

The roles of FOXP3 and CXCR4 in breast cancer

Stephen Mark Douglass



A thesis submitted for the degree of Doctor of Philosophy

January 2014

Acknowledgments

Undoubtedly, the most important people to thank is everyone at the Women's Cancer Detection Society (WCDS) and everyone who has donated to this fantastic charity. Without them I would not have had this opportunity. Other thoughts must be directed towards my supervisors, Professor John Kirby, Professor Simi Ali, Dr Annette Meeson and Mr David Browell who have supported me and gave the guidance and encouragement I needed to complete this project. Not forgetting all my friends, my family and everyone else who has helped me along the way.

Thank you.

It's been quite a ride!

List of abbreviations

ABC	Antigen binding capacity
ADH	Atypical ductal hyperplasia
ADP	Adenosine diphosphate
AML	Acute myeloid leukaemia
ANOVA	Analysis of variance
AP	Activator protein
APC	Allophycocyanin
ApE	A plasmid editor
ATF	Activating transcription factor
ATP	Adenosine triphosphate
BCA	Bicinchoninic acid
Bcl-2	B-cell Lymphoma 2
BGH	Bovine growth hormone
BRCA	Breast cancer susceptibility gene
BSA	Bovine serum albumin
CAMs	Cell-cell adhesion molecules
CD	Cluster of differentiation
CDK	Cyclin dependant kinase
chIP	Chromatin immunoprecipitation
CLIMA	Cell line integrated molecular marker
CML	Chronic myeloid leukaemia
CMV	Cytomegalovirus
(bio)COSHH	Control of (biological) substances hazardous to health
CREB	cAMP response binding element protein
Ct	Crossing threshold
CTLA	Cytotoxic T-lymphocyte antigen
DAB	3,3'-Diaminobenzidine
(k)Da	(Kilo) Daltons
DAPI	4',6-diamidino-2-phenylindole
(k)bp	(kilo) base pairs
DCIS	Ductal carcinoma <i>in situ</i>
DEPC	Diethyl pyrocarbonate
DMEM	Dulbeccos modified eagle medium
DMSO	Dimethyl sulphoxide
(c)DNA	(Complementary)Deoxyribonucleic acid
DNMT	DNA methyltransferase
DPX	Di-N-Butyle Phthalate in Xylene
<i>E.coli</i>	<i>Escherichia coli</i>
E1	Ubiquitin activating enzymes
E2	Ubiquitin conjugating enzymes
E3	Ubiquitin ligase enzymes
ECL	Enhanced chemoluminescence
EDTA	Ethylenediaminetetraacetic acid
ELISA	Enzyme-linked immunosorbent assay
ELR	Glutamic acid-leucine-arginine
EMT	epithelial-to-mesenchymal transition
ER	Oestrogen receptors
Erk	Extracellular signal regulated kinases

FACS	Fluorescent activated cell sorting
FAM	Carboxyfluorescein
FBS	Foetal bovine serum
FISH	Fluorescence <i>in situ</i> hybridisation
FITC	Fluorescein isothiocyanate
FOX	Forkhead box
FRT	Flp recombination target
FSH	Follicle stimulating hormone
GDP	Guanosine diphosphate
GFP	Green fluorescent protein
GPCR	G-protein coupled receptor
GTP	Guanosine triphosphate
HAT	Histone/protein acetyltransferase
HDAC	Histone deacetyltransferase
HEK	Human embryonic kidney cells
HER2	Human epidermal growth factor receptor 2
HES	Hairy-enhancer of split
HHV	Human herpes virus
HIF	Hypoxic inducible factor
HIV	Human immunodeficiency virus
HMEpC	Human mammary epithelial cells
HNM	Histidine asparagine methionine
HRP	Horseradish peroxidase
HSCTx	Haematopoietic stem cell transplant
HTA	Human tissue act
IDC	Invasive ductal carcinoma
IDT	Integrated DNA technology
IF	Immunofluorescence
IFN	Interferon
IgG	Immunoglobulin
IHC	Immunohistochemistry
IL	Interleukin
IPEX	Immunodysregulation polyendocrinopathy enteropathy X-linked syndrome
IκB	Inhibitor of κB
JAK	Janus kinase
LB	Lysogeny broth
LCIS	Lobular carcinoma <i>in situ</i>
LCK	Lymphocyte-specific protein tyrosine kinase
LH	Lutenizing hormone
MAPK	Mitogen activated protein kinase
MFI	Median fluorescence intensity
MMP	Matrix metalloproteinase
MRI	Magnetic resonance imaging
mTOR	Mammalian target of rapamycin
NCBI	National centre for bioscience institute
NFAT	Nuclear factor of activated T-cells
NF-κB	Nuclear factor κB
NHS	National health system
NICD	Notch intracellular domain

NLS	Nuclear localisation sequence
NPA	No primary antigen
NPI	Nottingham prognostic index
NST	No special type
PAGE	Polyacrylamide gel electrophoresis
PAK	p21-associated kinase
PBMC	Peripheral blood mononuclear cells
PBS	Phosphate buffered saline
PCNA	Proliferating cell nuclear antigen
PCR	Polymerase chain reaction
PDB	Protein data bank
PE	Phycoerythrin
PFA	Paraformaldehyde
pH	Power of hydrogen
PI	Propidium iodide
PI3K	Phosphoinositide 3-kinase
PIN	Prostate epithelial neoplasia
PKC	Protein Kinase C
PLCB	Phospholipase C β
PR	Progesterone receptor
PTEN	Phosphatase and tensin homologue
PTHrP	Parathyroid-related hormone protein
PTK	Protein tyrosine kinase
PVDF	Polyvinylidene fluoride
QE	Queen Elizabeth
RAFTK	Related adhesion focal tyrosine kinase
Rb	Retinoblastoma
RISC	RNAi silencing complex
(m)RNA	(messenger) Ribonucleic acid
RKKR	Arginine lysine lysine arginine
ROR	Retinoic receptor-related orphan receptor
RPMI	Royal park memorial institute
Runx	Runt-related transcription factor
RVI	Royal Victoria Infirmary
SCID	Severe combined immunodeficiency
SD	Standard deviation
SDS	Sodium dodecyl sulphate
siRNA	Small interfering RNA
SKP2	S-phase kinase protein 2
STAT	Signal transducer and activator of transcription
STR	Short tandem repeats
TAE	Tris-acetic acid-EDTA buffer
TAM	Tumour associated macrophages
TAMRA	Tetramethylrhodamine
TBS	Tris buffered saline
TCR	T-cell receptor
TDLU	Terminal ductal lobular units
TEB	Terminal end buds
Tet	Tetracycline
TetO2	Tetracycline operator sequences

TetR	Tetracycline repressor proteins
TGF	Transforming growth factor
Th	T-helper
TMB	3,3',5,5'-Tetramethylbenzidine
TNF	Tumour necrosis factor
Treg	Regulatory T-cell
TSG	Tumour suppressor gene
uPA	Urokinase plasminogen activator
UV	Ultraviolet
VCAM	Vascular cell adhesion molecule
VEGF	Vascular endothelial growth factor
WB	Western blot
YAP	Yes-associated protein

Abstract

The X-chromosome linked transcription factor, FOXP3, is expressed by epithelial cells from several organs. In these cells it is considered a potent tumour suppressor directly regulating the expression of many important oncogenes. The chemokine receptor, CXCR4, can also direct a number of processes relevant to the development of breast cancer. These include chemotaxis towards the sole ligand for CXCR4, CXCL12, which is expressed at the most common sites of metastatic spread. This study was designed to define further the role FOXP3 plays in metastatic breast cancer, with a particular focus on its potential to regulate CXCR4.

In comparison with normal primary breast epithelial cells, FOXP3 was downregulated at both transcript and protein levels in the breast cancer cell lines, MCF-7 and MDA-MB-231. In the more invasive MDA-MB-231, the remaining FOXP3 was located predominately within the cytoplasm and lacked the natural $\Delta 3$ isoform. Following stable FOXP3 overexpression in MDA-MB-231, significant decreases were observed in the expression of *ErbB2*, *SKP2*, *c-MYC* and *CXCR4*. In contrast, an increase in p21 expression led to inhibition of cell proliferation, with a greater proportion in the G1 phase of the cell cycle suggesting the induction of senescence. Specific knockdown of FOXP3 in normal breast epithelial cells with siRNA significantly increased *ErbB2*, *SKP2*, *c-MYC* and *CXCR4*, and decreased p21 expression. These cells also showed a significantly increased chemotactic response towards CXCL12, suggesting a role for FOXP3 influencing cell migration. The expression of FOXP3 and CXCR4 in normal breast tissue (n=2), and both lymph node negative (n=7) and lymph node positive (n=9) breast cancer samples was investigated by immunohistochemistry. Both epithelial and cancer cells in all the breast cancer samples showed increased CXCR4 expression in comparison to normal tissue. However, the expression of FOXP3 by epithelial or cancer cells did not appear different between all the samples examined.

Results from this study are consistent with FOXP3 functioning as an important tumour suppressor in breast cancer. Indeed, the functions of FOXP3 in breast epithelium can now potentially be extended to include influencing the expression of *CXCR4* and response to the pro-metastatic chemokine, CXCL12. Further studies should be directed to investigation of the molecular mechanisms involved in this influence of chemokine responsiveness by FOXP3.

Acknowledgements.....	i
List of abbreviations.....	ii
Abstract.....	vi
Contents pages.....	vii
List of figures.....	xii
List of tables.....	xvi
Reference list.....	314
Appendices.....	340

1 GENERAL INTRODUCTION	1
1.1 ANATOMY OF THE HUMAN BREAST.....	1
1.2 MAMMOGENESIS	1
1.3 THE LYMPHATIC SYSTEM.....	2
1.4 BREAST CANCER.....	5
1.4.1 Epidemiology.....	5
1.4.2 Signs and symptoms.....	8
1.4.3 Pathology and pathogenesis of breast cancer.....	8
1.4.4 The influence of growth factors and hormone receptors.....	13
1.4.4.1 Oestrogen and progesterone receptors	13
1.4.4.2 Human epidermal growth factor receptor 2	14
1.4.5 Oncogenes and tumour suppressor genes	15
1.4.5.1 BRCA1/2	16
1.4.5.2 p53	17
1.4.5.3 PI3K and PTEN	18
1.5 CHEMOKINE-DRIVEN CANCER PROGRESSION	18
1.5.1 Chemokines	20
1.5.1.1 Structure and classification.....	21
1.5.2 Chemokine receptors.....	22
1.5.3 Signal transduction.....	26
1.6 CHEMOKINE RECEPTORS AND BREAST CANCER METASTASIS	26
1.6.1 CXCR4 crystal structure	32
1.6.2 CXCR4-CXCL12 signalling.....	33
1.6.2.1 PI3K/Akt pathway	35
1.6.2.2 MAPK/Erk pathway	36
1.6.2.3 JAK/STAT pathway	37
1.6.2.4 HER2 upregulation	37
1.6.3 CXCR4 regulation	40
1.6.3.1 Hypoxia	40
1.6.3.2 HER2	41
1.6.3.3 NF- κ B.....	42
1.6.3.4 VEGF.....	43
1.6.3.5 Influence of cytokines.....	44
1.7 FOXP3.....	46
1.7.1 Forkhead box protein history and nomenclature	46
1.7.2 Structure.....	47
1.7.2.1 Gene.....	47

1.7.2.2	Protein.....	47
1.7.3	<i>Scurfy and IPEX</i>	54
1.7.4	<i>Natural isoforms</i>	55
1.7.5	<i>Intracellular trafficking</i>	56
1.7.6	<i>FOXP3 association with other transcription factors</i>	61
1.7.6.1	Homo-dimersation.....	61
1.7.6.2	NFAT.....	61
1.7.6.3	NF- κ B.....	62
1.7.6.4	Runx1.....	63
1.7.6.5	ROR- α	63
1.7.7	<i>Cellular expression of FOXP3</i>	64
1.7.7.1	Treg.....	64
1.7.7.2	Epithelial cells.....	65
1.7.8	<i>FOXP3 involvement in cancer</i>	67
1.7.9	<i>FOXP3, the X-linked tumour suppressor gene</i>	70
1.7.9.1	<i>LATS2</i>	71
1.7.9.2	<i>BRCA1</i>	72
1.7.10	<i>Regulation of FOXP3</i>	73
1.8	HYPOTHESIS OF THE STUDY.....	76
1.9	AIMS OF THE STUDY.....	77
2	GENERAL MATERIALS AND METHODS	78
2.1	CELL LINES.....	78
2.1.1	<i>Human mammary epithelial cells</i>	78
2.1.2	<i>MCF-7</i>	78
2.1.3	<i>MDA-MB-231</i>	78
2.1.4	<i>Validation of immortalised cancer cell lines</i>	79
2.1.5	<i>Flp-InTM T-RexTM Human embryonic kidney-293 cells</i>	79
2.2	CELL CULTURE METHODS.....	82
2.2.1	<i>Cryopreservation of cells</i>	82
2.2.2	<i>Cell counting</i>	82
2.2.3	<i>Growth media for immortalised cell lines</i>	83
2.2.4	<i>General maintenance of immortalised cell lines</i>	83
2.2.5	<i>General maintenance of primary cells</i>	83
2.2.6	<i>Mycoplasma testing</i>	84
2.3	DNA METHODS.....	85
2.3.1	<i>Agarose gel electrophoresis</i>	85
2.3.2	<i>DNA extraction and purification from agarose gel</i>	85
2.3.3	<i>DNA sequencing</i>	86
2.4	POLYMERASE CHAIN REACTION.....	86
2.4.1	<i>RNA isolation</i>	87
2.4.2	<i>Nucleic acid quantification</i>	87
2.4.3	<i>cDNA synthesis</i>	88
2.4.4	<i>Conventional PCR</i>	90
2.4.5	<i>Real-time PCR</i>	90
2.4.5.1	TaqMan® chemistry.....	91
2.4.5.2	Relative quantification of gene expression.....	94
2.5	PROTEIN METHODS.....	95
2.5.1	<i>Protein extraction</i>	95
2.5.2	<i>Fractionation of nuclear and cytoplasmic protein</i>	95
2.5.3	<i>Protein quantification</i>	95
2.5.4	<i>Flow cytometry</i>	98
2.5.4.1	Cell surface staining.....	98
2.5.4.2	Intracellular staining.....	99

2.5.5	Western blot.....	99
2.5.6	Immunofluorescence.....	100
2.6	LIST OF ANTIBODIES	101
2.7	STATISTICAL ANALYSIS	102
3	STUDY OF FOXP3 EXPRESSION IN NORMAL AND MALIGNANT BREAST CELL LINES.....	103
3.1	INTRODUCTION.....	103
3.1.1	<i>Dysregulated expression of FOXP3 in malignant breast epithelia</i>	103
3.1.2	<i>Cytokine-driven FOXP3 expression</i>	105
3.1.2.1	TGF- β	106
3.1.2.2	IL-2	107
3.2	AIMS AND OBJECTIVES	109
3.3	SPECIFIC MATERIALS AND METHODS	110
3.3.1	<i>Protein dialysis</i>	110
3.3.2	<i>ELISA</i>	110
3.3.3	<i>Primer design</i>	114
3.4	RESULTS.....	116
3.4.1	<i>Characterisation of inducible FOXP3 in transfected HEK cells</i>	116
3.4.2	<i>Validation of HMEpC</i>	119
3.4.3	<i>Determination of FOXP3 expression in cell lines</i>	121
3.4.4	<i>Quantification of subcellular distribution of FOXP3 in cell lines</i>	128
3.4.5	<i>Sequencing of FOXP3 in cell lines for mutations and splice variant isoforms</i>	130
3.4.5.1	Annealing temperature gradient for FOXP3 primer sets.....	130
3.4.5.2	Sequencing of FOXP3 primer set 1	132
3.4.5.3	Sequencing of FOXP3 primer set 2	135
3.4.5.4	Sequencing of FOXP3 primer set 3	135
3.4.6	<i>Effects of IL-2 and TGF-β on FOXP3 expression in breast cancer cell lines</i>	138
3.5	SUMMARY OF CHAPTER 3 RESULTS.....	140
3.6	DISCUSSION.....	141
3.6.1	<i>Validation of FOXP3 induction in transfected HEK cells</i>	141
3.6.2	<i>FOXP3 expression in normal and malignant cell lines</i>	142
3.6.3	<i>FOXP3 mutations and isoforms in breast cancer cells</i>	144
3.6.4	<i>p53 status in cancer cell lines and FOXP3 regulation</i>	148
3.6.5	<i>FOXP3 expression by cytokine-treatment in cancer cells</i>	148
3.7	CONCLUSION	151
4	IN VITRO MODELLING OF FOXP3 FUNCTIONS IN NORMAL AND MALIGNANT BREAST EPITHELIA.....	152
4.1	INTRODUCTION.....	152
4.1.1	<i>HER2 (ErbB2)</i>	152
4.1.2	<i>S-phase kinase-associated protein 2</i>	153
4.1.3	<i>c-Myc</i>	154
4.1.4	<i>p21 (CDKN1A)</i>	155
4.1.5	<i>CXCR4</i>	156
4.1.6	<i>The influence of FOXP3 on cellular function</i>	156
4.2	AIMS AND OBJECTIVES	159
4.3	SPECIFIC MATERIALS AND METHODS	160
4.3.1	<i>Bacterial cell culture methods</i>	160
4.3.1.1	Lysogeny broth	160
4.3.1.2	Transformation of chemically competent <i>E.coli</i>	160
4.3.1.3	Recovery of plasmid DNA from bacterial cell culture.....	161
4.3.1.4	Restriction enzyme digestion of DNA	161

4.3.2	<i>Transfection methods</i>	164
4.3.2.1	Stable transfection of MDA-MB-231 using Amaxa™Nucleofector™	165
4.3.2.2	Lipid-based transient transfections	165
4.3.3	<i>Selection of stably transfected cells using Zeocin™</i>	168
4.3.4	<i>Transfection of siRNA sequences</i>	170
4.3.5	<i>Functional studies</i>	173
4.3.5.1	Transwell chemotaxis	173
4.3.5.2	Transwell chemo-invasion assay	174
4.3.5.3	Proliferation assays	174
4.3.5.4	Cell cycle analysis	175
4.3.6	<i>Quantum™ Simply Cellular® Beads</i>	175
4.4	RESULTS.....	176
4.4.1	<i>Construction of a FOXP3-expressing plasmid</i>	176
4.4.2	<i>Transient transfection of pcDNA3.1/Zeo-FOXP3 into HEK cells</i>	180
4.4.3	<i>Transient transfection of pmax GFP into MDA-MB-231 using Amaxa™Nucleofector™</i> 180	180
4.4.4	<i>Zeocin™ killing curve using MDA-MB-231</i>	183
4.4.5	<i>Generation of stably transfected FOXP3 overexpressing MDA-MB-231</i>	185
4.4.6	<i>Effects of stable FOXP3 overexpression in MDA-MB-231</i>	189
4.4.6.1	Primer validation	189
4.4.6.2	Relative expression of genes following stable FOXP3 integration in MDA-MB-231	191
4.4.6.3	Effects of FOXP3 overexpression on MDA-MB-231 proliferation	193
4.4.7	<i>Optimising transient transfection of MDA-MB-231 using pmaxGFP</i>	196
4.4.8	<i>Optimisation of FOXP3 knockdown in HMEpC using FOXP3 specific siRNA sequences</i> 201	201
4.4.8.1	Choice of transfection reagent to knockdown FOXP3 in HMEpC	201
4.4.8.2	Choice of FOXP3 siRNA.....	201
4.4.9	<i>Effects of FOXP3 knockdown in HMEpC</i>	206
4.4.9.1	Relative expression of genes following FOXP3 knockdown in HMEpC.....	206
4.4.9.2	Changes in CXCR4 following FOXP3 knockdown in HMEpC	208
4.4.10	<i>Cytometric bead assay to determine anti-CXCR4 antibody binding capacity (ABC)</i> 210	210
4.4.10.1	Changes in CXCR4 ABC following FOXP3 knockdown in HMEpC	212
4.4.11	<i>Optimisation of chemoinvasion towards CXCL12 using MDA-MB-231</i>	214
4.4.12	<i>Effects of FOXP3 knockdown on invasiveness of HMEpC</i>	216
4.4.13	<i>Optimisation of chemotaxis assays towards CXCL12 using MDA-MB-231</i>	219
4.4.14	<i>Effects of FOXP3 knockdown on migration of HMEpC</i>	221
4.5	SUMMARY OF CHAPTER 4 RESULTS.....	224
4.6	DISCUSSION.....	226
4.6.1	<i>Generation of stable FOXP3 overexpressing MDA-MB-231</i>	227
4.6.2	<i>Effects of FOXP3 overexpression in MDA-MB-231</i>	228
4.6.3	<i>Effects of FOXP3 knockdown in HMEpC</i>	230
4.7	CONCLUSION	234
5	IN VIVO LEVELS OF FOXP3 AND CXCR4 EXPRESSION IN BREAST CANCER PATIENT SAMPLES	236
5.1	INTRODUCTION.....	236
5.1.1	<i>Tumour microenvironment</i>	236
5.1.1.1	T-cell infiltration.....	238
5.1.2	<i>Breast cancer classification</i>	239
5.1.2.1	Tumour grade.....	240
5.1.2.2	Tumour stage	243
5.2	AIMS AND OBJECTIVES	246
5.3	SPECIFIC MATERIALS AND METHODS	247

5.3.1	<i>Ethical approval</i>	247
5.3.2	<i>Selection of patient samples</i>	247
5.3.3	<i>RNA isolation from frozen patient samples using GentleMACS™ dissociator</i>	249
5.3.4	<i>RNeasy mini spin columns</i>	249
5.3.5	<i>IHC staining of breast tissue</i>	250
5.3.5.1	CD3 and CXCR4 staining.....	250
5.3.5.2	FOXP3 staining	251
5.3.5.3	List of antibodies used for IHC.....	258
5.3.6	<i>Quick score algorithm used for IHC staining</i>	258
5.4	RESULTS.....	260
5.4.1	<i>Separation of T-cells from frozen breast tumours</i>	260
5.4.2	<i>Optimisation of RNA isolation from frozen tumour sections</i>	262
5.4.3	<i>Selection of suitable housekeeping genes</i>	266
5.4.4	<i>Determination of T-cell infiltration in breast samples</i>	268
5.4.5	<i>Measurement of CXCR4 transcripts in breast samples</i>	272
5.4.6	<i>Optimisation of CXCR4 IHC staining</i>	274
5.4.7	<i>Measurement of CXCR4 protein expression in breast samples</i>	276
5.4.8	<i>Measurement of FOXP3 transcripts in breast samples</i>	280
5.4.9	<i>Optimisation of FOXP3 IHC staining and measurement in patient samples</i>	282
5.4.10	<i>Correlation of FOXP3 and CXCR4 protein expression in breast samples</i>	287
5.5	SUMMARY OF CHAPTER 5 RESULTS.....	289
5.6	DISCUSSION.....	291
5.6.1	<i>Correlation of lymph node status in selected patients and overall survival</i>	291
5.6.2	<i>The impact of T-cell infiltrates on real-time PCR results</i>	292
5.6.3	<i>Source of normal tissue for CXCR4 staining</i>	293
5.6.4	<i>FOXP3 IHC staining in normal tissue</i>	294
5.6.5	<i>FOXP3 and CXCR4 IHC staining in breast cancer patients</i>	295
5.7	CONCLUSION	297
6	DISCUSSION	298
6.1	THE ROLE OF FOXP3 IN BREAST CANCER.....	298
6.2	THE ROLE OF FOXP3 ON CXCR4 EXPRESSION.....	300
6.3	CONCLUDING THOUGHTS	303
6.4	POTENTIAL FOXP3 - CXCR4 MECHANISMS.....	304
6.5	THERAPEUTIC IMPLICATIONS.....	308
6.5.1	<i>FOXP3 therapies</i>	308
6.5.2	<i>CXCR4 inhibitors</i>	310
6.6	LIMITATIONS AND FUTURE DIRECTIONS FOR THE STUDY	311

List of figures

Figure 1-1 - Anatomy of the human breast and lymphatic system	4
Figure 1-2 - Risk of breast cancer development by age of women in the UK.....	7
Figure 1-3 - Disease progression witnessed in breast cancer and metastasis	12
Figure 1-4 - Classification of chemokines and the location of cysteine residues	24
Figure 1-5 - Chemokines and their constitutive receptors	25
Figure 1-6 - Distribution of CXCL12 and CCL21 in humans	31
Figure 1-7 - Signalling pathways involved with the CXCL12/CXCR4 axis	39
Figure 1-8 - Factors able to increase CXCR4 expression on epithelial cells.....	45
Figure 1-9 - Schematic representation of human FOXP3	49
Figure 1-10 - Loops and helixes of the forkhead domain in FOXP proteins.....	50
Figure 1-11 - Regions responsible for FOXP3-mediated gene repression	53
Figure 1-12 - Locations of Foxp3 nuclear sequences	60
Figure 1-13 - Organ specific expression of Foxp3 in epithelial cells	66
Figure 2-1 - Schematic representation of Flp-In TM T-Rex TM system.....	81
Figure 2-2 - Representative images of highly pure plasmid DNA isolated from bacteria and RNA from cell lines.....	89
Figure 2-3 - Schematic representation of TaqMan® real-time PCR reaction	92
Figure 2-4 - Representative standard curve to determine protein concentration	97
Figure 3-1 - Test principle of FOXP3 ELISA.....	112
Figure 3-2 - Standard curves for FOXP3 ELISA.....	113
Figure 3-3 - Manually designed primers for <i>FOXP3</i> sequencing.....	115
Figure 3-4 – Tetracycline-inducible expression of FOXP3 in transfected HEK cells	117
Figure 3-5 - Decline of FOXP3 expression following the removal of tetracycline from growth media.....	118
Figure 3-6 - Validation of HMEpC by staining for cytokeratins	120
Figure 3-7 - Confirmation of RNA integrity in cell lines	122
Figure 3-8 - Reaction efficiency of <i>FOXP3</i> and <i>GAPDH</i> Taqman® real-time PCR primers.....	123

Figure 3-9 - Determination of <i>FOXP3</i> transcripts in HMEpC and breast cancer cell lines	124
Figure 3-10 - Quantitative expression of FOXP3 protein levels in breast cell lines	126
Figure 3-11 - IF images of FOXP3 in cell lines	127
Figure 3-12 - Quantitative distribution of FOXP3 in subcellular fractions	129
Figure 3-13 - Annealing temperature gradient for <i>FOXP3</i> primers.....	131
Figure 3-14 - Sequencing of <i>FOXP3</i> in breast cancer cell lines using <i>FOXP3</i> primer set 1	133
Figure 3-15 - Electropherogram demonstrating <i>FOXP3Δ3</i> isoform in MCF-7 cells	134
Figure 3-16 - Sequencing of <i>FOXP3</i> in breast cancer cell lines using <i>FOXP3</i> primer set 2	136
Figure 3-17 - Sequencing of <i>FOXP3</i> in breast cancer cell lines using <i>FOXP3</i> primer set 3	137
Figure 3-18 - Effects of IL-2 and TGF- β treatment on <i>FOXP3</i> expression in breast cancer cell lines	139
Figure 4-1 - Conversion of MTS tetrazolium into Formazan	169
Figure 4-2 - Construction of pcDNA3.1/Zeo-FOXP3 vector	178
Figure 4-3 - Schematic representation of <i>FOXP3</i> insertion into the pcDNA3.1/Zeo(+)-vector	179
Figure 4-4 - Transient transfection of pcDNA3.1/Zeo-FOXP3 into HEK cells	181
Figure 4-5 - Transient transfection of pmaxGFP into MDA-MB-231	182
Figure 4-6 - Zeocin TM killing curve on MDA-MB-231	184
Figure 4-7 - Stable <i>FOXP3</i> overexpressing MDA-MB-231	187
Figure 4-8 - Subcellular distribution of FOXP3 within stably transfected MDA-MB-231	188
Figure 4-9 - Reaction efficiency of TaqMan® real-time PCR primers	190
Figure 4-10 - Changes in oncogene expression following FOXP3 overexpression in MDA-MB-231	192
Figure 4-11 - Effects of FOXP3 overexpression on the proliferation of MDA-MB-231	194
Figure 4-12 - Cell cycle analysis of MDA-MB-231 following FOXP3 overexpression.....	195

Figure 4-13 - Optimisation of pmaxGFP transfection into MDA-MB-231 using Lipofectamine®2000 after 24 hours	198
Figure 4-14 - Optimisation of pmaxGFP transfection into MDA-MB-231 using Lipofectamine®2000 after 48 hours	199
Figure 4-15 - Optimisation of pmaxGFP transfection into MDA-MB-231 using GenJet™	200
Figure 4-16 - Transfection of GAPDH-Cy ³ siRNA into HMEpC using Lipofectamine®2000 and siPORT™NeoFX™	203
Figure 4-17 - Determination of <i>FOXP3</i> knockdown in HMEpC using <i>FOXP3</i> specific siRNA	204
Figure 4-18 - Determination of <i>FOXP3</i> in HMEpC following transfection of <i>FOXP3</i> specific siRNA	205
Figure 4-19 - Changes in oncogene expression following <i>FOXP3</i> knockdown in HMEpC	207
Figure 4-20 - Effects on CXCR4 expression following <i>FOXP3</i> knockdown in HMEpC	209
Figure 4-21 - Cytometric bead assay to determine ABC of the anti-CXCR4 antibody	211
Figure 4-22 - Changes in CXCR4 ABC following <i>FOXP3</i> knockdown in HMEpC	213
Figure 4-23 - Optimisation of chemoinvasion towards CXCL12 using MDA-MB-231	215
Figure 4-24 - Chemoinvasion of HMEpC in response to 75nM of CXCL12 following transfection of <i>FOXP3</i> siRNA	217
Figure 4-25 - Chemoinvasion of HMEpC in response to 100nM of CXCL12 following transfection of <i>FOXP3</i> siRNA.....	218
Figure 4-26 - Optimisation of chemotaxis assays towards CXCL12 using MDA-MB-231	220
Figure 4-27 - Chemotaxis of HMEpC in response to 25nM of CXCL12 following <i>FOXP3</i> knockdown in HMEpC	222
Figure 4-28 - Chemotaxis of HMEpC in response to 50nM of CXCL12 following <i>FOXP3</i> knockdown in HMEpC	223
Figure 5-1 - Automated equipment used in frozen tissue homogenisation and paraffin embedded tissue IHC	255
Figure 5-2 - Schematic representation of the <i>ultraVIEW</i> detection kit	256
Figure 5-3 - Schematic representation of the <i>optiview</i> detection kit	256

Figure 5-4 - Schematic representation of the ABC Vectashield detection kit	257
Figure 5-5 – Determination of infiltrating CD3 ⁺ cells in dissociated breast tumours by flow cytometry	261
Figure 5-6 - Confirmation of RNA integrity following isolation from frozen cells using TRI reagent.....	264
Figure 5-7 - Confirmation of RNA integrity following isolation from frozen cells using RNeasy spin columns reagent	265
Figure 5-8 - Determining the most compatible housekeeping gene in frozen breast cancer tissues.....	267
Figure 5-9 - Determination of <i>CD3</i> transcripts in normal and breast cancer tissues	269
Figure 5-10 - IHC staining of CD3 in normal mammary breast tissue.....	270
Figure 5-11 - IHC staining of CD3 in breast cancer samples	271
Figure 5-12 - Determination of <i>CXCR4</i> transcripts in normal and breast cancer tissues	273
Figure 5-13 – Optimisation of CXCR4 IHC staining using human tonsil.....	275
Figure 5-14 - IHC staining of CXCR4 in normal breast tissue.....	277
Figure 5-15 - IHC staining of CXCR4 in LN-negative breast cancer samples.....	278
Figure 5-16 - IHC staining of CXCR4 in LN-positive breast cancer samples.....	279
Figure 5-17 - Measurement of <i>FOXP3</i> transcripts in normal and breast cancer frozen tissues	281
Figure 5-18 - Manual IHC staining of FOXP3 in normal breast tissue using FOXP3 clone 259D	284
Figure 5-19 - FOXP3 staining in LN-negative breast cancer samples.....	285
Figure 5-20 - FOXP3 staining in LN-positive breast cancer samples	286
Figure 5-21 - Quick scores for FOXP3 and CXCR4 expression in breast tissue	288
Figure 6-1 - Effects of CXCR4 expression following FOXP3 transfection into malignant breast and prostate cell lines	302
Figure 6-2 - Potential mechanisms of FOXP3 influencing CXCR4 expression.....	307

List of tables

Table 2-1 - List of TaqMan® primers used in real-time PCR	93
Table 2-2 - List of antibodies used in studies	101
Table 4-1 - Restriction enzymes used in plasmid cloning and linearization.....	163
Table 4-2 - List of siRNA used in experiments	172
Table 5-1 - Scoring system used for tumour grading.....	242
Table 5-2 - Table for Nottingham prognostic index ranges	244
Table 5-3 - Classification of the tumour-node-metastasis (TNM) system.....	245
Table 5-4 - Patient histories of selected breast cancer samples	248
Table 5-5 - List of antibodies used for IHC	259

Chapter

General introduction

1

General materials and methods

2

Study of FOXP3 expression in normal and malignant breast cell lines

3

In vitro modelling of FOXP3 expression in normal and malignant breast cell lines

4

In vivo levels of FOXP3 and CXCR4 expression in breast cancer samples

5

Discussion

6

List of references

7

Appendices

8

1 General introduction

1.1 Anatomy of the human breast

The adult breast is a special type of apocrine gland and is often described as a modified sweat gland which produces milk. It is made up of predominantly lobules, ducts and stroma (Elston and Ellis 1998). The lobules are the regions which contain the glands and are responsible for producing milk, whereas, the ducts are tubes which branch from the lobules towards the nipple and are responsible for carrying the milk. The rest of the breast is stroma, consisting mainly of adipose tissue and connective tissue which surrounds the ducts, lobules, blood vessels, lymphatic vessels and muscle. Each developed adult breast contains 15-20 lobes, and each lobe contains 20-40 lobules which branch into a network of ducts that terminate at the nipple (Elston and Ellis 1998). The terminal duct lobular units (TDLU) are the sites where milk is produced. These are found nearest to the pectoralis major muscle. From these lobular units, ducts branch out to form subsegmental ducts. As these ducts branch further out, they converge into slightly larger segmental ducts until they reach the areola region where they slightly dilate to form lactiferous sinuses. These are surrounded by muscle and control the opening and closing of the nipple during suckling (**figure 1.1 panel A**) (Elston and Ellis 1998).

1.2 Mammogenesis

The development of the mammary glands occurs during different growth cycles. In the embryonic stage, both sexes begin mammogenesis by forming rudimentary duct trees at birth. From this stage the development of the glands depends on systemic and maternal hormones but also the local regulation of paracrine communication between epithelial and mesenchymal cells by parathyroid-related hormone protein (PTHrP) (Sternlicht 2006). The development of lactiferous ducts is controlled by hormones and occurs during pre- and post-natal stages and again later during puberty (Sternlicht 2006). At the onset of puberty there is a change in the hormonal environment which is key in controlling further development of the mammary

glands. The anterior pituitary gland releases follicle stimulating hormone (FSH) and lutenizing hormone (LH) in a cyclic manner which stimulates the ovaries to synthesise oestrogens and progesterones. Oestrogen acts to further stimulate mesenchymal cells which results in an increase in the gland size as the ducts branch into the surrounding stroma (Sternlicht 2006). In males, testosterone acts on mesenchymal cells to inhibit mammogenesis. At this stage in females the gland is considered as matured, but remains inactive until pregnancy where a further onset of hormonal changes takes place (Sternlicht 2006).

During the first trimester, the ductal terminal branches elongate and the epithelial cells proliferate from stem cells distributed throughout the gland. During the second trimester, the glandular components of the breast enlarge as the adipose tissue and stroma progressively get thinner, and the lobules differentiate from terminal end buds (TEB). During the third trimester, the lobules mature as the epithelial cells become cuboidal and the rate of secretion increases (Sternlicht 2006). After menopause the mammary glands undergo involution as the amount of elastic tissue increases, adipose tissue decreases and the stroma becomes more fibrous and less cellular. As well as this, the levels of circulating ovarian hormones decrease and ductal elements begin to degenerate (Sternlicht 2006).

1.3 The lymphatic system

Lymph nodes are small bean shaped regions which are connected by lymphatic vessels. These vessels carry fluid (called lymph) away from the breast. Lymph is made up primarily of lymphocytes but also tissue fluid and waste products. The tissue in and around the breast is rich in lymph nodes and vessels, therefore, when breast cancer cells acquire the ability to invade the most common preliminary site they invade to is the lymph nodes. Once the cancer cells have reached the lymph nodes there is a high chance they will enter the bloodstream where they can then spread to other sites around the body. Most lymphatic vessels in the breast connect to the axillary lymph nodes which are situated mainly around the arm pit. The axillary lymph nodes consist of the pectoral lymph nodes, low axillary lymph nodes, mid axillary lymph nodes and brachial lymph nodes. Other lymph nodes are situated around either the clavical (infraclavicular lymph nodes, also known as higher

axillary) or near the sternum (supraclaviular lymph nodes and internal mammary lymph nodes) (Elston and Ellis 1998) (**figure 1.1 panel B**).

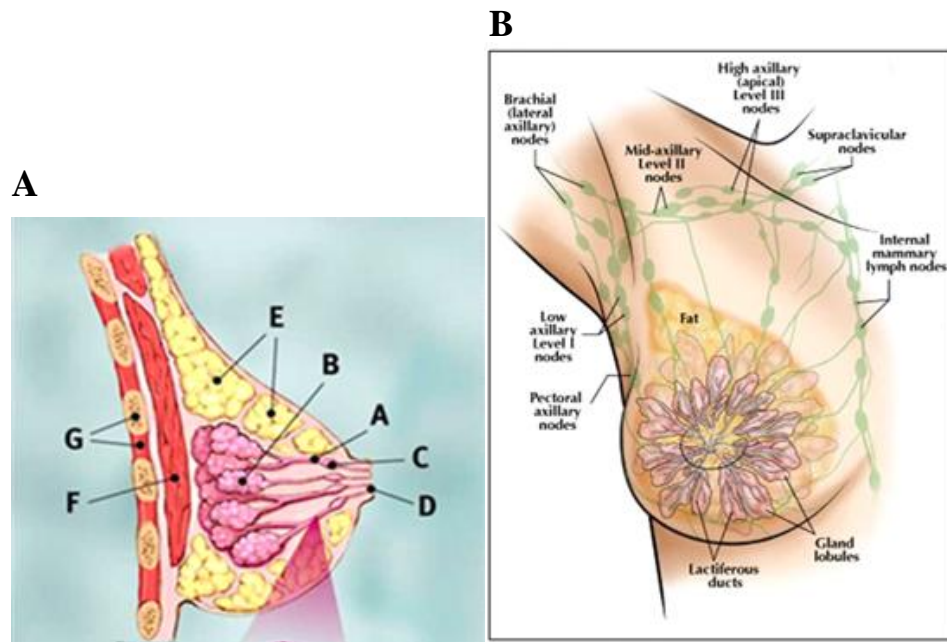


Figure 1-1 - Anatomy of the human breast and lymphatic system

Cross section of the human breast demonstrates the location of ducts (A,A) which stem from milk producing glands called lobes (A,B). The ducts branch and construct into subsegmental ducts (A,C) which are surrounded by muscle and terminate at the nipple (A,D). These glandular regions are surrounded by stroma which is predominantly made of adipose tissue (A,E). The breast tissue typically lies above the pectoralis major muscle (A,F) and extends from the level of third rib (A,G).

The lymphatic system surrounding the breast tissue is made up of a network of lymph nodes (B) which are responsible for draining lymph away from the breast. **Panel A** taken from (Breastcancer.org 2013), **panel B** taken from (Breastcancerbgone.com 2012).

1.4 Breast cancer

In ancient times autopsies were rare so cancers of internal organs were not reported. However, cancers of the breast were different as the tumour could be felt through the skin, and in later stages, can often ulcerate becoming more visible than other forms of cancer. On this basis, breast cancer is considered as one of the oldest diseases on record. One of the first descriptions of breast cancer was reported at around 1600BC in Egypt on the Edwin Smith papyrus (Aronowitz 2007).

Observations made by early physicians such as Bernardino Ramazzini in 1713 stated that Nuns had a higher risk of developing breast cancer. Ramazzini suggested the lack of sexual activity caused instability in the breast. Ramazzini stated that women who have never had child (nulliparity), or those who have children later in life have a higher relative risk of developing breast cancer.

In 1926, Janet Lane-Claypon conducted the first case-controlled study on breast cancer epidemiology. She published for the British Ministry of Health comparing 500 breast cancer patients with 500 control patients who had similar lifestyles and backgrounds asking many questions of the female lifestyles. Her conclusions still agree with many modern reviews on breast cancer susceptibility claiming age at menopause, age at first pregnancy (age at marriage used as a proxy), number of children, and lactation all impacted significantly on the risk of developing breast cancer (Winkelstein 2006).

1.4.1 Epidemiology

Breast cancer comprises 16% of all female cancers which makes it the most common malignancy in women worldwide (cancerresearchuk.org 2012). In 2010, more than 49,000 UK women were diagnosed with breast cancer. This is equal to roughly 136 women per day (cancerresearchuk.org 2012). Although breast cancer is much more common in woman, it can also occur in males and in 2010 approximately 400 men were diagnosed with breast cancer (cancerresearchuk.org 2012). From the mid-1970s, breast cancer rates in Britain have increased by almost 70% (cancerresearchuk.org 2012). This increase can be explained by the raise in awareness and screening programs which encourages the public to check for

symptoms more frequently and allows tumours to be diagnosed at an earlier stage making them potentially more treatable. These programs have been a huge success. In 2009/2010, the NHS screening programs detected nearly 16,500 cases of breast cancer in the UK. As well as highly successful screening and awareness programs, a clearer understanding of the disease has allowed the development of more innovative modern medicine which has also played a key part in improving survival rates.

During the 1970s it was estimated that only 5 out of 10 women survived beyond 5 years after the original diagnosis, however, more than 8 out of 10 women diagnosed now exceed 5 years (cancerresearchuk.org 2012). Although these figures are encouraging, breast cancer is still a major burden. In the UK breast cancer is now the second most fatal malignancy after lung cancer. The current lifetime risk of women developing breast cancer is 1 in 8 (cancerresearchuk.org 2012). Unfortunately, many developing countries do not have the same level of treatment, screening programs or awareness as more developed countries and possibly as a result of this, almost 69% of breast cancer deaths in 2004 occurred in developing countries (WHO.int 2013).

There are a number of risk factors which can influence the chances of breast cancer including child bearing, breast feeding, weight, diet, alcohol and smoking (discussed in further detail on cancer.org). However, the most prominent risk factor remains age and menopause stage. Unsurprisingly, as females get older their risk of acquiring breast cancer markedly increases (**figure 1.2**). Statistics suggest that the risk of women developing breast cancer before the age of 30 is approximately 1 in 2000, however, as age increases so does the risk (Breastcancer.org 2013).

Genetic inheritance of certain mutated genes also carries a significant risk of an individual's susceptibility to breast cancer. Therefore, inherited mutations also account for a large proportion of breast cancer cases. This is discussed further in section 1.4.5.

Estimated risk at birth up to and including:	UK (2008)
age 29	1 in 2,000
age 39	1 in 215
age 49	1 in 50
age 59	1 in 22
age 69	1 in 13
Lifetime risk	1 in 8

Figure 1-2 - Risk of breast cancer development by age of women in the UK

Data suggests a relatively low chance of breast cancer development in women aged below 29, however, as age increases the risk of developing breast cancer increases (Breastcancer.org 2013).

1.4.2 Signs and symptoms

In clinical practise in the UK, breast cancer presents through two main routes; one being symptomatic, and the other being asymptomatic. The majority of asymptomatic breast cancer cases are caught through the NHS breast screening programme. The most common symptomatic sign for the onset of breast cancer is a thickening of the skin or the formation of a lump in the breast. Other symptomatic changes of the breast which can act as an indicator include dimpling of the skin or the nipple, a change in size and shape of the breast, a rash on the breast or blood stained discharge from the nipple. Less common is where the cancer erodes or fungates through the skin in locally advanced cancer. Inflammatory breast cancer is a rare but aggressive form of breast cancer which often presents by the breast looking red, inflamed, sore and tougher to touch. Another rarer form of breast cancer is Paget's disease. Symptoms of Paget's disease can often be firstly misdiagnosed as eczema as a red and often scaly rash is found around the areola region.

In the UK, women aged between 43 and 72 are invited tri-annually for X-ray based mammographic screening. These patients are usually completely asymptomatic with no palpable abnormalilty within the breast. Some Hospitals involved in screening programmes have reported that the majority of breast cancers diagnosed are from asympmtomatic patients. This emphasises the benefits of breast sceening units in the UK.

1.4.3 Pathology and pathogenesis of breast cancer

Many lumps discovered in the breast are non-cancerous and are classed as benign as they are incapable of invasion and cannot spread outside the site of origin. Benign lumps can be formed at any stage of life in many women and are generally caused by fibrosis, which is the formation of scar tissue, or a cyst, which is a fluid-filled sac. However, when a lump is detected which is considered cancerous, it is classed as a carcinoma. An adenocarinoma is a carcinoma subset which originates from glandular tissue such as the ducts or lobules of the breast. Rarer cases of cancer exist which originate from the connective tissue, such as the muscle or adipose tissue. These tumours are classed as sarcomas.

Most breast cancers develop due to instability within the breast tissue. The initial stage of carcinogenesis is the formation of atypical ductal hyperplasia (ADH). If hyperplasia progresses into a breast carcinoma, the type of breast cancer is then divided into either *in situ* (non-invasive) or invasive breast cancer. Ductal carcinoma *in situ* (DCIS) is thought to be a true pre-invasive cancer and a precursor of true invasive ductal breast cancer, whereas, lobular carcinoma *in situ* (LCIS) is not considered to be a precursor of a true invasive cancer. However, LCIS is considered a marker of the potential for the development of both invasive lobular and ductal cancers. Because of its true malignant potential, DCIS is subdivided as either high or low grade based on the morphological appearance of the tumour cells. Tumours of a higher grade have a greater malignant potential and also have a greater tendency to reoccur after treatment.

There are basic histological types of invasive breast cancer. Those derived from the epithelial lining of the breast ducts, the ductal cancers of no special type (NST), and those not of a ductal origin or special type. The most common form of breast cancer is invasive ductal carcinoma (IDC). This accounts for approximately 80% of cases. The most common special type of breast cancer is derived from the lobular epithelial cells (lobular cancer). These account for approximately 10% of cases. Other less common forms of special type breast cancer can be mucinous (3%), tubular (3%) or medullary (2%) (Breastcancer.org 2013). Breast cancer classification is discussed further in section 5.1.2.

The development of a cancerous tumour is a multi-stage process. For a normal healthy cell to transform into a malignant cancer, it must acquire a number of traits that are dependent on a series of genetic changes that contribute to growth advantages. This notion was extensively reviewed by Hanahan and Weinberg (Hanahan and Weinberg 2000) who stated that a minimum of six alterations in the physiology of the cells are required before they transform into malignant cells. The six alterations stated were:

- Self sufficiency of growth signals
- Insensitive to anti-growth signals
- Evading apoptosis
- Limitless replication

- Promotion of angiogenesis
- Acquired potential to invade and metastasise

Normal cells require mitogenic growth signals delivered via transmembrane receptors which bind a distinct set of molecules. No normal healthy cell is able to proliferate in the absence of these signals, however, many oncogenes will allow the tumour to either mimic normal growth signals, or generate their own growth signals, thus reducing their dependence of stimulation from the tissue environment (Hanahan and Weinberg 2000). As well as receiving signals which encourage proliferation, the ability to ignore anti-growth signals is another key trait cancer cells require to prosper.

Performing cell cycle arrest and repairing damaged DNA, or undergoing apoptosis is a critical feature cells perform after detecting harmful mutations. As well as being able to expand in the number of cells within the tumour mass, the tumour cells also have an incessant ability to survive longer by evading apoptosis.

Research has shown *in vivo* that most, if not all, tumour cells have a limitless replicative potential where they can double many times beyond the specific number they should be able to (Hanahan and Weinberg 2000).

Vasculature is crucial for cell survival and function. Most cells are required to reside within approximately 100µm of a capillary blood vessel (Hanahan and Weinberg 2000). However, because of the increase in tumour mass, space becomes limited and cells are overcrowded leading to a lack of nutrients and oxygen levels supplied by the vascular system. During transformation, the malignant cells develop specific growth advantages, allowing them to survive better in hypoxic conditions. Cancer cells are able to promote angiogenesis and form new capillaries around the tumour mass providing the malignant cells with a fresh supply of nutrients and oxygen. One of the key mediators in this process is vascular endothelial growth factor (VEGF). VEGF is able to bind to transmembrane tyrosine kinase receptors on endothelial cells causing the receptors to dimerise and become activated (Veikkola and Alitalo 1999). The importance of VEGF in cancer is increasing and more frequently a subject of research as it has been extensively shown that many tumours have increased levels of VEGF compared to their normal tissue counterparts (Rak, Filmus et al. 1995; Rak,

Mitsuhashi et al. 1995; Ding, Chen et al. 2006; Luo, Jiang et al. 2008; Ding, Feng et al. 2012).

The most fatal characteristic of cancer is the ability to invade surrounding tissues leading to metastasis of the primary tumour. This stage forms in almost all types of cancer and generally occurs after the tumour has outgrown the primary site, and colonise in new areas of the body where space and nutrients are not limited (Hanahan and Weinberg 2000). When cells metastasise they are required to overcome a number of physical barriers, including penetration of the basement membrane, chemical barriers, such as hypoxia and pH changes, and also biological barriers, such as evasion of the immune system and various cytokines. Following transformation of the cancer cell, and its initial growth within the breast, these cells continue to grow as hyperplasia becomes more atypical. Overtime, atypical hyperplasia often results in the formation of a carcinoma *in situ*. The subsequent continuation of growth may not be restricted to the breast as the cells develop the ability to penetrate basement epithelia (**figure 1.3 panel A**). Once the cells have breached the epithelial cells lining the ducts or lobules they frequently metastasise to organs which are essential to maintaining life, initially migrating to the lymph nodes where they can then access the blood stream and metastasise to the lungs, liver, bone marrow and brain (**figure 1.3 panel B**). The ability of cells to metastasise, and the choice of site is non-random. This process is highly organised as the ‘seed and soil’ hypothesis describes (Fidler 2001; Fidler 2003; Langley and Fidler 2011).

The breast itself is not an essential organ. On this basis, metastasis in breast cancer is thought to contribute to approximately 90% of mortality (Bendre, Gaddy et al. 2003). The ability of cells to proliferate, evade apoptosis, invade and migrate is predomaniately mediated by the upregulation of growth factor receptors, hormone receptors, and several other types of proteins including cell-cell adhesion molecules (CAMs), and integrins (Aplin, Howe et al. 1998). The organ-specific targeting of breast cancer is now thought to be regulated by *chemotactic cytokines* produced in the target organ region. The expression of these factors and their constitutive receptors expressed on the malignant cells are key factors in the site-specificity of metastasis (Muller, Homey et al. 2001). The role of chemokines and chemokine receptors in breast cancer metastasis is discussed in sections 1.5 and 1.6.

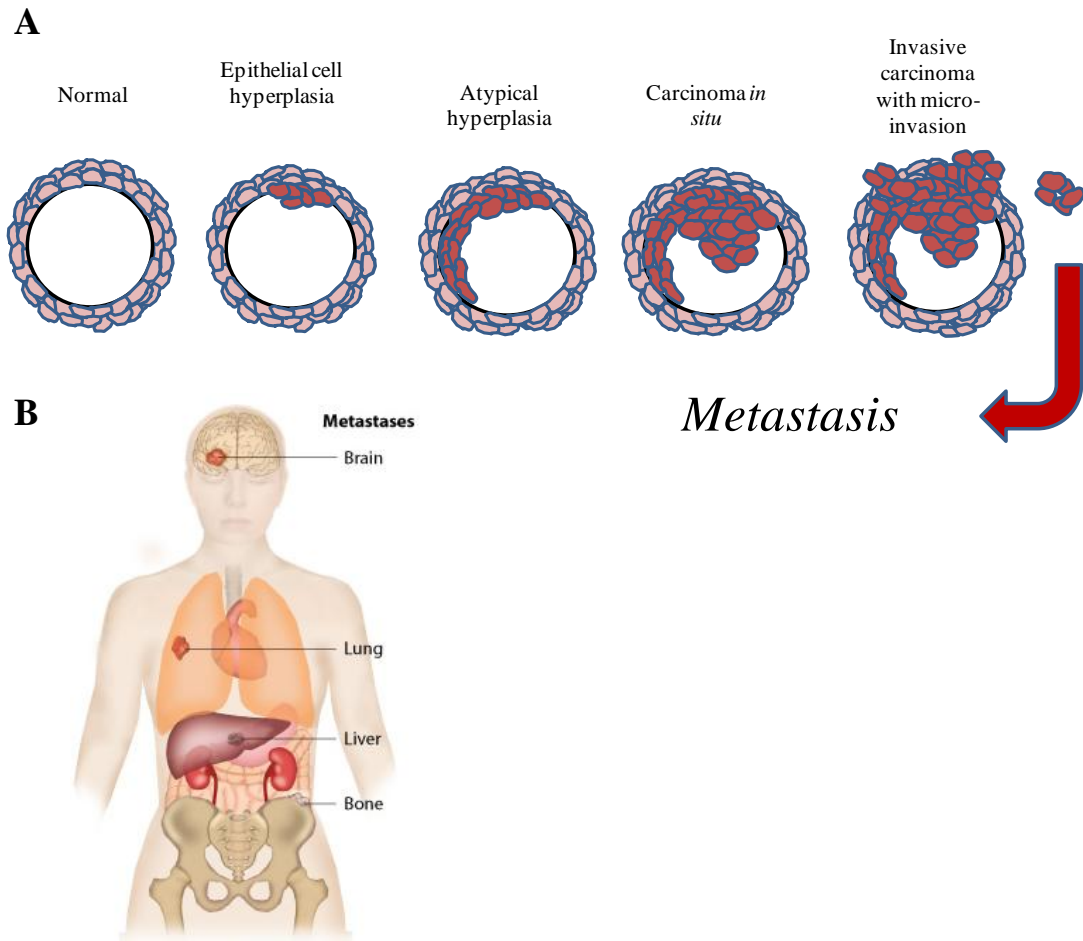


Figure 1-3 - Disease progression witnessed in breast cancer and metastasis

(A) Normal breast epithelia form a basement layer which surrounds the ducts and lobules of the breast. Mutations in genes which result in uncontrolled proliferation of cells may result in cellular hyperplasia, which may then lead onto more atypical hyperplasia. This can then form a carcinoma which may remain *in situ* or develop the ability to invade beyond the basement epithelia. (B) The cells often then metastasise to the lungs, liver, bone marrow and brain.

1.4.4 The influence of growth factors and hormone receptors

Malignant cells gain growth advantages over normal cells by upregulating hormone and growth factor receptors. There are three important receptors involved in breast cancer. Hormone receptors for oestrogen and progesterone and the growth factor receptor, HER2. The expression of these receptors is an important criterion when diagnosing breast cancer as they are considered as strong prognostic indicators.

1.4.4.1 Oestrogen and progesterone receptors

The importance of oestrogen receptors (ER) and progesterone receptors (PR) are two key prognostic markers used in breast cancer. It is estimated that approximately 80% of breast cancers have either individual or combined overexpression of ERs and PRs.

The main consequence of oestrogen and progesterone signalling is a rapid increase in the proliferation of cells. Oestrogen is a steroid hormone existing in three natural forms; estrone, estradiol and estriol. These hormones elicit their responses by diffusing across the cell membrane and binding to ERs located in the nucleus.

ERs were first identified by Elwood V. Jensen at the University of Chicago in 1958, for which Jensen was awarded the Lasker Award (Jensen and Jordan 2003). Two forms of ER exist: ER α and ER β . These receptors are often co-expressed, and when activated, form either homodimers ($\alpha\alpha$ or $\beta\beta$) or heterodimers ($\alpha\beta$) (Li, Huang et al. 2004). Reports demonstrate that as cancer progresses the levels of ER β decrease, whereas, ER α levels increase. For this reason most studies focus more specifically on the role of ER α (Bardin, Boulle et al. 2004). Tamoxifen and Raloxifene are two anti-oestrogen therapies which are successfully used to treat ER positive tumours (Platet, Cathiard et al. 2004).

ER signalling is thought to heavily impact a number of important processes involved with most stages involved in breast cancer progression. It has been reported that dysregulated ER-signalling can lead to aberrant expression of snail. This can lead to a loss of E-cadherin which is a key feature involved with epithelial-to-mesenchymal transition (EMT). ER-signalling has also been demonstrated to activate mitogen-activated protein kinase (MAPK), phosphoinositide 3-kinase (PI3K) and protein kinase C (PKC) signalling pathways (Chakravarty, Nair et al. 2010; Zheng, Huang et

al. 2011). ER α is able to promote invasiveness through increased expression of matrix metalloproteinase (MMP) 2 and MMP9 (Qin, Liao et al. 2008), and CXCR4 through control of HER2 (Li, Pan et al. 2004), therefore, increasing CXCL12-mediated migration. ER-signalling often cooperates through the interaction with several other factors. Many ER-coregulatory proteins are also differentially expressed in malignant breast tumours with their functions often altered as the tumour progresses (O'Malley 2006).

1.4.4.2 Human epidermal growth factor receptor 2

Human epidermal growth factor receptor 2 (HER2) also commonly known as Neu, CD340 or p185, is a member of the epidermal growth factor receptor family. These cell surface receptors are composed of four plasma membrane-bound tyrosine kinases which contain an extracellular ligand binding domain, a transmembrane domain and an intracellular domain which can interact with a number of signalling molecules (Roy and Perez 2009).

The HER2 protein is encoded by the gene *ErbB2* which is located on chromosome 17 (17q21-22). HER2 can activate many signal pathways involved in promoting the proliferation, survival, migration and invasion of cells often utilising MAPK, PI3K, PKC and signal transducer and activator of transcription (STAT) pathways (Roy and Perez 2009). Because these pathways are frequently activated and are responsible for a wide range of carcinogenic features in cells, the control of HER2 must be tightly regulated.

The overexpression of HER2 and the subsequent increase in HER2 signalling is very important in the pathogenesis of breast cancer which has led to its involvement being identified as an important biomarker. If left untreated, HER2 positive breast cancers generally have a worse prognosis than HER2 negative tumours as they not only proliferate more rapidly, but are also more resistant to hormone therapies and respond less to chemotherapies (Giai, Roagna et al. 1994; Stal, Sullivan et al. 1995; De Placido, Carlomagno et al. 1998). HER2 is overexpressed in approximately 30% of breast cancer cases (Slamon, Clark et al. 1987), however, it is also implicated in other aggressive malignancies including stomach (Jorgensen 2010; Jorgensen and

Hersom 2012), uterine (Santin, Bellone et al. 2008), and ovarian cancers (Slamon, Godolphin et al. 1989; Tuefferd, Couturier et al. 2007).

The main method of determining HER2 expression is by immunohistochemistry (IHC). The samples staining intensity is graded 0-3. Grade 0-1 is considered as HER2 negative, whereas grade 3 means the tumour is HER2 positive. If the tumour is graded 2 it means moderate levels are present and additional tests are carried out such as fluorescence *in situ* hybridisation (FISH) to detect over-amplification of the *ErbB2* oncogene.

Despite the aggressive nature of HER2 positive tumours, treatment with the monoclonal antibody Herceptin[®] is able to directly target HER2 and is very effective, thus, allowing HER2 positive tumours a better prognosis if they are diagnosed early and treated correctly. Use of Herceptin[®] was originally thought to have its most profound effects on the metastatic actions of breast cancer as it increased survival from 20.1 to 25.1 months (Hudis 2007). However, it has also been shown to be effective in early stages of disease as it can reduce the risk of relapse after surgery by an absolute risk of 9.5% and the risk of death by 3% (Moja, Tagliabue et al. 2012).

1.4.5 Oncogenes and tumour suppressor genes

Cancer is a complex group of diseases affecting a wide range of cells and tissues. Mutations that alter the expression of certain genes and their products are key features of all cancers. Research has demonstrated that a number of mutations in genes that disrupt steps in the cell cycle are prime candidates for studying carcinogenic transformation, and initial tumour growth and development. Generally speaking, the cell cycle is controlled by genes that function to suppress cell division, and genes which promote cell division. The first group of genes are termed as tumour suppressor genes (TSGs). These gene products prevent the passage through the cell cycle and, therefore, inhibit cell division. Only when these products are inactive will cell division occur. The second group of genes are termed oncogenes. These gene products function to promote cell division by the providing signals cells require to continue through the cell cycle. Therefore, the cell cycle is controlled through constant activation and inactivation of TSGs and oncogenes, therefore, these genes

must be very tightly regulated. Mutations which permanently inactivate TSGs or activate oncogenes will result in the control of the cell cycle being lost and the mutant cell begins to proliferate uncontrollably (Beckmann, Niederacher et al. 1997; Kenemans, Verstraeten et al. 2004).

Although cancer is a genetic disease, the majority of cancers are not classed as hereditary. Some cancers, such as retinoblastoma (Rb), carry a greater hereditary risk than other malignancies. However, breast cancer also carries a considerable inheritable factor.

A genetic link to cancer was first described by Theodor Boveri in 1902 (Ried 2009). Boveri stated that chromosomes with mutations could cause cells to divide more rapidly. More importantly, Boveri also stated that these chromosomal mutations could be inherited (Ried 2009). The risk of acquiring breast cancer significantly increases to almost double if a first degree relative has previously suffered breast cancer, which demonstrates that there is a clear inherited risk (Pharoah, Day et al. 1997). It is now estimated that environmental factors carry the greater risk as they contribute to over three quarters of breast cancer cases in the developed world (Key, Verkasalo et al. 2001). However, despite this increased risk, more than 85% of women with a close relative who has breast cancer do not develop the disease, whereas, more than 85% of women who do develop breast cancer have had no previous family history. Individuals who inherit a mutant TSG, such as *TP53*, *PTEN*, *STK11/LKB1*, *CDH1*, *CHEK2*, *ATM*, *MLH1*, and *MSH2* do carry a substantially increased risk of developing breast cancer (Walsh, Casadei et al. 2006; Campeau, Foulkes et al. 2008). This is a good illustration of how the development of breast cancer can be dictated on either genetic or environmental factors.

1.4.5.1 BRCA1/2

The majority of cases of familial breast cancers are accounted for by two autosomal dominant genes, breast cancer susceptibility gene 1 and 2 (*BRCA1* and *BRCA2*) (Lynch, Silva et al. 2008). The main functions of *BRCA* genes are to encode proteins which are key in repairing damaged DNA, or if damage is excessive, initiating apoptotic cascades resulting in cell death (Friedenson 2007).

It is estimated that 0.1% of the female population contain *BRCA* mutations. Moreover, inherited mutated forms of either *BRCA1* or *BRCA2* accounts for 5-10% of female breast cancers and 10-15% of ovarian cancers in the USA (Campeau, Foulkes et al. 2008). Mutations in either *BRCA1* or *BRCA2* are considered as high-penetrance as individuals who inherit a mutated *BRCA* gene have an estimated 30-70% risk of developing cancer (Aydin, Akagun et al. 2011) and a 45-60% risk of breast cancer by the age of 70 (Chen and Parmigiani 2007).

1.4.5.2 p53

TP53 is arguably, the most well known TSG. *TP53* is located on the short arm of chromosome 17 and encodes the protein p53. p53 is a transcription factor which has strong anti-cancer functions and is implicated in genome stability as approximately 50% of all human tumours have mutated p53 (Hollstein, Rice et al. 1994; Levine 1997).

p53 is able to perform cell cycle arrest, induce senescence and initiate apoptosis. For these reasons, p53 is often described as “*the guardian of the genome*”. p53 is one of the most studied proteins in research, however, because it is at the centre of an intricate protein network which determines a multitude of cellular responses, mapping the precise signalling pathways p53 is involved in is overwhelmingly complex.

p53 is tightly regulated and becomes activated in response to various DNA damaging agents, including ultraviolet (UV) radiation and oxidative stress (Han, Muller et al. 2008). The activation of p53 is thought to be triggered via MAPK family of proteins by phosphorylating the N-terminal transcriptional activation domain. When p53 is activated it accumulates in cells as the half-life drastically increases when DNA damage occurs (Maltzman and Czyzyk 1984; Price and Calderwood 1993; Maki and Howley 1997). The effects of p53 on cell cycle arrest is mediated primarily through p21 which is a molecule able to induce cell cycle arrest at the G1 phase (Elbendary, Cirisano et al. 1996). It has been reviewed that p53 contributes to inducing apoptosis through a number of mechanisms but the most common includes the activation of

pro-apoptotic genes such as members of the Bcl-2 family (Brouet, Rabian et al. 1984).

Because of the strong anti-cancer functions of p53, the prospect of restoring endogenous p53 to tumour cells has shown considerable promise as this caused regression of tumours *in vivo* (Ventura, Kirsch et al. 2007). However, subsequent studies have demonstrated that increasing p53 levels can cause premature aging (Tyner, Venkatachalam et al. 2002; Dumble, Gatz et al. 2004).

1.4.5.3 PI3K and PTEN

PI3KCA is an oncogene that encodes the catalytic subunit of PI3K which is a transducer of growth factor signalling. Constant activation of *PI3KCA* allows for constant signalling of PI3K which allows cancer cells to grow independently of external stimuli (Dillon, White et al. 2007).

Mutations causing somatic activation of *PI3KCA* are witnessed in approximately 25% of breast tumours (Bachman, Argani et al. 2004; Lai, Mau et al. 2008). The majority of signalling through PI3K is thought to act through Akt kinases which allow the cells to stimulate angiogenesis (Jiang and Liu 2009; Karar and Maity 2011), avoid apoptosis (Franke, Hornik et al. 2003) and increase the invasive and migratory potential of cancer cells (Du, Sun et al. 2010; Wander, Zhao et al. 2013).

An antagonist of PI3K signalling is a tumour suppressor called phosphatase and tensin homologue (PTEN). PTEN is able to repress growth factor induced cell division, apoptosis induction, and repression of invasion and angiogenesis (Dillon, White et al. 2007). The normal functioning of both PI3K and PTEN is essential in normal cell homeostasis and a loss of function in either genes results in high risk of breast cancer development (Dillon, White et al. 2007).

1.5 Chemokine-driven cancer progression

As described, metastasis remains the overwhelming cause of mortality in breast cancer. The process of metastasis is known to be the result from a number of

organised sequential steps. However, despite the clear importance of this process, the precise mechanism leading to metastasis remains one of the most poorly understood components of breast cancer pathogenesis.

Leukocyte biology has taught us that a specific set of small (8-10kDa) molecules called chemokines have the ability to regulate cell trafficking (Taichman, Cooper et al. 2002). It was hypothesised that tumour cells may also utilise the capabilities of chemokines and their constitutive chemokine receptors to govern the site-specific metastasis witnessed in breast cancer (Muller, Homey et al. 2001; Ali and Lazennec 2007).

As chemokines have roles in normal homeostasis, low levels of chemokines are present within normal tissues. For example, normal breast milk is known to contain CXCL1, 2, 3, 5, 6, 7 and 8 (Maheshwari, Christensen et al. 2003). Certain chemokines are also located within the normal breast but lost in carcinogenic tissues. These chemokines include CXCL1, 2, 5, 6, 8, 20, and also CCL2 and CCL7 (Porter, Krop et al. 2001).

Strong evidence, from a large degree of literature, has demonstrated that chemokines and chemokine receptors play a pivotal role in driving tumour progression by directing cell migration. Chemokine-chemokine receptor interactions are involved in many steps of tumour development including cell transformation, survival, growth and angiogenesis (Tanaka 2002; Luker and Luker 2006). For instance, CXCL8 has been frequently found overexpressed at transcript and protein levels within a number of malignancies including breast cancer (Chavey, Bibeau et al. 2007). CXCL8 is able to bind not only to its natural chemokine receptor CXCR2, but also a G-protein coupled receptor (GPCR) encoded by tumourigenic virus', such as Human Herpes virus 8 (HHV-8), which develop lesions similar to Kaposi's sarcoma in mice (Yang, Chen et al. 2000). Reports have demonstrated that several melanoma cell lines express CXCR2 (Varney, Li et al. 2003), and also produce CXCL1 (Payne and Cornelius 2002) and CXCL8 (Singh, Gutman et al. 1994). However, blocking either the ligands or the receptors inhibits the growth of these cells (Singh, Gutman et al. 1994; Norgauer, Metzner et al. 1996). This demonstrates that the CXCR2-CXCL1/CXCL8 axis acts in an autocrine/paracrine manner.

Tumours are not simply a solid mass of cancer cells. Tumours are made up of a number of non-malignant cells, with the non-malignant cells often outnumbering the malignant cells (Balkwill and Mantovani 2001). Chemokines are able to recruit various leukocytes into the tumour environment. The recruitment of these inflammatory cells is able to drive cancer progression by releasing various cytokines, proteases or release more chemokines. The infiltration of tumour associated macrophages (TAMs) is well documented in cancer and is discussed further in section 5.1.1 (Leek and Harris 2002; Laoui, Movahedi et al. 2011; Mukhtar, Nseyo et al. 2011). Other reports now indicate that CCL5 is abundant in the tumour environment of breast cancer which attracts macrophage infiltration (Luboshits, Shina et al. 1999), whereas, CCL2 is responsible for macrophage infiltration in oesophageal cancers (Ohta, Kitadai et al. 2002).

Sarcomas, gliomas and a number of malignancies of the breast, pancreas and ovaries have high levels of CC chemokines which are produced by both the malignant cells and the stromal cells. These chemokines are reported to be important for homing of macrophages and lymphocytes to the tumour mass (Bottazzi, Polentarutti et al. 1983; Balkwill and Mantovani 2001).

1.5.1 Chemokines

Chemokines are a family of small *chemotactic cytokines* which are secreted by cells. These small proteins are present in all vertebrates as well some viruses and bacteria, however, they have not been reported in invertebrates (DeVries, Kelvin et al. 2006). They induce their actions by binding to their constitutive chemokine receptors located on cell surfaces. The main function of chemokines is to direct the migration of target cells (Tarrant and Patel 2006). Cells are attracted to chemokines which follow a signal of increasing chemokine concentration towards the source of the chemokine.

Chemokines which direct cell migration during normal processes, such as lymphocyte homing to the lymph nodes to screen for pathogens, are classed as homeostatic chemokines (Zlotnik, Burkhardt et al. 2011). These chemokines are constitutively expressed within specific tissues. Other chemokines which are

involved in processes such as inflammation are referred to as inflammatory chemokines. The expression of inflammatory chemokines must be tightly regulated as they are only induced at the onset of specific inflammatory stimuli (Zlotnik and Yoshie 2000). These chemokines are key in aspects such as in infections, immune disorders and diseases associated with acute and chronic inflammation such as cancer (Zlotnik and Yoshie 2000).

1.5.1.1 Structure and classification

Chemokines consist of between 92-130 amino acids and are organised by their structural characteristics and not just their ability to attract cells (Garton, Gough et al. 2001). When chemokines are synthesised they are created as pro-peptides that contain a signal peptide of approximately 20 amino acids which is cleaved from the active (or mature) region when they are secreted by the cells (Baggiolini 2001).

Most chemokines contain four conserved cysteine residues which interact with each other in pairs via intracellular disulphide bonds. The organisation of these residues dictates the 3-dimensional shape of the chemokine. Typically, the first and third cysteines (as they appear in the protein sequence) interact, as do the second and fourth residues. The first two cysteines are located near the N-terminal of the active protein, whereas, the third cysteine is located near the centre of the protein, and the fourth cysteine is towards the C-terminal (**figure 1.4**).

Chemokines are predominantly made up of loops, and strands (Fernandez and Lolis 2002). After the first two residues, approximately 10 amino acids form a loop referred to as the N-loop. After the N-loop, there is a single turn helix (referred to as the 3_{10} -helix), followed by three β stands and finally a C-terminal α helix. These helices and strands are connected by turns referred to as 30s loops, 40s loops and 50s loops. The third cysteine is located within the 30s loop, and the fourth cysteine is located in the 50s loop (Fernandez and Lolis 2002).

Chemokines are categorised into four groups based on their spacing of the first two cysteine residues (**figure 1.4**). Most chemokines fall into the CC or CXC subfamilies. CC chemokines have two adjacent cysteines near their amino terminus. Most members of this subgroup contain four cysteine residues, however, CCL1,

CCL15, CCL21, CCL23 and CCL28 contain six cysteine residues. In CXC chemokines, the two N-terminal cysteines are separated by a single amino acid (denoted as X in the CXC term). C chemokines are unique as, they only contain two cysteine residues; one located at the N-terminal and one downstream. Finally, the CX₃C chemokines only contains one member and is defined by three amino acids separating the first two cysteine residues. Interestingly, because of its cell surface location, it is thought that this chemokine acts as both a chemoattractant and an adhesion molecule (Fernandez and Lolis 2002).

Within mammals 17 CXC chemokines have been identified. These chemokines are subcategorised as either glutamic acid-leucine-arginine (ELR) positive or negative (Strieter, Polverini et al. 1995; Ali and Lazenec 2007). The ELR positive chemokines are CXCL1, CXCL2, CXCL3, CXCL5, CXCL6, CXCL7 and CXCL8 (Moser and Willmann 2004). Based on the NH₂-terminal motif being demonstrated in angiogenesis, ELR negative chemokines are known to be angiostatic, whereas, ELR positive chemokines are angiogenic (Strieter, Polverini et al. 1995).

1.5.2 Chemokine receptors

Chemokine receptors are GPCRs. There are approximately 19 chemokine receptors which are subdivided into four categories depending on the chemokine they can bind (**figure 1.5**).

These receptors share many structural features. They all contain seven transmembrane domains made up from a single polypeptide chain of approximately 350 amino acids. Each receptor has three extracellular loops and three intracellular loops. The C-terminal end of the receptor is coupled with G-proteins which allows the initiation of intracellular signalling after the specific chemokine has bound and activated the receptor (Murdoch and Finn 2000).

Each chemokine receptor is highly specific for certain chemokines and can only bind and become activated from chemokines with the conserved cysteine residue in the correct location. Hence, only CXC chemokines bind CXC receptors (CXCR), CC chemokines bind CC receptors (CCR), the two XC chemokines bind to the XC

receptor (XCR1) and the sole CX₃C chemokine binds to CX₃C receptors. The majority of chemokines are able to bind to more than one receptor.

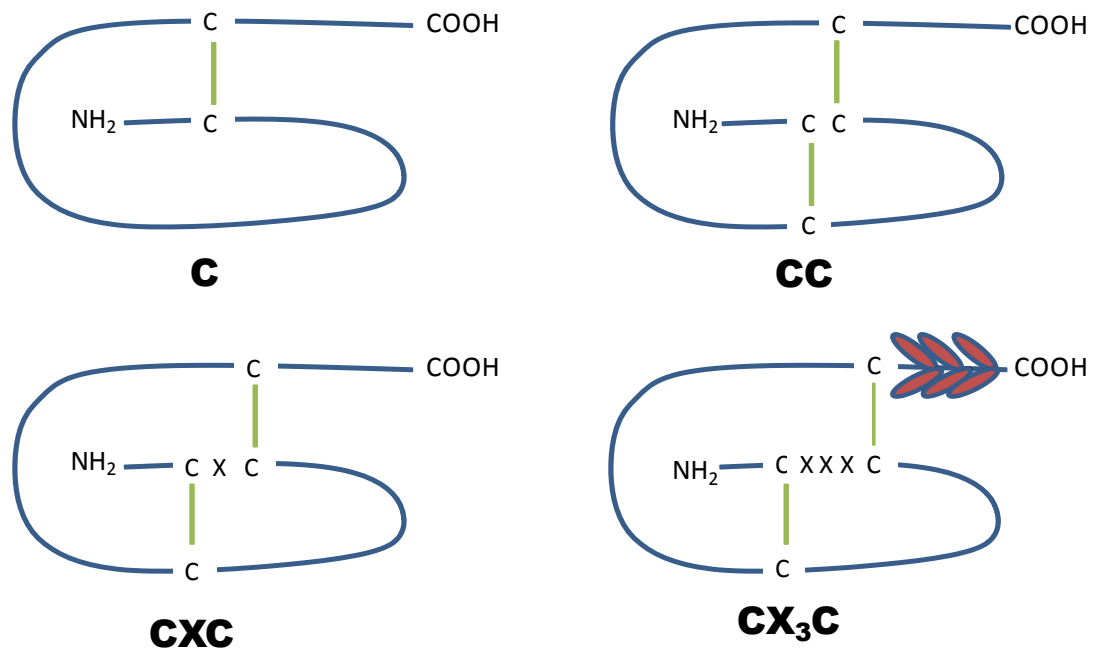


Figure 1-4 - Classification of chemokines and the location of cysteine residues

Chemokines are subclassed into four individual categories depending on the location of the cysteine residues present. Blue lines represent the peptide chain, whereas, the green lines represent disulphide bonds connecting the cysteine residues. CX₃C chemokines also have a mucine-like domain illustrated in red.

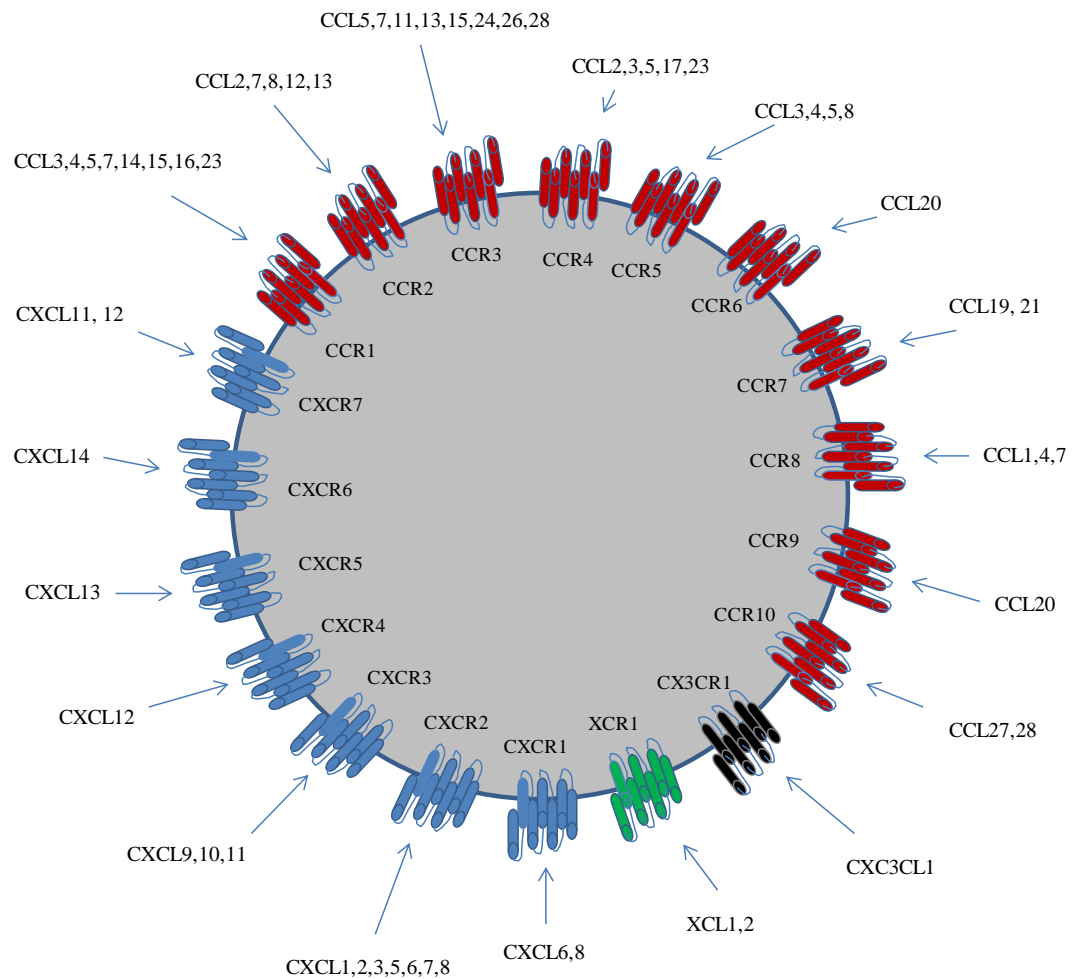


Figure 1-5 - Chemokines and their constitutive receptors

Chemokine receptors are categorised into four families which are defined by the type of chemokine they can bind. The location and number of the highly conserved cysteine residue in the chemokine defines the receptor it can interact with. Some chemokines can bind several receptors. Image adapted from (Balkwill 2004).

1.5.3 Signal transduction

Chemokine-chemokine receptor interactions are dependent on intracellular heterotrimeric G-proteins. These G-proteins consist of $G\alpha$, $G\beta$ and $G\gamma$ subunits which remain associated to guanosine diphosphate (GDP) at the basal state (Mukherjee and Zhao 2013).

When the appropriate chemokine binds to its constitutive receptor, the receptors undergo homo- hetero- dimerisation. GDP is released and replaced with guanosine triphosphate (GTP) which leads to the receptor undergoing a change in its tertiary structure via the separation of the G-protein subunits into a $G\alpha$ monomer and two $G\beta\gamma$ dimers. $G\alpha$ can exist in four different forms; $G\alpha_s$, $G\alpha_i$, $G\alpha_q$ or $G\alpha_{12}$ (Mukherjee and Zhao 2013). Originally it was thought that CXCR4 was primarily a $G\alpha_i$ -associated G-protein coupled receptor, however, recently it has been demonstrated that CXCR4 can associate with any of the $G\alpha$ subunits (Rubin 2009).

The chemokine receptor associating with the G-protein then initiates a number of downstream signalling cascades such as PI3K, MAPK, phospholipase- $C\beta$, p21-activated kinase, NF- κ B, calcium mobilisation and the activation of extracellular signal regulated kinases 1 and 2 (Rossi and Zlotnik 2000).

When a biological response such as inflammation is over, it is important to cease the reaction and restore normal homeostasis. Chemokine receptors have the ability to mediate this. Upon ligand binding, the $G\alpha$ subunit of the receptor protein tyrosine kinase (PTK) becomes activated causing phosphorylation of serine and threonine residues at the tail of the chemokine receptor where it becomes inactivated. Alternatively, it can enter the lysosomal compartment to be degraded, or become rapidly internalised and recycled in the perinuclear region of the cell where it can be trafficked into the plasma membrane and stored (Neel, Schutyser et al. 2005).

1.6 Chemokine receptors and breast cancer metastasis

The importance of chemokines and their receptors at various stages of tumour progression is well documented (Muller, Homey et al. 2001; Ali and Lazennec 2007). A comprehensive report by Muller et al (Muller, Homey et al. 2001)

quantitatively analysed the mRNA expression of all known chemokine receptors in seven breast cancer cell lines. They reported three separate patterns of expression. Firstly, CXCR2 was expressed on the normal mammary cells but expressed at much lower levels on their malignant counterparts. Secondly, CCR7 was expressed on both malignant and normal mammary cells, whereas, the final scenario demonstrated that CXCR4 was absent on normal mammary cells, but was markedly upregulated amongst malignant cell lines.

Despite being present on normal breast cells, CCR7 is still frequently increased on breast carcinomas. CCR7 has two major ligands, CCL19 and CCL21. These chemokines are expressed at high levels within the lymph nodes and is therefore thought to act primarily as a lymph node homing chemokine receptor in breast cancer metastasis (**figure 1.6 panel A**) (Cunningham, Shannon et al. 2010). Wiley et al (Wiley, Gonzalez et al. 2001) used murine studies to demonstrate that treatment using neutralising anti-CCL21 antibodies was able to reduce the metastasis of B16 melanoma cells to the regional lymph nodes in comparison to control IgG antibodies. This demonstrates that CCR7 was functionally active.

CXCR4 is the chemokine receptor which is most frequently upregulated in both human and murine cancers (Balkwill 2004; Balkwill 2004). In fact, it has now been reported that over 23 human malignancies frequently overexpress CXCR4 (Balkwill 2004) including; acute myeloid leukaemia (AML) (Mohle, Schittenhelm et al. 2000), Non-Hodgkin Lymphoma (Weng, Shahsafari et al. 2003), chronic myeloid leukaemia (CML), (Peled, Hardan et al. 2002), multiple myeloma (Moller, Stromberg et al. 2003), pancreatic cancer (Koshiba, Hosotani et al. 2000), prostate cancer (Taichman, Cooper et al. 2002), breast cancer (Muller, Homey et al. 2001), ovarian cancer (Scotton, Wilson et al. 2001; Scotton, Wilson et al. 2002), thyroid cancer (Hwang, Chung et al. 2003), colorectal cancer (Zeelenberg, Ruuls-Van Stalle et al. 2003), kidney cancer (Schrader, Lechner et al. 2002), glioma (Rempel, Dudas et al. 2000), small cell lung cancer (Kijima, Maulik et al. 2002), and melanoma (Robledo, Bartolome et al. 2001; Murakami, Maki et al. 2002; Payne and Cornelius 2002; O'Boyle, Swidenbank et al. 2013).

Further emphasis on the importance of CXCR4 in breast cancer can be drawn on the basis that despite the sole CXCR4 ligand, CXCL12, being expressed relatively

constitutively in the body, its highest concentrations are found within the primary sites of breast cancer metastasis (**figure 1.6 Panel B**) (Muller, Homey et al. 2001). Intriguingly, it has been reported that stromal cells such as myofibroblasts within tumours are able to produce increased levels of CXCL12 in these regions (Allinen, Beroukhi et al. 2004). The upregulation of CXCR4 has been reported to occur as early as ADH and increases as cancers progress from this stage to invasive cancer. This suggests CXCR4 upregulation occurs early in carcinogenesis and could contribute to the early stages of tumour progression, and more than just cell migration (Schmid, Rudas et al. 2004; Luker and Luker 2006).

As well as *in vitro*, *in vivo* studies have highlighted that the expression of CXCR4 in breast cancer patients, and other malignancies including melanoma patients, correlated with an increased risk of metastasis and a poorer prognosis (Muller, Homey et al. 2001; Altundag, Morandi et al. 2005; Xu, Shen et al. 2013). Treatment with the CXCR4 inhibitor, AMD3100, decreases the invasiveness of colorectal (Li, Yu et al. 2008) and ovarian cancer cells via the downregulation of MMP9 and VEGF (Righi, Kashiwagi et al. 2011). The importance of CXCR4 in breast cancer has also been demonstrated using *in vivo* murine models (Muller, Homey et al. 2001; Kang, Mansel et al. 2005). Severe combined immunodeficiency (SCID) mice intravenously injected with MDA-MD-231 cells developed spontaneous tumours. CXCR4 was detected at mRNA and protein levels within the primary tumours and also lung metastases' (Muller, Homey et al. 2001). However, if SCID mice were injected with MDA-MB-231 cells and administered anti-human CXCR4 monoclonal antibodies, after 28 days, metastasis to the lung was significantly reduced in comparison to mice which were treated with an isotype control antibody (Muller, Homey et al. 2001). *In vitro* experiments have also demonstrated that CXCR4 expressing breast cancer cells grow significantly faster than CXCR4 negative cells (Lapteva, Yang et al. 2005). Kang et al (Kang, Mansel et al. 2005) validated these findings further by injecting MDA-MB-231 into mice to produce metastases to the bone. When the metastatic cells were recovered microarray identified *CXCR4* as one of few genes that was enriched in the population.

As mentioned, the sole ligand for CXCR4 is CXCL12. However, CXCL12 is not a ligand specific for just CXCR4. CXCL12 can also able to bind to CXCR7.

CXCR7 is considered by many to be an atypical chemokine receptor as it is reported to lack many functions commonly associated with other chemokine receptors. Upon binding of CXCL12, CXCR7 does not release intracellular calcium stores (Burns, Summers et al. 2006; Odemis, Boosmann et al. 2010), and there are conflicting reports on its ability to activate PI3K and MAPK pathways, and direct cell migration (Balabanian, Lagane et al. 2005; Hartmann, Grabovsky et al. 2008; Zabel, Wang et al. 2009; Zheng, Li et al. 2010).

However, similar to CXCR4, CXCR7 has also been implicated in promoting the growth of a number of malignancies including breast, lung, prostate and liver cancers (Zheng, Li et al. 2010) (Burns, Summers et al. 2006; Miao, Luker et al. 2007; Wang, Shiozawa et al. 2008). Within these malignancies, CXCR7 has been reported to enhance the adhesion of cancer cells to fibronectin and endothelial cells (Burns, Summers et al. 2006; Wang, Shiozawa et al. 2008; Zheng, Li et al. 2010), and increase cell survival by evading apoptosis (Burns, Summers et al. 2006; Wang, Shiozawa et al. 2008). One factor CXCR7 has been shown to influence is the release of various angiogenic factors such as VEGF (Wang, Shiozawa et al. 2008; Zheng, Li et al. 2010).

Interestingly, despite both receptors being targeted by CXCL12, and both receptors being reported in breast cancer, the roles they are reported to influence in breast cancer appear to oppose one another. A comprehensive report by Hernandez et al (Hernandez, Magalhaes et al. 2011) demonstrated these opposing roles by overexpressing either CXCR4 or CXCR7 into the rat adenocarcinoma cell line, MTLn3, and investigating the changes in primary tumour growth and also the metastatic changes. They suggested that the overexpression of CXCR4 resulted in increased chemotaxis towards CXCL12 *in vivo* and *in vitro*. CXCR4 overexpression also increased extravasation and motility of cancer cells within the primary tumour *in vivo*. However, CXCR4 overexpression appeared to have little impact on the growth of the primary tumour, therefore implying CXCR4 plays the most profound effects on the metastatic aspects of breast cancer.

On the other hand, CXCR7 overexpression did increase the primary tumour growth and angiogenesis through upregulation of VEGF-A. However, when CXCR7 was overexpressed alone, it had little effect on cancer cells chemotaxis or invasion

towards CXCL12 *in vitro*, whereas *in vivo*, invasion, intravasation and the formation of metastases seemed to decrease. This would suggest that CXCL12 is a key mediator in breast cancer progression through selective activation of CXCR7 in early stages of tumour development, and CXCR4 in latter stages and metastatic formation.

Interestingly, the same report by Hernandez et al (Hernandez, Magalhaes et al. 2011) demonstrated that when CXCR7 was overexpressed into cells with high level CXCR4 expression, it resulted in an increase in chemotaxis *in vitro*. This suggests CXCR7 may increase migration by working cooperatively alongside CXCR4.

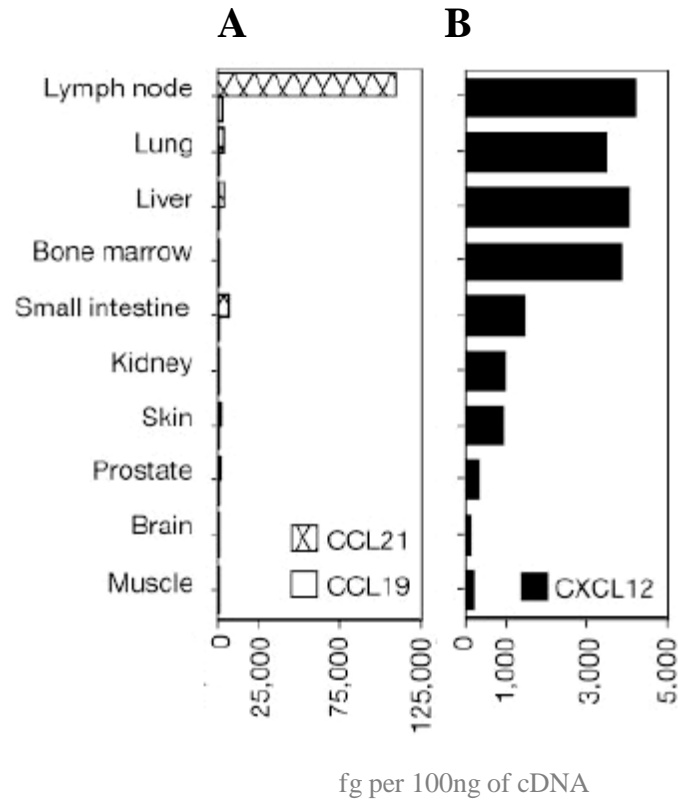


Figure 1-6 - Distribution of CXCL12 and CCL21 in humans

The CXCR4 ligand CXCL12 is found within the highest quantities in regions most common to breast cancer metastasis including the lymph nodes, lungs, liver and bone marrow (**A**) whereas the CCR7 ligand, CCL21, is found within extremely high quantities within the lymph nodes (**B**). Taken from (Muller, Homey et al. 2001).

1.6.1 CXCR4 crystal structure

As mentioned in section 1.5.2, most chemokine receptors share many structure characteristics. The CXCR4 crystal structure was comprehensively described by Wu et al (Wu, Chien et al. 2010). This made CXCR4 the first chemokine receptor to be crystallised.

Firstly, similar to other chemokine receptors, the main fold of CXCR4 consists of 7 transmembrane α -helices. These are similar to other 7 transmembrane α -helical GPCR which have been crystallised; however, Wu et al (Wu, Chien et al. 2010) described 6 main differences in the CXCR4 structure:

- 1) The extracellular end of helix I is shifted slightly towards the central axis of the receptor.
- 2) Helix II makes a tighter helical turn at Pro92 which causes a 120° rotation of its extracellular end.
- 3) Both the intracellular and extracellular tips of helix IV substantially deviate from their consensus positions in other GPCR.
- 4) The extracellular end of helix V is about 1 turn longer.
- 5) The extracellular end of helix VI is relatively similar shape in all structures as it is characterised by a sharp kink at Pro254, however, its extracellular end is shifted by approximately 3 Å in CXCR4.
- 6) The extracellular end of helix VII is 2 helical turns longer than other GPCRs.

The extracellular region of CXCR4 consists of 34 N-terminal residues, extracellular loop 1 (consists of residues 100-104) which links helices II and III, extracellular loop 2 (residues 174-192) which links helices IV and V and extracellular loop 3 (residues 267-273) which links helices VI and VII (Wu, Chien et al. 2010).

Clear density is apparent from Pro27 (which is adjacent to Cys28). This residue pins the base of the N-terminal of Cys274 at the tip of helix VII via a disulphide bond. Extracellular loop 2 is the largest loop in CXCR4. This is formed by a second disulphide bond between Cys109 and Cys186. Interestingly, the length, sequence and secondary structure of extracellular loop 2 is considerably different amongst most GPCRs. However, the disulphide bond connecting extracellular loop 2 with the extracellular end of helix III is highly conserved in chemokine receptors. These two

disulphide bonds are functionally very important in CXCR4 as they form an entrance to the ligand binding pocket (Zhou and Tai 2000).

The intracellular region of CXCR4 contains intracellular loop 1 (residues 65-71) which links helices I and II, intracellular loop 2 (residues 140-149) which links helices III and IV, and intracellular loop 3 (residues 225-230) which links helices V and VI. The intracellular structure of CXCR4 is reported to be more structurally conserved with other GPCRs than the extracellular region (Wu, Chien et al. 2010).

1.6.2 CXCR4-CXCL12 signalling

Unlike most chemokine receptors which are able to bind several ligands, CXCL12 is the sole ligand specific for CXCR4 (Ma, Jones et al. 1998). Two different isoforms of CXCL12 have been identified in humans (α and β) (Luker and Luker 2006). Splice variant isoforms of this chemokine are not widely reported as they are almost identical in structure, differing only by the addition of four amino acids on the carboxyl terminus of CXCL12- β (Kryczek, Wei et al. 2007).

Also, structure-function studies have demonstrated that the binding of CXCL12 to CXCR4 is dependent on the amino terminal, and both isoforms bind to CXCR4 and do not differ in their functions as ligands for the receptor (Crump, Gong et al. 1997). It is thought that the interaction between CXCL12 and CXCR4 occurs between residues 12-17 of CXCL12 and 2-26 of CXCR4 (Huang, Shen et al. 2003). Many of these signals promote proliferation (Murakami, Maki et al. 2002; Orimo, Gupta et al. 2005), migration and invasion of cancer cells (Allinen, Beroukhi et al. 2004), as well as the ability to evade apoptosis (Broxmeyer, Kohli et al. 2003) and survive, thus demonstrating their importance in cancer.

To cease the actions of CXCL12, it has been demonstrated that both isoforms are cleaved by a number of enzymes including dipeptidyl peptidase/CD26 (Lambeir, Proost et al. 2001), MMPs (McQuibban, Butler et al. 2001) and cathepsin G (Delgado, Clark-Lewis et al. 2001). These remove 2-5 amino acids from the amino terminus of CXCL12 which inactivates the ability of CXCL12 to interact with CXCR4. Following CXCL12 binding, and the subsequent release from CXCR4, the

receptor is often internalised and sorted into the lysosome for degradation. However, some GPCRs can be also be recycled back to the surface of the membrane (Marchese, Chen et al. 2003). CXCR4 can be either recycled or degraded. However, the extent of receptor recycling to the surface is poor following CXCL12 stimulation (Signoret, Oldridge et al. 1997; Tarasova, Stauber et al. 1998). An alternative paper has demonstrated that CXCR4 is ubiquitinated, sorted to the lysosome and degraded (Marchese and Benovic 2001). The E3 ubiquitin ligase AIP4 is thought to mediate this degradation (Marchese and Benovic 2001).

Specific interaction between CXCL12 and CXCR4 has been demonstrated as CXCR4 expressing MDA-MB-231 potently migrated and invaded through matrigel coated membranes in a CXCL12 dose-dependent manner (Muller, Homey et al. 2001). Consistent with the actions of MDA-MB-231, primary tumour cells, isolated from patients via pleural effusion, also exhibited a strong chemotactic response to CXCL12 (Muller, Homey et al. 2001). Further emphasising the importance of this interaction, treatment with anti-CXCR4 antibodies is able to neutralise the response (Muller, Homey et al. 2001). This demonstrates that directional migration and invasion of breast cancer cells is CXCL12-mediated.

One of the prerequisites for cell motility and migration is actin polymerisation which initiates the formation of pseudopodia and directional migration as well as invasion through a reconstituted membrane (Burger, Burger et al. 1999). Human breast cancer cells exhibited a transient 2.2-fold increase in filamentous actin within 20 seconds after being stimulated with 100nM of CXCL12 (Muller, Homey et al. 2001).

CXCR4 signalling also drives the adhesive capacity of cells by upregulating various components of extracellular matrix involved in cellular adhesion including collagen, fibronectin and integrins $\alpha 2$, $\alpha 4$, $\alpha 5$ and $\beta 1$ (Cardones, Murakami et al. 2003; Hartmann, Burger et al. 2005). Cardones et al (Cardones, Murakami et al. 2003) demonstrated that when B16 cells were exposed to shear stress conditions, the overexpression of CXCR4 caused more than a 10-fold increase in adhesion to VCAM1-expressing lung endothelial cells which were stimulated with TNF- α . CXCR4 also activates members of src family of protein tyrosine kinases. These family members activate components of focal adhesion complexes like RAFTK/Pyk2 Crk and paxillin (Fernandis, Prasad et al. 2004).

MMPs are heavily involved in degradation of extracellular matrix, thereby providing a mechanism for cancer cells to penetrate basement membranes aiding invasion. It has been demonstrated that CXCL12-dependant activation of CXCR4 is able to increase the secretion of MMP2 and MMP9 in MDA-MB-231, and increases their capacity to invade (Kang, Mansel et al. 2005).

The ability of cells to survive in suboptimal conditions is also increased following CXCL12-CXCR4 interactions. When cells of several cancer types, including ovarian (Scotton, Wilson et al. 2002) and basal cell carcinoma, (Chen, Yu et al. 2006) were cultured in suboptimal conditions (such as low serum), the cancer cells which had been stimulated with CXCL12 survived and proliferated to a greater extent than those which weren't stimulated.

Signalling through CXCR4 has been reported to activate a number of downstream pathways, many of which are thought to be responsible for these processes. A number of these pathways are discussed;

1.6.2.1 PI3K/Akt pathway

PI3K is an important pathway which regulates a multitude of biological processes including apoptosis, metabolism, cell proliferation and cell growth (Carnero, Blanco-Aparicio et al. 2008). The constant activation and signalling of the PI3K is a key trait in many primary and metastatic cancers which has made it an important target for drug design (Carnero, Blanco-Aparicio et al. 2008).

Binding of CXCL12 to CXCR4 is able to stimulate PI3K which subsequently activates its major downstream effector Akt. Based on the wide range of diverse functions Akt is involved in, it is thought that many of the responses involved in CXCR4 signalling in breast cancer are governed by the activation of PI3K and Akt (Murakami, Maki et al. 2002). Breast cancer cells treated with CXCL12 *in vitro* caused activation of Akt kinase within 15 minutes and this activation was sustained for at least 4 hours (Prasad, Fernandis et al. 2004).

As demonstrated in several cancer cell lines, once Akt is activated it is able to phosphorylate a number genes involved in inhibiting apoptosis and prolonging cell

survival (Luo, Manning et al. 2003). One gene controlled by Akt is NF- κ B (Sovak, Bellas et al. 1997). NF- κ B is often activated in a range of malignancies and is discussed further in section 1.6.3.3.

Another report has demonstrated that CXCR4 activation is able to promote the expression of VEGF through activation of the Akt pathway (Liang, Brooks et al. 2007). Western blot analysis demonstrated that following incubation with CXCL12, MDA-MB-231 had a time-dependant increase in phosphorylated Akt with a maximum phosphorylation witnessed after 30 minutes incubation (Liang, Brooks et al. 2007). The presence of CXCL12 also demonstrated an increase in VEGF expression. When MDA-MB-231 were incubated with the CXCR4 antagonist, TN14003, the CXCL12-induced Akt phosphorylation was reduced. This blocking of CXCR4 also resulted in a decreased expression of VEGF. To demonstrate that the control of VEGF by CXCR4 was Akt dependant, MDA-MB-231 treated with the Akt inhibitor, LY294002 decreased the VEGF secretion (Liang, Brooks et al. 2007).

1.6.2.2 MAPK/Erk pathway

Following the binding of a mitogen to cell surface receptors, this causes the activation of Ras by phosphorylating GDP to GTP. Ras can then activate Raf which in turn phosphorylates MAPKK (also known as MEK). Finally, phosphorylated MEK activates MAPK leading to the activation of transcription factors such as c-Myc, which can influence the expression of specific genes. Because of the order these proteins are activating in, this pathway is sometimes referred to as Ras-Raf-MEK-ERK pathway (Fresno Vara, Casado et al. 2004).

This pathway was originally synonymous with its role in cell proliferation. However, dysregulation of this pathway is now linked to many aspects of tumour phenotypes. A mutation in any of these proteins will result in an altered phosphorylation state, and as a consequence, signalling will be constantly “on” or “off”. It has now been predicted that approximately one-third of all human cancers have dysregulated MAPK (Dhillon, Hagan et al. 2007). Because of its clear importance in cancer, many compounds have now been developed to target and inhibit steps of the MAPK pathway as a cancer therapeutic (Downward 2003; Sebolt-Leopold 2008).

CXCR4 is able to activate MAPK which is the upstream activator of Erk1/2 (Kryczek, Wei et al. 2007). Erk1/2 are often termed as the same effectors as they both activate the same downstream transduction pathways. Incubation of breast cancer cells with CXCL12 caused activation of Erk1/2 within 15 minutes (Zhou, Luo et al. 2002; Prasad, Fernandis et al. 2004). Activation of Erk1/2 are able to phosphorylate a number of downstream transcription factors and genes involved in promoting proliferation and cancer cell survival (Pearson, Robinson et al. 2001).

1.6.2.3 JAK/STAT pathway

Another pathway involved in CXCR4 signalling is Janus Kinase (JAK)/STAT. Once activated by CXCL12, JAK1, 2 and 3 associate with CXCR4. JAK then activates STAT members and recruit them to the nucleus where they transcribe genes involved in motility within cells which are not usually involved in migration such as epithelial cells (Soriano, Serrano et al. 2003). JAK signalling in breast cells is also able to promote proliferation *in vitro* (Li and Shaw 2004) as well as promoting the polymerisation of actin to enhance cells motility.

1.6.2.4 HER2 upregulation

Evidence of CXCL12-CXCR4 signalling activating HER2 has been demonstrated in breast (Cabioglu, Summy et al. 2005) and prostate (Chinni, Yamamoto et al. 2008) cancers. Using the CXCR4 and HER2 overexpressing breast cancer cells, MDA-MB-231 and SKBr3, Cabioglu et al (Cabioglu, Summy et al. 2005) reported that inhibitors for HER2, CXCR4, and Src kinase all inhibited CXCL12-induced cell migration. The same report also demonstrated that blocking the Src kinase using an inhibitor was also able to inhibit HER2 signalling, suggesting that the CXCL12-CXCR4 axis is able to transactivate HER2 through the Src kinase pathway (Cabioglu, Summy et al. 2005). A similar method of CXCL12 induced HER2 expression involving Src kinase was described in prostate cancer (Chinni, Yamamoto et al. 2008)

A schematic representation of some the responses involved with CXCL12-CXCR4 interactions is provided in **figure 1.7**.

To summarise this section, there are a number of specific molecules which regulate the metastatic dissemination of tumour cells to specific anatomical sites. These molecules must follow a specific criterion (Muller, Homey et al. 2001). Firstly, they have to be expressed at the principle sites of metastasis. Next, adhesion target cells to the endothelium and transendothelium migration needs to be promoted. The molecules must be capable of mediating invasion of cells in to tissues, and finally, the process requires the expression of a distinct receptor repertoire by the target cells. Based on this evidence, the CXCR4-CXCL12 axis fits the criteria for molecules key in mediating breast cancer spread and illustrates its importance in dictating the anatomical specificity witnessed in the metastatic dissemination of breast tumour cells.

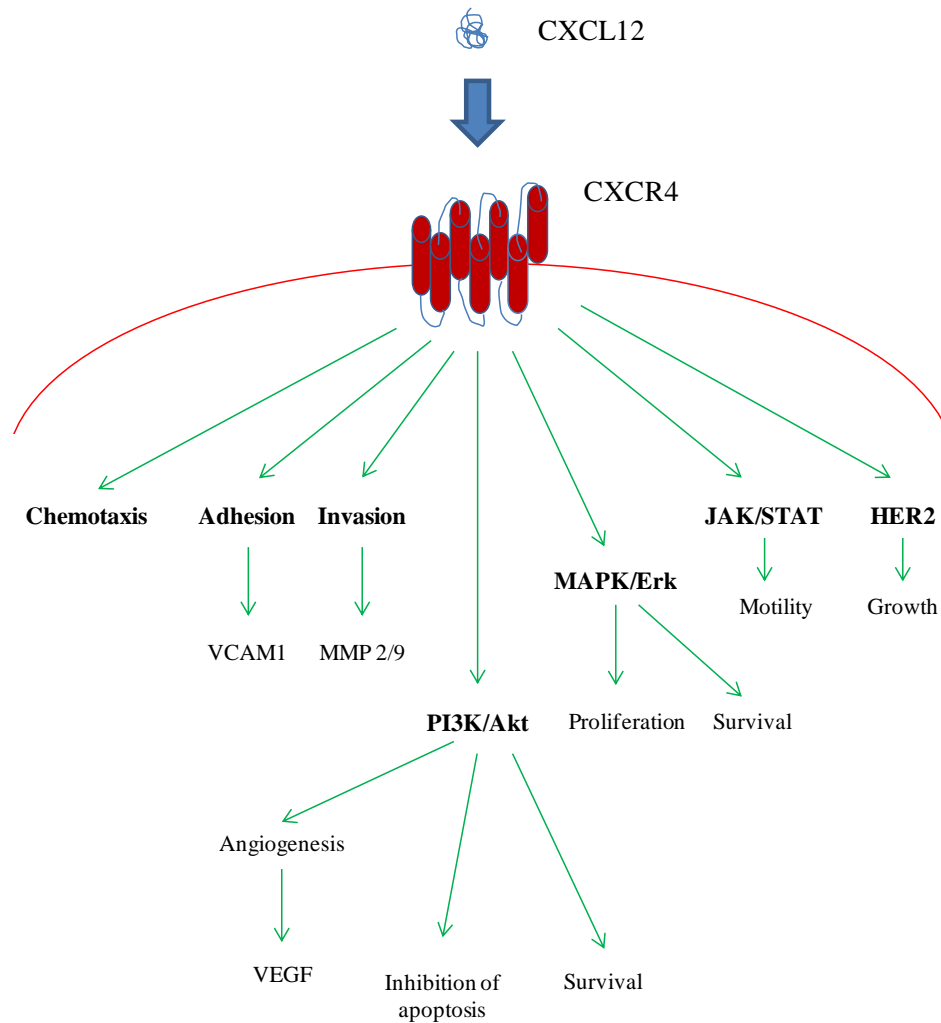


Figure 1-7 - Signalling pathways involved with the CXCL12/CXCR4 axis

Following binding of CXCL12 to CXCR4 a number of actions involved with tumour development and metastasis are initiated including chemotaxis, adhesion, invasion, proliferation, angiogenesis, cell growth, and increased survival mechanisms. Many of these are governed through signalling of PI3K/Akt, MAPK/Erk and JAK/STAT pathways which have also been reported to be activated through CXCL12 binding.

1.6.3 CXCR4 regulation

1.6.3.1 Hypoxia

During cancer metastasis, the invading and migrating cells frequently encounter harsh conditions such as low oxygen levels (hypoxia) and diminished nutrients, mainly due to overcrowding of cancerous cells within the tumour mass.

Schioppa et al (Schioppa, Uranchimeg et al. 2003) demonstrated that a number of cells including monocytes, macrophages, endothelial cells, epithelial cells and a variety of cancer cells including MCF-7 and MDA-MB-231, increase the mRNA levels and surface expression of CXCR4 when cultured in hypoxic conditions for 4-6 hours in comparison to the same cells cultured in normal 20% oxygen levels. These cells release hypoxic inducing factor-1 α (HIF-1 α) when they experience these conditions. HIF-1 α is a transcription factor which has been well demonstrated on several lines of evidence to be frequently expressed in conditions of low oxygen and is considered as the most defined molecule involved in the systemic mechanism of oxygen homeostasis. HIF-1 α promotes the expression of a number of target genes including CXCR4 (Staller, Sulitkova et al. 2003).

Using the ovarian epithelial cancer cell line, CAOV3, Schioppa et al (Schioppa, Uranchimeg et al. 2003) performed chromatin immunoprecipitation (chIP) assay demonstrating that HIF-1 α directly upregulated CXCR4 by binding to its promoter. Not only does HIF-1 α directly cause upregulation of CXCR4 at both transcript and protein level, this increase in CXCR4 surface expression correlated with an increased migratory response towards CXCL12 (Matteucci, Locati et al. 2005). The HIF-1 α mediated increase in CXCR4 on these cells is reversible as the transcript and protein levels of CXCR4 were returned to baseline levels after 24 hours of reoxygenation. Interestingly, the hypoxic conditions also increased the expression of VEGF which could also increase tumour cells oxygen and nutrient levels (Liu, Cox et al. 1995; Forsythe, Jiang et al. 1996).

1.6.3.2 HER2

As well as CXCR4 being expressed on up to 90% of primary breast tumours and being heavily implicated in cancer metastasis, HER2 is also overexpressed in approximately 30% of breast tumours, and is associated with particularly aggressive forms of cancer carrying a high risk of forming metastasise (Yu and Hung 2000).

Within the literature there is clear evidence of interplay between HER2 and CXCR4 expression. Li et al (Li, Pan et al. 2004) generated two independent HER2 overexpressing MDA-MB-435 breast cancer cells and used flow cytometry, Western blot and fluorescent microscopy to demonstrate that each stable transfectant had approximately a 3-fold increase in CXCR4 expression compared to empty vector transfected cells. Moreover, when the HER2 overexpressing MDA-MB-435 were treated with Herceptin[®], there was a subsequent decrease in CXCR4 expression in comparison to the same cells which were treated with a control IgG (Li, Pan et al. 2004). To further validate these findings, BT-474 cells (HER2 overexpressing breast cancer cells) were also treated with Herceptin[®] and a comparable decrease in CXCR4 surface expression was witnessed. Similar findings were observed when BT-474 was treated with HER2-specific siRNA (Li, Pan et al. 2004).

HER2 signalling can activate Akt which, in turn, can activate mammalian target of rapamycin (mTOR). This is known as the PI3K/Akt/mTOR pathway (Zhou, Hu et al. 2000). To test whether mTOR signalling is involved in the HER2-mediated enhancement of CXCR4, inhibitors of HER2 tyrosine kinase, PI3K and mTOR were administered to HER2 overexpressing breast cancer cells. Results demonstrated that treatment with each inhibitor reduced the levels of CXCR4, suggesting that the PI3K/Akt/mTOR pathway may be activated by HER2-induced CXCR4 expression (Li, Pan et al. 2004).

Signalling of CXCL12 through CXCR4 usually causes ubiquitination of the CXCR4 receptor. This suggests that CXCR4 expressing cancer cells which reach their CXCL12 enriched organs would have partial degradation of the CXCR4 receptor (Yu and Hung 2000). Following CXCL12 stimulation, CXCR4 expression on MDA-MB-435 was rapidly degraded with approximately 40% of the receptor being lost within 1 hour (Marchese and Benovic 2001; Li, Pan et al. 2004). However, the levels of CXCR4 on MDA-MB-435 stably transfected with HER2 remained almost the

same after 1 hour of CXCL12 stimulation (Li, Pan et al. 2004). A pulse-chase assay further demonstrated that ligand-induced protein degradation of CXCR4 in HER2 transfected cells was significantly reduced, therefore, allowing cancer cells to maintain high level expression of CXCR4 and extended signalling through the receptor potentially contributing to other steps involved in metastasis (McQuibban, Butler et al. 2001).

An *in vivo* link was also demonstrated between CXCR4 and HER2 expression as there was a statistically significant positive correlation between the two in human breast tumour samples. The majority of HER2 positive samples also expressed CXCR4, whereas, most HER2 negative tumours lacked detectable expression of CXCR4 (Li, Pan et al. 2004).

Because CXCL12-CXCR4 signalling has been reported to induce HER2 expression in cancer cells, and HER2 signalling has been shown to increase CXCR4 expression, this provides an intriguing potential feedback loop between CXCR4 and HER2 signalling to increase each others expression.

1.6.3.3 NF- κ B

NF- κ B is a heterodimeric transcription factor which is made up from a complex of Rel family proteins that are physically restricted to the cytoplasm of normal cells by interaction with a NF- κ B inhibitor.

NF- κ B is able to upregulate the expression of pro-cancer genes including IL-6, IL-8, urokinase plasminogen activator (uPA), MMP9 and VEGF (Baeuerle and Henkel 1994; Nakshatri, Bhat-Nakshatri et al. 1997; Karin and Lin 2002). Because of this ability to promote metastasis and angiogenesis, NF- κ B activation has been implicated in a variety of cancers (Bargou, Emmerich et al. 1997; Sovak, Bellas et al. 1997; Dong, Chen et al. 1999; Cogswell, Guttridge et al. 2000). In addition to this, inhibitors of NF- κ B are able to reduce the metastasis in xenograft models (Andela, Schwarz et al. 2000).

NF- κ B is expressed within a wide range of cell types and each cell type has its own specific heterodimers, however the most predominant subtype is made up of p50 and p65 subunits.

MDA-MB-231 have a constitutively active NF- κ B, however, MDA-MB-231 generated to overexpress the I κ B super-repressor have significantly lowered *CXCR4* transcripts. These cells also had a significantly reduced ability to migrate in response to CXCL12 (Helbig, Christopherson et al. 2003). Following transient transfection of *CXCR4* into MDA-MB-231, the migratory potential of the cells was restored (Helbig, Christopherson et al. 2003). The direct control of *CXCR4* by NF- κ B was validated by chIP assay which demonstrated that the NF- κ B subunits p65 and p50 bind directly to sequences between -66 and +7 in the *CXCR4* promoter region (Helbig, Christopherson et al. 2003).

Another potential feedback loop could exist between NF- κ B and *CXCR4* as *CXCR4* signalling through the PI3K/Akt pathway is able to directly regulate NF- κ B.

1.6.3.4 VEGF

VEGF is a signal protein important in angiogenesis and vasculogenesis, functioning to promote the formation of new blood vessels which provide essential nutrients to tumour cells. The overexpression of VEGF has been implicated in several diseases including aggressive forms of breast cancer. Interestingly, it has been reported that the expression of VEGF is also able to upregulate *CXCR4* in cancer cells (Kijowski, Baj-Krzyworzeka et al. 2001; Bachelder, Wendt et al. 2002).

When brain microvascular endothelial cells were exposed to 50ng/ml of VEGF, the mRNA expression of *CXCR4* increased 3-fold by 8 hours, and continued to increase up to approximately 10-fold after 16 and 24 hours. These findings were similarly demonstrated at a protein level where the upregulation of *CXCR4* was significantly increased after 24 hours (Zagzag, Lukyanov et al. 2006). *In vivo* studies have demonstrated that inhibition of the CXCL12-*CXCR4* axis is able to decrease tumour growth by inhibiting angiogenesis in a VEGF-dependant manner (Guleng, Tateishi et al. 2005).

1.6.3.5 Influence of cytokines

A number of cytokines have been shown to cause an increase in CXCR4 expression in a variety of cell types. The cytokines IL-2 (Moriuchi, Moriuchi et al. 1997) IL-4, IL-7, IL-15 (Jourdan, Vendrell et al. 2000), IL-10 and TGF- β 1 (Wang, Murakami et al. 2001) have all been shown to increase the expression of CXCR4. Interestingly, a number of these cytokines are present in tumour environments, and could therefore lead to the increased expression of CXCR4 and contribute to cancer progression. Cancers exist in a state of chronic inflammation where high levels of the inflammatory cytokines TNF- α and IFN- γ and IL-1 β are present. Interestingly, all these cytokines have been reported as causing downregulation of CXCR4 (Feil and Augustin 1998; Gupta, Lysko et al. 1998; Han, Wang et al. 2001).

A schematic representation of factors able to influence an increase in CXCR4 expression is provided in **figure 1.8**.

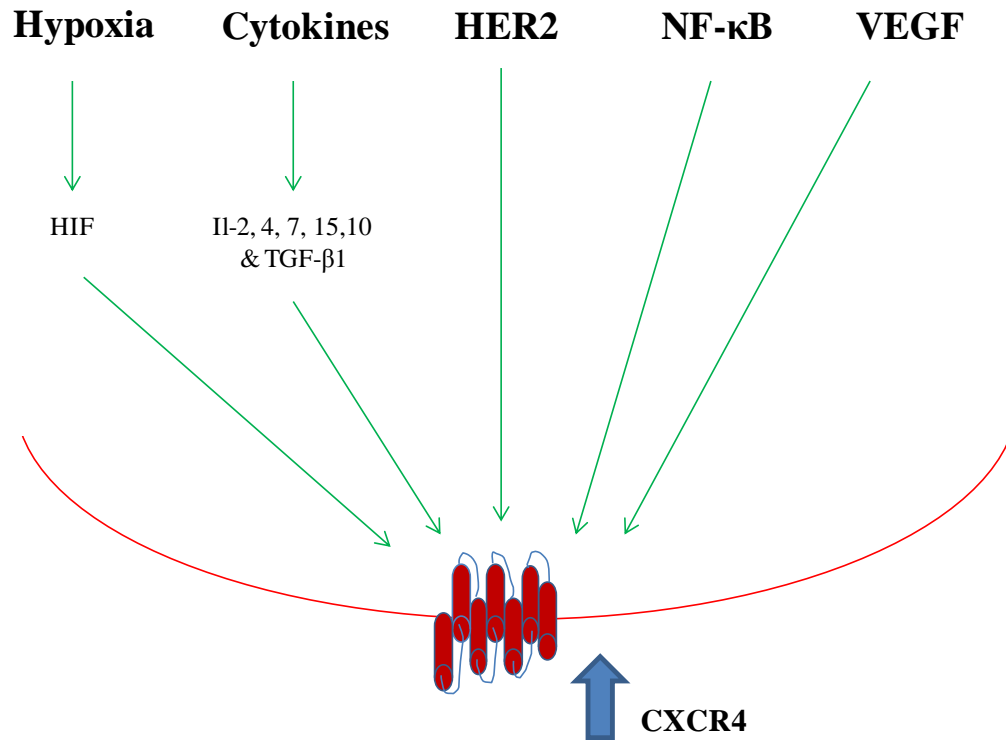


Figure 1-8 - Factors able to increase CXCR4 expression on epithelial cells

CXCR4 upregulation on epithelial cells has been reported to be influenced by a number of factors including hypoxia via HIF-1 α , HER2, NF- κ B, VEGF and also a number of cytokines such as IL-2, 4, 7, 15, 10 and also TGF- β 1.

1.7 FOXP3

FOXP3 is a forkhead box transcription factor. As a transcription factor, FOXP3 is able to work in cooperation with other proteins or directly bind to regulate the expression of target genes. FOXP3 is highly expressed in regulatory T-cells (Tregs) and governs many of its most characteristic features (Hori, Nomura et al. 2003). In addition to Tregs, FOXP3 can also be transiently upregulated in naive T-cells conveying many phenotypic features of Tregs, but not the immunosuppressive function associated with them (Wang, Ioan-Facsinay et al. 2007). Interestingly, FOXP3 has recently been identified within epithelial cells of specific organs. This is discussed in the following sections.

1.7.1 Forkhead box protein history and nomenclature

The first forkhead box (FOX) protein was discovered in the fruit fly *Drosophila melanogaster* in 1990 by Weigel and Jackle (Weigel, Jurgens et al. 1989). It was initially identified as a factor required for pattern formation in the terminal regions of the embryo (Weigel, Jurgens et al. 1989). Since this discovery, more than 100 FOX proteins have been identified in organisms ranging from yeast to humans. The number of FOX genes has increased at a greater pace in vertebrates than in invertebrates. Within the human genome there are 43 identified FOX genes (Katoh 2004). These proteins have diverse roles in the body ranging from the development and regulation of the immune system (Coffer and Burgering 2004), to development of hair (Hong, Noveroske et al. 2001), and hearing and speech (Lai, Fisher et al. 2001).

The first international meeting on forkhead transcription factors was held in 1998 at La Jolla (California, USA) to agree on a common nomenclature. Prior to this meeting forkhead genes were originally given different names such as FKH, FREAC and HFH (Kaestner, Knochel et al. 2000). However, because of their common DNA binding forkhead box domain, the term FOX was used to describe all chordate transcription factors which contain this unique region (Kaestner, Knochel et al. 2000). FOX proteins are divided into 17 subclasses (denoted A-Q) based on their amino acid sequence composition within the forkhead domain. Finally a letter

denotes each individual member within the subclass (Kaestner, Knochel et al. 2000). The final proposal on this nomenclature was endorsed by more than 20 scientists as well as the Human and Mouse Gene Nomenclature Committees. The convention for naming human FOX proteins is that all letters are capitalised (e.g. FOXP3) whilst in mice, only the first letter is capitalised (e.g. Foxp3) and for all other chordates, the first letter and the subclass is capitalised (e.g. FoxP3). Italic script is used to describe the genes (e.g. *FOXP3* [human]) (Kaestner, Knochel et al. 2000).

1.7.2 Structure

1.7.2.1 Gene

The *FOXP3* gene is relatively well conserved in mammals (Ziegler 2006). It is located on the p arm of the X-chromosome at Xp.11.23. It contains 11 coding exons (1–11) and three non-coding exons. The two 5' non-coding exons (–2a and –2b) are located significantly upstream of the coding exons and are spliced into a single common non-coding exon (–1) (Lal and Bromberg 2009). There remains controversy in the literature over the number of *FOXP3* exons; those who describe 11 exons do not count the initial –1 non-coding exon which lies outside the protein coding region.

1.7.2.2 Protein

The full length FOXP3 protein is made up of 431 amino acids. FOXP3 has a relatively short half-life of approximately 21 minutes as it undergoes rapid polyubiquitination and proteosomal degradation (Lee, Gao et al. 2008).

FOXP3 contains four main domains; a repressor domain, a zinc finger, a leucine zipper motif, and the DNA-binding forkhead domain which defines the FOX protein membership (**figure 1.9**). All known FOX proteins share a common, highly conserved DNA-binding forkhead box domain. This domain is located towards the carboxyl terminus of the protein and contains approximately 80-100 amino acids. This alignment of amino acids produces three α helices, two β strands and two loops (**figure 1.10**) (Kaestner, Knochel et al. 2000). The arrangement of these helix-turn-helix proteins and the crystal structure when bound to DNA is often said to resemble

the wings on a butterfly. As a consequence, this region has been referred to as a “winged helix” (Clark, Halay et al. 1993).

This winged helix is typically invariant across the FOX proteins and the organisms they are expressed in; however, the location of the forkhead domain within the protein is not so consistent. FOXP3 has similar structural characteristics to all other FOXP3 members. FOXP1, FOXP2 and FOXP4 all have centrally located zinc fingers, leucine zippers and forkhead domains. However, FOXP3 has the forkhead domain located towards the C-terminus (Lopes, Torgerson et al. 2006). This region is the primary domain responsible for binding to DNA where the transcription of specific genes is regulated. As well as having a relatively invariant forkhead domain, a considerable degree of homology in the amino acid composition of FOXP3 across different organisms is also maintained. Human FOXP3 shares the greatest resemblance with FoxP3 of the rhesus monkey (97%). Interestingly, cows, cats, dogs and horses have between 89-90% homology, whereas, mouse Foxp3 shares 86% homology to humans (Banham, Lyne et al. 2009).

A zinc finger is a small structural motif often found in proteins. The term zinc finger was first used when describing the finger like appearance in the structure of the transcription factor IIA found in the African clawed frog *Xenopus laevis* (Klug and Rhodes 1987). Many zinc finger domains utilise zinc ions to stabilise the folding of the protein, however, despite the name, zinc fingers will bind other metals such as iron or even non-metals (Krishna, Majumdar et al. 2003). Zinc fingers are frequently found in transcription factors, where the vast majority demonstrate a strong capacity to interact. Studies frequently report zinc fingers interacting with DNA, RNA, proteins and other small molecules depending on their amino acid sequence within the finger domain (Krishna, Majumdar et al. 2003). The zinc finger present in FOXP3 is classed as a C2H2 (Cys₂-His₂) which is most common form in mammalian transcription factors (Krishna, Majumdar et al. 2003). The full function of the zinc finger present in FOXP3 has yet to be fully elucidated, with no current reports demonstrating a conclusive role.

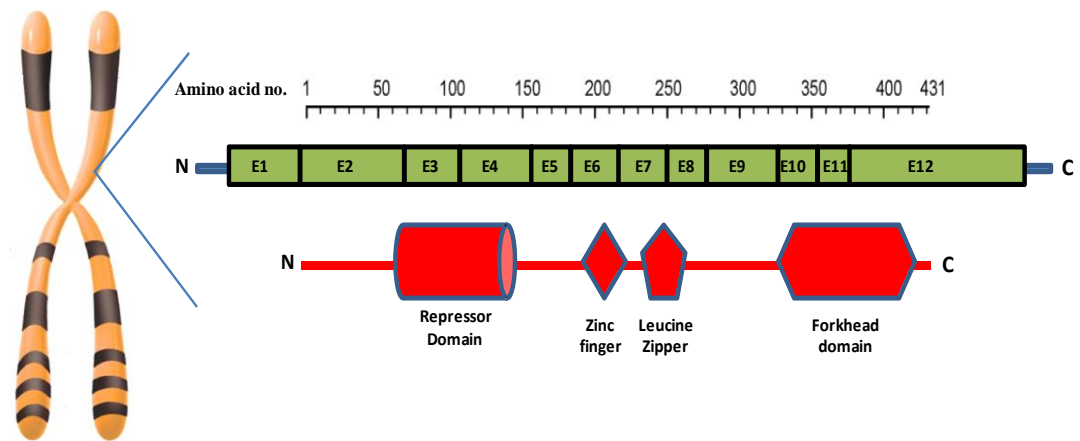


Figure 1-9 - Schematic representation of human FOXP3

The X-chromosome located FOXP3 gene consists of 11 coding exons and 1 non-coding exon, which is located towards the N-terminal. Full length FOXP3 is made up 431 amino acids and 4 domains. Image taken from (Douglass, Ali et al. 2012).

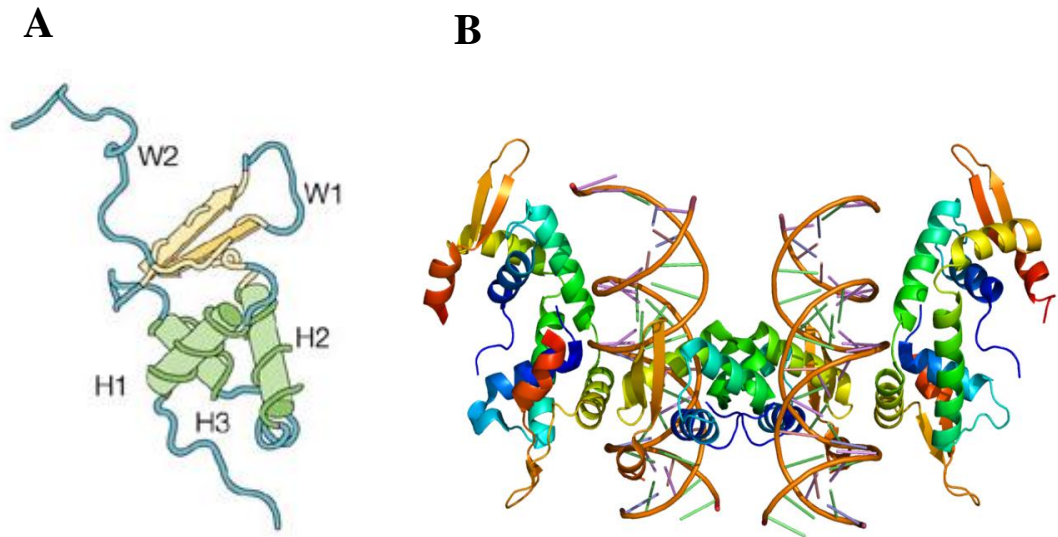


Figure 1-10 - Loops and helices of the forkhead domain in FOXP proteins

(A) The Forkhead domain in FOX proteins consists of two wings (W1 & W2) and three helices (H1-H3) (Coffer and Burgering 2004). (B) When these helices and wings are arranged they are said to resemble the “wings on a butterfly” (image of FOXP2, taken from Protein Data Bank (PDB) rendering based on 2a07).

It has been reported that FOXP3 regulates approximately 700 genes in humans, functioning as either a transactivator or repressor to these genes (Zheng, Josefowicz et al. 2007).

Despite the difference in location of the forkhead domain in FOXP3, FOXP proteins have considerable homology between the forkhead domain, leucine zipper and zinc finger domains, however, main differences between FOXP proteins are found within the N-terminal region (Lopes, Torgerson et al. 2006). FOXP1, FOXP2 and FOXP4 contain polyglutamine tracts (Wang, Lin et al. 2003), however, FOXP3 contains a proline rich region allowing for kinks and turns in the protein (Lopes, Torgerson et al. 2006). As with many transcription factors, reports have demonstrated that transcriptional repression of specific genes by FOXP3 is dependent on regions outside of the DNA-binding forkhead domain (Lopes, Torgerson et al. 2006). Mutant FOXP3 proteins lacking the forkhead domain have an ability to repress transcription to a similar level as wild type FOXP3. In addition, this ability to repress transcription was not significantly affected in mutants lacking the leucine zipper and zinc finger as well as the forkhead domain. However, a FOXP3 mutant lacking the N-terminal 198 amino acids was not able to significantly repress transcription (**figure 1.11**). Therefore, between amino acids 67-132 in FOXP3 have been termed as the repressor domain (Lopes, Torgerson et al. 2006).

Most transcription factors bind to DNA in a homo-multimeric fashion, or as part of a complex containing other transcription factors. However, the majority of FOX proteins exist as monomers in a solution and when they bind to DNA (Li and Tucker 1993). The ability to heterodimerise extends the range of biological functions within the FOXP subfamily (Shu, Yang et al. 2001).

It has been demonstrated that FOXP1, FOXP2 and FOXP4 are all capable of interacting with each other either as homodimers or heterodimers (Li, Weidenfeld et al. 2004). In addition, it has been demonstrated that FOXP1 and FOXP3 are capable of interacting in *in vitro* assays (Wang, Lin et al. 2003). FOXP3 is also capable of homodimerisation. The leucine zipper is the domain which is both necessary and sufficient for this activity as mutations affecting this region result in loss of homodimerisation (Lopes, Torgerson et al. 2006).

As mentioned previously, FOXP3 often functions through the interactions of several transcription factors such as Runt-related transcription factor 1 (Runx1) and nuclear factor of activated T-cells (NFAT), thereby proving its ability to heterodimerise. The association of FOXP3 with other transcription factors is discussed in section 1.7.6.

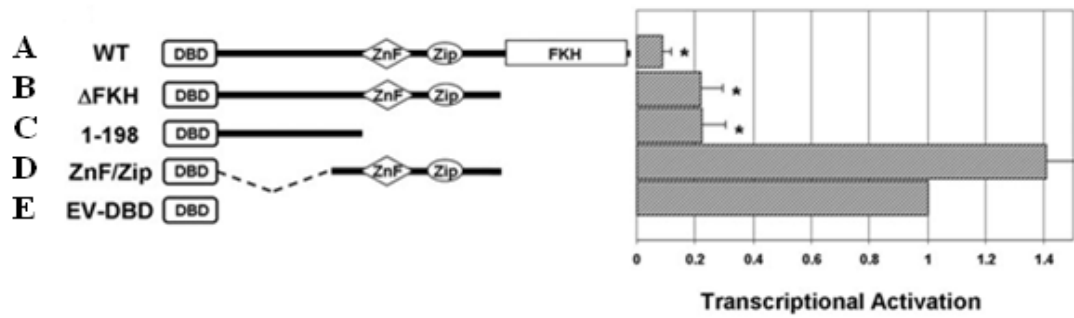


Figure 1-11 - Regions responsible for FOXP3-mediated gene repression

Image demonstrates that wild type FOXP3 (A) and FOXP3 mutants missing the forkhead domain (B) and a mutant only containing the first 1-198 amino acids (C) are capable of significant gene repression, however, a mutant FOXP3 missing amino acids 1-198 and the forkhead domain (D) and also a mutant only containing the forkhead (E) are unable to repress the transcription of gene (Lopes, Torgerson et al. 2006).

1.7.3 Scurfy and IPEX

The *Foxp3* gene was first discovered in mice as a result of a spontaneous mutation at the Oak Ridge National Laboratory in 1949 (Godfrey, Wilkinson et al. 1991; Chatila, Blaeser et al. 2000). This condition was later described as scurfy, whereas, the human equivalent of scurfy is known as Immune dysregulation, Polyendocrinopathy, Enteropathy, X-linked syndrome (IPEX). A mutation in *FOXP3* is the only cause of IPEX syndrome. Although, a number of IPEX-like syndromes also exist. These individuals have many clinical symptoms of IPEX patients, but they do not have mutated *FOXP3*. Many patients with IPEX-like syndrome also have defective Treg development, however, despite having functional *FOXP3*, studies have described these patients as having dysfunctional CD25 expression on CD4⁺ T-cells, a lack of sensitivity to IL-2 (since CD25 is the α -chain of the IL-2 receptor and encoded by *IL2RA*) and reduced IL-10 expression (Caudy, Reddy et al. 2007).

The first IPEX syndrome was reported by Powell et al (Powell, Buist et al. 1982) in 1982 who described a clinical triad of features including watery diarrhoea, eczematous dermatitis and endocrinopathy. IPEX unfortunately has high motility rates with symptoms typically presenting within the first year and the majority of mortality occurring within the first or second year of life.

As the master regulator of the function and development of Tregs, it is no surprise that the major problems encountered by IPEX patients occur as a result of overwhelming chronic autoimmunity due to a lack of Tregs.

IPEX symptoms generally present within the first few months of life. A number of distinctive and defined symptoms are associated with IPEX. These include enteropathy as the immune system attacks the intestinal epithelial cells causing severe diarrhea. This is usually the first symptom associated with IPEX. This also causes a failure to gain weight and grow at the expected rate with observable cachexia. Dermatitis and psoriasis, with heavy inflammation of the skin and eczema is also commonly witnessed. IPEX individuals often develop multiple disorders associated with the endocrine glands, hence the term polyendocrinopathy. Type 1 diabetes mellitus is the most common endocrinopathy associated with IPEX, although the thyroid gland may also be affected. Autoimmune blood disorders such

as anaemia, thrombocytopenia and neutropenia have also been reported in patients, although these are less frequent.

IPEX patients are treated using a haematopoietic stem cell transplant (HSCTx). Although there are a number of complications associated with HSCTx, this treatment has been demonstrated to be highly effective in alleviating the clinical symptoms. In attempts to limit the effects of autoimmunity, immunosuppressive drugs are administered until a suitably matched donor is found for the HSCTx. The adoptive transfer of FOXP3⁺ T-cells is able to prevent the onset of scurfy in mice (Fontenot, Gavin et al. 2003; Huter, Punkosdy et al. 2008).

1.7.4 Natural isoforms

Human CD4⁺CD25^{hi} Tregs express two natural FOXP3 isoforms (Allan, Passerini et al. 2005). This notion was also supported in normal breast epithelial cells (Zuo, Wang et al. 2007). Both Tregs and epithelial cells of specific organs express a full length version (FOXP3FL) and a version with a complete deletion of exon 3 (FOXP3Δ3) (or 2 depending on the authors preference to numbering exons), which is approximately 4kDa smaller in size than its full length counterpart. It is thought that these isoforms are expressed in approximately equal ratio. When originally reported, exon 3 was thought to lie in a relatively uncharacterised region which did not have any known protein domains.

Full length and Δ3 variants of FOXP3 were transiently transfected into Jurkat cells and measured to see if either isoform could repress the expression of IL-2 by suppressing the activation of the *IL2* promoter (Smith, Finney et al. 2006). Co-expression of the isoforms resulted in significant repression of *IL2* by both isoforms. Importantly, the level of suppression on the promoter was almost identical which suggested that FOXP3Δ3 also acts as a transcriptional repressor (Smith, Finney et al. 2006). A contrasting report by Allan et al (Allan, Passerini et al. 2005) demonstrated that expression of FOXP3Δ3 is less effective than the full-length version at suppressing *IL-2* therefore leaving the functional capabilities of FOXP3Δ3 unclear.

Since the report by Allen et al (Allan, Passerini et al. 2005) was published it has been shown that the region where exon 3 lies has been demonstrated as a repressor domain

(described previously in section 1.7.2.2). In T-cells, the region where exon 3 lies has been shown to interact and inhibit retinoic receptor-related orphan receptor- α (ROR- α). This leads to the expression of genes responsible for generating Th17 cells, and on this basis, it is thought that only full length versions of FOXP3 are capable of regulating the differentiation of Th17. It is thought that the FOXP3 Δ 3 version acts as the dominant negative isoform (Ziegler 2006). It is important to note that unlike in humans, mice only express the full length Foxp3 variant which represents the orthologue for human FOXP3 (Allan, Passerini et al. 2005).

1.7.5 Intracellular trafficking

As a transcription factor, the ability to transport to the nucleus is a prerequisite for effective functioning of FOXP3. However, because the FOXP3 protein is synthesised in the cytoplasm, it must then be actively transported to the nucleus of cells. Despite this, few reports have studied the mechanisms involved in the transport of FOXP3 to the nucleus.

A consensus arginine-lysine-lysine-arginine (RKKR) sequence has been reported as critical in the localisation of proteins to the nucleus (Mikami, Hori et al. 2005; Lopes, Torgerson et al. 2006; Song, Waataja et al. 2006). This sequence is found towards the C-terminus of the forkhead domain in FOXP3 and is conserved between human and mouse FOXP3.

Hancock and Ozkaynak (Hancock and Ozkaynak 2009) reported that three domains were required for nuclear localisation of full length Foxp3 (**figure 1.12**). These regions were subsequently defined as nuclear localisation sequences (NLS). Firstly, the authors reported that in murine Foxp3, the RKKR sequence does not act as a classic NLS in full length Foxp3, but is required in shortened versions of the protein.

Several constructs were designed where single or multiple residues of the RKKR sequences were replaced with unrelated amino acids in a full length Foxp3 protein. Results showed that none of these constructs altered the proteins ability to translocate to the nucleus (Hancock and Ozkaynak 2009). Two further constructs were designed where the C-terminal 12 amino acids were cleaved from the protein revealing a C-short protein. One of these constructs had the RKKR sequence maintained, whereas,

the other construct had the entire RKKR sequence replaced with unrelated amino acids. Results demonstrated that the C-short construct, with the maintained RKKR sequence, transported at a similar rate as a full version, whereas, the construct with mutated RKKR suffered a significantly slower rate of nuclear localisation with the majority remaining in the cytoplasm (Hancock and Ozkaynak 2009). However, removal of this domain appeared to slow the rate of transport, as after 5 days the mutant protein was found to be exclusively located in the nucleus (Hancock and Ozkaynak 2009).

When the C-terminal 12 amino acids were restored to the construct, which lacked the wild type RKKR sequence, the ability to translocate to the nucleus was also restored (Hancock and Ozkaynak 2009). Therefore, the C-terminal 12 amino acids were subsequently defined as NLS-1. The fact that the removal of this domain did not completely abrogate transport suggests other domains are also involved.

The second region, defined as NLS-2, lies directly N-terminal to the forkhead domain and consists of two histidine–asparagine–methionine (HNM) repeats separated by five amino acids (Hancock and Ozkaynak 2009). Foxp3 proteins which contain mutations in this region have a significantly impaired ability to translocate to the nucleus. Within the five amino acids separating the HNM repeats is a lysine residue. When this lysine residue is maintained, the nuclear translocation rate was only minimally affected, indicating that this residue plays an important role (Hancock and Ozkaynak 2009).

The final region (NLS-3) is located within the first N-terminal 51 amino acids. A protein lacking these amino acids also had a significantly reduced rate of nuclear translocation (Hancock and Ozkaynak 2009). Mutant Foxp3 proteins which lacked all three of these NLS regions were located almost exclusively in the cytoplasm.

In contrast to these findings, Lopes et al (Lopes, Torgerson et al. 2006) made a GFP-FOXP3 fusion protein with a series of overlapping mutations or deletions. Their data demonstrated that changing two basic amino acids to acidic amino acids within the RKKR sequence abrogated the nuclear import of the protein, thus suggesting this sequence was important in the nuclear localisation of FOXP3.

When IPEX patients were screened for point mutations, no patients were found to contain mutations within the RKKR sequence (Lopes, Torgerson et al. 2006). However, one patient did contain a mutation which did slightly abrogate nuclear localisation (Lopes, Torgerson et al. 2006). This mutation was found at the opposite side of the forkhead domain, and even then nuclear localisation was only slightly reduced. These regions either side of the forkhead domain have also been demonstrated as NLS in hepatocyte NF-3 β which is another forkhead family member (Qian and Costa 1995).

There are possible explanations for these conflicting reports on the RKKR domain in murine Foxp3 and the GFP-FOXP3 construct.

- ❖ There are 3 proline residues in the 12 amino acid tail of mouse Foxp3 but 4 proline residues in the 14 amino acid tail in human FOXP3. This may induce changes in the secondary structure of FOXP3 which may alter the function of the RKKR sequence.
- ❖ Because of the size of GFP, the use of a GFP-tagged human FOXP3 may affect the overall structure of the protein, altering the function of specific regions.
- ❖ Despite considerable homology between human and murine, FOXP3 changes are apparent which could have profound consequences on nuclear translocation

Finally, particular caution should be taken regarding results based around the murine GFP-FOXP3 construct. The addition of the 238 amino acids GFP protein to the N-terminus of FOXP3 causes steric hindrance, and thus abrogates the function of FOXP3 including the ability to physically interact with other transcriptional partners (Darce, Rudra et al. 2012). Based on this finding, much of what we have discovered about the functions of FOXP3 using the GFP-FOXP3 construct may be an artefact because of the hypomorph. It should also be noted that FOXP3 does not necessarily always interact with other transcription factors through its N-terminal domain; it is known that FOXP3 is capable of interacting with other FOXP family members

through the leucine zipper region and interacts with NFAT through the FKH domain (Wu, Borde et al. 2006). This is discussed in the next section.

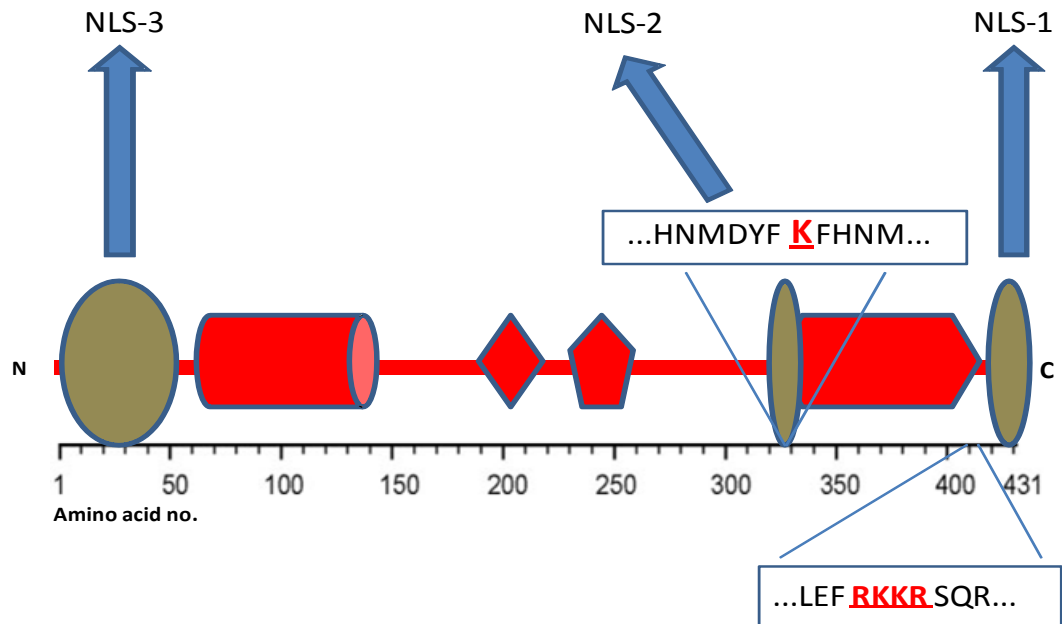


Figure 1-12 - Locations of Fxp3 nuclear sequences

Schematic representation of sequences and regions demonstrated to be responsible for Fxp3 nuclear localisation. Brown ovals highlight each individual as highlighted by Hancock & Ozkaynak (Hancock and Ozkaynak 2009). The location of the RKKR sequence deemed important by Lopes et al (Lopes, Torgerson et al. 2006) is also demonstrated towards the C-terminus of the protein. Image taken from (Douglass, Ali et al. 2012).

1.7.6 FOXP3 association with other transcription factors

An increasing amount of data is being produced to demonstrate that many normal functions of FOXP3 are reliant on interactions with other proteins.

FOXP3 contains conservative non-coding sequences. One of these sequences lies 5' to the transcriptional start site and has been reported to act as a proximal promoter region (Zhang, Meng et al. 2008). This region contains several important sequences including TATA, GC and CAAT boxes which are considered the key sequences for binding transcription factors suggesting FOXP3, like many other transcription factors, works in cooperation with other proteins. This notion was further enhanced as a mutation in this region significantly decreased the activity of FOXP3 (Mantel, Ouaked et al. 2006).

1.7.6.1 Homo-dimersation

As described in section 1.7.2.2, FOXP3 contains a leucine zipper motif which is primarily responsible for the interaction with other transcription factors. It has been reported that FOXP3 is able to form both homo-tetramers and homo-oligomers (Zuo, Liu et al. 2007). Interestingly, it was also demonstrated that FOXP3 with a mutated leucine zipper is also unable to bind the NFAT/forkhead site of the *IL-2* promoter which suggests that the ability of FOXP3 to homo- hetero-dimerise is a prerequisite for transcriptional repression (Lopes, Torgerson et al. 2006; Zuo, Liu et al. 2007).

On the other hand, it would appear that the actions of FOXP3 are not always solely dependent on the interactions with other proteins via the leucine zipper, as a FOXP3 mutant missing amino acid 250 is still able to suppress IFN- γ (Chae, Henegariu et al. 2006).

1.7.6.2 NFAT

NFAT is a transcription factor imperative for the transcription of activation-associated genes in T-cells, hence the name. Cooperation of FOXP3 and NFAT is relatively well documented. Unsurprisingly, many genes including *IL2*, *CD25* and

CTLA4 which are regulated by FOXP3 are also closely linked to NFAT, suggesting a high level of interaction between the two proteins (Rao, Luo et al. 1997; Hori, Nomura et al. 2003; Wu, Borde et al. 2006).

It has since been demonstrated that FOXP3 does control many NFAT-mediated genes by forming a cooperative complex. Amongst the genes involved in this cooperation are *IL2*, *CD25* and *CTLA4* (Rao, Luo et al. 1997; Hori, Nomura et al. 2003). This suggests the complex of FOXP3 and NFAT are crucial in the development and function of Tregs (Bettelli, Dastrange et al. 2005; Wu, Borde et al. 2006). Further evidence of this hypothesis is provided by data demonstrating that a mutant version of FOXP3, which is incapable of interacting with NFAT, is unable to suppress IL-2 production and also fails to upregulate CTLA-4 and CD25. Moreover this mutant was also unable to suppress autoimmunity *in vivo* (Wu, Borde et al. 2006). NFAT and another transcription factor, activator protein 1 (AP-1) also work closely together, however, since it has been shown that FOXP3 is able to directly interact with NFAT as well as AP-1 DNA target sequences, it is thought that NFAT binds to FOXP3 preferentially and replaces AP-1 (Wu, Borde et al. 2006).

1.7.6.3 NF- κ B

The interaction of FOXP3 and NF- κ B has been demonstrated in non-immune cells by several reports, however, this interaction has not yet been demonstrated within immune cells, therefore, suggesting this interaction could be key for epithelial cell homeostasis but not for T-cell function.

Within non-immune cells, FOXP3 is able to inhibit the transcription of NF- κ B mediated genes (Bettelli, Dastrange et al. 2005; Kwon, So et al. 2008) and also the expression of NF- κ B itself (Zhang and Sun 2010; Loizou, Andersen et al. 2011).

NF- κ B is usually located within the cytoplasm and inhibited by I κ B. However, after activation, the I κ B is removed and the protein is actively transported to the nucleus. Kwon et al (Kwon, So et al. 2008) produced data which demonstrated that the expression of FOXP3 enhanced the stability of I κ B which prevented the nuclear translocation of NF- κ B (Kwon, So et al. 2008). A separate report highlighted that FOXP3 directly interacts with c-Rel to inhibit NF- κ B expression (Loizou, Andersen

et al. 2011). Interestingly, c-Rel has also been demonstrated to influence the activation of IL-2 (Huang, Chen et al. 2001).

1.7.6.4 Runx1

Runx1 is a member of the runt-related family of transcription factors which also contains Runx2 and Runx3. Runx1 is expressed within Tregs and T-effector cells and has been highlighted as a regulator of IL-2 and IFN- γ (Ono, Yaguchi et al. 2007). Within amino acids 278-336 of FOXP3, a region between the leucine zipper and the forkhead domain, lies a Runx1 binding domain (Ono, Yaguchi et al. 2007).

Interactions between Runx1 and FOXP3 appear to have important effects on the function of Tregs as a mutant version of FOXP3, unable to bind Runx1, was also unable to effectively suppress IL-2 production (Ono, Yaguchi et al. 2007). In addition to this, Runx1 knockdown in human Tregs abrogated their suppressive capacity (Ono, Yaguchi et al. 2007). A mutation within the Runx1 binding region of FOXP3 has also been reported in IPEX patients (Bacchetta, Passerini et al. 2006).

1.7.6.5 ROR- α

The FOXP3-ROR- α interaction has been confirmed using chIP studies (Du, Huang et al. 2008). However, FOXP3 repression of ROR- α is relatively unique. Unlike many other interactions, which reportedly require the forkhead domain or the leucine zipper, FOXP3 repression of ROR- α is dependent on a region within exon 3, therefore, only full length FOXP3 variants are able to fulfil this interaction (Du, Huang et al. 2008). ROR- α has recently been identified as a key mediator in the development of Th17 cells which has since lead to the hypothesis that FOXP3, and moreover, specific FOXP3 isoforms are involved in Th17 development.

1.7.7 Cellular expression of FOXP3

1.7.7.1 Tregs

Through evolution, our bodies have developed an almost perfect mechanism to protect ourselves from pathogens. This is referred to as tolerance. Our central tolerance is based within the thymus which aims to delete auto-reactive T-cells before they are released into the circulation. However, as effective as this is, some harmful T-cells may escape the positive/negative selection process as we now have evidence from the presence of various autoimmune disorders. Therefore, we have developed a secondary mechanism called peripheral tolerance which attempts to combat the autoreactive T-cells that have escaped central tolerance. The main effectors involved in peripheral tolerance are Tregs; these cells are capable of modulating the activation and proliferation of potentially harmful T-cells. Tregs make up approximately 1-2% of whole blood and 5-10% of CD4⁺ T-cells in humans (Long, Cerosaletti et al. 2010). In comparison to regular T-cells, Tregs have several distinguishable characteristics, most of which are directly controlled through FOXP3 interactions. FOXP3 is therefore commonly used as the most reliable marker for Tregs.

The ability of FOXP3 to act as a transcriptional activator and repressor of specific genes is well documented and can be best demonstrated within the roles it plays in defining the most characteristic features of Tregs. As well as expressing CD4, Tregs have characteristically high level expression of the IL-2 α -chain receptor (CD25), therefore, being referred to as CD4⁺CD25^{hi} T-cells. However, unlike other T-cells, despite this high level expression of the IL-2 receptor, they fail to synthesise and secrete IL-2, but do require the cytokine to survive (Sakaguchi 2005). FOXP3 has been demonstrated to bind directly to the 5' promoter region of the *IL2ra* gene (which results in the activation and expression of CD25) and also the *IL2* gene (which results in the repression of the gene responsible for producing IL-2) (Chen, Rowell et al. 2006). Tregs also have high expression of CTLA-4, a cell surface molecule which is able to interact with CD80 and CD86 which delivers inhibitory signals and is thought to be responsible for the direct cell-cell suppression by Tregs. FOXP3 binds directly to promoter regions in the *CTLA4* gene and is therefore also responsible for high level CTLA-4 expression on Tregs (Chen, Rowell et al. 2006).

Other key features of Tregs governed directly by FOXP3 are the low level expression of IL-7R (by repressing *IL7ra*) and lack of IFN- γ (by binding to *IFNG* locus) (Chen, Rowell et al. 2006).

1.7.7.2 Epithelial cells

Because of the high expression and influence FOXP3 has in Tregs it was originally thought that FOXP3 was restricted to cells of the lymphocyte lineage. However, pioneering research from Chen et al (Chen, Chen et al. 2008) demonstrated the expression of Foxp3 within the nucleus of epithelial cells in select organs of mice (**figure 1.13**). FOXP3 has now been demonstrated within the epithelial cells of the breast (Zuo, Liu et al. 2007; Zuo, Wang et al. 2007; Chen, Chen et al. 2008; Merlo, Casalini et al. 2009; Li, Wang et al. 2011), prostate (Wang, Liu et al. 2009; Li, Wang et al. 2011), lung (Chen, Chen et al. 2008), ovaries (Zhang and Sun 2010) and brain (Frattoni, Pisati et al. 2012). Organ specificity was also demonstrated as Foxp3 was not located within liver, intestine or kidney epithelia (Chen, Chen et al. 2008). Despite a number of reports demonstrating clear presence of FOXP3 in some epithelial tissues, it should also be noted that it is expressed at levels significantly lower than the levels found in Tregs, where it is expressed at similar level of housekeeping genes (Wang, Liu et al. 2009).

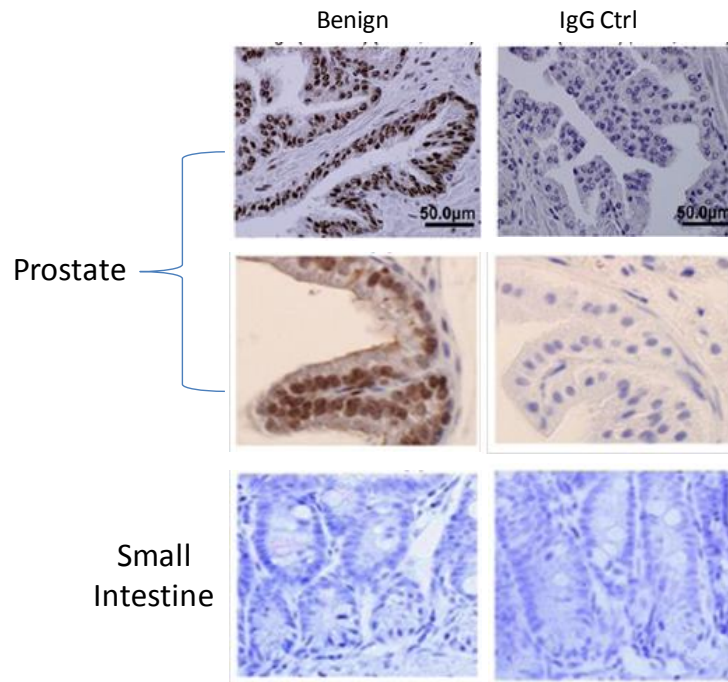


Figure 1-13 - Organ specific expression of Foxp3 in epithelial cells

Foxp3 is found in epithelial cells of specific organs such as the prostate. However, Foxp3 is not found within the small intestine. Images taken (Wang, Liu et al. 2009) (top image) and (Chen, Chen et al. 2008).

1.7.8 FOXP3 involvement in cancer

A number of malignancies have been linked to FOXP3 expression including colorectal cancer (Somasundaram, Jacob et al. 2002), head and neck cancer (Schaefer, Kim et al. 2005), hepatocellular carcinoma (Unitt, Marshall et al. 2006), cancers of the breast (Zuo, Liu et al. 2007; Zuo, Wang et al. 2007; Merlo, Casalini et al. 2009; Li, Wang et al. 2011), pancreas (Liyanage, Moore et al. 2002), gastrointestinal tract (Sasada, Kimura et al. 2003; Kawaida, Kono et al. 2005), lung (Woo, Chu et al. 2001), ovarian cancer (Zhang and Sun 2010), melanoma (Baumgartner, Wilson et al. 2007; Ahmadzadeh, Felipe-Silva et al. 2008; Gerber, Munst et al. 2013), cervical cancer (Fattorossi, Battaglia et al. 2004), lymphoma (Berger, Tigelaar et al. 2005) and leukemia (Ghiringhelli, Larmonier et al. 2004; Beyer, Kochanek et al. 2005). However, FOXP3 appears to act as a “double edged sword” in many of these malignancies, with its expression often reported as either favourable or bad. The opposing scenarios are often dependant on the cells where FOXP3 expression is investigated.

The filtration of various leukocytes into the tumour microenvironment is well established. T-cells, in particular are found in high quantities around the tumour mass. Many of these T-cells are Tregs, therefore, FOXP3 is often reported to be increased in many malignant tissues and represents a worse prognosis (Matsuura, Yamaguchi et al. 2009; Rech, Mick et al. 2010; Yuan, Chen et al. 2010; Gupta, Babb et al. 2011). This infiltration of Tregs is thought to act as a mechanism of immune evasion by the tumour as the presence of Tregs within the tumour microenvironment can suppress the anti-cancer properties of other immune cells recruited to the region. In addition to this, it has been demonstrated that many tumours produce and secrete high levels of TGF- β (Liu, Wong et al. 2007), therefore, this could also enhance the induction of FOXP3 in CD4⁺CD25⁻ T-cells and drive the differentiation of naive T-cells into acquired Tregs, therefore, contributing further to the suppression. Infiltration of T-cells and Tregs into the tumour environment is discussed further in section 5.1.1.

Wang et al (Wang, Liu et al. 2009) were the first group to examine the expression of FOXP3 within the epithelial cells of both normal and malignant prostate tissue. Firstly, they demonstrated that 85/85 normal prostate tissues examined contained

nuclear FOXP3, whereas, only 31.5% of malignant tissue contained nuclear FOXP3 (Wang, Liu et al. 2009). They also observed that FOXP3 was significantly downregulated within samples with clearly identifiable prostate epithelial neoplasia (PIN) in comparison to healthy tissues, thus suggesting that FOXP3 downregulation occurred at an early stage of carcinogenesis (Wang, Liu et al. 2009).

When the mRNA levels of *FOXP3* were investigated in benign and malignant tissue from matched patients, it was demonstrated that 14 out of 18 malignant tissues had a 2-10-fold reduction of *FOXP3*. In addition to this, 6 out of 18 cases also contained PIN. When these lesions were microdissected it was also demonstrated that *FOXP3* was downregulated, once again emphasizing that *FOXP3* downregulation within prostate cancer occurs in an early stage of carcinogenesis (Wang, Liu et al. 2009).

Next, fluorescence *in situ* hybridisation (FISH) was used to determine whether the *FOXP3* gene was deleted in any prostate cancer samples. Out of 165 prostate cancer tissues they found that 23 samples had *FOXP3* deletions (Wang, Liu et al. 2009). Moreover, 5 of these 23 cases had X-chromosome polysomy. Interestingly, the *FOXP3* deletion was observed in all X chromosomes thus demonstrating that the X polysomy occurs after *FOXP3* is deleted (Wang, Liu et al. 2009). Evidence of somatic *FOXP3* mutations in primary prostate was demonstrated when DNA from malignant and normal tissue from 20 matched patients was compared. Results demonstrated that five of the cancer samples contained single base-pair changes. Four of these mutations were missense mutations. Two of the samples had clear PIN and when these lesions were microdissected they found that both patients contained the same mutations as the patients with malignancy (Wang, Liu et al. 2009).

The presence and importance of FOXP3 regulation within ovarian epithelial cells has also been demonstrated by Zhang and Sun (Zhang and Sun 2010). IHC demonstrated that FOXP3 protein was found within the normal ovarian epithelium samples, however, weak or no expression was found in the malignant samples. Similar results were observed when *FOXP3* transcripts were compared by real-time PCR in the malignant and normal samples. In all 26 cancer samples analysed, *FOXP3* transcripts were significantly lower than those found in normal ovarian specimens (Zhang and Sun 2010).

A similar report by Frattini et al (Frattini, Pisati et al. 2012) demonstrated that despite normal FOXP3 levels within the human brain, FOXP3 was strongly downregulated within the majority of 35 human glioblastoma samples. Interestingly, using murine glioma cells they found that Foxp3 was detectable within early stages of tumour development, but diminished through tumorigenesis (Frattini, Pisati et al. 2012). Therefore, this data would suggest that Foxp3 expression could be involved in tumour progression more so than initial carcinogenic transformation, thus opposing the findings from Wang et al (Wang, Liu et al. 2009).

A similar scenario of FOXP3 expression within malignant and normal breast tissue has also been described in several reports and is discussed in 3.1.1.

Despite these findings, alternative reports have demonstrated a completely different scenario where FOXP3 expression is restricted to cancer cells. Hinz et al (Hinz, Pagerols-Raluy et al. 2007) used IHC to demonstrate that normal human pancreatic duct cells did not express FOXP3, however, in the pancreatic cancer cells FOXP3 was clearly identifiable. The fact that the majority of the FOXP3 staining in these cells was cytoplasmic would question the contribution of FOXP3 in these cells. However, the same authors (Hinz, Pagerols-Raluy et al. 2007) also demonstrated that FOXP3 expressing pancreatic cell lines were able to inhibit the proliferation of activated T-cells, therefore, suggesting a potential mechanism of conveying immune evasion by epithelial cells.

A similar scenario was described in melanoma cells by Ebert et al (Ebert, Tan et al. 2008) who used real-time PCR to demonstrate the presence of both natural FOXP3 isoforms in melanoma cells, but not in normal human melanocytes. IHC also demonstrated the presence of FOXP3 protein in the melanoma cells which, in these cell, was nuclear.

It should be noted that these alternative findings could be attributed to differing epithelial subsets and therefore the behaviour of FOXP3 in certain epithelia could also differ.

1.7.9 FOXP3, the X-linked tumour suppressor gene

A female's genetic makeup consists of two X-chromosomes (XX), whereas a male's consists of one X-chromosome and one Y-chromosome (XY). In both males and females, the X-chromosome is gene rich and is estimated to contain more than 1000 genes. Because of this, if both X-chromosomes were activated in females this "double dosage" would be potentially toxic. In order to equalise this, females have a unique way to neutralise this effect by inactivating one of their X-chromosomes and silencing one set of X-linked genes. The decision of which X-chromosome is deactivated is random and begins at the early stages of embryonic stem cell differentiation. Once deactivated, the X-chromosome is condensed into a compact structure called a barr body (Boumil and Lee 2001). Because of this dose compensation, X-linked genes are frequently referred to as dose compensated.

The vast majority of TSGs (discussed in section 1.4.5) are located on non-sex chromosomes and are autosomal and are inherited in a recessive manner. Therefore, autosomal recessive genes require two genetic events to inactivate them. This process was first described by Knudson in his two hit hypothesis (Knudson 1971).

It has been generally accepted now that within epithelial cells FOXP3 acts a TSG by controlling the expression of a number of genes implicated in cancer. FOXP3 is able to directly repress the expression of the oncogenes *ErbB2* (Zuo, Wang et al. 2007), *SKP2* (Zuo, Liu et al. 2007) and *c-MYC* (Wang, Liu et al. 2009) whereas, it is able to upregulate the expression of a number of anti-cancer genes including *CDKN1A* (Liu, Wang et al. 2009). This emphasises the importance of normal FOXP3 expression in epithelial cells. The importance of the aforementioned genes in driving carcinogenesis and the control FOXP3 has on them is discussed in section 4.1, whereas, the role it plays in *LATS2* and *BRCA1* regulation is discussed in sections 1.7.9.1 and 1.7.9.2.

Due to its genetic location on the X-chromosome, FOXP3 is classed as an X-linked TSG. This makes FOXP3 the first X-linked TSG to be identified, however, the consequence of being an X-linked TSG is that unlike autosomal TSG's, they are hemizygous and will only require a single genetic event to inactivate them, thus increasing the risk of carcinogenic transformation. Based on this, it is important to acknowledge and carefully monitor females who carry a recessive FOXP3 mutant.

Although these females will not display any phenotypic changes, should this wild type gene become damaged or inactivated, the recessive mutant gene will be expressed which could lead to a change in the woman's phenotype and a much increased risk of developing breast or ovarian cancer. Women who are genotyped as FOXP3 mutant carriers should perhaps undergo screening more frequently.

1.7.9.1 *LATS2*

The Hippo-pathway is made up of the key components Yes-associated protein (YAP), LATS1/2 and Mst1/2 (Li, Wang et al. 2011). YAP is a transcription factor which functions in an unphosphorylated state where it is able to regulate gene expression. When YAP is phosphorylated it is rapidly degraded. The enzymes which are responsible for this phosphorylation are LATS1/2 (Zhao, Li et al. 2010). Therefore LATS2 largely regulates cell cycle proliferation and apoptosis by repressing the expression of YAP.

YAP-overexpression has been reported in several cancers including the prostate, liver (Zhao, Wei et al. 2007; Xu, Yao et al. 2009), breast, colon, lung (Wang, Dong et al. 2010) and ovaries (Steinhardt, Gayyed et al. 2008), whereas, LATS2 is significantly downregulated in cancers of the breast (Takahashi, Miyoshi et al. 2005), prostate (Powzaniuk, McElwee-Witmer et al. 2004), brain (Jiang, Li et al. 2006) and various blood-born cancers (Jimenez-Velasco, Roman-Gomez et al. 2005).

FOXP3 has been reported to directly bind and upregulate *LATS2* in human prostate and breast epithelial cells. Li et al (Li, Wang et al. 2011) stained human tumours for FOXP3 and LATS2 and demonstrated that 71% of FOXP3 positive tumours also expressed LATS2, whereas, only 46% of FOXP3 negative tumours expressed LATS2. The same report (Li, Wang et al. 2011) used FOXP3-inducible MCF-7 cells to demonstrate that following FOXP3 induction, *LATS2* transcripts were increased 10-fold after 3 days. Further evidence was provided when a major reduction of *LATS2* transcripts was witnessed following FOXP3 knockdown in TSA (mouse breast cancer cell line) and MCF-10A cells, whereas, an increase in YAP phosphorylation was reported when FOXP3 was transfected into 293 cells (Li, Wang et al. 2011).

This demonstrates that FOXP3 regulates the phosphorylation of YAP by directly regulating *LATS2* expression.

1.7.9.2 *BRCA1*

Li et al (Li, Katoh et al. 2013) demonstrated that FOXP3 directly binds and represses the expression of *BRCA1* and that silencing of FOXP3 in human sarcoma cells increased the rate of DNA repair. This suggests that FOXP3 is able to inhibit DNA repair and suggests that in contrast to other reports demonstrating the strong tumour suppressor properties of FOXP3, it may also work to promote tumorigenesis.

The influence of FOXP3 on *BRCA1* expression was further validated using several lines of evidence by Li et al (Li, Katoh et al. 2013). Firstly, silencing of FOXP3 in MCF-10A cells resulted in an increase in *BRCA1* transcripts and protein, whereas induction of FOXP3 in MCF-7 cells also resulted in a decreased expression of *BRCA1* transcripts and protein (Li, Katoh et al. 2013). Similar findings were witnessed in mammary cells isolated from scurfy mice which also had increased levels of *BRCA1* (Li, Katoh et al. 2013). The ability of FOXP3 to repress *BRCA1* activity was tested in 10 breast and prostate cancer samples which had FOXP3 missense mutations. Results demonstrated that all samples had significantly reduced ability to repress the *BRCA1* promoter (Li, Katoh et al. 2013).

Radiation is used in therapies for approximately 50% of cancer patients (Delaney 2005; Begg, Stewart et al. 2011). Despite this, many malignancies acquire resistance to irradiation (Delaney, Jacob et al. 2005; Bhide and Nutting 2010). Irradiation works by inducing DNA damage and initiating apoptosis to cancer cells. However, because the main role of *BRCA1* is involved with DNA repair, Li et al (Li, Katoh et al. 2013) investigated whether the ability of FOXP3 to control *BRCA1* has any correlation with radiotherapy-resistance in cancer patients. TSA cells were transfected with; FOXP3 shRNA, *BRCA1* shRNA, FOXP3/*BRCA1* shRNA or scrambled shRNA. Each cell was then exposed to irradiation or not. They then measured tumour cell survival using a colony forming assay to investigate the colony growth after these effects.

FOXP3 silencing in cells which were not exposed to irradiation had no effect however, if these cells were subjected to irradiation, at all doses, there was a

significant increase in the number of colonies (Li, Katoh et al. 2013). This therefore demonstrates that the presence of FOXP3 is required for the effects of irradiation through the direct repression of *BRCA1* and that a lack of FOXP3 in cancer cells can increase the chances of radio-resistance in cancer therapy.

1.7.10 Regulation of FOXP3

Despite an increasing interest in FOXP3 in both cancer and immunological research, much work has focused on various downstream targets of the transcription factor, whereas, the underlying mechanisms which regulate FOXP3, particularly in epithelial cells, remain undefined. T-cell biology has produced a number of reports which have highlighted several mechanisms involved in the transcription of FOXP3.

The *FOXP3* promoter region is located approximately -6200bp upstream of the transcriptional start site. This region contains sequences specific for six NFAT and AP-1 binding sites, TATA sequences and CAAT boxes (Mantel, Ouaked et al. 2006). This promoter is highly conserved between mice and humans.

At an epigenetic level it has been relatively well reported that methylation of CpG sequences within the promoter region of genes inhibits acetylation of histones and binding of transcription factors to DNA, whereas, demethylation of CpG sequences and the acetylation of histones are features of activated genes. Reports suggest that control of FOXP3 occurs by a similar mechanism involving the methylation status of CpG sequences in the promoter of FOXP3 (Janson, Winerdal et al. 2008).

The epigenetic regulation of CpG methylation at specific sites in T-cells is a key factor involved in differentiation of T-cells (Lee, Fitzpatrick et al. 2001; Lee, Kim et al. 2006; Wilson, Rowell et al. 2009).

It has been reported that in naïve $CD4^+CD25^-$ T-cells, approximately 10-45% of CpG motifs in the proximal *Foxp3* promoter are methylated, whereas all were demethylated in natural Tregs (Kim and Leonard 2007). Further importance of methylation at the proximal promoter is suggested as Kim et al (Kim and Leonard 2007) demonstrated that in $CD4^+CD25^{lo}$ cells this site was approximately 70% methylated, whereas, in the $CD4^+CD25^{hi}$ cells only approx 5% were methylated.

Methylation of these sites within the *FOXP3* promoter can block the binding of transcription factors which have been reported to be involved in the activation of FOXP3 such as CREB and ATF (Kim and Leonard 2007).

Several reports have now demonstrated that conventional CD4⁺ T-cells are able to transiently upregulate FOXP3 following activation through the T-cell receptor (TCR) (Morgan, van Bilsen et al. 2005; Gavin, Torgerson et al. 2006; Tran, Ramsey et al. 2007). The level of FOXP3 expression after activation is thought to be comparable to that of resting Tregs but is significantly lower than that of a similarly activated Tregs (Allan, Crome et al. 2007). Moreover, the expression of FOXP3 in these cells is only transient and is unable to convey a suppressive phenotype as these cells fail to suppress T-cell division and cytokine production (Morgan, van Bilsen et al. 2005; Gavin, Torgerson et al. 2006).

These findings demonstrate that conversion of CD4⁺ T-cells to acquired Tregs requires more than just FOXP3 expression and is perhaps more dependent on the magnitude and the stability of FOXP3 expression.

As well as the epigenetic control of FOXP3, various reports have also investigated the extrinsic regulation of FOXP3 by various cytokines, such as IL-2 and TGF- β (discussed in section 3.1.2) and antibiotics demonstrating that it can be regulated at both an epigenetic level and a genetic level. A good example of this is NK-cells which do not express FOXP3, are able to upregulate and express FOXP3 when they are treated with a DNA methylation inhibitor 5-aza-2'deoxyctidine (Zorn, Nelson et al. 2006).

The notch pathway has been reported in various stages of T-cell maturation and also FOXP3 transcription (Anastasi, Campese et al. 2003; Vigouroux, Yvon et al. 2003). Blockage of the Notch pathway using anti-Notch1 antibodies is capable of inhibiting the suppressor function of Tregs *in vitro* (Asano, Watanabe et al. 2008). Interestingly, Notch1 signalling is thought to control FOXP3 expression in a bi-phasic manner as low magnitude notch signalling resulted in activation of the FOXP3 promoter via a notch intracellular domain (NICD)-RBP-J complex, however high magnitude signalling repressed the promoter via HES1 (hairy-enhance of split 1) (Ou-Yang, Zhang et al. 2009).

IL-6, which acts as an inflammatory cytokine, also is thought to influence FOXP3 expression indirectly as it is able to suppress the development and function of Tregs (Lal, Zhang et al. 2009). A report by Lal et al (Lal, Zhang et al. 2009) demonstrated that IL-6 is able to induce DNMT1 expression. This is then able to induce STAT3-dependant methylation of the FOXP3 enhancer by DNMT1 in Tregs which results in the repression of *Foxp3* in these cells (Lal, Zhang et al. 2009).

A report by Tone et al (Tone, Furuuchi et al. 2008) published data which demonstrated that Smad3 and NFAT work in cooperation to activate FOXP3 expression. They showed that NFAT bound to the FOXP3 enhancer, whereas, Smad3 was responsible for the regulation of the enhancer activity and that subsequent FOXP3 induction is dependent on the binding of Smad3 and NFAT to the 5' enhancer of *FOXP3*.

As discussed in section 1.4.5.2, p53 is one of the most well known TSG involved with cancer. Interestingly, FOXP3 has been suggested as a potential direct target of p53 in breast cells. Jung et al (Jung, Jin et al. 2010) used chIP which suggested that one motif approximately -1408bp to -1399bp from the transcriptional start site of FOXP3 shared strong homology with the binding consensus sequence of p53 (Jung, Jin et al. 2010). This indicates that the regulation of FOXP3 by p53 could be direct and the tumour suppressor function and induction of FOXP3 in breast epithelial cells is largely regulated and dependant on functional p53.

Lymphocyte-specific protein tyrosine kinase (LCK) is a member of Src family of non-receptor protein tyrosine kinases which is predominately expressed in T-cells, however, it is also present in normal breast tissue and breast cancer cell lines (Koster, Landgraf et al. 1991). A recent report by Nakahira et al (Nakahira, Morita et al. 2013) identified LCK as a binding partner of FOXP3. LCK is able to upregulate FOXP3 in breast cancer cell lines by phosphorylating the protein at tyrosine-342 (Tyr-342) (Nakahira, Morita et al. 2013).

1.8 Hypothesis of the study

The majority of breast cancer mortality is due to the metastatic dissemination of the primary tumour to organs more imperative to maintaining life such as the lungs, bone marrow, and brain.

FOXP3 is a transcription factor recently demonstrated to be expressed within the nucleus of epithelial cells of specific organs. Within these cells it has been demonstrated to act as a potent TSG repressing the expression of several oncogenes including *HER2*, *SKP2*, and *MYC*. In correlation it has also been widely reported that within most aggressive forms of breast cancer, FOXP3 is found to be downregulated, often mutated, or restricted to the cytoplasm. Chemokines such as CXCL12 and chemokine receptors such as the CXCL12 ligand CXCR4 has been heavily implicated in breast cancer metastasis due to their roles in cell migration and invasion. Normal breast epithelia fail to express chemokine receptors, whereas, approximately 80% of primary breast tumours upregulate CXCR4. Moreover, the CXCR4 positive breast cancer cells frequently metastasise to sites in the body most enriched with CXCL12 which are the lymph nodes, lungs and bone marrow. These sites are also the most common sites of metastasis.

This study was designed to test the hypothesis that the presence of constitutive nuclear FOXP3 in mammary epithelial cells is important in preventing tumour metastasis by regulating the expression of key oncogenes and specific chemokine receptors which enhances the cells ability to migrate and invade in response to ligand. This may provide a potential mechanism for chemokine-mediated breast cancer metastasis.

1.9 Aims of the study

- Investigate the expression, distribution and potential mutations in FOXP3 within breast cancer cell lines and normal mammary epithelial cells.

- Investigate the transcriptional, proteomic and functional consequences of restoring FOXP3 into an invasive breast cancer cell line and also effects following knockdown of wild type FOXP3 in HMEpC.

- Investigate potential correlations between FOXP3 and CXCR4 expression in breast cancer samples in patients with aggressive and progressive cancer and patients in early disease development.

Chapter

General introduction 1

General materials and methods 2

Study of FOXP3 expression in normal and malignant breast cell lines 3

In vitro modelling of FOXP3 expression in normal and malignant breast cell lines 4

In vivo levels of FOXP3 and CXCR4 expression in breast cancer samples 5

Discussion 6

List of references 7

Appendices 8

2 General materials and methods

2.1 Cell lines

2.1.1 Human mammary epithelial cells

Human mammary epithelial cells (HMEpC) were purchased from Invitrogen (Paisley, UK). HMEpC are a primary cell line isolated from reduction mammoplasty tissue. Before delivery the cells are tested for the expression of normal mammary cell markers including cytokeratins 5, 6, 8, 18 and E-cadherin. An independent laboratory confirmed the complete absence of Hepatitis B, C and HIV-1 viruses.

2.1.2 MCF-7

MCF-7 was provided by the University of Texas, MD Anderson Cancer Center (Houston, TX, USA). MCF-7 is an immortalised human breast adenocarcinoma cell line derived from the pleural effusion of a 69-year-old Caucasian female in 1970. The woman previously underwent two mastectomies in a five-year span. The tissue removed at the first mastectomy was benign, but the second mastectomy revealed a malignant adenocarcinoma. Over three years she was treated with radiotherapy and hormone therapy for local recurrences. *In vivo* these cells are capable of forming primary tumours in nude mice but they are incapable of penetrating a collagen fibroblast matrix and have a low activity in a boyden chemo-invasion assay (Soule, Vazquez et al. 1973). MCF-7 are therefore considered as low-to-non invasive *in vitro*.

2.1.3 MDA-MB-231

MDA-MB-231 was provided by the University of Texas, MD Anderson Cancer Center. MDA-MB-231 is an immortalised human breast adenocarcinoma cell line derived from the pleural effusion of a 51-year-old Caucasian female in 1973. The patient underwent a mastectomy and radiotherapy before removal of the specimen.

MDA-MB-231 has a 23-hour doubling time and therefore grow rapidly. MDA-MB-231 will form mammary and metastatic tumours in nude mice, are extremely active in both chemotaxis and chemo-invasion assays, and are considered highly invasive *in vitro* and *in vivo* (Cailleau, Young et al. 1974).

2.1.4 Validation of immortalised cancer cell lines

Immortalised cancer cell lines were validated by STR (short tandem repeats) DNA fingerprinting using the AmpF STR Identifier kit (Applied Biosystems, Paisley, UK) according to manufacturers instructions. STR fingerprinting is a popular method required by many journals to validate cell lines. STR are regions of microsatellite instability with defined tri- or tetrad-nucleotide repeats located throughout the chromosome. PCR reactions using primers on non-reactive flanking regions generate products of varying sizes depending on the number of repeats they contain in the region. When between 8 and 16 of these STR loci are combined it is possible to identify the sample.

The STR profiles were compared to known ATCC fingerprints (ATCC.org), and to the Cell Line Integrated Molecular Authentication database (CLIMA) version 0.1.200808 (<http://bioinformatics.istge.it/clima/>) (Nucleic Acids Research 37:D925-D932 PMID: PMC2686526). The STR profiles matched known DNA fingerprints or were unique.

2.1.5 Flp-InTM T-RexTM Human embryonic kidney-293 cells

The transfected human embryonic kidney-293 cell line (referred to as HEK) was a gift from Dr Marcin Pekalski (Cambridge University, UK). This system was generated from the Flp-InTM T-RexTM 293 cell line purchased from Invitrogen. This system allows the generation of stably transfected cell lines that have homogeneous expression of a protein of interest within the Flp-InTM expression vector. These tetracycline repressor expressing cells contain an integrated Flp recombination target (FRT) site which allows stable genomic incorporation of a specific gene. The control of this gene is then governed by tetracycline presence. Transfected HEK cells were

grown in complete Royal Park Memorial Institute (RPMI) medium (Sigma-Aldrich, Dorset, UK) containing 10% Foetal Bovine Serum (FBS) (Lonza, Slough, UK) which was sterile filtered through a 0.22µm pore sterile syringe filter, (VWR international, Leicestershire, UK), 100U/ml penicillin, 100µg/ml streptomycin, and L-glutamine (200mM) (Sigma-Aldrich) in culture flasks. Hygromycin B (100µg/ml) (Sigma-Aldrich) was used a selection antibiotic to select transfected cells. The expression of FOXP3 was induced by tetracycline (Tet) (100µg/ml) (Sigma-Aldrich). A schematic overview of the Tet-on mechanism is provided in **figure 2.1**. Briefly, the Flp-InTM T-RexTM operator system works utilising a plasmid which contains Tet operator sequences (TetO2). The construct also transcribes for the production of Tet repressor Proteins (TetR) which are capable of homo-dimersing and binding to the TetO2 sequences which are directly upstream of the gene of interest, in this case FOXP3. Once the TetR proteins are bound to the TetO2 sequences these blocks and prevents the transcription of the gene. The presence of tetracycline in the growth culture is able to bind to the TetR which causes a conformational change and prevents the TetR from being able to bind to the TetO2 sequences and thus allows transcription of FOXP3.

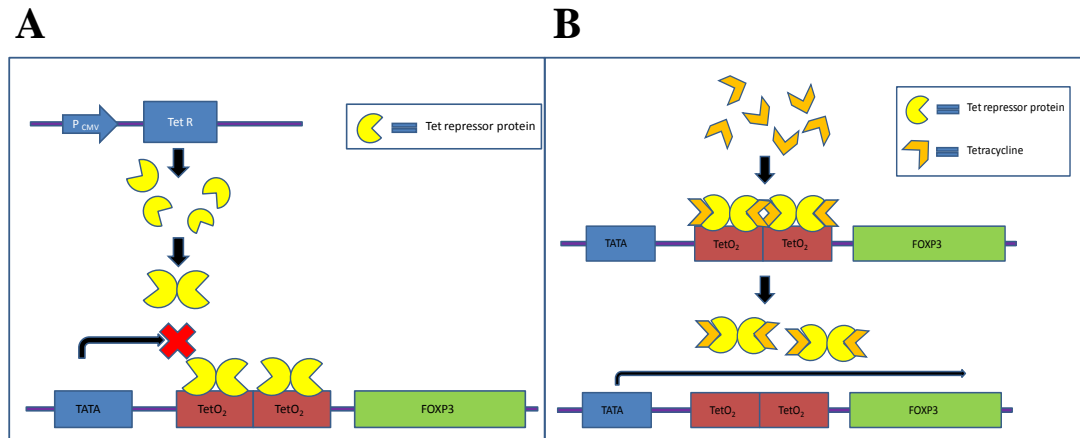


Figure 2-1 - Schematic representation of Flp-In™ T-Rex™ system

In the absence of tetracycline (**A**), Tet repressor gene encodes for the tetracycline repressor proteins. These proteins homodimerise and bind to TetO₂ sequences which prevent the transcription of the *FOXP3* gene. When tetracycline is present (**B**), it binds to the homodimerised Tet repressor proteins which causes a conformational change in the shape. This prevents the Tet repressor proteins from binding to the tetO₂ sequences and allows the transcription of *FOXP3* to occur.

2.2 Cell culture methods

All cell culture methods were performed within class II laminar flow hoods in sterile conditions with equipment which was autoclaved prior to use. All cell lines and chemicals had the relevant COSHH and bioCOSHH forms signed prior to use.

2.2.1 Cryopreservation of cells

Cells were routinely cryopreserved in liquid nitrogen for long term storage. Cells were centrifuged to pellet and then resuspended in 90% FBS (sterile filtered through 0.22µm filter) and 10% dimethyl sulphoxide (DMSO) (Sigma-Aldrich) in a final volume of 1ml. The suspension was then transferred to a cryogenic vial which is placed in an isopropyl alcohol freezing medium and transferred to a -80°C freezer to cool the vials at 1°C/minute. The gradual freezing process prevents the cells from being “shocked” after taken from room temperature to a freezing temperature and therefore improves cell viability when the cells are re-cultured. When cells had been stored at -80°C for approximately 6 hours they can be transferred to liquid nitrogen for long-term storage. Cells were recovered by rapid thawing of the vial at 37°C and centrifuged to pellet in 10ml of their appropriate growth medium. Cells were then resuspended in growth medium and cultured appropriately.

2.2.2 Cell counting

Some experiments require a specific number of cells to be used. Prior to these experiments, cells were mixed at an equal ratio with trypan blue (Sigma-Aldrich) to determine cell viability and counted using an improved Neubauer haemocytometer (VWR, international). Only viable cells were considered in cell counts. Cells located within each 4 corner grids and centre grid of the 25 square grid were counted. The cell number was divided by 0.02 and multiplied by 1000 to obtain the number of cells/ml. To find the total number of cells, this number was multiplied by the total volume the cells were resuspended in. These fields were counted twice and the average was taken to avoid error.

2.2.3 Growth media for immortalised cell lines

MCF-7 and MDA-MB-231 were cultured in Dulbeccos Modified Eagle Media (DMEM) without phenol red (Sigma-Aldrich,) supplemented with 10% FBS which was sterile filtered through a 0.22µm pore sterile syringe filter, 100U/ml penicillin, 100µg/ml streptomycin, and L-glutamine (200mM) in culture flasks.

2.2.4 General maintenance of immortalised cell lines

Adherent cells were seeded into either 25cm² (T25) or 75cm² (T75) vented flasks (Greiner Bio-One, Gloucestershire, UK) and cultured in normal growth conditions within a 37°C humidified incubator with 5% CO₂ in a horizontal position. The cells were split at a ratio of 1:3 when they were approximately 80-90% confluent. Medium was changed as required. Adherent cells were detached from the surface of the flask by washing the cells in phosphate buffer saline (PBS) (Sigma-Aldrich) followed by incubation at 37°C for 3-5 minutes with 1mM Trypsin-EDTA solution (Sigma-Aldrich). Complete growth media containing 10% FBS was added to inactivate the trypsin before centrifugation to remove cells from suspension. Cell pellets were re-suspended in an appropriate volume of fresh medium before passage into new flasks.

2.2.5 General maintenance of primary cells

HMEpC were cultured in T25 flasks in normal growth conditions within a 37°C humidified incubator with 5% CO₂. Cells were seeded into T25 flasks at a density recommended by the manufacturers (2.5x10³/cm²). When the cells were at least 50% confluent, growth medium was replaced until the cells reached 90% confluency, which were then passaged into new flasks. Because HMEpC are a primary cell line, they can only undergo a limited number of doublings and must be used at early passage. In this study, HMEpC were not used beyond three passages as cells beyond this stage begun to de-differentiate.

2.2.6 Mycoplasma testing

Mycoplasma is a specific genus of bacteria which lacks a cell wall allowing resistance to antibiotics like penicillin and streptomycin. Mycoplasma cannot be seen by microscopy as they are one of the smallest known cells and have a diameter of approximately 0.15-0.3µm. Mycoplasma is often found in laboratories as a result of contamination from the individual or from cell media. They can induce cellular changes, chromosome alterations and changes in metabolism and growth.

Mycoplasma testing was carried out within the laboratory using mycoAlert™ mycoplasma testing kit (Lonza). This kit is a biochemical test which utilises the activity of mycoplasma enzymes found in the vast majority of the 180 mycoplasma species. Mycoplasma testing was carried out routinely according to the manufacturers protocol. Briefly, 100µl of culture media was incubated with 50µl of mycoAlert™ reagent for 5 minutes. After 5 minutes the luminescence was measured (TD-20/20 turner design luminometer, Promega, Southampton, UK). Next, 50µl of mycoAlert™ substrate was added and left to incubate for a further 10 minutes, followed by a second luminescence reading. A ratio between the first reading and the second reading of more than 1.5 demonstrates mycoplasma presence.

The addition of the mycoAlert™ reagent lyses mycoplasma releasing mycoplasma enzymes. The addition of mycoAlert™ substrate catalyzes the conversion of adenosine diphosphate (ADP) to adenosine triphosphate (ATP) which is detected by luminescence. If these enzymes are not present there will be no increase in the two readings, however, if enzymes are present they will be converted by the mycoAlert™ substrate into ATP, causing a detectable increase in luminescence.

Cells positive for mycoplasma were quarantined in a separate incubator and treated with 0.5µg/ml of mycoplasma removal agent (Abd Serotec, Kidlington, UK). Since this antibiotic does not affect eukaryotic cell growth, mammalian cells can still be grown in the presence of this antibiotic. Contaminated cells were treated in quarantine for one week and re-tested.

2.3 DNA methods

2.3.1 Agarose gel electrophoresis

Agarose gels (1.2%) were prepared by heating and dissolving agarose powder (Bioline, London, UK) in TAE buffer (1L stock consists of 48g Tris base, 11ml acetic acid and 20ml 0.5M EDTA at pH8.0, all purchased from Sigma-Aldrich). After allowing the agarose liquid to cool, ethidium bromide (0.5µg/ml) (Promega) was added to the gel and allowed to set in a plastic casting stand. Ethidium bromide is a DNA intercalating agent which causes DNA to fluoresce under UV light. After setting, the gel was transferred to an electrophoresis tank filled with TAE buffer. DNA Ladders (Fermentas, Sunderland, UK) were used to establish the size of the bands. The nucleic acid was mixed with orange G (10% of final volume) and run at 120V for approximately 1 hour. Following electrophoresis, bands were visualised using an Alpha Imager® Instrument (Alpha Innotech Corporation, San Leandro, CA, USA).

2.3.2 DNA extraction and purification from agarose gel

Extraction of DNA from agarose gels was performed using a QIAquick Gel Extraction Kit (QIAGEN, Manchester, UK). This kit uses silica-binding technology and spin columns and ensures greater than 80% recovery of DNA which is free from primers, nucleotides, enzymes, salts, agarose and ethidium bromide. DNA was extracted according to the manufacturers protocol. Briefly, bands were visualised under UV light and cut out of the gel using a sterile scalpel. The gel was dissolved in an agarase containing buffer (3x the weight of the extracted gel) for 10 minutes in a water bath at 45°C. When the gel had completely dissolved, iso-propanol was added (1x the weight of the extracted gel) to precipitate the DNA, the contents was added to the spin column and centrifuged for 1 minute at 13000xg. This was followed by two wash steps using an ethanol containing buffer, before being eluted from the column into a fresh collection tube using 20µl of an elution buffer.

2.3.3 DNA sequencing

DNA Sanger sequencing was performed at Source Bioscience (Nottingham, UK). Sequencing data was analysed using A Plasmid Editor (ApE) software to align sample sequences against wild type sequences acquired from National Centre for Bioscience Institute (NCBI.gov).

2.4 Polymerase chain reaction

The polymerase chain reaction (PCR) was developed in 1986, with the significance of this technique being fully acknowledged later when Kary Mullis was awarded the Nobel Prize for Chemistry in 1993 (Mullis 2013). PCR is a technique which allows scientists to generate many copies of a specific DNA sequence using *in vitro* reactions. For instance, 25 cycles of PCR increase DNA copies by more than 10^6 .

PCR is based on the fact that DNA polymerases are primer dependant. A pair of primers is designed and synthesised complementary to a sequence of interest on both the coding and complementary DNA strands. The polymerase will then extend these primers past the sequence of interest by incorporating new complementary bases.

A PCR cycle consists of three phases; heating to denature DNA double helices, followed by a cooler temperature which allows the primers to anneal to the DNA along with complementary oligonucleotides. The final phase is another heated step which allows the DNA polymerase enzyme to extend the primers and copy the sequence of interest.

Because the temperatures used are so high it is important that the DNA polymerase enzymes used are thermostable and can withstand high temperatures without denaturing. *Taq* polymerase was used in conventional PCR experiments. *Taq* was originally isolated from hyperthermophilic archaea (*Thermus aquaticus*). It is stable at high temperatures and has an error rate of approximately 1.3×10^{-5} . The *Taq* enzyme used in the reaction is a hot-start enzyme. This means it contains a mixture of *Taq* polymerase enzyme and a monoclonal antibody which binds to the enzyme until a reaction temperature is raised to denature the antibody and release it from the

enzyme. Therefore, an initial 95°C step is required to activate the enzyme before the cycles start.

2.4.1 RNA isolation

Total RNA was isolated from cells using TRI reagent (Sigma-Aldrich) unless specified. All RNA work was carried out with ribonuclease-free and contaminant-free apparatus. All water used in RNA work and analysis was diethyl pyrocarbonate (DEPC) treated. Cells were released from the flask using 1mM trypsin-EDTA as described in 2.2.4. The pellet was resuspended and lysed in 1ml TRI reagent and left for 5 minutes at room temperature. 200µl of chloroform (Sigma-Aldrich) was added and the homogenate was shaken vigorously for 15 seconds, incubated on ice for 2-3 minutes then centrifuged at 12000xg for 15 minutes at 4°C. The aqueous phase was removed and RNA was precipitated by adding an equal volume of iso-propanol (Sigma-Aldrich). This was left to incubate for 15 minutes followed by centrifugation at 12000xg for 10 minutes at 4°C. The supernatant was removed and the RNA pellet was washed and precipitated with 75% ethanol before being centrifuged at 12000xg for 10 minutes at 4°C. The RNA was resuspended in an appropriate amount of DEPC water, and the concentration and quality of RNA was assessed using a nanodrop spectrophotometer (nanodrop ND-1000 spectrophotometer, Thermo Scientific, Waltham, MA, USA).

2.4.2 Nucleic acid quantification

The concentration and quality of the isolated nucleic acid was assessed using the nanodrop spectrophotometer (**figure 2.1**). The spectrophotometer measures three absorbances; the 230nm readout measures organic solvents, the 260nm readout measures nucleic acids and the 280nm readout measure the protein content. The 260/280 ratio provides an estimate of nucleic acid purity. Pure preparations of DNA and RNA have OD_{260/280} values of between 1.8 and 2.0 respectively. Isolated nucleic acid which fell below a 260/280 ratio of 1.8 was not used.

2.4.3 cDNA synthesis

cDNA synthesis was performed using a tetro cDNA synthesis kit purchased from Bioline. cDNA was synthesised according to the manufacturers protocol. Briefly, up to 5µg of total RNA was mixed with 1µl of Oligo dT, 10mM dNTP mix, 5x reverse transcriptase buffer, 1µl ribosafe RNase inhibitor and 200u/µl of MMLV tetro reverse transcriptase. DEPC was used to make a final reaction volume of 20µl. The reaction was incubated at 45°C for 30 minutes followed by 5 minutes of incubation at 85°C to terminate the reaction. cDNA synthesis was carried out using a T100 thermal cycler (BIO-RAD, Hercules, CA, USA).

Prepared cDNA was immediately stored at -20°C. cDNA was not frozen and thawed more than twice to ensure quality was maintained.

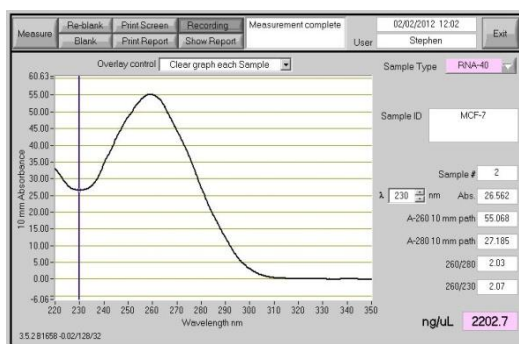
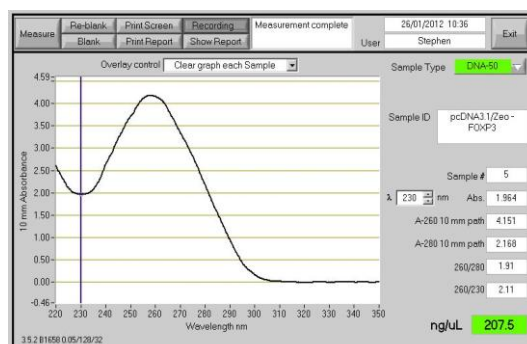
A**B**

Figure 2-2 - Representative images of highly pure plasmid DNA isolated from bacteria and RNA from cell lines.

The nanodrop spectrometer is able to determine the RNA (**A**) and DNA (**B**) purity from cell lines and bacteria can measure the absorbance levels of protein (280nm), nucleic acid (260nm) and the presence of organic solvents (230nm).

2.4.4 Conventional PCR

Conventional PCR was performed using synthesized cDNA in a reaction typically consisting of 5µl of cDNA template, 0.5µg/µl of forward/reverse primers (manually designed and purchased from IDT, [Leuven, Belgium], and listed in section 3.3.3) and 25µl master mix (2x) (Bioline) (consisting of: dNTPs, which provide the nucleotides required to construct each daughter strand after each cycle, divalent cations such as magnesium and monovalent cations such as potassium ions, and a buffer solution to provide the correct chemical environment). The reaction was made up to a final volume of 50µl using DEPC-treated water.

PCR was carried out using a T100 thermal cycler. A typical PCR cycle comprised of; 30 seconds at 95°C to denature, 30 seconds at the optimum temperature for the primers to anneal, followed by 1 minute at 70°C for the elongation of the primers by the polymerase enzyme. The cycles were repeated 40 times and PCR products were ran on 1.2% agarose gels as described in section 2.3.1.

2.4.5 Real-time PCR

In real-time PCR, after the completion of each cycle fluorescence is emitted and measured by a detector which allows determination of the amount of template DNA being amplified as the reaction progresses. This is a key feature in real-time PCR and is the major difference compared to conventional PCR, which is only capable of detecting amplified DNA at the end-point. Real-time PCR allows for both the detection and quantification of DNA, where the quantity can be expressed as absolute number of copies, or relative gene expression when compared to the expression of an endogenous control. Real-time PCR also uses primers and follows the same 3 steps of denaturation, primer annealing and elongation as described in section 2.4.

All real-time PCR was conducted using a StepOnePlus™ PCR machine (Applied Biosystems) using TaqMan® probes (Applied Biosystems). A list of TaqMan® primers used is provided in **table 2.1**.

2.4.5.1 TaqMan® chemistry

TaqMan® chemistry is based around an oligonucleotide probe which has a fluorophore covalently attached to the 5' end and a quencher at the 3' end. The fluorophore used was 6-carboxyfluorescein (FAM) and the quencher was tetramethylrhodamine (TAMRA). The purpose of a quencher is to inhibit fluorescence emitted by the fluorophore which is excited by the cyclor's light source. As long as the quencher is in close proximity to the fluorophore, the degree of auto-fluorescence will be inhibited. The TaqMan® probes are designed so that they will bind to a target sequence of the single stranded DNA which will be amplified by a specific set of primers.

A schematic representation of the principle behind TaqMan® chemistry is provided in **figure 2.2**. Briefly, during the PCR reaction, as the *Taq* polymerase enzyme extends the primers and synthesises a new strand adjacent to the template DNA, the polymerase enzyme will degrade the TaqMan® probe which subsequently breaks the close proximity set between the quencher and the fluorophore and allows the fluorophore to fluoresce which is detected by a source. The specificity of the hybridization between the target sequence and probe is essential to cause fluorescence signals. This therefore reduces both the chance of false positives and background fluorescence.

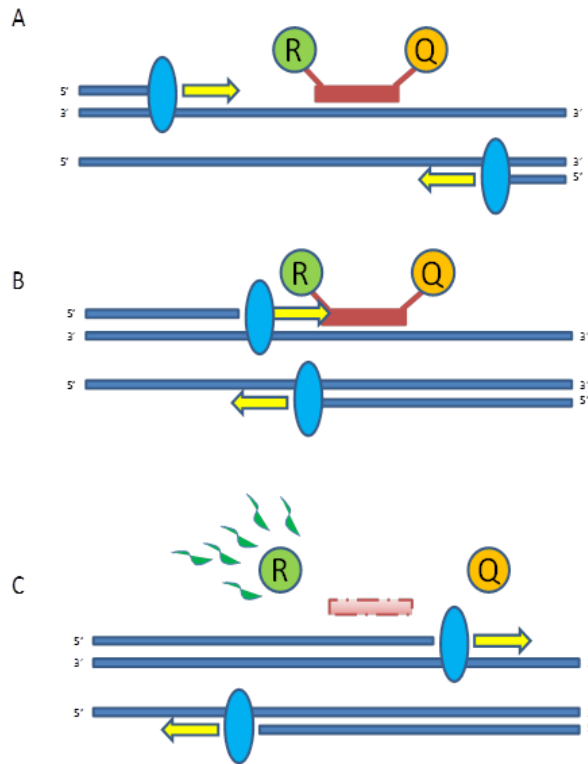


Figure 2-3 - Schematic representation of TaqMan® real-time PCR reaction

TaqMan® probes with FAM fluorochrome (labelled R) and a TAMRA quencher (labelled Q) anneal to specific sequences within the target DNA which are up-stream of the primers (**A**). As the primers extend along the template the polymerase degrades the probes (**B**) and releases the fluorochrome from the proximity of the quencher causing fluorescence (**C**).

Target gene	Assay ID (Applied Biosystems)
<i>GAPDH</i>	H202758991_g1
<i>β-ACTIN</i>	Hs01060665_g1
<i>β-TUBULIN</i>	Hs00258236_m1
<i>FOXP3</i>	Hs01085834_m1
<i>CXCR4</i>	Hs00607978_s1
<i>HER2</i>	Hs01001580_m1
<i>SKP2</i>	Hs01021864_m1
<i>CDKN1A</i>	Hs00355782_m1
<i>MYC</i>	Hs00153408_m1

Table 2-1 - List of TaqMan® primers used in real-time PCR

2.4.5.2 Relative quantification of gene expression

In order to measure changes in the expression of a gene, two methods can be used. A standard curve, or the comparative crossing threshold (Ct). Comparative $\Delta\Delta\text{Ct}$ method was used in all experiments and relies on determining the expression levels of the gene of interest relative to a normal housekeeping gene.

Before carrying out the experiment, the efficiency of primers was assessed using serial dilutions of template cDNA from 1 μl (neat) to 0.0625 μl (1:16) and examining how the Ct varies with the template dilution. The slope of the linear regression witnessed is then used to determine the efficiency of amplification. A number of variables can affect the efficiency of a PCR reaction including length of the amplicon, the quality of the primers and the quality of the cDNA template. Examples of primer validation are included in section 3.4.3 (**figure 3.8**) and section 4.4.6.1 (**figure 4.9**).

When calculating the relative expression of a gene of interest in two or more different samples, one of the samples should act as a reference to normalise against.

The comparative $\Delta\Delta\text{Ct}$ method starts by initially determining the ΔCt of each sample:

$\Delta\text{Ct} = \text{Ct of the gene of interest in each sample} - \text{Ct of the housekeeping gene in each sample.}$

Following this, the $\Delta\Delta\text{Ct}$ of each sample can be calculated. This involves finding the difference between the ΔCt of the test sample and the ΔCt of the normalised sample (or sample to which it is to be compared against):

$\Delta\Delta\text{Ct} = \Delta\text{Ct of gene of interest in sample of interest} - \Delta\text{Ct of the gene of interest in the normalised sample.}$

The final calculation is to determine the comparative expression level of the gene in the sample compared to normalised sample and is done so using the following equation:

Comparative expression level = $2^{-\Delta\Delta\text{Ct}}$.

2.5 Protein methods

2.5.1 Protein extraction

Total protein was isolated from cell lines after being released from culture flasks as described in section 2.2.4. The cell pellet was resuspended in a cell lysis buffer (Ambion, Paisley, UK) which contained protease and phosphatase inhibitors. Cells were mixed every 5 minutes whilst on ice for 20 minutes. The suspension was then sonicated (Soniprep 150 sonicator, MSE, London, UK) on ice, and centrifuged at 15000xg for 20 minutes at 4°C. The supernatant was removed and dispensed into a fresh Eppendorf to be used for future experiments or stored at -20°C for long term storage.

2.5.2 Fractionation of nuclear and cytoplasmic protein

To define the subcellular distribution of FOXP3, the nuclear and cytoplasmic protein contents were separated using a NE-PER® nuclear and cytoplasmic extraction kit (Thermo scientific). Cells in culture were released from the flask as described in section 2.2.4. The pellet was resuspended in a solution, supplemented with protease inhibitors, to cause lysis of the cell membrane, vortexed and incubated on ice for 10 minutes. A second cytoplasmic lysis reagent was added to the reaction and was centrifuged at 16000xg for 5 minutes. The cytoplasmic content within the supernatant was collected into a fresh tube. The nuclear extract within the pellet was resuspended in a third lysis buffer causing nuclear membrane disruption. The reaction was vortexed and centrifuged for 10 minutes at 16000xg. Nuclear contents within the supernatant were placed into a fresh tube.

2.5.3 Protein quantification

Protein in prepared cell lysates was quantified using a Pierce® BCA protein assay kit (Thermo scientific). The assay is based around two chemical reactions. Firstly, peptide bonds in the protein reduce Cu^{+2} from cupric sulphate to Cu^{+1} . This reduction of Cu^{+2} to Cu^{+1} is directly proportional to the amount of protein present in the solution. Following this initial reduction reaction, two molecules of bicinchoninic

acid (BCA) (present in the highly alkaline reagent) chelate with each Cu^{+1} ion to form a purple coloured product which can be measured at 562nm using a microplate reader (DYNEX, OPSYS MR).

A standard curve was prepared in 96-well plates using albumin supplied by the company and was diluted between $0\mu\text{g/ml}$ to $2000\mu\text{g/ml}$. The protein concentration in prepared samples was determined by pipetting $25\mu\text{l}$ of sample into appropriate wells along with $200\mu\text{l}$ of working reagent (50 parts of reagent A containing; sodium carbonate, sodium bicarbonate, bicinchoninic acids and sodium tartrate in 0.1M sodium hydroxide, with 1 part of reagent B containing 4% cupric sulphate). The plate was then mixed thoroughly and incubated for 30 minutes at 37°C . Following incubation, the absorbance of each well was measured at 562nm and the sample concentration was determined by reading off the standard curve (**figure 2.4**).

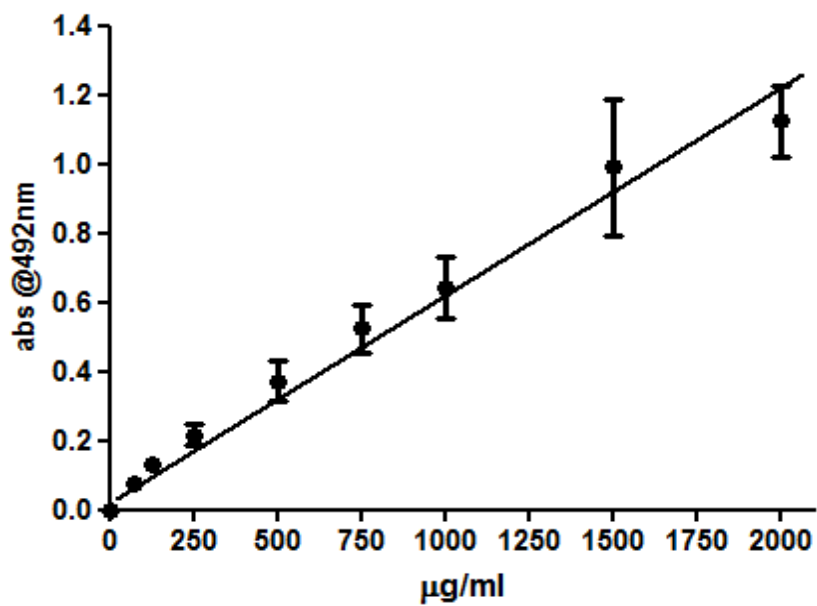


Figure 2-4 - Representative standard curve to determine protein concentration

A standard curve was prepared using Pierce® BCA protein assay kit ranging from 0μg/ml to 2000μg/ml. Protein in samples were quantified by reading off the standard curve. Error bars are representative of mean \pm standard deviation (n=2).

2.5.4 Flow cytometry

Flow cytometry is a technique used to measure the physical characteristics of cells. Cells are suspended in a fluid and passed through the cytometer in a stream of single cells. As the cells pass through the machine they are subjected to a stationary laser light. When the light hits the cells it causes scattering and is deflected off the cells and is detected in two directions. Light which is scattered in the plane of the excitation laser is proportional to the size of the cell and is called forward scatter. Light which is scattered at right angles to the path of the excitation laser is side scatter. Side scatter is proportional to cell granularity.

Flow cytometry utilises antibodies which are conjugated to fluorochromes to detect specific antigens on or in the cells. The detection of these molecules is based on fluorescence which occurs when the fluorochrome is stimulated by light of a particular wavelength. However, the wavelength of the light used for excitation needs to be removed from that of the fluorescence to allow separation of both wavelengths. Dichronic mirrors and optical filters are used to reflect and absorb the light which is deflected into photomultiplier tubes and converted into an electric current. This current is then fed into an amplifier creating a signal which is proportional to the number of photons that reach the photodetector.

All flow cytometry was carried out using a Becton Dickinson FACS canto II flow cytometer (Becton Dickinson, Franklin Lakes NJ, USA). Data was analysed using FlowJo software (Becton Dickinson).

2.5.4.1 Cell surface staining

Cells to be stained were released from culture using trypsin-EDTA, counted and 1×10^6 cells were pelleted by centrifugation at 500xg for 5 minutes in complete growth media. All staining was performed in FACS tubes. Cells were resuspended in 50 μ l of PBS+2% FBS (referred to as FACS buffer) and primary antibody (according to the manufacturers datasheet). Cells were incubated at 4°C for 1 hour with the primary antibody. At the end of the incubation, cells were washed twice in 1ml of FACS buffer and resuspended in 300 μ l of FACS buffer before run on the canto II flow cytometer.

2.5.4.2 Intracellular staining

As a transcription factor, the nuclear localisation of FOXP3 is imperative to its function. Therefore, in order to detect FOXP3, cells must firstly be permeabilised to allow antibodies to pass through the plasma membrane to reach its target. FOXP3 was stained using a FOXP3 staining buffer set (eBioscience, Hatfield, UK). This kit has been formulated and optimised for a number of monoclonal FOXP3 antibodies including PCH101 and 236A/E7.

Intracellular staining was performed following cell surface staining. Cells in FACS tubes were centrifuged at 12000xg to pellet cells. Cells were then fixed and permeabilised using a fix/Perm buffer which contains formaldehyde and a detergent. This buffer was prepared at a 1:3 ratio of fix/perm concentrate to fix/perm diluent. Cells were incubated at 4°C in fix/perm buffer for 30 minutes. Cells were washed in perm buffer followed by 1 hour incubation with the FOXP3 antibody for 1 hour. Cells were washed twice in perm buffer before being resuspended in FACS buffer and ran on the canto II flow cytometer.

The expression of FOXP3 and CXCR4 was assessed by performing cell surface staining followed by intracellular staining. Matched isotype controls which have no relevant specificity were used to separate non-specific staining from the specific antibody staining. The antibodies used are included in **table 2.2**.

2.5.5 Western blot

Western blot is a technique which is used to detect proteins in a sample. It used sodium dodecyl sulphate-polyacrylamide gel electrophoresis (SDS-PAGE) to separate denatured proteins by size. Proteins are then transferred onto a membrane which is then probed with antibodies in attempt to detect specific proteins in the sample. Depending on the experiment, protein was isolated from cells as described in section 2.5.1 or 2.5.2.

Protein samples were prepared in Laemmli loading buffer (12% SDS, 60% [v/v] of 20% glycerol, 30% [v/v] 0.0012% bromophenol blue [all purchased from Sigma-Aldrich], 0.37M Tris-base at pH6.8), β -mercaptoethanol (Sigma-Aldrich) and the

final sample volume was made up to 20µl with distilled water. Each sample was boiled at 100°C for 5 minutes before loading into a 10% acylamide gel with a pre-stained protein ladder (Fermentas).

The gel was then transferred onto a polyvinylidene fluoride (PVDF) membrane (GE healthcare) at 30V overnight in transfer buffer (25 mM Tris, 192 mM glycine, 10% methanol, 0.1% SDS [all purchased from Sigma-Aldrich]). The membrane was then blocked in 5% milk powder in PBS for 3 hours before being incubated at 4°C overnight with the primary antibody (all antibodies used included in **table 2.2**) with 5% milk powder in PBS. The membrane was washed 3 times for 10 minutes in 0.1% PBS/tween (Sigma-Aldrich) followed by incubating at room temperature with a horseradish peroxidase (HRP)-conjugated secondary antibody (included in **table 2.2**) for 1 hour.

The membrane peroxidase activity was detected using ECL (Thermo scientific) and then exposed to photographic film (Koodak). Membranes were stripped using harsh stripping buffer (10% SDS, 0.5M Tris-Hcl [pH 6.8] and 0.8ml β-mercapnoethanol) for 30 minutes at 50°C and then re-probed with the appropriate primary antibody.

2.5.6 Immunofluorescence

Immunofluorescence (IF) was performed on cells grown in chamber slides (5x10⁴ cells/chamber) overnight in normal growth conditions. The next day, growth media was removed and cells were fixed with 4% paraformaldehyde (PFA) for 30 minutes. Following fixation, cells were permeabilised using 0.1% Triton X-100 (Sigma-Aldrich) for 15 minutes at 4°C. Each chamber was then blocked using PBS+5%FBS for 1 hour before being incubated at 4°C overnight with the primary antibody (included in **table 2.2**), which was diluted in PBS+5%FBS. Slides were then incubated with a FITC-conjugated secondary antibody (included in **table 2.2**) for 2 hours at 4°C, then counter stained with 4',6-diamidino-2-phenylindole (DAPI) and mounted using Vectashield (Vector LABORATORIES, Peterborough, UK). Cells were viewed using a Leica fluorescent microscope.

2.6 List of antibodies

Experiment	Target antigen	Reactive species	Species raised in	Company	Isotype	Concentration/ Working concentration
WB/ IF	FOXP3	Human	Mouse	Abcam (Cambridge, UK)	(236A/E7) IgG ₁	1:100
WB	IgG (2°)	Mouse	Rabbit	Sigma-Aldrich	IgG	1:5000
IF	IgG (2°)	Mouse (FITC conjugate)	Goat	Abcam	IgG	1:1000
IF	CK8	Human	Mouse	Santa Cruz	IgG _{2a}	1:250
IF	CK18	Human	Mouse	Santa Cruz	IgG ₁	1:250
WB	Anti-TATA	Human	Mouse	Abcam	IgG ₁	1:1000
WB	β-Actin	Human	Mouse	Sigma-Aldrich	IgG _{2a}	1:5000
Flow cytometry	FOXP3	Human (APC conjugate)	Rat	eBioscience	PCH101 (IgG _{2a} κ)	0.5µg (5µl)
Flow cytometry	-	Human (APC conjugate)	Rat	eBioscience	eBR2a (IgG _{2a} κ)	0.25µg (2.5µl)
Flow cytometry	CXCR4	Human (FITC conjugate)	Mouse	Becton Dickinson	IgG _{2a}	10µl
Flow cytometry	-	Human (FITC conjugate)	Mouse	Biolegend	IgG _{2a} κ	10µl
Flow cytometry	CD3	Human (PE conjugate)	Mouse	Becton Dickinson	IgG _{2b} κ	10µl

Table 2-2 - List of antibodies used in studies

2.7 Statistical analysis

Data was organised and analysed using Microsoft office Excel 2007 and GraphPad Prism 5. Quantitative values were plotted as the mean \pm standard deviation (SD). Unless stated, a direct comparison between two columns was performed using the unpaired Students t-test. Multiple column analysis was performed with one-way ANOVA. Values <0.05 were considered as statistically significant. Outliers from experiments were excluded using the Grubbs' test on Prism.

	Chapter
General introduction	1
General materials and methods	2
Study of FOXP3 expression in normal and malignant breast cell lines	3
<i>In vitro</i> modelling of FOXP3 expression in normal and malignant breast cell lines	4
<i>In vivo</i> levels of FOXP3 and CXCR4 expression in breast cancer samples	5
Discussion	6
List of references	7
Appendices	8

3 Study of FOXP3 expression in normal and malignant breast cell lines

3.1 Introduction

3.1.1 Dysregulated expression of FOXP3 in malignant breast epithelia

The expression of FOXP3 within normal and malignant breast tissue has been investigated by a number of groups. Each group have consistently demonstrated the presence of nuclear FOXP3 within normal mammary epithelial cells (Zuo, Liu et al. 2007; Zuo, Wang et al. 2007; Merlo, Casalini et al. 2009; Wang, Liu et al. 2009; Zhang and Sun 2010; Lal, Chan et al. 2013). However, within the malignant breast cells several scenarios have been described and are summarised within this section.

FOXP3 is well known for its role in the immune system as the master regulator of the development and function of Tregs. Until several years ago it was thought FOXP3 expression was restricted to the lymphocyte lineage. However, it has now been well documented that FOXP3 is also expressed in non-immune cells. Chen et al (Chen, Chen et al. 2008) used Rag2^{-/-} mice and scurfy mice to demonstrate that Foxp3 was expressed at transcript and protein levels in the nucleus of epithelial cells within the breast, prostate and lung. Separate reports have also demonstrated the expression of FOXP3 within ovarian epithelial cells (Zhang and Sun 2010) and the brain (Frattoni, Pisati et al. 2012). Within Tregs, *FOXP3* is expressed at a similar level to housekeeping genes such as *GAPDH*, however, within epithelial cells the expression is significantly lower, approximately 100-fold less than levels found in Tregs (Wang, Liu et al. 2009).

Several studies have investigated the expression and distribution of FOXP3 within human breast epithelial cells and have consistently demonstrated that FOXP3 is expressed constitutively within the nucleus of normal breast epithelial cells (Zuo, Wang et al. 2007; Merlo, Casalini et al. 2009). The expression of FOXP3 within breast cancer samples is slightly more ambiguous. Some cases demonstrated levels

of *FOXP3* which were comparable to normal breast epithelia, whereas, the majority of cases had significantly dysregulated expression of *FOXP3*, being completely absent, downregulated, mutated or being predominately restricted to the cytoplasm of the cells (Zuo, Liu et al. 2007; Zuo, Wang et al. 2007; Merlo, Casalini et al. 2009; Wang, Liu et al. 2009; Zhang and Sun 2010).

Merlo et al (Merlo, Casalini et al. 2009) published a comprehensive report focusing on the subcellular distribution of *FOXP3* from two trials (Milan 1 and Milan 3) amongst a large cohort of breast cancer patients. The Milan 3 trial, which analysed 183 patient samples, revealed that 78 samples had no detectable levels of *FOXP3*, 44 samples were weakly positive, and 61 samples were strongly positive. However, within the samples which stained strongly positive, the majority of samples expressed *FOXP3* predominately restricted to the cytoplasm with very few samples expressing nuclear *FOXP3*. This demonstrates that *FOXP3* is frequently unregulated in breast cancer.

The same authors (Merlo, Casalini et al. 2009) then correlated the localisation of *FOXP3* to the overall survival of the patients. Patients with no detectable levels of *FOXP3* generally had a worse prognosis than those with normal *FOXP3*, situated within the nucleus. Interestingly, patients which had detectable *FOXP3* restricted to the cytoplasm, had a similarly poor, or worse prognosis as the patients with no detectable *FOXP3* (Merlo, Casalini et al. 2009). This suggests that the failure to recruit *FOXP3* to the nucleus could be an important prognostic indicator of aggressive (or the potential to be aggressive) forms of breast cancer.

Another study (Zuo, Wang et al. 2007) analysed the expression of *FOXP3* by IHC in 50 normal breast samples and 275 breast cancer samples. It was found that only 21% of tumours expressed *FOXP3* within the nucleus, whereas, 80% of normal healthy tissues expressed nuclear *FOXP3*. The same report (Zuo, Wang et al. 2007) then analysed the mRNA expression of *FOXP3* in ten breast cancer cell lines and two non-malignant breast cell lines by real-time PCR. The two non-malignant epithelial cell lines expressed relatively normal levels of *FOXP3* and also expressed both natural isoforms. On the other hand, all ten malignant cell lines had significantly fewer *FOXP3* transcripts than the normal cell lines. Moreover, all the malignant cell lines failed to express a full length *FOXP3*, each consistently missing certain exons.

Some cell lines expressed only the FOXP3 Δ 3 isoform, whereas others expressed versions missing exons 3 and 4 and exons 3 and/or 8.

The same study (Zuo, Wang et al. 2007) examined 50 normal and cancerous tissues from matched patients suffering IDC and showed that when cancerous tissues were compared with the normal tissues, 36% showed somatic *FOXP3* mutations. Of these samples, 38% of cases had lost the wild type allele. Moreover, when similar *FOXP3* mutations were witnessed in IPEX patients, they were deemed as important for normal FOXP3 functioning (Ziegler 2006). This data demonstrates the wide spread dysregulated expression of FOXP3 at protein and transcript level within malignant breast epithelial cells.

An alternative report by Lal et al (Lal, Chan et al. 2013) quantitatively assessed the levels of Treg and epithelial cell derived-FOXP3 in 32 breast tumours from DCIS and IDC with synchronous normal epithelial cells. In line with other reports in the literature, Lal et al (Lal, Chan et al. 2013) reported that FOXP3 expressing Tregs significantly increased with malignant progression. However, although this study reported that FOXP3 was expressed within normal breast epithelial cell, they also reported that epithelial cell derived-FOXP3 expression also increased with invasive progression. This demonstrates the slight ambiguity within the literature regarding epithelial cell FOXP3 expression and breast cancer.

3.1.2 Cytokine-driven FOXP3 expression

A number of reports have investigated the effects of FOXP3 expression in T-cells after treatment with various cytokines. The greatest increase in FOXP3 expression was produced by treatment with IL-2 (Zorn, Nelson et al. 2006) and TGF- β (Nishihara, Ogura et al. 2007; Xiao, Jin et al. 2008; Yang, Anderson et al. 2008; Zhou, Lopes et al. 2008). Although recently, Frattini et al (Frattini, Pisati et al. 2012) reported that TGF- β is unable to increase the mRNA or protein levels of FOXP3 in glioblastoma cells, the effect of cytokines on FOXP3 expression in breast epithelial cells remains largely unreported.

3.1.2.1 TGF- β

TGF- β has been evolutionary conserved between vertebrates and invertebrates (Massague, Blain et al. 2000). Although no TGF- β response elements have been identified in or around the *FOXP3* gene, TGF- β has long been identified as a key regulator of FOXP3 expression in Tregs of animals and humans (Yamagiwa, Gray et al. 2001; Schramm, Huber et al. 2004). The effects of TGF- β on the differentiation of T-cells appears to be dose-dependent as low levels of TGF- β are able to promote the development of Th17 cells, whereas, higher concentrations of TGF- β favour the differentiation of FOXP3⁺ Tregs (Nishihara, Ogura et al. 2007; Xiao, Jin et al. 2008; Yang, Anderson et al. 2008; Zhou, Lopes et al. 2008).

Many of the actions of TGF- β are governed through the interactions with Smad proteins as these are classed as signal transducers of TGF- β (Derynck, Zhang et al. 1998). A report by Tone et al (Tone, Furuuchi et al. 2008) discovered a conserved enhancer site within FOXP3 which is able to bind Smad3, therefore, suggesting TGF- β influences FOXP3 expression through Smad3 dependant signalling mechanisms.

Differentiation of naïve CD4⁺ T-cells to acquired (CD4⁺)CD25^{hi}FOXP3⁺ Tregs can be achieved by TGF- β in both mouse and human. In fact, these naïve peripheral T-cells which are activated in the presence of TGF- β or IL-2 are also able to gain an immunosuppressive characteristic both *in vitro* (Chen, Jin et al. 2003; Zheng, Wang et al. 2006) and *in vivo* (Andersson, Tran et al. 2008; Huter, Punkosdy et al. 2008). However, Floess et al (Floess, Freyer et al. 2007) reported that the removal of TGF- β from the environment caused a rapid reduction in FOXP3 expression suggesting that TGF- β is a key mediator of FOXP3 development in induced Tregs.

As previously discussed in section 1.7.10, the methylation status of CpG sites in the promoter of *FOXP3* is key in regulating expression of the *FOXP3* gene in T-cells. Interestingly, TGF- β was demonstrated to cause demethylation at these sites in CD4⁺CD25⁻ T-cells to induce FOXP3 in naïve T-cells, however, the expression of FOXP3 was only transient (Kim and Leonard 2007).

It has also been reported that TGF- β can influence FOXP3 expression via other indirect mechanisms. TGF- β is able to inhibit the phosphorylation of Erk which

results in the inhibition of DNA methyltransferases (DNMT) (Luo, Zhang et al. 2008). The subsequent inhibition of DNMTs in T-cells has been reported to increase the expression of FOXP3, therefore providing an alternative indirect mechanism.

3.1.2.2 IL-2

T-cells express the IL-2 receptor, however, upon antigenic stimulation of the TCR, these cells then secrete IL-2 which provides a feedback loop between IL-2/IL-2 receptor, and promotes cell growth, differentiation and survival (Beadling and Smith 1993; Beadling and Smith 2002).

Studies using different patient populations have consistently demonstrated the effects of IL-2 on FOXP3 expression in T-cells (Sereti, Imamichi et al. 2005; Ahmadzadeh and Rosenberg 2006). Zorn et al (Zorn, Nelson et al. 2006) demonstrated using T-cells from healthy donors that IL-2 caused rapid upregulation of FOXP3 at transcript and protein levels after 2 hours of culture in CD4⁺CD25⁺ T-cells, but not in CD4⁺CD25⁻ cells (Zorn, Nelson et al. 2006). *In vitro* studies often use IL-2 for the expansion of FOXP3⁺ Tregs as these cells, despite not secreting IL-2, require the cytokine to survive. *In vivo* studies have also demonstrated that low doses of IL-2 are capable of expanding Tregs, however, the effects are only transient as removal of IL-2 caused a decrease in Treg numbers (Zorn, Nelson et al. 2006). These effects of IL-2 on FOXP3 expression are governed by IL-2 receptor-mediated signalling cascades which act through JAK (Frank, Robertson et al. 1995). JAKs are able to activate STATs by tyrosine phosphorylation which causes them to dimerise and translocate to the nucleus where they can regulate gene transcription. In particular STAT5 is a key member of the IL-2 signalling pathway. Evidence suggests the effects of IL-2 on FOXP3 could be governed through STAT5 as it has been reported that a deficiency in STAT5 leads to autoimmunity because of a lack of natural Tregs (Tsuji-Takayama, Suzuki et al. 2008; Tsuji-Takayama, Suzuki et al. 2008). *In vitro* studies have demonstrated that STAT5a/b directly bind to the *Foxp3* gene and were required for the induction of gene expression (Snow, Abraham et al. 2003; Yao, Kanno et al. 2007; Passerini, Allan et al. 2008). Further evidence of IL-2 signalling-mediated induction of FOXP3 involving both JAK and STAT pathways, is provided as mice with JAK3 knockout have a complete lack of FOXP3⁺ cells (Mayack and Berg

2006), whereas, STAT5 knockout mice have strongly reduced FOXP3 expression (Yao, Kanno et al. 2007). Interestingly, IL-2 is not the only cytokine to induce STAT5 signalling. Studies have since demonstrated that IL-7 and also IL-15 can phosphorylate STAT5 which subsequently results in increased transcription of FOXP3 in Tregs (Bayer, Lee et al. 2008; Mazzucchelli, Hixon et al. 2008).

3.2 Aims and objectives

- To confirm the tetracycline-inducible expression of *FOXP3* in transfected HEK cells and validate these cell lines as good positive and negative controls for *FOXP3*.
- To quantitatively determine the expression levels of *FOXP3* protein and transcripts in breast cancer cell lines and HMEpC.
- To investigate the subcellular distribution of *FOXP3* protein in breast cancer cell lines and HMEpC.
- To investigate potential mutations and/or alternative splice variant isoforms of *FOXP3* within breast cancer cell lines.
- To investigate the effects of IL-2 and TGF- β on *FOXP3* expression in breast cancer cell lines.

3.3 Specific materials and methods

3.3.1 Protein dialysis

Before use, protein lysates from cell lines underwent dialysis to remove low molecular weight contaminants such as detergents which could interact and affect results. The membranes in the dialysis cassettes (Slide-A-Lyzer[®] Dialysis cassettes, Thermo Scientific) are composed of low-binding regenerated cellulose and have a sealed sample chamber which maintains high sample retention. The cassettes were hydrated for 2 minutes, and then the excess liquid was removed gently by tapping the edge of the cassette. Each sample was added slowly to separate cassettes using a syringe. The samples were then dialysed overnight at room temperature in dialysis buffer containing 25% acetic acid. The sample was removed from the cassette by initially injecting a small pocket of air to separate the membranes, then gently collecting the sample by injecting air into the cassette to make a pocket and extract the liquid via a needle.

3.3.2 ELISA

A pre-coated human FOXP3 ELISA kit (Biorbyt, Cambridge, UK) was used to quantify FOXP3 protein expression in cell lines. Samples and controls were prepared to contain 20µg of protein in 100µl. FOXP3 quantification was performed according to the manufacturers protocol. Briefly, samples and standards were added to individual wells and incubated at 37°C for 2 hours. Liquid was then removed from the wells and a reagent containing a biotin-conjugated polyclonal antibody was added and left to incubate for 1 hour at 37°C. Excess reagent was removed from each well before being washed three times in ELISA wash solution. Next a reagent containing avidin conjugated to HRP was added to each well and incubated for 30 minutes at 37°C. Excess reagent was removed from wells before washing with an ELISA wash buffer a further three times before finally adding 3,3',5,5'-Tetramethylbenzidine (TMB) and incubating for 25 minutes at 37°C. The reaction between TMB and HRP is based on TMB acting as a hydrogen donor in reducing hydrogen peroxide to water by the presence of peroxidase in HRP. This results in a blue coloured solution which can be measured at wavelengths of 650nm. The addition of sulphuric acid stopped the

reaction and turned the TMB solution a stable yellow colour which can be measured at 450nm. The intensity of the yellow product is proportional to the FOXP3 concentration in the sample. The absorbance was measured using a microplate reader at 450nm. A schematic representation of the test principle is provided in **figure 3.1**. FOXP3 concentration was determined by plotting absorbance against the prepared standard curve (**figure 3.2**).

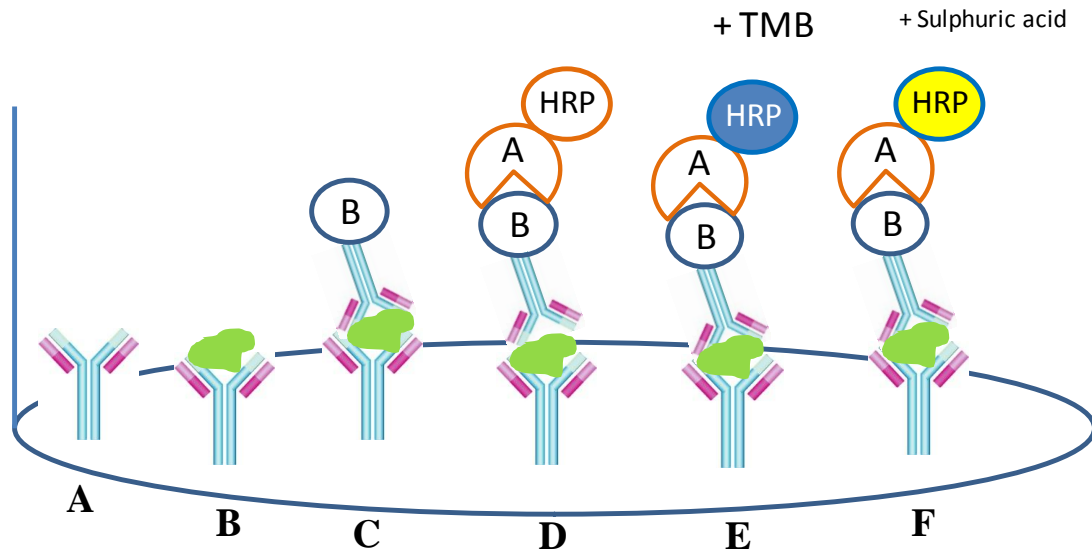


Figure 3-1 - Test principle of FOXP3 ELISA

Each well is coated with a monoclonal antibody specific for human FOXP3 (**A**) which will detect and bind any FOXP3 present in the sample lysates (**B**). A reagent which contains a secondary antibody directly conjugated to biotin is then added to each well (**C**) followed by a reagent containing avidin-HRP (**D**). When TMB is added to the well, it oxidises to TMB diimine resulting a blue colour change (**E**). Sulphuric acid is added to cease the reaction and cause a stable yellow colour change (**F**) which is measured using a microplate reader at 540nm.

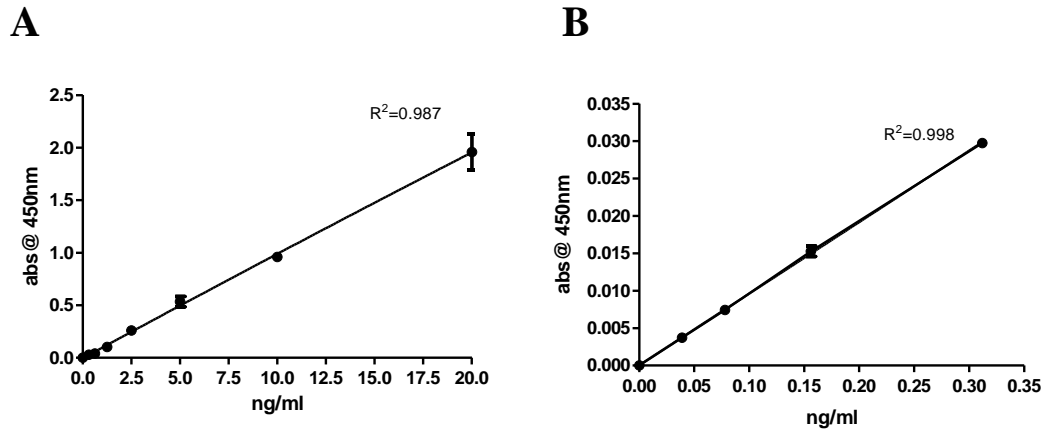


Figure 3-2 - Standard curves for FOXP3 ELISA

A FOXP3 standard curve was constructed using seven points of concentration. Standard concentration points were prepared by reconstituting standard concentrate with the provided diluent producing a double dilution series ranging from 20ng/ml to 0.312ng/ml and a blank sample (0ng/ml) (A). A separate curve was produced which further diluted the 0.312ng/ml sample producing four further points to determine test sensitivity at concentrations below 0.312ng/ml (B).

3.3.3 Primer design

All primers were manually designed and purchased from IDT. Information for each primer is listed in **figure 3.3**. Primers are generally 15 to 30 base pairs in length and have a large degree of homology with the target sequence. The melting temperature of a primer is one parameter which dictates the primer to template DNA stability. This melting temperature is the temperature when one half of a DNA duplex will dissociate and becomes single stranded. Primers with melting temperatures between 52-58°C generally produce best results; temperatures over 65°C increase the risk of secondary annealing. The actual melting temperature is heavily influenced by several parameters including concentrations of magnesium, potassium and co-solvents, however, a simple formula for calculating the melting temperature is;

$$T_m = 4(G+C) + 2(A+T) ^\circ C.$$

The primers should have a G/C content of approximately 50% of the primer sequence. Because the annealing temperature for the reaction can only be held at one temperature, the G/C content determines annealing temperature for the reaction. Therefore, the forward and reverse primers should have approximately the same G/C percentage content to produce a compatible annealing temperature. Typically, this is no more than 5°C difference. To ensure that designed primers are specific only for the sequence of interest, a BLAST search was carried out on each primer used (<http://blast.ncbi.nlm.nih.gov/Blast.cgi>).

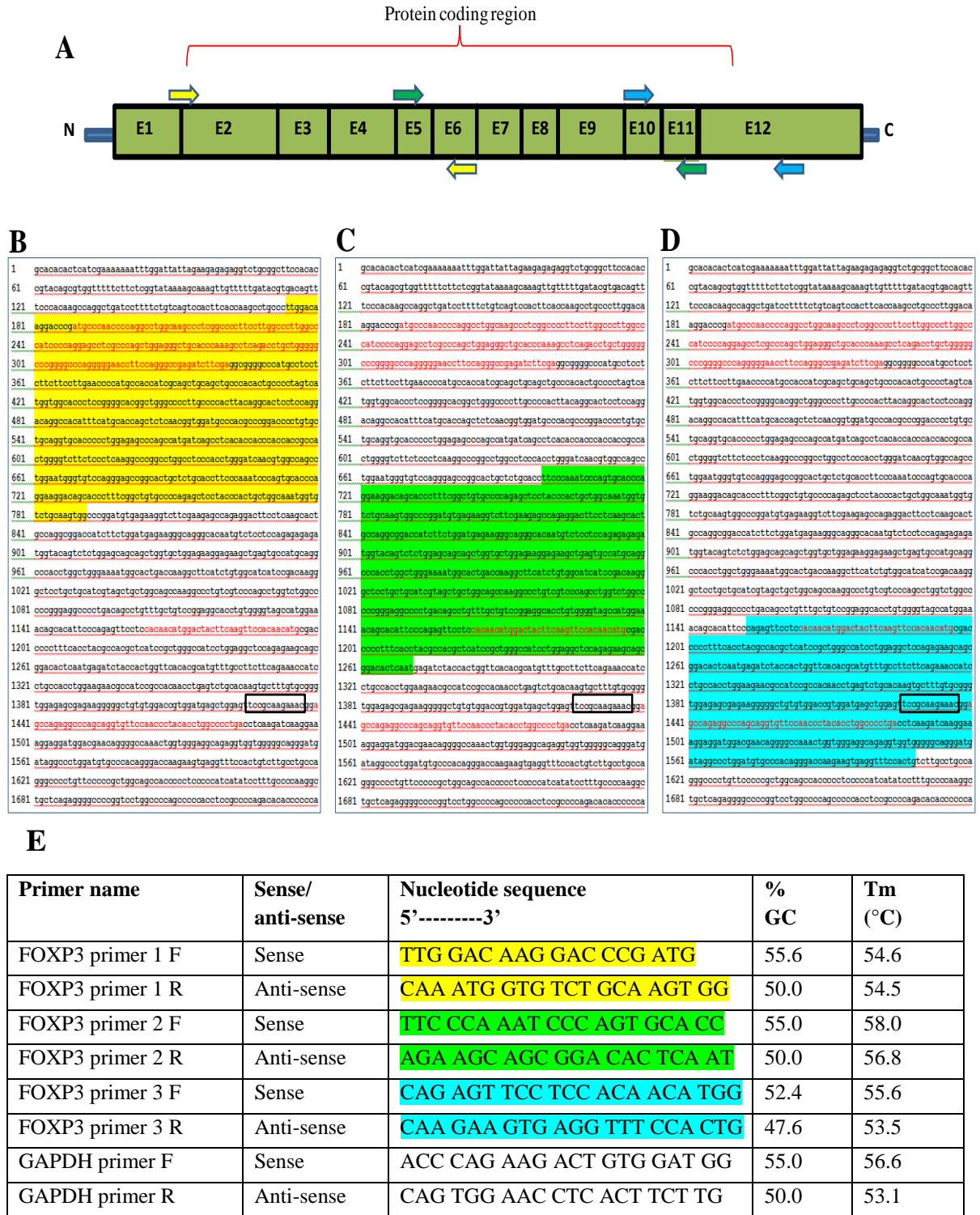


Figure 3-3 - Manually designed primers for *FOXP3* sequencing

Three sets of *FOXP3* primers were designed to span the entire *FOXP3* protein coding domain. Sequences in red regions highlighted represent the 3 NLS regions identified by Hancock and Ozkaynak (Hancock and Ozkaynak 2009). **Panel A:** Schematic diagram of the forward and reverse primer locations on *FOXP3*. **Panel B;** sequences covered by 1st primer set, **panel C;** sequences covered by the 2nd primer set and **panel D;** sequences covered by the 3rd primer set. Black boxes represent the RKKR sequence identified by Lopes et al (Lopes, Torgerson et al. 2006) as responsible for nuclear localisation. The Table (**panel E**) represents the information for each primer set.

3.4 Results

3.4.1 Characterisation of inducible FOXP3 in transfected HEK cells

The transfected HEK system utilises the presence of tetracycline to induce the expression of FOXP3 (as described in section 2.1.5). Cells cultured with tetracycline to induce FOXP3 expression are referred to as HEK+'ve Tet, whereas, HEK cells cultured without tetracycline are referred to as HEK-'ve Tet. The construct also confers the ability to resist the antibiotic Hygromycin B, therefore, cells which are stably transfected have correctly integrated the plasmid into their genome and can be successfully grown in the presence of 100µg/ml Hygromycin B.

The ability of transfected cells to induce FOXP3 was determined using IF and Western blot (**figure 3.4 panel A and B**). Wild type HEK cells do not naturally express FOXP3. Cells successfully cultured in Hygromycin B similarly expressed no detectable expression of FOXP3, however, following the addition of tetracycline to the growth culture, there was a rapid increase in FOXP3 expression in these cells. When the nuclear and cytoplasmic fractions from these cells were isolated, results demonstrated that FOXP3 was exclusively expressed within the nucleus (**figure 3.4 panel C**).

The specificity of tetracycline-mediated FOXP3 induction in these cells was demonstrated when tetracycline was removed from the media, the FOXP3 expression declined in a time-dependant manner (**figure 3.5**). Despite a marked decrease, FOXP3 was still detectable 72 hours after tetracycline removal, however, expression levels returned to a non-detectable baseline level by 96 hours. Transfected HEK cells were used as positive and negative controls for subsequent experiments.

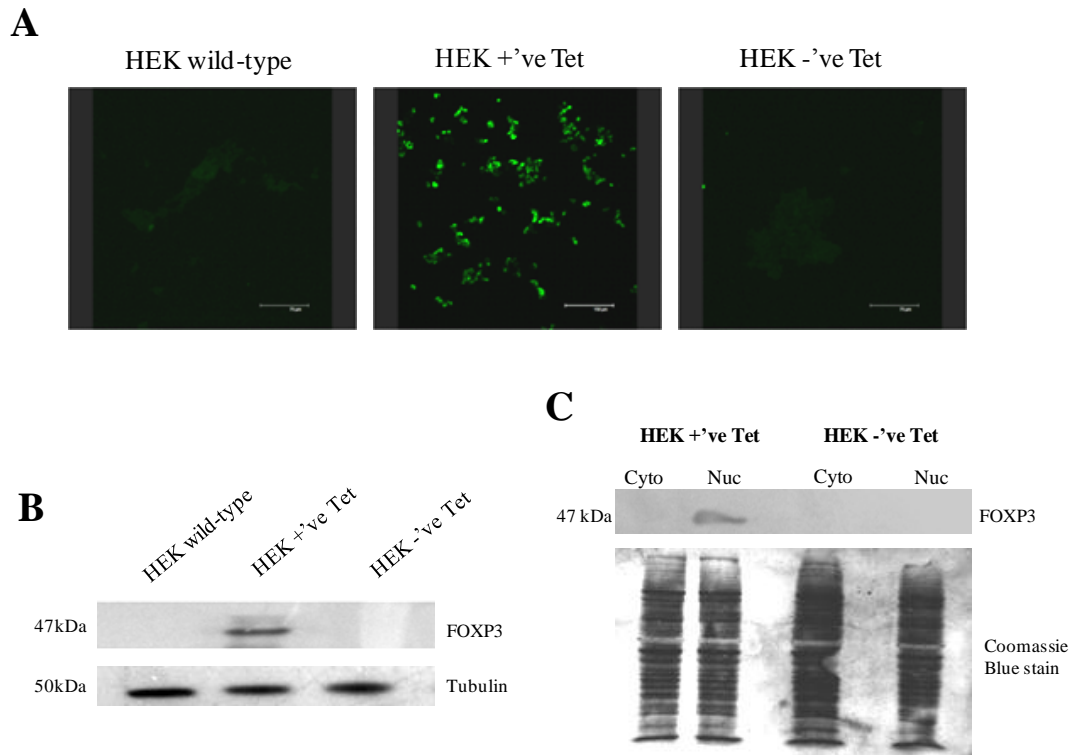


Figure 3-4 – Tetracycline-inducible expression of FOXP3 in transfected HEK cells

(A) Representative IF images of tetracycline induced FOXP3 expression. HEK wild type and transfected HEK cells were seeded into chamber slides and left to grow overnight. The following day, cells were fixed, permeabilised and stained using a human anti-FOXP3 primary antibody and a FITC-conjugated secondary antibody. (B) Western blot was also used to demonstrate FOXP3 expression in transfected HEK cells cultured with and without tetracycline. (C) Subcellular distribution of FOXP3 in transfected HEK cells was determined by Western blot following isolation of nuclear (Nuc) and cytoplasmic (Cyto) domains. The coomassie blue stained gel was used to demonstrate equal loading between samples

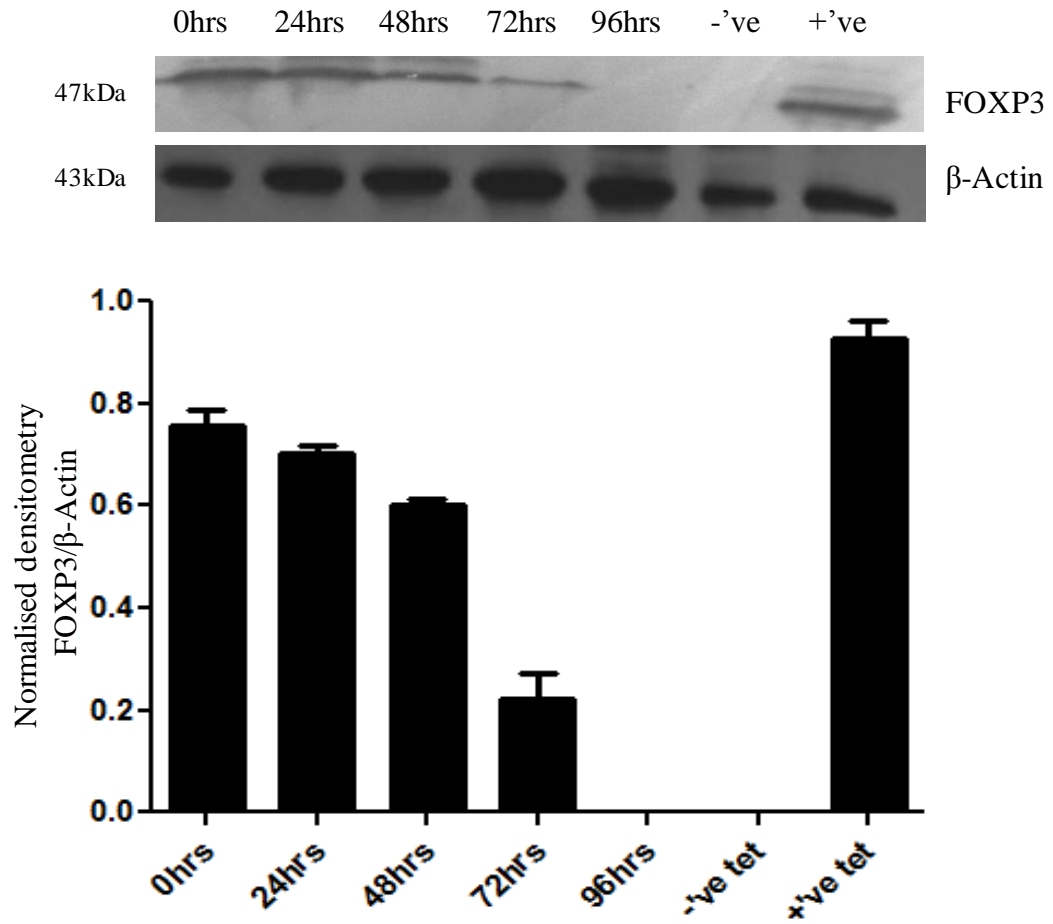


Figure 3-5 - Decline of FOXP3 expression following the removal of tetracycline from growth media

Culture flasks of HEK+'ve Tet were seeded with 100ng/ml tetracycline. Each day (24 hours) one flask had growth culture removed, was washed in PBS and replaced with fresh media without tetracycline. Total protein from all samples was isolated after 96 hours and Western blot was performed (upper panel). Densitometry of bands demonstrates decline in FOXP3 expression (lower panel). HEK-'ve Tet (-'ve Tet) was used as a negative control and HEK+'ve Tet (+'ve Tet) was used as a positive control.

3.4.2 Validation of HMEpC

Primary HMEpC were purchased from Invitrogen. Each vial of cells was routinely tested for several markers of normal mammary epithelial cells including cytokeratins 5, 6, 8, 18 and E-Cadherin before delivery. They were also tested for the absence of viruses including HIV-1, Hepatitis B & C, bacteria, yeast and fungi to ensure the cells are to highest standard for usage. Upon arrival of HMEpC, the cells were stained for cytokeratin 8 and 18 to validate the quality of these cells. IF demonstrated high level expression of both cytokeratin 8 and 18 (**figure 3.6**).

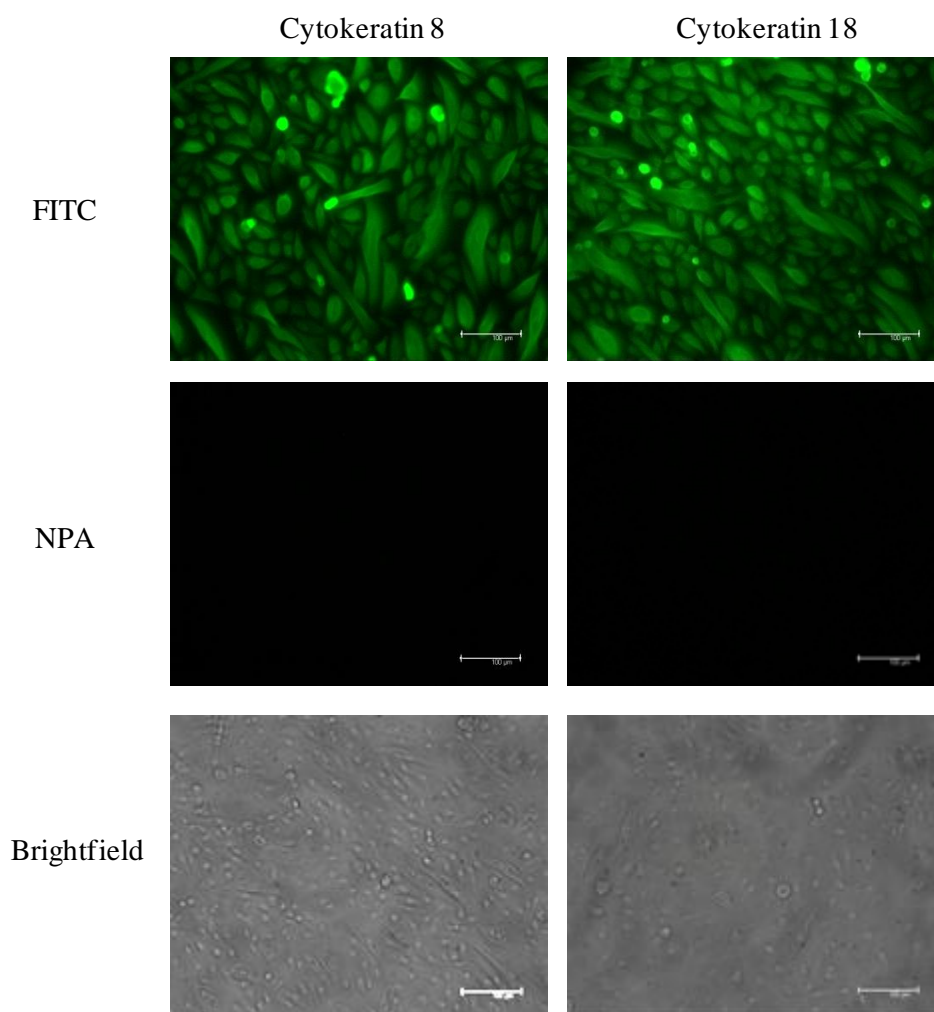


Figure 3-6 - Validation of HMEpC by staining for cytokeratins

HMEpC were stained with primary monoclonal human anti-cytokeratin 8 and anti-cytokeratin 18 antibodies and FITC conjugated secondary antibodies. No primary antibody (NPA) and brightfield images included as controls.

3.4.3 Determination of *FOXP3* expression in cell lines

The expression of *FOXP3* at transcript and protein levels was determined in HMEpC, MCF-7 and MDA-MB-231. Prior to PCR, the integrity of RNA was determined by running a sample of the isolated RNA in a 1.2% agarose gel. The presence of the ribosomal subunits, 18S and 28S, confirmed good quality RNA from cell lines (**figure 3.7**). RNA was reverse transcribed and *FOXP3* transcripts were determined using real-time PCR with TaqMan® probes specific for *FOXP3*. The reaction efficiency of *FOXP3* and *GAPDH* (which was used as a housekeeping gene) real-time PCR primers was assessed by preparing serial dilutions of a template cDNA (**figure 3.8**). A linear drop in Ct value with declining levels of template cDNA demonstrates primer specificity and high reaction efficiency. Both *FOXP3* and *GAPDH* primers had efficiencies greater than 98% for both primers.

Real-time PCR results demonstrated that *FOXP3* was expressed constitutively in HMEpC, however, in both MCF-7 and MDA-MB-231 *FOXP3* was significantly downregulated in comparison to HMEpC (**figure 3.9**).

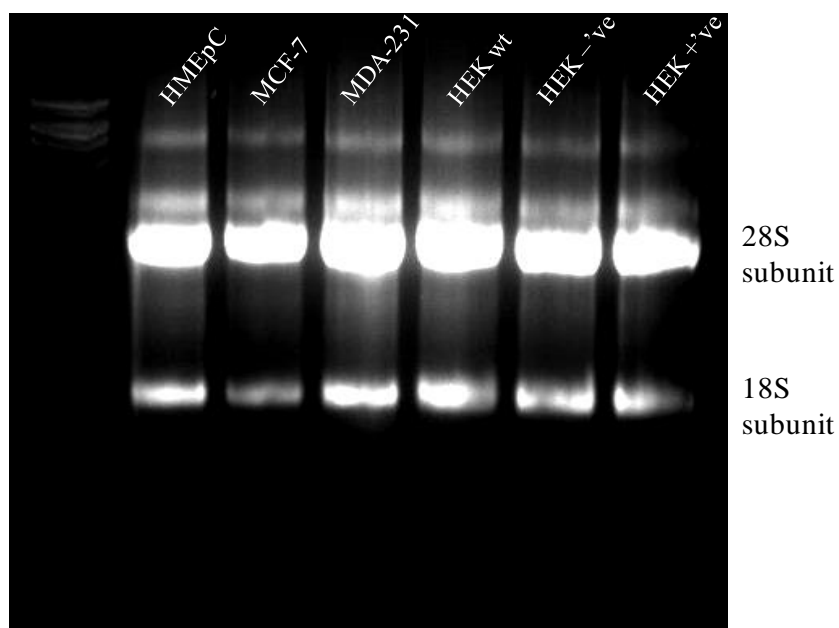


Figure 3-7 - Confirmation of RNA integrity in cell lines

Total RNA was extracted from cell lines using TRI reagent. Following quantification of RNA by the nanodrop spectrophotometer, the quality of isolated RNA was confirmed by agarose gel (1.2%) electrophoresis by demonstrating ribosomal RNA subunits (28S & 18S).

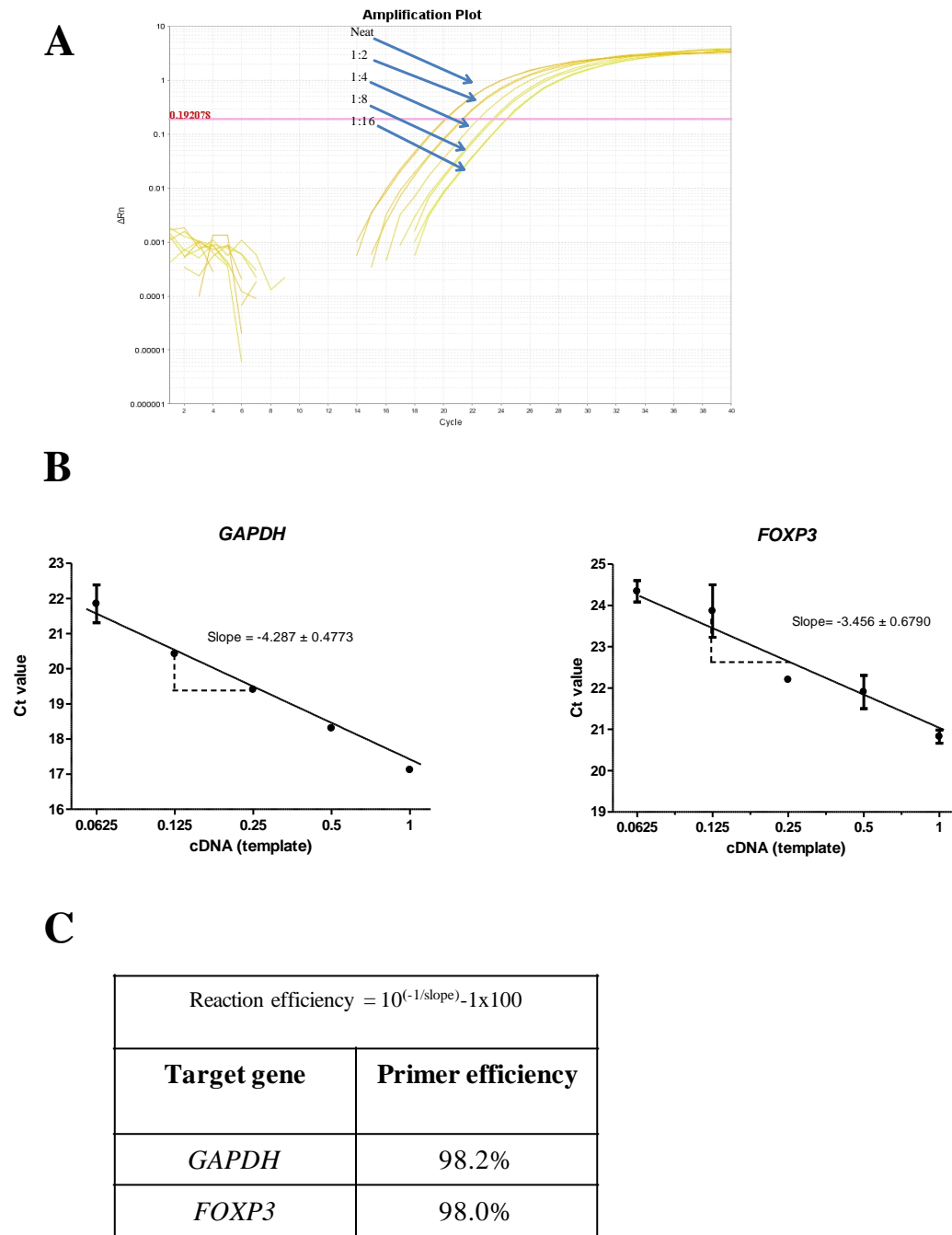


Figure 3-8 - Reaction efficiency of *FOXP3* and *GAPDH* Taqman® real-time PCR primers

HEK+^{ve} Tet cDNA was used to measure reaction efficiency of *GAPDH* and *FOXP3* TaqMan® primers. cDNA was serially diluted and ran for 35 cycles (representative image from *FOXP3* amplification plot) (A). Ct values obtained were plotted against cDNA input in log₂ format and represented as linear regression line plot of Ct value versus cDNA input (B). Reaction efficiency from each primer was calculated incorporating the slope of the linear regression into the equation:

Reaction efficiency = $10^{(-1/\text{slope})} - 1 \times 100$ (C).

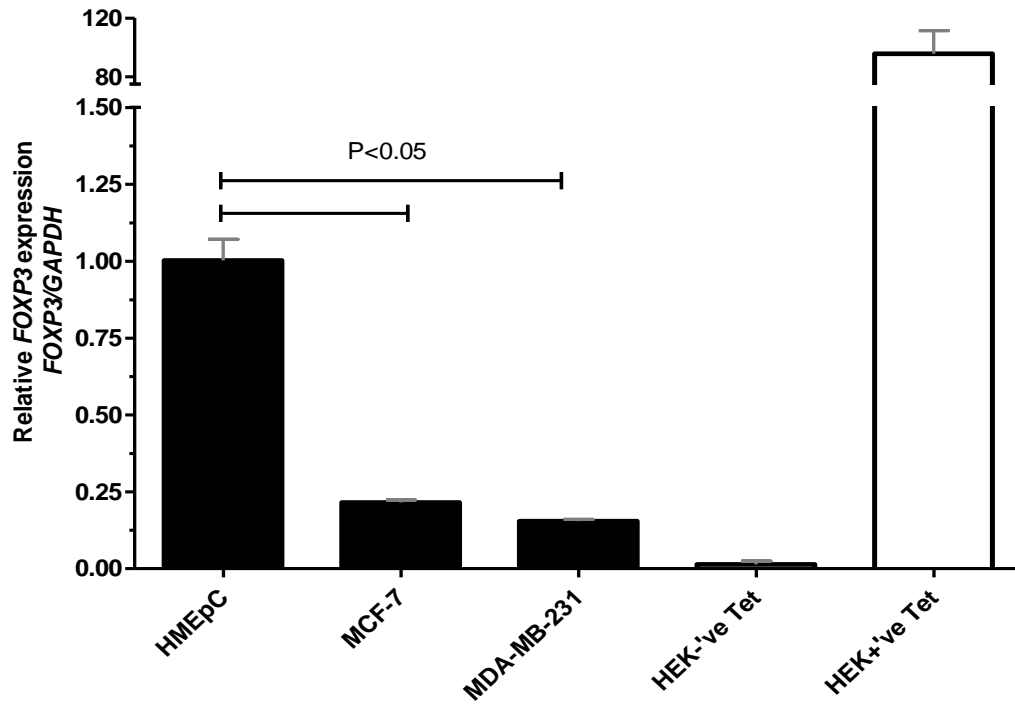


Figure 3-9 - Determination of *FOXP3* transcripts in HMEpC and breast cancer cell lines

Data represents relative levels of *FOXP3* transcripts. After normalising against endogenous *GAPDH*, the amounts of transcripts were compared to those from HMEpC, which was arbitrarily defined as 1.0. Data shown are means and SD of duplicate (n=3). Statistical analysis was performed using an unpaired t-test.

Initially Western blot was used to determine protein levels of FOXP3. However, because the expression of FOXP3 in breast epithelial is low, limited success was achieved using this technique. High level protein loading and extended exposures were required to achieve any form of signal in lysates from HMEpC, MCF-7 and MDA-MB-231 (**figure 3.10 panel A**). Results determined from Western blots suggested the presence of two bands within the HMEpC. The upper band at 47kDa represented the full length variant of FOXP3, and a band of lower molecular weight at 44kDa represented the other FOXP3 isoform (FOXP3 Δ 3). Although the bands were not as strong as those in HMEpC, two distinct bands were also produced at the same molecular weights in MCF-7. FOXP3 expression was barely detectable in MDA-MB-231. Because of the difficulty in detecting FOXP3 using Western blot a more sensitive and quantitative technique was required.

A FOXP3 ELISA was purchased which has a reported minimum sensitivity level of less than 0.085ng/ml. ELISA results quantitatively demonstrated FOXP3 was expressed by HMEpC, whereas, FOXP3 was significantly lower in both MCF-7 and MDA-MB-231 (**figure 3.10 panel B**). This correlates with findings produced in Western blots. These findings were further validated by IF (**figure 3.11**). Furthermore, the IF images highlight that FOXP3 expression was predominately located within the nucleus in HMEpC.

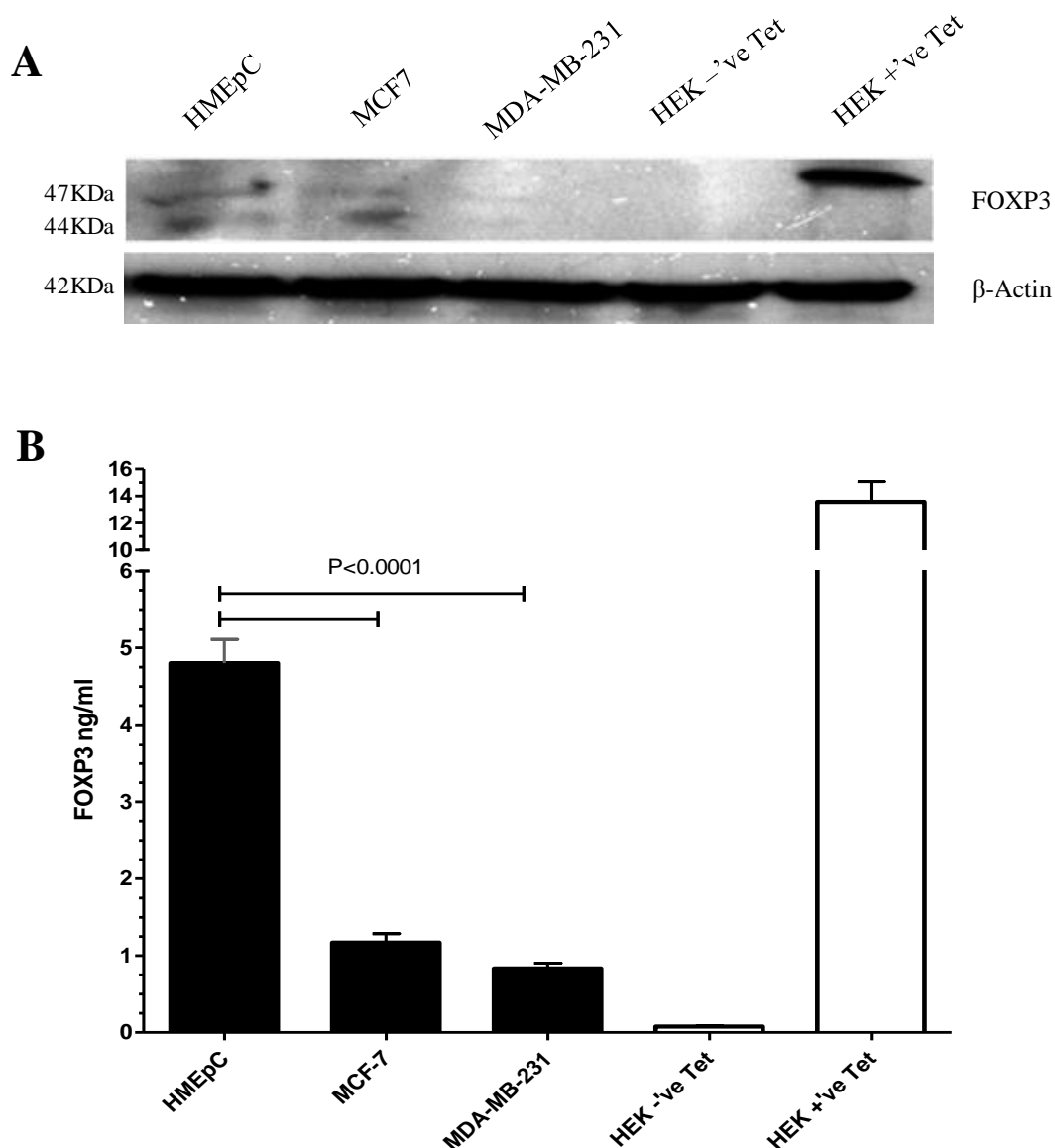


Figure 3-10 - Quantitative expression of FOXP3 protein levels in breast cell lines

Total protein was extracted from cell lines using a cell lysis buffer supplemented with protease and phosphatase inhibitors. Following quantification of protein concentrations, Western blot was performed using 100µg of total protein separated by SDS-PAGE and probed for FOXP3 using a human anti-FOXP3 primary antibody and a HRP-conjugated secondary antibody. β-actin was used as a loading control (**A**). ELISA was used to quantify FOXP3 protein present in 20µg of total protein from each cell line lysate (**B**). Absorbance's of each sample was measured by spectrophotometry using a microplate reader at 450nm. Concentrations of FOXP3 protein was determined by comparing absorbance values of samples against a standard curve after subtracting background readout. Error bars show SD of means from experiments performed in duplicate (n=5). Statistical analysis was performed using an unpaired t-test.

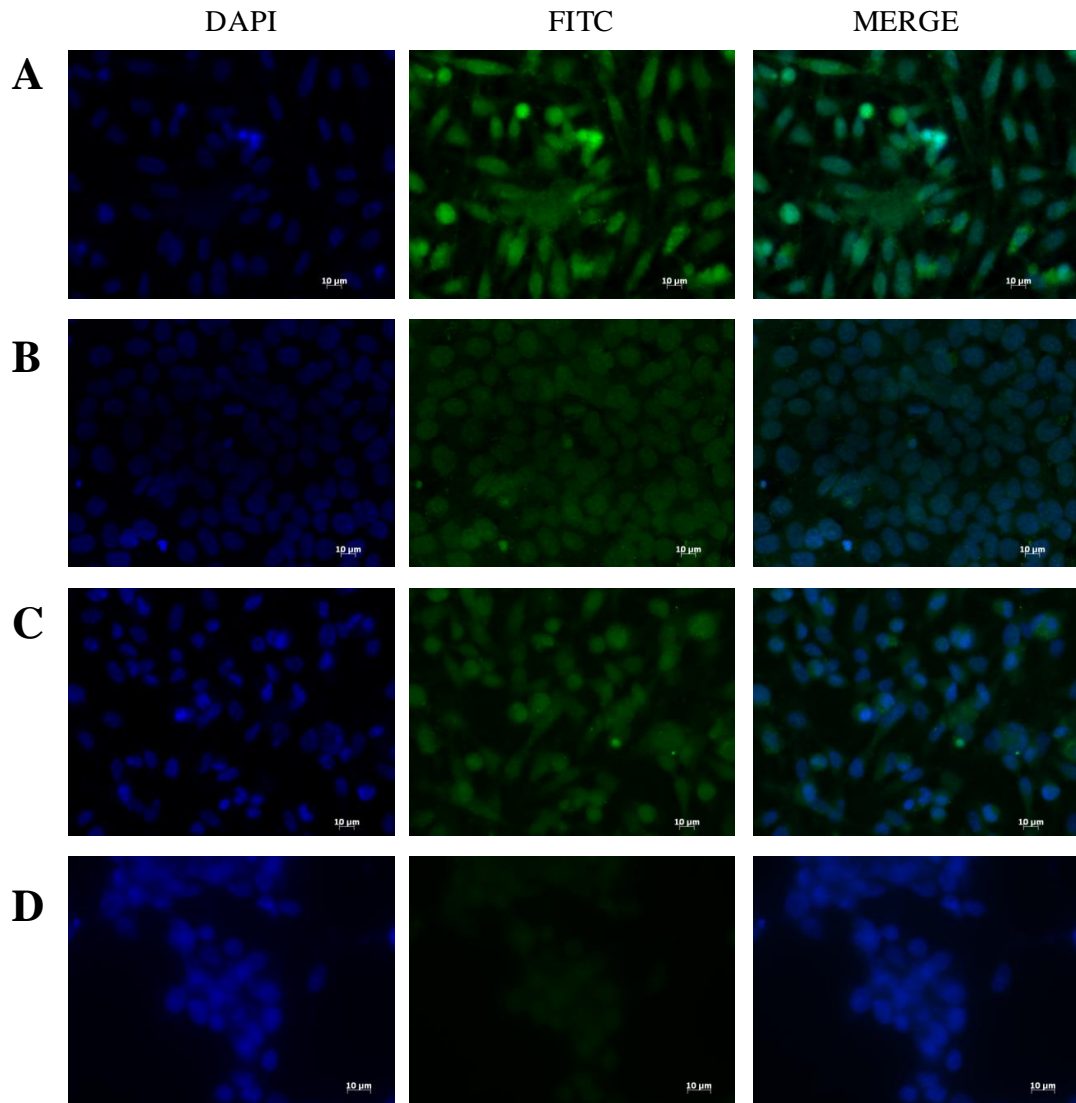


Figure 3-11 - IF images of FOXP3 in cell lines

Cells were seeded into chamber slides and grown in normal growth conditions overnight. The following day cells were fixed, permeabilised and stained using a human anti-FOXP3 primary antibody and a FITC-conjugated secondary antibody. Cells were also counter stained with DAPI to demonstrate nuclear localisation. (A) HMEpC, (B) MCF-7, (C) MDA-MB-231 and (D) HEK-'ve Tet.

3.4.4 Quantification of subcellular distribution of FOXP3 in cell lines

After confirming the presence, albeit at low levels, of FOXP3 within each cancer cell line, the subcellular distribution of FOXP3 in each of these cell lines was investigated. Results in section 3.4.3 (**figure 3.11**) demonstrated that FOXP3 was predominantly nuclear in the HMEpC. However, because the expression of FOXP3 in each cancer cell line was significantly reduced, the IF images could not be used to determine the distribution of the protein in the cancer cells.

Using the subcellular NE-PER® fractionation kit, the nuclear and cytoplasmic proteins from each cell line was isolated and FOXP3 protein from each domain was quantified using the FOXP3 ELISA kit (**figure 3.12 panel A**). Before quantifying protein levels in each domain, Western blots were produced to determine the levels of cross contamination between domains. The NE-PER® fractionation kit has a reported less than 10% cross contamination level which was demonstrated by Western blots using antibodies specific for each domain (**figure 3.12 panel B**). Results once again showed that FOXP3 was lower within MCF-7 and MDA-MB-231 when compared to the HMEpC. FOXP3 protein levels were higher within nuclear fractions of the HMEpC, however, a proportion of FOXP3 protein was also detected within the cytoplasm. This level of cytoplasmic FOXP3 in HMEpC could be explained as the synthesis of FOXP3 occurs in the cytoplasm, and is then actively transported to the nucleus. FOXP3 was found at relatively equal proportions in the nuclear and cytoplasmic fractions in MCF-7 with slightly higher levels in the nuclear fraction. On the other hand, MDA-MB-231 had a significantly greater proportion within the cytoplasmic domain.

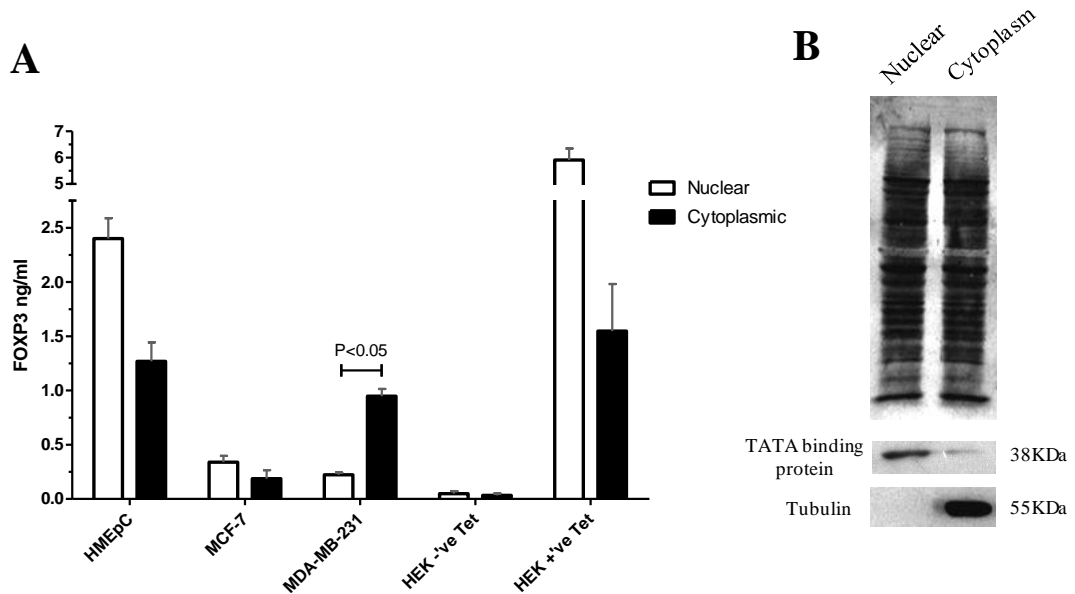


Figure 3-12 - Quantitative distribution of FOXP3 in subcellular fractions

Nuclear and cytoplasmic proteins were isolated from cell lines using a NE-PER® fractionation kit. Following quantification of protein levels in each sample, 35µg of protein was used from each sample to maintain equal loading, except for HEK+’ve Tet which had 10µg loaded in order to make sure values did not exceed the kit sensitivity. The absorbance of each samples were determined by spectrophotometry using a microplate reader at 450nm using a microplate reader and protein levels were quantified by measuring the samples absorbance against a standard curve after subtracting background readout (**A**). Error bars show SD of means from experiments performed in duplicates (n=4). To demonstrate the low cross contamination levels between fractions, a Western blot was performed on protein samples using antibodies specific for nuclear (human anti-TATA binding protein) and cytoplasmic (human anti-tubulin) fractions (**B**). Statistical analysis was performed using an unpaired t-test.

3.4.5 Sequencing of *FOXP3* in cell lines for mutations and splice variant isoforms

Dysregulation of *FOXP3* within breast cancer is widely reported and discussed in section 3.1.1. Having demonstrated that *FOXP3* is downregulated within both MCF-7 and MDA-MB-231, and is also found predominately within the cytoplasm of MDA-MB-231, possible mutations or splice variant isoforms which could be responsible for this was investigated by sequencing the *FOXP3* protein coding region in all cell lines. Particular interest was focused around the three NLSs identified by Hancock & Ozkaynak (Hancock and Ozkaynak 2009) and the RKKR sequence identified by Lopes et al (Lopes, Torgerson et al. 2006) as these have been demonstrated to be relevant in protein nuclear localisation of *FOXP3*.

3.4.5.1 Annealing temperature gradient for *FOXP3* primer sets

FOXP3 primers were manually designed, ensuring that the entire protein coding region of each exon was completely spanned by the primers. This ensures that any splice variant isoforms of *FOXP3* which may lack specific exons will be detected. Despite maintaining a relatively similar melting temperature between the forward and reverse primer pairs in each set, annealing temperature gradients were carried out to determine an optimum temperature to produce the greatest amount of product. *FOXP3* primer sets were optimised using varying annealing temperatures ranging from between 40°C to 65°C. Results for each primer produced a single band at the correct number of base pairs, therefore, highlighting their specificity and thermostability. Temperatures between 51°C and 58°C seemed to produce the most product for each primer set (**figure 3.13**). The annealing temperature for each primer was set to 55°C.

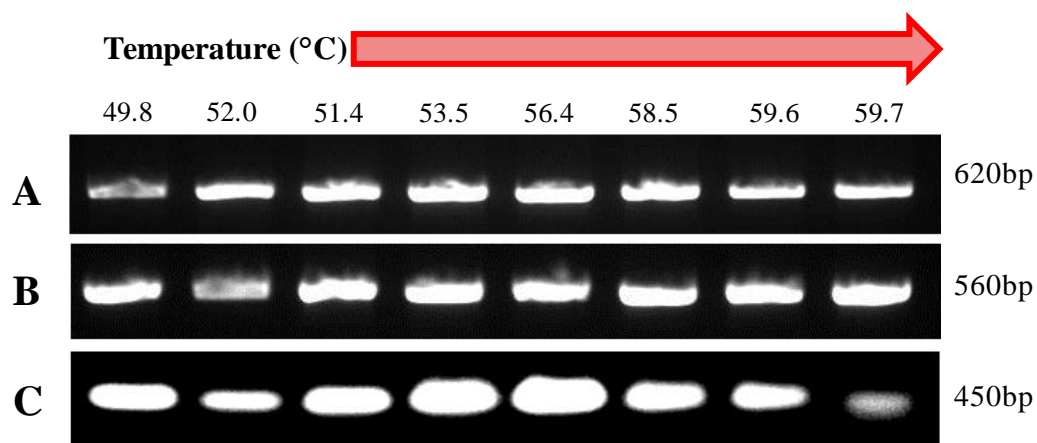


Figure 3-13 - Annealing temperature gradient for *FOXP3* primers

Primers for conventional PCR were designed manually. Each set of primers: *FOXP3* primer set 1 (A), *FOXP3* primer set 2 (B), and *FOXP3* primer set 3 (C) were designed so melting temperatures were no more than 5°C apart. Conventional PCR with a temperature gradient ranging from 48.9°C to 59.7°C was used to determine the optimal temperature each primer set annealed. 30 cycles of PCR using HEK+’ve Tet cDNA as a template for *FOXP3* primer set 1 and set 2, whereas, MCF-7 cDNA was used as a template for *FOXP3* primer set 3 as the reverse primer falls outside of the *FOXP3* region cloned into transfected HEK cells. Samples were ran on 1.2% agarose gel supplemented with 0.5µg/ml ethidium bromide.

3.4.5.2 Sequencing of *FOXP3* primer set 1

High quality RNA was isolated from cell lines and reverse transcribed into cDNA. Using *FOXP3* primer set 1, cDNA was amplified for 35 cycles followed by the amplified product being run on a 1.2% agarose gel supplemented with 0.5µg/ml ethidium bromide. The PCR product was visualised under UV light and single bands were excised from the gel. DNA was eluted from the gel and sent for sequencing.

FOXP3 primer set 1 used primers which completely span exons 2 (starting from the protein coding region in exon 2) to exon 5. Agarose gel PCR demonstrated that both HMEpC and MCF-7 produced two single bands after amplification using *FOXP3* primer set 1. When these were sequenced the upper band of 620bp contained no missing exons or mutations. However, in HMEpC and MCF-7 the lower band of 510bp was completely missing exon 3 (**Figure 3.14**). Representative electropherograms from MCF-7 sequencing illustrating the deletion of exon 3 in the lower band is provided in **figure 3.15**. MDA-MB-231 only produced a single band at 620bp which also contained no mutations.

The findings from *FOXP3* primer set 1 show that HMEpC, MCF-7 and MDA-MB-231 all contain a *FOXP3* isoform containing exons 2-5 with no mutations, whereas, HMEpC and MCF-7 also contain a separate isoform which completely lacks exon 3. These results also demonstrate that all cell lines and *FOXP3* isoforms contained no mutations within the NLS-1.

Sequencing results for HMEpC using *FOXP3* primer set 1 are provided in **appendix 1**.

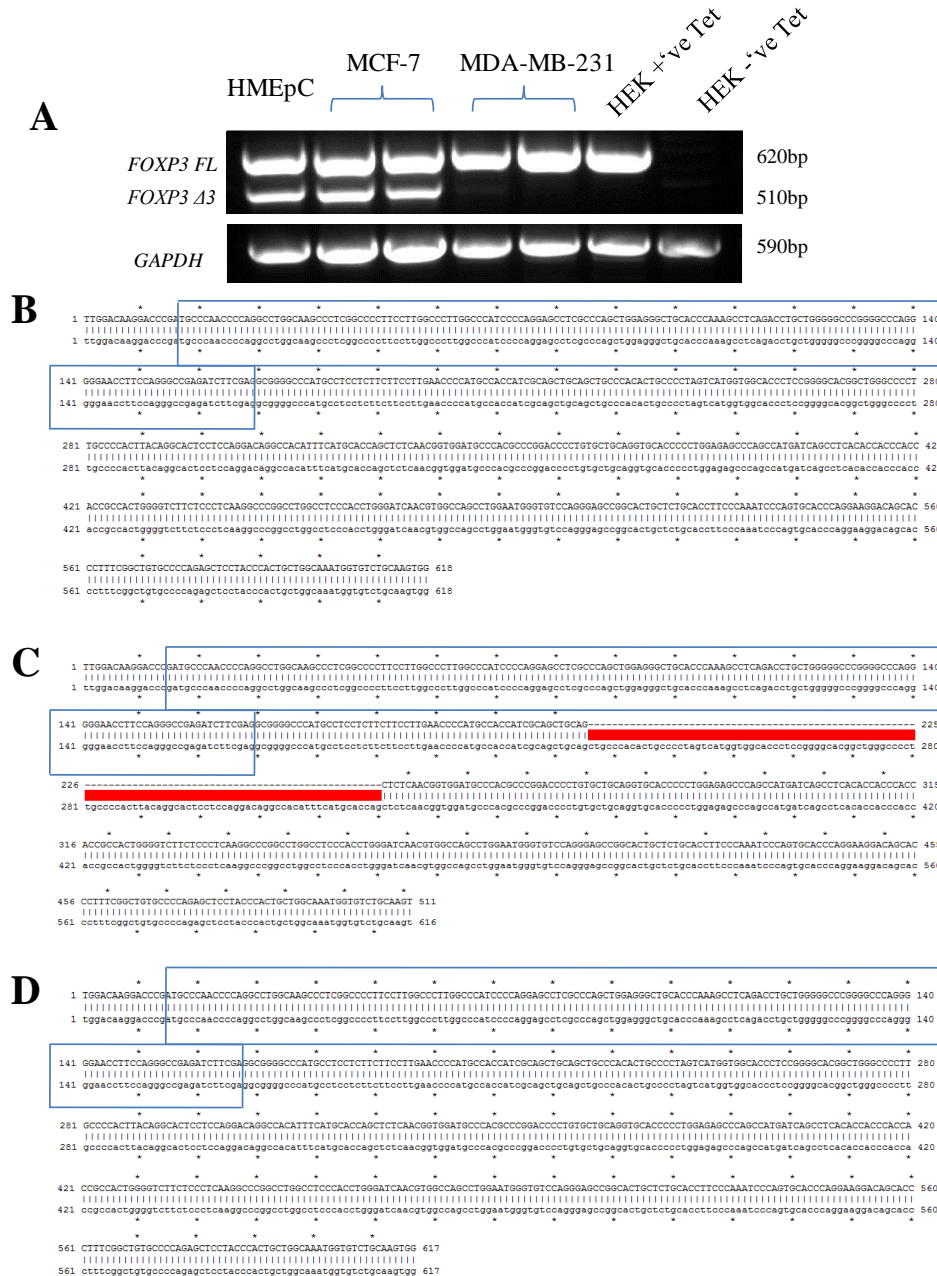


Figure 3-14 - Sequencing of *FOXP3* in breast cancer cell lines using *FOXP3* primer set 1

Following 35 cycles of PCR with a previously determined annealing temperature for *FOXP3* primer set 1, the final product was ran on a 1.2% agarose gel (A). *GAPDH* primers were used as a loading control between samples and to ensure cDNA quality. cDNA from HEK+ve Tet was used as a positive control, whereas HEK-ve Tet was used as a negative control. Sequencing data from the upper band of MCF-7 (B), the lower band in MCF-7 (C) and MDA-MB-231 (D) was analysed and aligned alongside wild type *FOXP3* (accession number NM_014009.3) using ApE software. Upper rows represent sample sequences and lower rows represent wild type. Blue boxes represent NLS-1 identified by Hancock and Ozkaynak (Hancock and Ozkaynak 2009). Data is representative of two experiments which produced similar results.

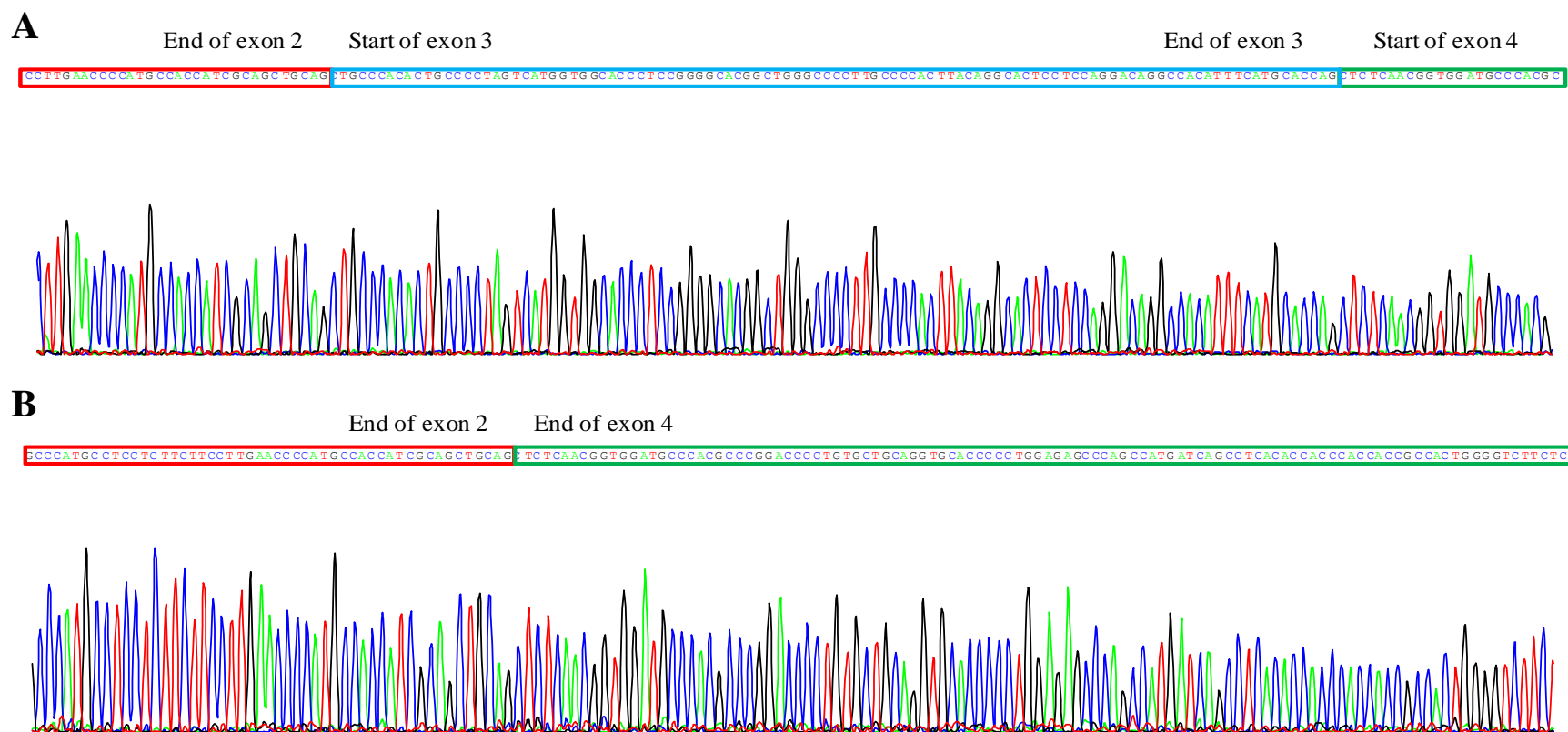


Figure 3-15 - Electropherogram demonstrating *FOXP3A3* isoform in MCF-7 cells

(A) Sequencing data from upper band in MCF-7 demonstrates the presence of exons 2, 3 and 4. (B) Data from lower band in MCF-7 cells demonstrates complete deletion of exon 3. Data was analysed using ApE software.

3.4.5.3 Sequencing of *FOXP3* primer set 2

FOXP3 primer set 2 completely spans exons 6-10. Results highlighted that HMEpC, MCF-7 and MDA-MB-231 produced a single band at approximately 560bp which demonstrates a single isoform. Moreover, all cell lines contained no missing exons between exon 6 and 10. Sequencing these products also illustrated that no mutations were detected in any cell lines (**figure 3.16**). *FOXP3* primer set 2 also covers NLS-2 which also contained no mutations.

3.4.5.4 Sequencing of *FOXP3* primer set 3

FOXP3 primer set 3 completely spans exon 11 and slightly downstream of the protein coding domain in exon 12. Once again, single bands were produced in each cell line with no mutations detected (**figure 3.17**). Both NLS-3 and the RKKR sequences were covered by *FOXP3* primer set 3. No mutations were detected in either cell line.

No positive control was used for this primer set. In previous studies we have used HEK+^{ve} Tet as a positive control however this primer set uses a reverse primer which lies outside of the *FOXP3* gene which was cloned into the vector therefore meaning it is not detectable with these primers.

Sequencing results using *FOXP3* primer sets 2 and 3 for HMEpC are provided in **appendix 2**.

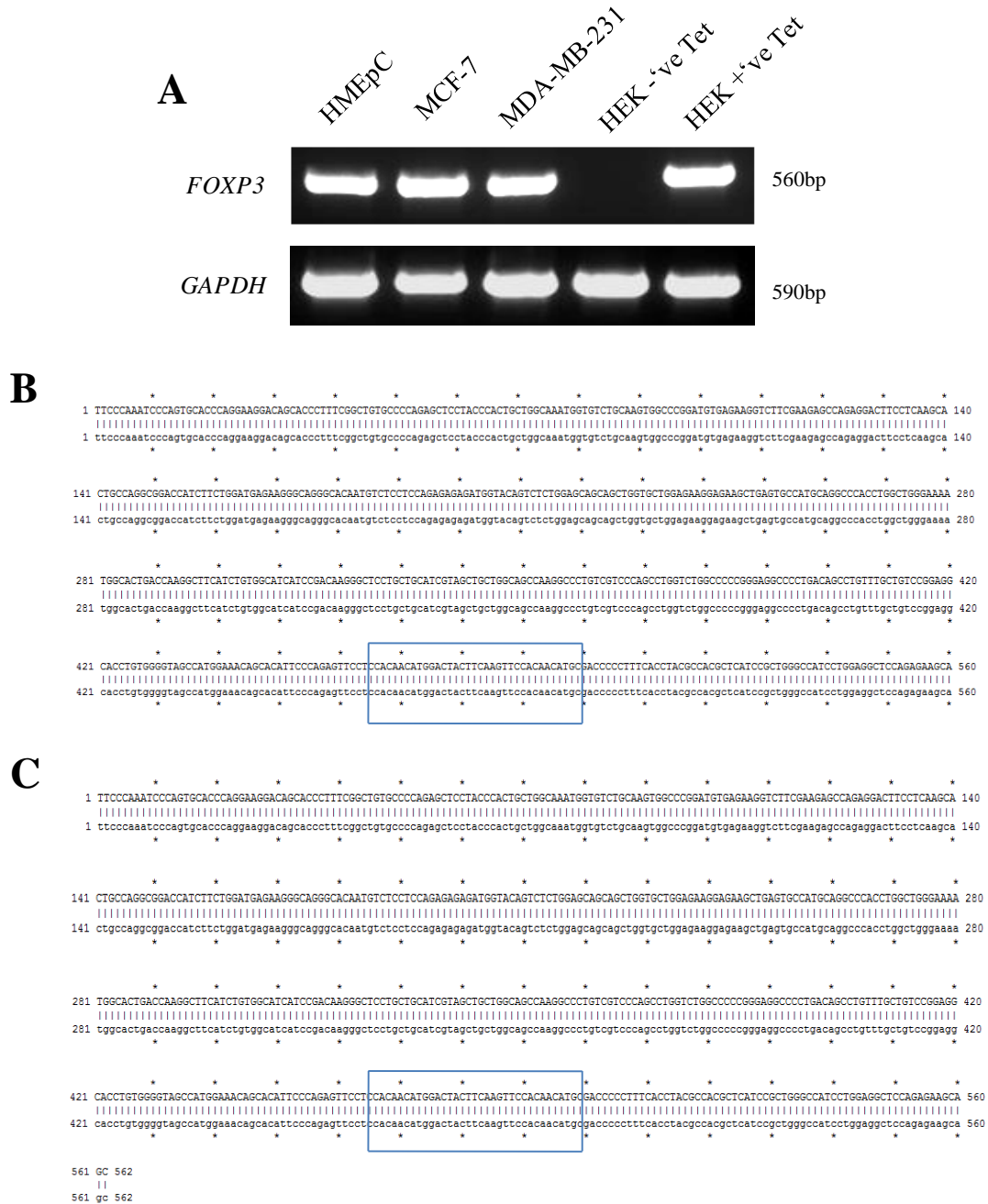


Figure 3-16 - Sequencing of *FOXP3* in breast cancer cell lines using *FOXP3* primer set 2

Following 35 cycles of PCR with a previously determined annealing temperature for *FOXP3* primer set 2, the final product was ran on a 1.2% agarose gel (A). *GAPDH* primers were used as a loading control between samples and to ensure cDNA quality. cDNA from transfected HEK+^{ve} Tet was used as a positive control whereas HEK-^{ve} Tet was used as a negative control. Sequencing data from MCF-7 (B) and MDA-MB-231 (C) was analysed and aligned alongside wild type *FOXP3* (accession number NM_014009.3) using ApE software. Upper rows represent sample sequences and lower rows represent wild type *FOXP3*. Blue boxes represent NLS-2 identified by Hancock and Ozkaynak (Hancock and Ozkaynak 2009). Data is representative of two experiments which produced similar findings.

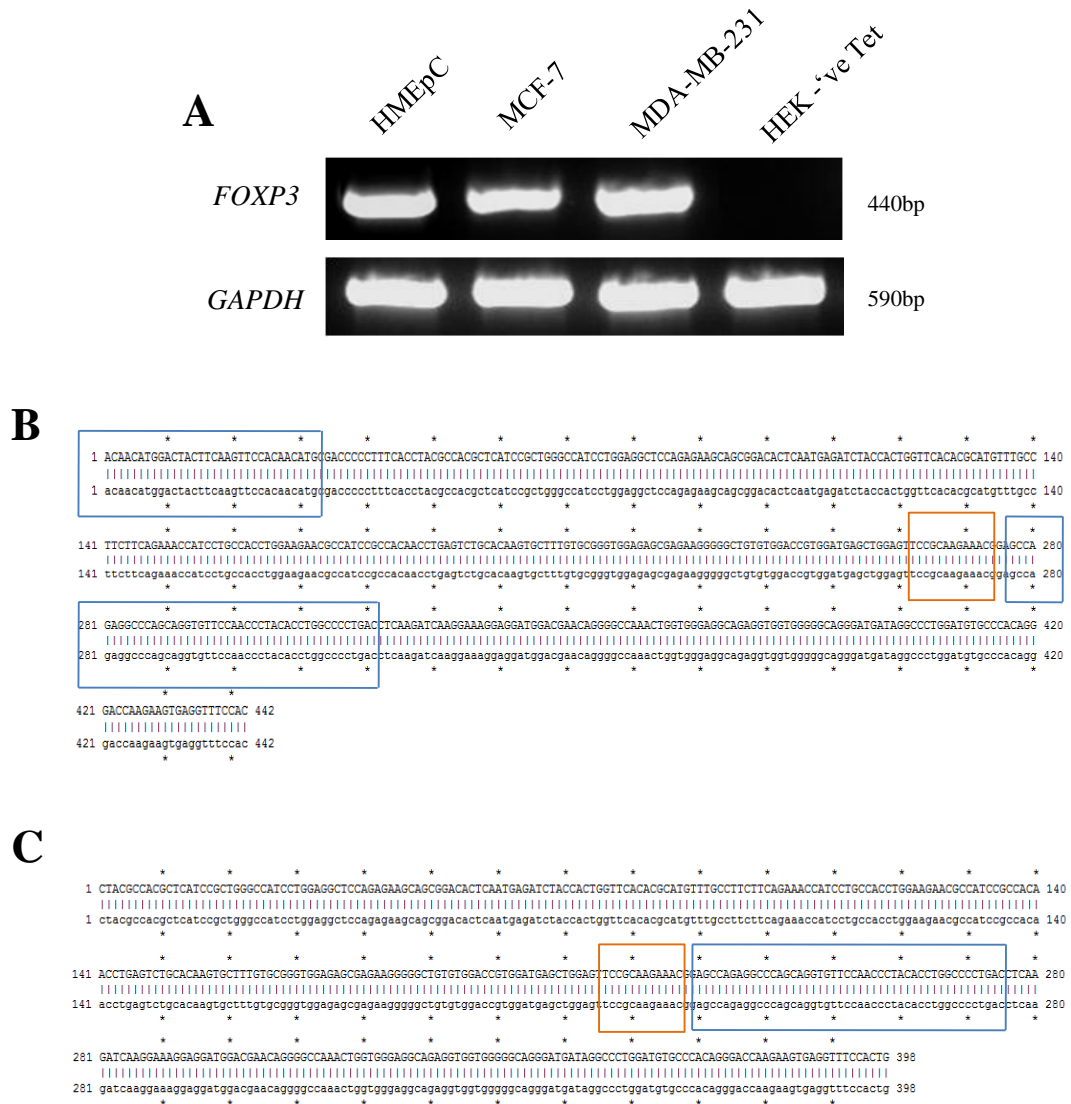


Figure 3-17 - Sequencing of *FOXP3* in breast cancer cell lines using *FOXP3* primer set 3

Following 35 cycles of PCR with a previously determined annealing temperature for *FOXP3* primer set 3, the final product was ran on a 1.2% agarose gel (A). *GAPDH* primers were used as a loading control between samples and to ensure cDNA quality. cDNA from transfected HEK-ve Tet was used as a negative control. Sequencing data from MCF-7 (B) and MDA-MB-231 (C) was analysed and aligned alongside wild type *FOXP3* (accession number NM_014009.3) using ApE software. Upper rows represent sample sequences and lower rows represent wild type *FOXP3*. Blue boxes represent NLS-3 identified by Hancock and Ozkaynak (Hancock and Ozkaynak 2009) whereas orange boxes represent RKKR sequences identified by Lopes et al (Lopes, Torgerson et al. 2006). Data is representative of two experiments which produced similar findings.

3.4.6 Effects of IL-2 and TGF- β on *FOXP3* expression in breast cancer cell lines

Several reports have demonstrated that cytokines including TGF- β and IL-2 can increase the expression of *FOXP3* in T-cells (Zorn, Nelson et al. 2006; Nishihara, Ogura et al. 2007; Xiao, Jin et al. 2008; Yang, Anderson et al. 2008). However, no reports have investigated whether these cytokines can also influence *FOXP3* expression in breast cancer cells.

MDA-MB-231 and MCF-7 were treated with either 10ng/ml or 20ng/ml of either TGF- β or IL-2 for up to 24 hours and the transcript expression of *FOXP3* was analysed by real-time PCR (**figure 3.18**). Results demonstrate that treatment with TGF- β and IL-2 did not significantly increase the expression of *FOXP3* in either MDA-MB-231 or MCF-7 even after increasing both concentrations and incubation periods. CD4⁺ T-cells were also treated with 20ng/ml TGF- β and IL-2 for 24 hours and despite a marked increase in *FOXP3* after TGF- β treatment, there was no increase after IL-2 treatment.

This demonstrates that neither TGF- β nor IL-2 can increase *FOXP3* expression in breast cancer cell lines.

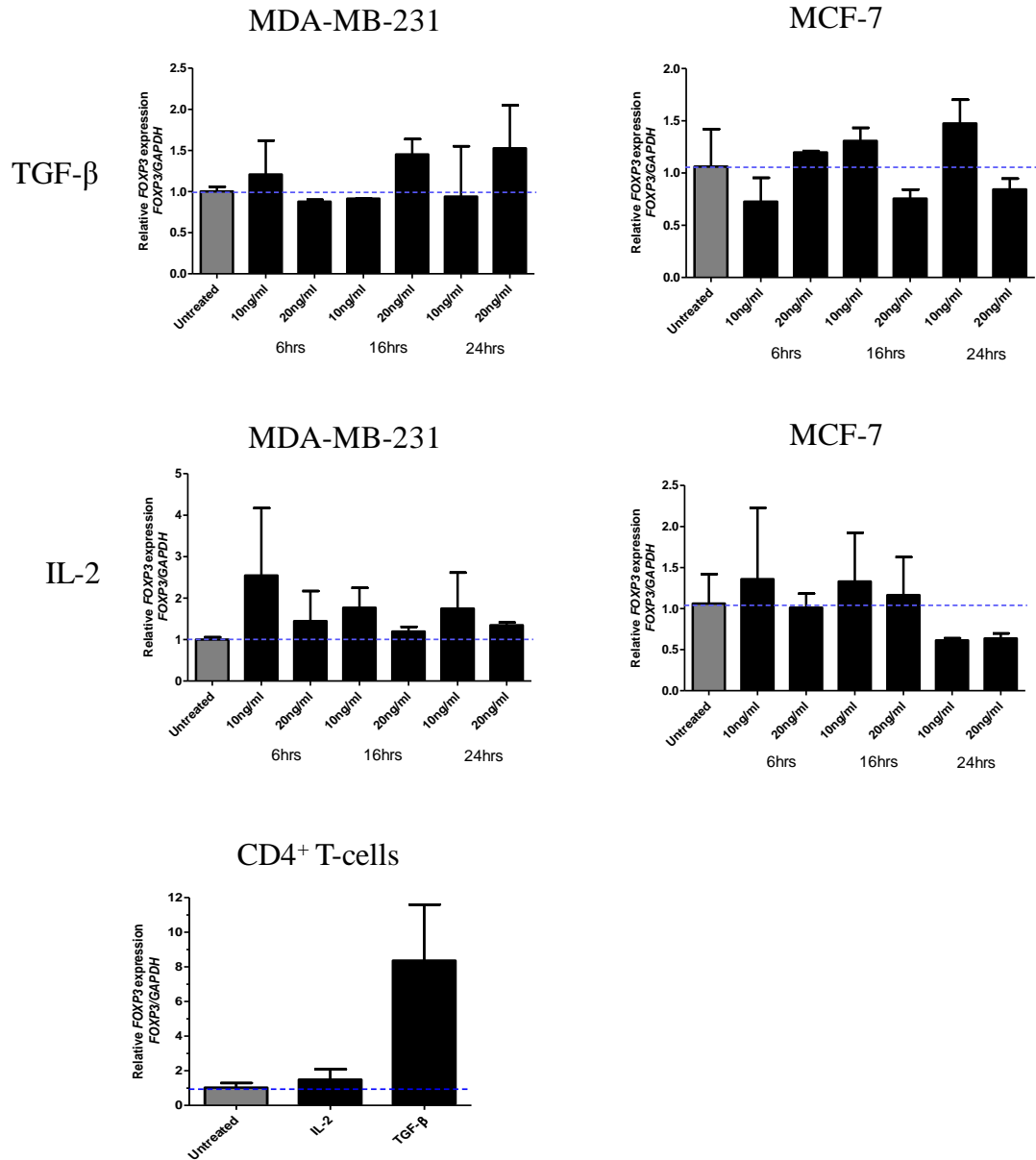


Figure 3-18 - Effects of IL-2 and TGF-β treatment on *FOXP3* expression in breast cancer cell lines

MDA-MB-231 and MCF-7 were seeded into 6-well plates and cultured with either 10ng/ml or 20ng/ml of TGF-β or IL-2. After 6, 16 and 24 hours RNA was isolated. Freshly isolated CD4⁺ T-cells were treated with 20ng/ml of TGF-β and IL-2 for 24 hours as a positive control. cDNA was synthesised and real-time PCR was performed for *FOXP3* transcripts after normalising against endogenous *GAPDH* (n=2). Statistical analysis was performed using a paired t-test.

3.5 Summary of chapter 3 results

- ✓ Following the introduction of tetracycline to the growth media, *FOXP3* was rapidly induced in transfected HEK cells. When tetracycline was removed the *FOXP3* protein was degraded and undetectable after approximately 96 hours.
- ✓ *FOXP3* is significantly downregulated at both a protein and transcript level in MCF-7 and MDA-MB-231 cell lines in comparison to HMEpC.
- ✓ *FOXP3* is located predominantly within the cytoplasm of the typically more invasive MDA-MB-231 cell line, whereas it remains predominantly nuclear in less invasive MCF-7 cells.
- ✓ HMEpC and MCF-7 cells contained both natural *FOXP3* isoforms (*FOXP3FL* and *FOXP3Δ3*) at approximately equal levels, whereas, MDA-MB-231 only expressed a full length variant.
- ✓ Neither IL-2 nor TGF- β was able to upregulate *FOXP3* in either MDA-MB-231 or MCF-7 breast cancer cells.

3.6 Discussion

Following the discovery of FOXP3 in epithelial cells, research has now demonstrated that FOXP3 is frequently dysregulated in a number of malignancies at protein and transcript levels. This has demonstrated that FOXP3 is more than just a marker for Treg function and development, it is also a potent tumour suppressor required for maintaining epithelial cell homeostasis. Studies have reported a number of scenarios including downregulation, mutations, splice variants, skewed cellular distribution and even normal nuclear expression of FOXP3 in several forms of malignancy (Zuo, Liu et al. 2007; Zuo, Wang et al. 2007; Merlo, Casalini et al. 2009; Wang, Liu et al. 2009; Zhang and Sun 2010; Frattini, Pisati et al. 2012).

However, a recent report by Lal et al (Lal, Chan et al. 2013) reported that both Treg and epithelial cell derived FOXP3 expression increased with malignancy. On this basis, the aim of this chapter was to further investigate the expression of FOXP3 within primary normal mammary epithelial cells and two breast cancer cell lines, with different invasive capacities.

3.6.1 Validation of FOXP3 induction in transfected HEK cells

The first aim of this chapter was to validate the tetracycline-inducible FOXP3 system in transfected HEK cells generated by Dr Marcin Pekalski. Following the addition of tetracycline, the expression of FOXP3 was rapidly increased within transfected HEK cells. As a transcription factor, it is important that FOXP3 is located within the nucleus. When FOXP3 was induced in these cells the expression was found to be exclusively within the nucleus. This demonstrates that the inducible system described acts as a good positive and negative control for FOXP3 expression for subsequent experiments. The inducible induction of FOXP3 in the transfected HEK cells is reversible as the removal of tetracycline from the growth media resulted in a time-dependant decrease in FOXP3 expression. This emphasises that the induction of FOXP3 in the HEK cells was tetracycline-dependant.

It has been reported in T-cells that the FOXP3 protein is relatively unstable and has a half-life of approximately 21 minutes before it undergoes rapid polyubiquitination and the protein is degraded (Lee, Gao et al. 2008). However, when tetracycline was

removed from the growth media FOXP3 was still detectable for up to 72 hours and completely absent after 96 hours. This extended presence of FOXP3 could be explained on the basis that FOXP3 is not a native protein to these cells, and they may lack the required mechanisms to effectively degrade the protein. This demonstrates that the presence of FOXP3 in these cells acts as a good control for expression but not as a functioning protein. Another aspect to be considered is the promoter stability in the transfected HEK cells. The tetracycline-inducible FOXP3 expression in the transfected HEK cells is under the control of a CMV promoter which could be more stable for longer periods than the natural FOXP3 promoter found in T-cells.

3.6.2 FOXP3 expression in normal and malignant cell lines

In Tregs, FOXP3 is expressed at high levels and is therefore considered a good marker for these cells. However, the expression in epithelial cells is considerably lower (Wang, Liu et al. 2009). Three methods of detecting FOXP3 were attempted in this aspect of the study. Each technique used antibodies which detect FOXP3 epitopes outside of exon 3, therefore, both FOXP3FL and FOXP3 Δ 3 isoforms will be detected. Initially, Western blot was used to detect the expression of FOXP3 in cell lines. However, even after excessive protein loading, extended incubation periods and exposure times, the FOXP3 signal produced in all breast epithelial cells (including HMEpC) was weak. This finding demonstrates the presence of FOXP3 in these cells, albeit at a low level. This finding was further validated by IF. In order to amplify the signal, a more sensitive technique was used in the form of a FOXP3 ELISA which has a reported minimum sensitivity of less than 0.085ng/ml. In order to quantify FOXP3 levels, a standard curve was produced using concentrations ranging from 20ng/ml down to 0.312ng/ml. The accuracy and sensitivity was demonstrated by further serial diluting the 0.312ng/ml sample four more times to reach to concentration of 0.039ng/ml which still produced a measurable signal with relatively low error bars.

ELISA results enabled, for the first time, the quantification of FOXP3 expression in normal mammary cells. The level of FOXP3 within these cells was low. This finding is consistent with the literature. FOXP3 protein and transcripts within MCF-7 and MDA-MB-231, were significantly less in comparison to HMEpC. The levels of

FOXP3 protein and transcripts were approximately the same in MCF-7 and MDA-MB-231 which could indicate that FOXP3 downregulation may have occurred at earlier stages of carcinogenesis rather than latter stages. On the contrary, Frattini et al (Frattini, Pisati et al. 2012) reported that Foxp3 was still present within early stages of tumours in glioblastoma, however, the expression diminished as the tumour progressed, possibly suggesting that FOXP3 plays a greater role in later stages of tumorigenesis.

After confirming the presence of FOXP3 within both breast cancer cell lines, the cytoplasmic and nuclear distribution of FOXP3 was investigated. Since FOXP3 is synthesised within the cytoplasm and actively transported into the nucleus, it is often referred to as a shuttling protein. On this basis, it is expected that some FOXP3 would be present within the cytoplasm. Findings demonstrated that a proportion of FOXP3 was located within the cytoplasm in HMEpC although the nuclear content was clearly greater. Combined levels of nuclear and cytoplasmic FOXP3 contents from MCF-7 were less than that found in HMEpC. MCF-7 appeared to contain both nuclear and cytoplasmic FOXP3. However, when the distribution within MDA-MB-231 was investigated, the proportion of FOXP3 within the cytoplasm was significantly greater than the nuclear content. One question which can be posed from this finding is: Does the skewed distribution of FOXP3 have further detrimental effects to epithelial cells when it is present in the cytoplasm? As a transcription factor, the primary role of FOXP3 is to bind to DNA and influence gene expression. To carry out this function, FOXP3 needs to be present within the nucleus. Although the presence of FOXP3 has been observed in the cytoplasm in several reports (Hinz, Pagerols-Raluy et al. 2007; Merlo, Casalini et al. 2009; Wang, Liu et al. 2009), the exact consequences of this dysregulated distribution have never been investigated. This suggests that FOXP3 acting detrimentally in the cytoplasm is less likely, with the mere absence of FOXP3 from the nucleus being more important. However, in contrast to this, when Merlo et al (Merlo, Casalini et al. 2009) looked at the distribution of FOXP3 in a large cohort of breast cancer patients they reported that patients with FOXP3 restricted to the cytoplasm had an equal, or worse, prognosis to those who had no detectable FOXP3. This suggests that the cytoplasmic location could be more detrimental than a complete absence of the protein.

The levels of FOXP3 within the nuclear compartment of MCF-7 and MDA-MB-231 were relatively equal. This suggests that if the level of nuclear FOXP3 within MCF-7 was at a functioning level, then it should be equally functional within MDA-MB-231, proposing that a cytoplasmic distribution could be consistent with a worse prognosis.

Acetylation is the process of adding an acetyl group into a chemical compound, generally by replacement of an active hydrogen atom. This is catalyzed by enzymes which contain histone/protein acetyltransferases (HATs). Acetylation is an important part of biology as it can regulate the expression and stability of proteins. Interestingly, Foxp3 is a protein demonstrated to be influenced heavily by acetylation. Deacetylase inhibitors can increase acetylation of Foxp3 which results in an increased suppressive function in Tregs *in vitro* and *in vivo* (Hansen, Baeuerle et al. 1994). Indeed, HAT p300 in particular can cause acetylation of Foxp3 which subsequently increases the protein stability in transfected cells, whereas, inhibition of HAT p300 is able to inhibit the function of Tregs through impaired Foxp3 function (Liu, Wang et al. 2013). Interestingly, the effects of Foxp3 acetylation in normal or malignant epithelial cells have not been reported and, therefore, require further investigation. Acetylation has been reported to be important in nuclear translocation of proteins, whereas, lysine residues are often targeted in the acetylation of proteins. These residues are also involved in nuclear translocation of proteins, including the RKKR sequence in FOXP3 reported by Lopes et al (Lopes, Torgerson et al. 2006). However, despite the importance of HAT p300 in controlling Foxp3, a report by Van Loosdregt et al (van Loosdregt, Vercoulen et al. 2010) has demonstrated that the acetylation of Foxp3 by HAT p300 does not influence the subcellular distribution of Foxp3.

3.6.3 FOXP3 mutations and isoforms in breast cancer cells

It is well established that mutations can cause significant downregulation of gene expression which subsequently affects the protein expression. In addition to being downregulated, the distribution of FOXP3 in many cancers is found to be restricted to the cytoplasm (Merlo, Casalini et al. 2009; Wang, Liu et al. 2009). Hancock and Ozkaynak (Hancock and Ozkaynak 2009) used murine Foxp3 to demonstrate three

regions which are imperative to nuclear transport and have highly conserved homology within human FOXP3. A separate report from Lopes et al (Lopes, Torgerson et al. 2006) demonstrated the importance of an RKKR sequence in human FOXP3. This sequence is important for nuclear translocation of other proteins (Mikami, Hori et al. 2005; Song, Waataja et al. 2006) including FOXP3 in prostate cells (Wang, Liu et al. 2009). Therefore these regions were of particular interest.

HMEpC contained both natural FOXP3 isoforms and no mutations. MCF-7 also contained both natural isoforms with no mutations. However, MDA-MB-231 only contained the full length variant and is therefore missing the natural FOXP3 Δ 3 isoform. Interestingly, these findings also match the results from Western blots, which showed the presence of two faint bands, one at approximately 47kDa, and one approximately 4kDa smaller in HMEpC and MCF-7. This finding was validated from the sequencing results which demonstrated the presence of FOXP3FL and FOXP3 Δ 3 in HMEpC and MCF-7.

These findings show that FOXP3 is downregulated within both non-invasive and invasive breast cancer cell lines. However, FOXP3 in the invasive cell line is not only predominately restricted to the cytoplasm, but also missing a natural isoform therefore posing another question: Because MDA-MB-231 still contains a full length isoform, does the specific absence of the Δ 3 isoform contribute to cancer invasion? To address this question, understanding the role of the Δ 3 isoform, and perhaps exon 3, is of particular importance. Unfortunately, the functional differences between the two isoforms are still largely unclear (Allan, Passerini et al. 2005; Ziegler 2006).

A report by Zuo et al (Zuo, Wang et al. 2007) investigated the expression of FOXP3 in ten malignant breast cancer cell lines. They reported that FOXP3 was downregulated between 1.5- and 20-fold in all malignant cell lines including MCF-7 and MDA-MB-231, a similar finding to results in this study. The same report also determined the presence of splice variant isoforms in each cell line. Firstly, 70% of the malignant lines still expressed the *FOXP3 Δ 3* variants demonstrating that the absence of exon 3 was most consistent between the cell lines. However, even the immortalised non-malignant MCF-10A cell line expressed only the Δ 3 isoform. Secondly, they reported that MCF-7, as well as missing a full length variant, also lacked exon 3 and 4, whereas, MDA-MB-231 was missing the full length and exons

3 and 8. Although these findings are inconsistent with results in this study, they do suggest widespread lack of exon 3 amongst breast cancer cell lines and suggest an important role of exon 3 in normal homeostasis.

Both full length and $\Delta 3$ FOXP3 versions have been demonstrated in Tregs and epithelial cells (Allan, Passerini et al. 2005; Zuo, Wang et al. 2007). However, very little has been reported regarding the role of the $\Delta 3$ isoform. FOXP3 $\Delta 3$ has been described as the dominant negative isoform (Ziegler 2006). Exon 3 is located within amino acids 72-106 of FOXP3 and is located within the repressor domain which is known to specifically interact and inhibit ROR- α which leads to the expression of genes responsible for Th17 generation (Du, Huang et al. 2008). Therefore, it is thought that only full length FOXP3 in T-cells can generate Th17 lineage.

Although many reports have demonstrated downregulation of FOXP3, along with mutations and missing isoforms, few reports have investigated the role of FOXP3 $\Delta 3$ in epithelial cells. A recent report by Frattini et al (Frattini, Pisati et al. 2012) is the only paper to date which has investigated the functional aspects of each FOXP3 isoform within non-immune cells. Interestingly, they reported that overexpression of either FOXP3FL or FOXP3 $\Delta 3$ resulted in a reduced proliferation rate (Frattini, Pisati et al. 2012). However, only the FOXP3 $\Delta 3$ isoform was able to reduce the migratory potential of these cells (Frattini, Pisati et al. 2012). Transfection of the full length isoform failed to significantly inhibit migration. This would suggest that the FOXP3 $\Delta 3$ isoform has a greater importance in controlling the migration of cells than the full length isoform, and the lack of FOXP3 $\Delta 3$ in MDA-MB-231 could be responsible for promoting the invasive phenotype.

Because exon 3 interacts with ROR- α , only full length FOXP3 can inhibit ROR- α . ROR- α has been implicated in several forms of malignancy including cancers of the prostate (Moretti, Montagnani Marelli et al. 2002), colon (Lee, Kim et al. 2010) and breast (Xiong, Wang et al. 2012). Within these malignancies, ROR- α is often downregulated, indicating strong anti-cancer properties. Moreover, the presence of ROR- α is reported to inhibit tumour invasiveness (Xiong, Wang et al. 2012). Because both HMEpC and MCF-7 express both FOXP3 isoforms, and T-cell biology has demonstrated that only full length FOXP3 is capable of inhibiting ROR- α , we

could speculate that *FOXP3*^{FL} and *FOXP3*^{Δ3} work in an antagonistic fashion to control the expression of ROR- α .

As MDA-MB-231 lack the *FOXP3*^{Δ3} isoform, and only expresses a full length isoform which represses ROR- α , MDA-MB-231 maybe inhibiting and repressing the expression of ROR- α . Therefore, could this be a key factor in contributing to the invasive capacity of MDA-MB-231?

Although we did not find any mutations within our cell lines, the presence of mutations in *FOXP3* is widespread and well documented in both breast and prostate cancers (Zuo, Wang et al. 2007; Wang, Liu et al. 2009). Zuo et al (Zuo, Wang et al. 2007) sequenced 65 breast cancer patient samples with matched normal tissue and found that 23 out of 65 samples (35%) contained somatic mutations in *FOXP3*. When these mutations were mapped, only 2 of the samples had mutations in exon 3, with the majority lying towards the C-terminal in regions around the forkhead domain or the zinc finger. Similar findings were demonstrated in a study which investigated *FOXP3* mutations in prostate cancer samples (Wang, Liu et al. 2009) and IPEX patients (Lopes, Torgerson et al. 2006). This would suggest that regions towards the C-terminus are more frequently affected in diseases and may be more important for *FOXP3* functioning.

It could be asked why the *FOXP3* sequencing results for MCF-7 and MDA-MD-231 differ from findings of the Zuo group (Zuo, Wang et al. 2007). One possibility is that the cell lines used were in fact not the ones thought to be used. It has been reported that specific cell lines within laboratories can have similar appearances and also grow consistently with other cell lines. For instance it is estimated that between 10-20% of *in vitro* cell lines may have HeLa cell contamination, an issue risen by Stanley Gartler in 1967 (Gartler 1967) and Walter Nelson-Rees in 1975 (Nelson-Rees, Flandermeyer et al. 1974). The cells used in this study were provided by the MD Anderson centre (Houston, TX, USA) and are thoroughly validated as described in section 2.1.4. The most plausible conclusion is that within each cell line there is considerable heterogeneity and not all cell lines are exactly the same. This concept has been reviewed by Baguley and Leung (Baguley and Leung 2011) who have demonstrated a large degree of heterogeneity in growth factor receptors and signalling pathways in breast cancer cell lines. The way cells are currently and

previously looked after (i.e. previous experiments performing knockdown etc), the culture methods and even passage number can alter the expression and profile of each cell line.

3.6.4 p53 status in cancer cell lines and FOXP3 regulation

As reported, the level of FOXP3 is correlated with tumour development which suggests FOXP3, as a TSG, moderates cellular responses to genotoxic stress (Jung, Jin et al. 2010). We have demonstrated that FOXP3 was further dysregulated in the invasive MDA-MB-231 in comparison to the less invasive MCF-7. This suggests that as breast cancer progresses, FOXP3 becomes increasingly dysregulated.

As mentioned in section 1.7.10, a report by Jung et al (Jung, Jin et al. 2010) suggested that FOXP3 was directly regulated by p53. Following treatment with the DNA damaging agent, doxorubicin, levels of FOXP3 was significantly increased in MCF-7, but not in MDA-MB-231, MDA-MB-453 or MDA-MB-157 (Jung, Jin et al. 2010). Interestingly, of these cell lines, only MCF-7 expressed wild type p53. Furthermore, when p53 specific siRNA was used to knockdown the wild type expression of p53 in MCF-7, the induced expression of FOXP3 by doxorubicin previously witnessed was significantly hindered (Jung, Jin et al. 2010). This suggests that MCF-7 is able to successfully upregulate FOXP3 expression under genotoxic stress through the interactions of p53 which restores capacity to function or localise to the nucleus and possibly inhibits the potential to invade. However, because MDA-MB-231 fails to express functional p53 they are unable to upregulate FOXP3 expression under genotoxic stresses and potentially promotes the more aggressive phenotype.

3.6.5 FOXP3 expression by cytokine-treatment in cancer cells

As discussed in section 3.1.2, certain cytokines, particularly TGF- β and IL-2, increase the expression of FOXP3 in T-cell subsets. It has been reported that breast epithelial cells respond to TGF- β and, therefore, have TGF- β receptors (Miettinen, Ebner et al. 1994; Dore, Edens et al. 1998). IL-2 receptors have also been

demonstrated on intestinal and lung epithelial cells (Ciacci, Mahida et al. 1993; Lesur, Arsalane et al. 1997), whereas, a study by Garcia-Tunon et al (Garcia-Tunon, Ricote et al. 2004) demonstrated IL-2 receptor presence on cells from breast cancer patients.

Treatment of the breast cancer cell lines MDA-MB-231 and MCF-7 with TGF- β or IL-2 failed to induce any change in *FOXP3* expression after 6, 16 and 24 hours. As a positive control, freshly isolated CD4⁺ T-cells were also treated with IL-2 and TGF- β . An increase in *FOXP3* expression was witnessed after TGF- β treatment but not with IL-2. Zorn et al (Zorn, Nelson et al. 2006) reported that treatment of IL-2 increased *FOXP3* in CD4⁺CD25⁺ cells but not in CD4⁺CD25⁻ cells. Because CD25 is the α chain of the IL-2 receptor, this could therefore suggest IL-2 may only have its effects on expanding pure Tregs which are defined as CD25^{hi} and therefore have high levels of IL-2 receptors. Tregs make up approximately 5-10% of human CD4⁺ T-cells (Long, Cerosaletti et al. 2010) and the content of Tregs in our CD4⁺ isolation may have been too low to witness the effects of IL-2 treatment. This data demonstrates, for the first time, that *FOXP3* within breast epithelial cells does not respond to TGF- β and IL-2. Similar findings have been demonstrated by Frattini et al (Frattini, Pisati et al. 2012) who reported that treatment of TGF- β 1 and TGF- β 2 did not influence the mRNA or protein levels of *FOXP3* in three glioblastoma cell lines.

As described, *FOXP3* downregulation is widespread amongst breast cancer patients, whereas, even the level of *FOXP3* in healthy epithelial cells is still relatively low. TGF- β is a cytokine which is key in homeostasis and tumour suppression. However, when cancer cells lose responsiveness of TGF- β , they can use this cytokine to their advantage as reviewed by Massague (Massague 2008). Because TGF- β is often enriched in tumour environments, if TGF- β was able to cause increased *FOXP3* expression in epithelial cells, it would seem unlikely that the majority of breast cancers and breast epithelia would have downregulated or low levels of *FOXP3*.

The importance of TGF- β in cancer can be further illustrated by several lines of evidence. As mentioned in section 1.7.8, chronic inflammation is associated with breast cancer where T-cell infiltration is high. Infiltration of Tregs are also frequently witnessed and thought to act as a mechanism of immune evasion. Therefore, the presence of TGF- β could increase the levels of Tregs within the tumour environment

by converting CD4⁺ T-cells into acquired Tregs and thus leading tumour progression via immune evasion.

3.7 Conclusion

This chapter has demonstrated dysregulation of FOXP3 in breast cancer cell lines of both low and high level invasive capacity. Data in this chapter for the first time quantifies the levels of FOXP3 in breast epithelia as well as quantifying the subcellular distribution of the protein in breast cancer cell lines. Although these aspects are consistent with data in other reports, the data from sequencing *FOXP3* in breast cancer does not fit in with the current literature. Despite the discovery of a missing natural *FOXP3* variant in MDA-MB-231, data from the experiments reported here failed to show any mutations in either breast cancer cell lines. There is much debate around the relevance of using cell lines and this data further emphasises the high level of heterogeneity in cell lines, and emphasises the importance of cell line validation.

Because data in this chapter has demonstrated the high level dysregulation of FOXP3 in the invasive breast cancer cell line MDA-MB-231 and regular constitutive expression of FOXP3 in the HMEpC, it would be of interest to investigate the effects of restoring wild type FOXP3 in MDA-MB-231, and also what the consequences are if wild type FOXP3 was knocked down in HMEpC. This is addressed in the next chapter.

	Chapter
General introduction	1
General materials and methods	2
Study of FOXP3 expression in normal and malignant breast cell lines	3
<i>In vitro</i> modelling of FOXP3 in normal and malignant breast cell lines	4
<i>In vivo</i> levels of FOXP3 and CXCR4 expression in breast cancer samples	5
Discussion	6
List of references	7
Appendices	8

4 *In vitro* modelling of FOXP3 functions in normal and malignant breast epithelia

4.1 Introduction

As a transcription factor the primary role of FOXP3 is to regulate the expression of genes (Zheng, Josefowicz et al. 2007). Many of the genes reported as FOXP3 targets are considered as oncogenes as they are frequently overexpressed in cancer cells. The influence of FOXP3 on a number of specific oncogenes has been reviewed by Douglass et al (Douglass, Ali et al. 2012) and is briefly discussed.

4.1.1 HER2 (*ErbB2*)

The importance of HER2 in breast cancer has been discussed in section 1.4.4.2. The *ErbB2* gene encodes the HER2 protein which is a transmembrane receptor tyrosine kinase and member of the epidermal growth factor receptor family. Overexpression of HER2 has been linked to more aggressive forms of breast cancer. On this basis, it has recently emerged as an important prognostic marker in breast cancer diagnosis (Slamon, Clark et al. 1987; Press, Bernstein et al. 1997).

HER2 activation is dependent on phosphorylation of specific tyrosine residues on the intracellular region of HER2 which act as binding sites for molecules linking HER2 to downstream pathways which include MAPK and PI3K leading to cell growth and survival (Roy and Perez 2009).

The potential of FOXP3 to modify the expression of HER2 in breast epithelial cells has been demonstrated on several lines of evidence by Zuo et al (Zuo, Wang et al. 2007). Following transfection of a FOXP3 expressing vector into a HER2 overexpressing mouse breast cancer cell line (TSA) there was a significant reduction of *ErbB2* transcripts. Whereas, when FOXP3 was silenced in normal mammary cells there was a subsequent increase in *ErbB2* transcripts. Further evidence of this repression was provided when the 5' sequence of the *ErbB2* gene was analysed and

revealed multiple binding motifs for the forkhead domain of FOXP3 (Zuo, Wang et al. 2007). This demonstrates that the effects of FOXP3 on *ErbB2* are direct. *In vitro* experiments using human breast cancer cell lines have produced results similar to those observed from *in vivo* (Zuo, Wang et al. 2007). Analysis of ten malignant breast cancer cell lines, all with significantly reduced levels of *FOXP3*, revealed that seven cell lines overexpressed *ErbB2* transcripts in comparison to normal epithelial cells (Zuo, Wang et al. 2007). However, the fact that the other three cell lines did not overexpress HER2, demonstrates that FOXP3 is most likely not the sole regulator of HER2 expression. Finally, when wild type FOXP3 was silenced using siRNA in normal mammary epithelial cells, a 7-fold increase was observed in *ErbB2* mRNA and cell-surface expression of HER2 (Zuo, Wang et al. 2007).

4.1.2 S-phase kinase-associated protein 2

S-phase kinase-associated protein 2 (SKP2) has been reported in a wide variety of cancers (Nakayama and Nakayama 2006) and is overexpressed in nearly 50% of breast cancers (Sonoda, Inoue et al. 2006). SKP2 overexpression in these malignancies generally correlates with a poor prognosis (Signoretti, Di Marcotullio et al. 2002; Radke, Pirkmaier et al. 2005).

Cell cycle progression is controlled by a number of short lived enzymes called cyclin dependant kinases (CDK) and CDK inhibitors. The expression of these enzymes must be tightly regulated and are frequently degraded by the proteolytic ubiquitin–proteasome pathway. This pathway consists of three enzymes, ubiquitin-activating enzymes (E1), ubiquitin-conjugating enzymes (E2) and ubiquitin ligase enzymes (E3). SKP2 is an essential component of E3 ubiquitin ligase and has specificity for degrading the CDK inhibitor p27 (Nakayama, Nagahama et al. 2004). As well as regulating cell cycle, overexpression of SKP2 has also been suggested to influence the migration and invasiveness of cancer cells (Einama, Kagata et al. 2006).

The expression of SKP2 and FOXP3 has been investigated in a panel of malignant human breast tissues (Zuo, Liu et al. 2007). It was found that 30% of FOXP3 positive samples overexpressed SKP2. However, only 56% of FOXP3 negative samples overexpressed SKP2 (Zuo, Liu et al. 2007). It was also shown that MCF-7

with inducible FOXP3 expression had an 8-fold increase in *SKP2* transcripts 48 hours after FOXP3 expression was un-induced (Zuo, Liu et al. 2007). This highlights that FOXP3 is able to rapidly reduce the expression of *SKP2*. Similarly, *SKP2* was increased when FOXP3 was silenced in an early passage of HMEpC, whereas, when wild type FOXP3 was transfected into TSA cell lines, *SKP2* expression was reduced between 10- and 20-fold (Zuo, Liu et al. 2007). chIP assay demonstrated a number of FOXP3-specific binding regions located within the *SKP2* gene, and a deletion in either binding site results in an increased level of *SKP2* expression (Zuo, Liu et al. 2007). This confirms that FOXP3 directly represses the expression of *SKP2* in breast epithelial cells.

4.1.3 c-Myc

c-Myc is overexpressed in more than 30% of human cancer cases. This has led it to becoming one of the most researched genes in cancer (Grandori, Cowley et al. 2000). The *c-Myc* gene is located on chromosome 8 and encodes a transcription factor which is an integral part of controlling cell cycle progression, as it acts as a CDK inhibitor with high affinity for p21 (Jung, Menssen et al. 2008) and p15 (Iavarone and Massague 1997).

Although the effects of FOXP3 controlling c-Myc expression have never been reported in breast cancer, a report by Wang et al (Wang, Liu et al. 2009) suggested that FOXP3 is able to regulate the expression of c-Myc in prostate epithelia. This is based on several strong lines of evidence. Firstly, when wild type FOXP3 was knocked down in human prostate cells, an increase in *c-Myc* transcripts and protein was observed resulting in an increased rate of proliferation (Wang, Liu et al. 2009). Corresponding to this, when FOXP3 was transfected into two human prostate cancer cell lines, the expression of *c-Myc* was almost completely abrogated (Wang, Liu et al. 2009). As demonstrated by chIP assay, using prostate epithelial cells, FOXP3 directly regulates the expression of *c-Myc* as an abundance of forkhead binding motifs was revealed within the 5' region of the transcriptional start site in the *c-Myc* gene (Wang, Liu et al. 2009).

4.1.4 p21 (*CDKN1A*)

p21 is a protein encoded by the *CDKN1A* gene. Dysregulated expression of p21 has been implicated in many forms of cancer, particularly breast cancers (Pinto, Andre et al. 2005). Interestingly, in these cancers, p21 itself is often not mutated (Pinto, Andre et al. 2005), suggesting that the association between p21 expression and cancer is due to its role as a downstream target of other genes (el-Deiry, Tokino et al. 1993; Dulic, Kaufmann et al. 1994; Somasundaram, Zhang et al. 1997).

p21 is a CDK inhibitor with specificity for CDK1 and CDK2. p21 causes cell cycle arrest in the G₁ phase and is therefore, important in cell cycle progression and senescence (Xiong, Hannon et al. 1993). As well as causing cell cycle arrest, it can interact with proliferating cell nuclear antigen (PCNA), which is an accessory factor for DNA polymerase and is important in DNA synthesis and repair (Cayrol, Knibiehler et al. 1998).

Although p21 itself is not thought to influence the migration of cells (Goetze, Scholz et al. 2010) it has recently been suggested that p21 is able to influence the migration and invasion of cancer cells through other mechanisms such as p21-activated kinase 4 (PAK4) (Li, Katoh et al. 2013).

In addition to repressing the expression of several oncogenes, FOXP3 can also upregulate factors involved in reducing tumour growth. FOXP3 binds to intron 1 in *CDKN1A* and increases histone H3 acetylation by reducing the binding of HDAC2 and HDAC4, providing a potential mechanism for upregulation of p21 expression (Liu, Wang et al. 2009). When FOXP3 was knocked down in MCF-7 and human mammary epithelial cells, there was a decrease in the expression of p21 (*CDKN1A*) transcripts and protein (Liu, Wang et al. 2009). This knockdown also correlated with an increase in the size and number of the colonies compared to wild type cells (Liu, Wang et al. 2009). The link between FOXP3 and p21 regulation in breast cancer was further validated when 62 human breast cancer cases were assessed for FOXP3 and p21. Results demonstrated that only 30% of FOXP3 negative cases expressed p21 (Liu, Wang et al. 2009). Despite these important findings, it should be noted that other TSGs such as p53 (el-Deiry, Tokino et al. 1993) and *BRCA1* (Somasundaram, Zhang et al. 1997) are also able to control p21 levels.

A recent report has also demonstrated that FOXP3 is able to bind directly to the transcriptional start site of both p21 and *c-MYC* within glioblastoma stem cell-like cells and control the expression of these genes in a similar manner as described in breast epithelia (Frattini, Pisati et al. 2012).

4.1.5 CXCR4

Although the potential of FOXP3 to influence CXCR4 expression has never been reported in epithelial cells, Zheng et al (Zheng, Josefowicz et al. 2007) performed a genome-wide analysis of FOXP3 target genes in Tregs and demonstrated that *CXCR4* is a gene directly under the influence of FOXP3 in thymic T-cells. Interestingly, the gene for another chemokine receptor heavily associated with breast cancer metastasis, CCR7, was also reported to be regulated by FOXP3 in Tregs. However, the influence of FOXP3 on CXCR4 is yet to be fully defined.

4.1.6 The influence of FOXP3 on cellular function

As discussed by Douglass et al (Douglass, Ali et al. 2012), many of the genes regulated by FOXP3 in epithelial cells encode receptors which control the growth, proliferation, migration and invasion of cells. Several *in vitro* and *in vivo* reports using breast, brain, prostate and ovarian epithelial cells have now shown that dysregulated FOXP3 expression does not merely affect the expression of the aforementioned genes and proteins, but is also able to alter the function of these cells (Zuo, Wang et al. 2007; Liu, Wang et al. 2009; Wang, Liu et al. 2009; Zhang and Sun 2010; Li, Wang et al. 2011; Frattini, Pisati et al. 2012; Li, Katoh et al. 2013; Nakahira, Morita et al. 2013).

When FOXP3 DNA was transfected into two human breast cancer cell lines, MCF-7 and SKBr3, and one mouse breast cancer cell line, TSA (all of which lack normal FOXP3 expression), the colonies grew at significantly reduced rate, whereas, cells transfected with an empty vector grew rapidly (Zuo, Wang et al. 2007). This demonstrates that FOXP3 is able to suppress the growth of breast cancer cells. *In vivo* studies have also demonstrated the intrinsic importance of Foxp3 and the effects

of *Foxp3* deletions. A strain of mice with a floxed *Foxp3* locus was generated so these mice contain prostate specific deletions of *Foxp3* within the epithelia (Wang, Liu et al. 2009). By 8-12 weeks there was a 16-fold decrease in *Foxp3* expression which was validated at protein level by Western blot (Wang, Liu et al. 2009). After 12-15 weeks there was a 5-fold increase in the percentage of Ki67⁺ proliferating cells in comparison to wild type mice. MRI scans also demonstrated a significant enlargement of the prostate in live mice (Wang, Liu et al. 2009). After 14-16 weeks, 5 out of 6 *Foxp3* deficient mice showed hyperplasia. After 23-26 weeks, 80% of the *Foxp3*-floxed mice showed extensive hyperplasia, whereas none of the age matched mice showed this pathology (Wang, Liu et al. 2009). Finally, by 43-60 weeks, all the mice with prostate specific *Foxp3* deletions showed extensive hyperplasia (Wang, Liu et al. 2009).

The data by Wang et al (Wang, Liu et al. 2009) demonstrates that a lack of *Foxp3* in prostate epithelial cells leads to spontaneous tumour growth in mice which began the process of sexual maturity. This finding could have profound clinical significance on male IPEX patients. As described in section 1.7.3, IPEX patients undergo HSCTx which has a high success rate in alleviating chronic autoimmunity. However, IPEX patients will still have mutated versions of FOXP3 within their epithelial cells and, similar to the mice reported in the study by Wang et al (Wang, Liu et al. 2009), may have an increased risk of developing prostate hyperplasia and tumour formation when they begin puberty. This would suggest that from this stage, IPEX patients should be monitored carefully for the formation of prostate specific tumours.

When a FOXP3 vector was re-introduced into an ovarian cancer cell line, the growth and proliferation of these cells was significantly reduced (Zhang and Sun 2010). There was also significant inhibition of cell cycle associated proteins as a predominant accumulation of FOXP3 transfected cells were caught in the G0-G1 phase of the cell cycle. In addition to this, the metastatic potential of these cells was reduced as the migration and invasive potential of these cells was inhibited following FOXP3 transfection. It is thought that the majority of these effects can be attributed to inhibiting the signalling of NF- κ B and mTOR and the expression of uPA and *MMP2* and *MMP9* (Zhang and Sun 2010). The ability FOXP3 to influence the expression of *MMP9* was also suggested in MCF-7 (Nakahira, Morita et al. 2013). Nishihira et al (Nakahira, Morita et al. 2013) reported that following the activation of

FOXP3 through LCK, the invasiveness of MCF-7 cells was significantly decreased. Interestingly the same report also demonstrated that FOXP3 expression resulted in a decrease in *VEGFA* expression (Nakahira, Morita et al. 2013).

As described in section 1.7.8, *FOXP3* has also been reported to be downregulated within the majority of glioblastoma cases (Frattini, Pisati et al. 2012). The same report investigated the functional effects of FOXP3 overexpression in a FOXP3 deficient glioblastoma cell line, and also the effects of FOXP3 knockdown in a glioblastoma cell line within constitutive FOXP3 expression and an adequate proliferation rate. Results demonstrated that overexpression of either of the natural FOXP3 isoforms were able to reduce proliferation, however, only isoform b (also referred to as FOXP3Δ3) was able to reduce the migration of these cells (Frattini, Pisati et al. 2012). On the other hand, FOXP3-silencing resulted in an increase in the proliferation and migration of these cells in comparison to scrambled shRNA transfected cells (Frattini, Pisati et al. 2012).

Similar findings were reported *in vivo* as mice injected with FOXP3 silenced glioblastoma cells developed tumours which were FOXP3 negative. As measured by Ki67⁺ cells, these mice also had a significantly higher proliferation and reduced survival in comparison to mice with scrambled shRNA transfected cells (Frattini, Pisati et al. 2012).

4.2 Aims and objectives

- Construct a FOXP3-expressing plasmid.
- Generate stably transfected FOXP3-overexpressing MDA-MB-231.
- Knockdown wild type FOXP3 expression in HMEpC using commercial siRNA.
- Following FOXP3 transfection into MDA-MB-231 and FOXP3 knockdown in HMEpC:
 - Use real-time PCR to determine transcriptional changes in *ErbB2*, *SKP2*, *MYC*, *CXCR4* and *CDKN1A*.
 - Use flow cytometry to determine the changes in cell surface expression of CXCR4.
 - Assess functional changes affecting cell cycle, cell proliferation, invasion and migration in response to CXCL12.

4.3 Specific materials and methods

4.3.1 Bacterial cell culture methods

A culture of chemically competent EB5α *E.coli* (BioEdge, Gaithersburg, MD, USA) (Referred to as *E.coli* from here on) was used in cloning and the generation of a FOXP3-expression plasmid. FOXP3 DNA was transformed into *E.coli* and used to generate large quantities of plasmid DNA for transfections.

4.3.1.1 Lysogeny broth

The original formula of lysogeny broth (LB) was published in 1951 in the first paper of Bertani on bacterial lysogeny (Bertani 2004). The recipes have not changed greatly since. LB is a nutritionally rich medium that is primarily used for the growth of bacteria. LB (Sigma-Aldrich) consists of 10g/L bacto-tryptone, 5g/L bacto-yeast extract, and 10g/L NaCl (at pH7). To make LB agar, 10g/L agar was added and heated to dissolve.

Everything needed for optimum growth of a bacterial suspension is provided in the recipe. Peptides and peptones are provided by tryptone and vitamins, and certain trace elements are provided by yeast extract, sodium ions for transport and osmotic balance is provided by sodium chloride. All media was sterilised by autoclaving at 121°C for 15 minutes.

Bacteria were grown on LB media agar plates at 37°C, or in liquid LB at 37°C overnight on a shaker. Bacterial stocks were made for long term storage by freezing cells in LB with 50% glycerol (Sigma-Aldrich) at -80°C.

4.3.1.2 Transformation of chemically competent *E.coli*

Chemical competence refers to the ability of cells to take up extracellular DNA from its environment. Competent *E.coli* were transformed by defrosting 25µl of cells on ice, followed by incubating with 2µg of DNA on ice for 30 minutes. This allows the DNA to adsorb onto the surface of cells. The cells were then heat shocked for 90

seconds at 45°C and returned to ice for 2 minutes. This process causes the cells to open pores in their membranes allowing the DNA to enter, whilst incubation on ice causes the pores on the membrane to close, thereby trapping DNA in the cells. The cells were then grown in 1ml of LB for 2 hours at 37°C before being spread onto LB agar plates containing an appropriate concentration of the selection antibiotic for the plasmid type (Ampicillin for FOXP3-vector and Kanamycin for pmaxGFP-vector). The LB agar plates were incubated at 37°C overnight and the following day individual colonies were picked for further analysis. Negative controls were used which consisted of LB agar plates with antibiotic but no cells.

4.3.1.3 Recovery of plasmid DNA from bacterial cell culture

Plasmid DNA was isolated from *E.coli* cultures using a QIAgen mini-prep kit (QIAgen). This technique utilises silica-binding technology and spin columns. Universal tubes containing 10ml of LB, antibiotic and previously transformed *E.coli* were grown overnight on a shaker at 37°C. The following day the cells were pelleted by centrifugation at 500xg for 5 minutes. Bacteria were then resuspended in 250µl of buffer containing RNase followed by lysis of cells using 250µl of an alkaline SDS solution. 350µl of a neutralising buffer was added to stop the reaction. The lysate was centrifuged at 13000xg for 10 minutes to pellet cell debris, protein, chromosomal DNA and lipids. The clear lysate produced was then added to a silica spin column and centrifuged for 1 minute at 13000xg. The eluate was disposed of and the plasmid DNA was washed twice in an ethanol containing buffer before being eluted from the column into a fresh sterile collection tube with 50µl of elution solution.

4.3.1.4 Restriction enzyme digestion of DNA

Restriction enzymes recognise short, symmetrical base pairs and cut DNA into small specific segments. Depending on the endonuclease selected, enzymatic digestion can produce either blunt or sticky ends. A blunt ended digestion can ligate to any other

blunt end digested DNA, however, a sticky end can only bind to other sequences with the same overhanging sequence. This produces specific annealing of complementary ends and restoration of the original restriction site. It is generally accepted that 1 unit of enzyme (Promega) is used to digest 1µg of DNA in 1 hour at 37°C. Digestions were left for between 3-6 hours at 37°C, however, for complete digestion of larger DNA quantities additional time may be required and was often left overnight. The restriction enzymes used are listed in **table 4.1** along with their target sequences.

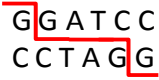
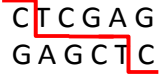

Restriction enzyme	Target sequence	Experiment used in
<i>BamHI</i>	 GGATCC CCTAGG	Digest pcDNA3.1/Zeo(+) plasmid to allow FOXP3 insert to ligate
<i>XhoI</i>	 CTCGAG GAGCTC	Digest pcDNA3.1/Zeo(+) plasmid to allow FOXP3 insert to ligate
<i>ScaI</i>	 AGTACT TCATGA	Used to linearise the pcDNA3.1/Zeo-FOXP3 plasmid for stable transfections

Table 4-1 - Restriction enzymes used in plasmid cloning and linearization

When cloning the *FOXP3* gene into the pcDNA3.1/Zeo(+) backbone *BamHI* and *XhoI* were used. To linearise the plasmid for transfection, *ScaI* was used which cuts specifically at a site within the ampicillin resistance gene region.

4.3.2 Transfection methods

Transfection is a common technique used in biological research where the aim is to genetically manipulate a cell by deliberately introducing new nucleic acid. The aim of transfection can be either to upregulate expression of a specific gene of interest, often delivered in the form of a plasmid, or to knockdown the expression of a wild type gene which is expressed within the target cell.

Many methods of transfection have been developed. These methods are best categorised as chemical, electrical or viral based methods. Chemical and electrical methods were used in this study.

Electrical-based transfection is electroporation (also known as nucleofection). This technique is based on physical parameters instead of chemical. It uses electrical pulses to significantly increase the electrical conductivity and permeability of the cells plasma membrane. The mechanism of electroporation occurs through a number of phases: The initial phase is the application of a current (generally between 300-400mV) for less than 1ms across the plasma membrane. This current results in a migration of ions into the surrounding solution which charges the membrane and results in a rearrangement in the morphology of the lipids making pores approximately 0.3nm in size allowing linearised DNA to enter the cells. Finally, the pores will heal and reseal, or, if the critical size was exceeded, the pore will expand causing the cell to rupture resulting in cell death.

The most commonly performed chemical-based transfection is referred to as lipofection (also known as lipid-based transfection). This technique is highly effective as it uses transfection reagents which contain cationic lipid subunits which form liposomes in aqueous environments. The positively charged lipids can then encapsulate negatively charged plasmid DNA when the two are mixed. The liposomes containing the DNA are then able to fuse directly with the cells negatively charged plasma membrane and enter the cell. Once inside the cell, the liposome avoids the endosomal pathway and enters the nucleus.

Transfections can be either transient or stable. When the genetic material is only transiently transfected, the foreign DNA will not be incorporated into the host cells genome therefore the expression of the exogenous DNA will only be present in the

cell for a limited time whilst the cell undergoes mitosis and eventually dilutes the DNA out. However, if the DNA is incorporated into the genome, when the cell undergoes mitotic division, each new daughter cell will also express the transfected DNA. Stably transfected cells are often selected from non-transfected cells via the use of a selection antibiotic. The plasmid contains a gene to encode the resistance to the antibiotic, therefore, cells which survive in the presence of the antibiotic are considered to have incorporated the plasmid DNA into their genome.

4.3.2.1 Stable transfection of MDA-MB-231 using AmaxaTMNucleofectorTM

Cell lines were transfected with plasmid DNA using the AmaxaTMNucleofectorTM (all NucleofectorTM equipment was purchased from Lonza). Prior to electroporation, cells were grown in T75 flasks until 80-90% confluent. Cells were released from the flask surface (as described in section 2.2.4) and counted. 1×10^6 cells were resuspended in 100 μ l of AmaxaTMNucleofectorTM solution V. Plasmid DNA (5 μ g) was added to the culture, mixed gently by pipetting, and then transferred to an AmaxaTMNucleofectorTM electroporation curvette. The curvette was then inserted into the AmaxaTMNucleofectorTM machine and program X-13 (MDA-MB-231) or A-23 (HEK-293) was selected. After electroporation was complete, the curvette was removed from the machine and placed on ice for 5 minutes to help the healing of pores on the cell membrane. Finally, cells were removed from the curvette and placed directly into fresh growth media and cultured. Growth media was replaced the following day and the transfection efficiency was checked 24 and 48 hours post-transfection.

4.3.2.2 Lipid-based transient transfections

In this study transient transfections were attempted using a number of lipid-based transfection reagents. Each of these has a similar mechanism of action and vary slightly in their protocols. The transfections were performed in 6-well plates. Protocols for each reagent are described briefly below:

Lipofectamine®2000 (Invitrogen): Lipofectamine®2000 is lipid-based transfection reagent which has been widely reported as successful in transfecting plasmid DNA, including a FOXP3 plasmid into an ovarian cancer cell line (Zhang and Sun 2010). It has also been reported to be successful in transfecting MDA-MB-231 cells (Chen, Kang et al. 2001; Wu, Chan et al. 2005; Thakur, Sun et al. 2008).

Transfection complexes were formed by diluting 4µg of freshly isolated plasmid DNA, and either 4µl, 8µl or 12µl of Lipofectamine®2000 reagent each in 50µl of basal DMEM. Tubes were left to incubate at room temperature for 5 minutes before being combined and left to incubate for a further 25 minutes at room temperature allowing the liposomes and DNA to form complexes. At the end of incubation, the transfection complexes were added drop by drop to each well and the plate was gently mixed to disperse complexes. Cells were seeded at a concentration of 0.5×10^6 /ml into 6-well plates in 2ml of growth media without serum or antibiotics and incubated overnight in normal growth conditions. The following day, old media was removed and replaced with fresh complete growth media. The transfection efficiency was determined 24 and 48 hours post-transfection.

JetPRIME™ (Polyplus, Illkirch, France): Prior to transfection, cells were serum starved for 2 hours. Transfection complexes were formed by diluting 2µg of plasmid DNA in 200µl of JetPRIME™ buffer followed by the immediate addition of 4µl, 6µl, 8µl or 10µl of JetPRIME™ reagent. These complexes were left to incubate at room temperature for 10 minutes before being dispensed onto the surface of the culture plate. Cells (0.5×10^6 /ml) were then immediately added to the wells and left to incubate in the normal growth conditions, in 2ml growth media without antibiotics. Transfection complexes were removed after 6 hours and replaced with fresh complete growth media. Transfection efficiency was assessed 24 and 48 hours post-transfection.

GenJet™ (SignaGen® Laboratories, Peterborough, UK): GenJet™ transfection reagent (Ver.II) is an upgraded version of the original GenJet™ reagent, and according to the manufacturers protocol, it is able to increase transfection efficiencies up to 20 times higher than the previous GenJet™ reagent. MDA-MB-231 were transfected with plasmid DNA using an advanced protocol supplied by the

manufacturers specifically for transfecting MDA-MB-231 cells. This protocol was also optimised to increase transfection efficiencies and cell viability.

GenJet™ reagent and DNA complexes were prepared by diluting 2µg of highly pure plasmid DNA and either 4µl, 6µl or 8µl of GenJet™ reagent into 100µl of basal DMEM in separate tubes. Each tube was gently vortexed and centrifuged at a low speed to bring drops to the bottom of the tube. The diluted GenJet™ reagent was then immediately added to the diluted DNA solution and mixed by pipetting 3-4 times and then left to incubate for 15 minutes at room temperature. During this period, 1.2×10^6 cells were pelleted by centrifugation at 150xg for 10 minutes and the supernatant was completely removed. After the transfection complexes had incubated for 15 minutes at room temperature, they were used to resuspend the cell pellet. The cells were then incubated at 37°C for a further 20 minutes with the transfection complexes. Following incubation, the cell suspension was dispensed into a 6-well plate with 2ml of complete growth media. The transfection efficiency was determined 24 and 48 hours post-transfection.

TurboFect™ (Fermentas): Transfection of plasmid DNA was attempted using TurboFect™ according to the manufacturers protocol. Briefly, transfection complexes were prepared by diluting 2µg of DNA in 100µl of basal DMEM. 2µl, 4µl or 6µl of TurboFect™ reagent was immediately added to the DNA complexes and incubated at room temperature for 15 minutes. Transfection complexes were evenly distributed onto the surface of the 6-well plate and 0.25×10^6 /ml cells were dispensed on top of complexes in 2ml growth media. Transfection efficiency was determined 24 hours post-transfection.

GeneJuice® (EMB Millipore, Billerica, MA, USA): Cells were prepared at a final density of 0.5×10^6 in 3ml of growth media. Transfection complexes were prepared by diluting 6µl of GeneJuice® reagent in 100µl of basal DMEM and incubated for 5 minutes at room temperature. Next, 2µg of DNA was added to the solution, mixed gently by pipetting, and incubated for a further 10 minutes at room temperature. Transfection complexes were then placed onto the surface of the culture plate and cells were dispensed into wells and incubated in normal growth conditions. Transfection efficiency was determined after 24 hours.

4.3.3 Selection of stably transfected cells using ZeocinTM

When generating stably transfected cell lines, it is imperative to determine the lowest concentration of antibiotic which is required to kill untransfected cells and select cells which have integrated plasmid DNA, and can therefore grow in the presence of the selection antibiotic.

When cells are metabolising they frequently produce reducing equivalents as a by-product. These reducing equivalents pass on their electrons to an electron transfer reagent which reduces tetrazolium into a purple coloured aqueous formazan product. This can then be detected at 490nm. When cells are no longer viable they fail to reduce the tetrazolium product to formazan, therefore, cell metabolism and viability is proportional to the intensity of the purple colour (**figure 4.1**).

The lowest concentration of ZeocinTM (Invitrogen) required to kill untransfected MDA-MB-231 was determined using a CellTiter 96® Non-radioactive cell proliferation assay (Promega). This assay uses a tetrazolium substrate (3-(4,5-dimethylthiazol-2-yl)-5-(3-carboxymethoxyphenyl)-2-(4-sulfophenyl)-2H-tetrazolium, inner salt; MTS) and an electron coupling reagent (phenazine methosulphate, inner salt; PMS) to determine cell viability. Approximately 5×10^4 MDA-MB-231 were dispensed into 96-well plates and grown overnight in normal conditions. The following day, growth media was removed and replaced with fresh growth media containing ZeocinTM at concentrations ranging from 0 µg/ml to 700 µg/ml, with 100 µg/ml increments. Each day cell viability was determined by adding 100 µl of a MTS/PMS complex (1:20, MTS:PMS) and incubated at 37°C for 2 hours. The intensity of colour change was determined using microplate reader at 490nm. Cell viability was determined as a percentage using healthy cells grown in the absence of antibiotic, arbitrarily set as 100%.

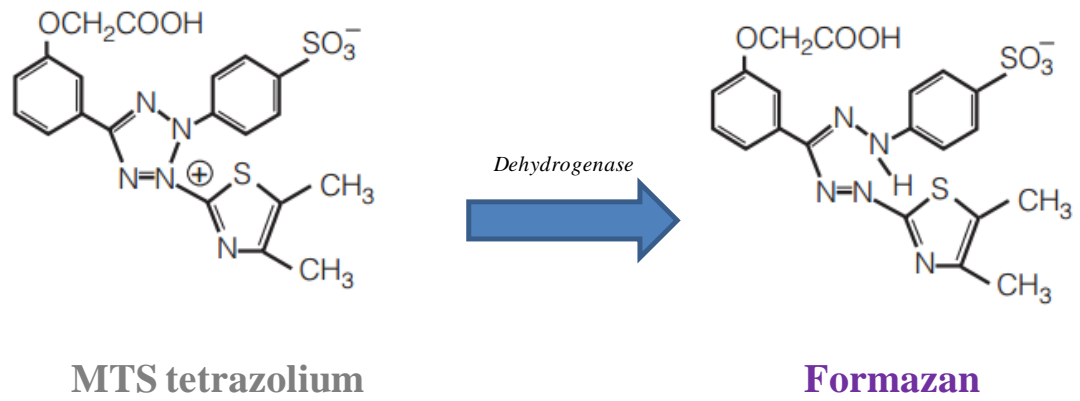


Figure 4-1 - Conversion of MTS tetrazolium into Formazan

The conversion of MTS tetrazolium into soluble formazan is catalysed by dehydrogenase enzymes which are located within metabolically active cells. Therefore, the extent of cells which are growing and viable are proportional to the formazan product which can be measured at 490nm using a microplate reader.

4.3.4 Transfection of siRNA sequences

siRNA stands for small interfering RNA. During translation, mature mRNA produced within the nucleus is transported into the cytoplasm of the cells where they are translated into protein. siRNA sequences which enter the cell via liposomes form a complex with ribonucleic proteins called RISC (RNAi silencing complex). Part of this complex is a catalytic protein called argonaute which binds to non-coding RNAs such as siRNA. siRNA sequences then direct the complex to the complementary mRNA sequence and where they exhibit their endonuclease slicer activity (Tolia and Joshua-Tor 2007). The cleaved mRNA is then destroyed by the cells as it is recognised as aberrant. Thus, siRNA inhibits the protein production by silencing the expression of the gene within the cytoplasm of cells.

siPORTTMNeoFXTM (Ambion) is a lipid-based transfection reagent which has high specificity for delivering siRNA into cells. Because siRNA is composed of short specific bases it is substantially smaller than plasmid DNA, therefore, reagents used to deliver siRNA sequences are generally less cytotoxic than those used to deliver plasmids. Delivery of siRNA sequences was performed using commercial siRNA sequences and the transfection reagents Lipofectamine®2000 and siPORTTMNeoFXTM. Transfections were carried out according to the manufacturers protocol. The transfection process using Lipofectamine®2000 is described in section 4.3.2.2. All knockdown experiments were performed in 12-well plates. Transfection using siPORTTMNeoFXTM was carried out according to the manufacturers protocol. Briefly, 3µl of siPORTTMNeoFXTM transfection reagent and 1µM of *silencer*® select FOXP3 siRNA were combined, in separate tubes, with basal growth media to make a final volume of 50µl. The tubes were left to incubate at room temperature for 10 minutes before being combined and left to incubate for a further 10 minutes at room temperature. Following incubation, complexes were dispensed onto the surface of a culture plate and 1ml of the cells (0.2×10^6) were dispensed on top of the transfection complexes and left to incubate at 37°C in normal growth conditions. This now makes a final siRNA concentration of 5nM. The knockdown efficiency was assessed at transcript and protein levels after 24 hours.

All siRNA used in experiments were purchased from Ambion. FOXP3 specific sequences and are listed in **table 4.2**. Control siRNA sequences were also purchased

from Ambion (*Silencer*® select Negative Control No.1 siRNA, catalogue no.4390843).

siRNA name	Assay ID
FOXP3 siRNA-1	s27191
FOXP3 siRNA-2	s27192
FOXP3 siRNA-3	s27190

Table 4-2 - List of siRNA used in experiments

All FOXP3 specific siRNA sequences were purchased from Ambion. Specific assay ID's are provided.

4.3.5 Functional studies

A number of functional assays were used to determine the effects on cell behaviour following FOXP3 transfection into MDA-MB-231 and FOXP3 knockdown in HMEpC.

4.3.5.1 Transwell chemotaxis

Transwell chemotaxis assays were carried out using specially designed 24-well plates (Becton Dickinson) which contain a “lip” on which the transwell chamber can rest. Before allowing cells to migrate, the chemotaxis plates were blocked using basal media containing 0.1% BSA (Sigma-Aldrich) and 1% L-Glutamine (referred to as chemotaxis buffer) and incubated at 37°C for 1 hour. This ensures the chemokine remains in suspension and it prevents it from sticking to the surface of the plate. Human breast cancer cells require a fibronectin matrix to adhere to, so the underside of 8µm-pore chemotaxis filters (Becton Dickinson) were coated with 2.5µg/ml fibronectin (Sigma-Aldrich) and incubated at room temperature for 30 minutes. Excess fibronectin was removed and the filters were left to air dry for a further 30 minutes.

Each well contained an optimised concentration of CXCL12 (Almac, Craigavon, UK) which was dispensed into the lower chamber of the well in 800µl of chemotaxis buffer. 0.2×10^6 mammalian cells (previously serum starved for 2 hours) were suspended in 500µl of chemotaxis buffer and dispensed into the upper chamber. Chemotaxis assays were then incubated at 37°C in normal growth conditions for an optimised period of time.

Following migration, filters were removed and the insert swabbed with a cotton bud to remove non-migrated cells. Migrated cells were fixed by placing the filters at -20°C in ice cold methanol for at least 2 hours. After fixation, the filters were washed in tap water and stained in haematoxylin for 1 minute. Filters were then washed by submerging in Scott’s tap water to help develop the colour. The cells were then dehydrated by passing the filters through ethanol (50%-75%-90%-100%) before being left to dry at room temperature for 2 hours. Filters were cut and mounted onto cover slides using Di-N-Butyle Phthalate in Xylene (DPX) (Sigma-Aldrich) and

counted using a light microscope (counting 6 high powerfields/filter). Cells within pores were also counted as migrated. Duplicates of each assay were counted and validated by a blind count from another member of the group.

4.3.5.2 Transwell chemo-invasion assay

Chemo-invasion assays were prepared in the same way as chemotaxis assays (section 4.3.5.1); however, prior to fibronectin coating, a thin layer of matrigel was added on the surface of the membrane inside the filter and left to set at 37°C. Matrigel is extremely temperature sensitive. It remains in an aqueous solution when kept at 4°C but becomes increasingly viscous as temperature increases. On this basis, matrigel (Becton Dickinson) was added to filter inserts at 4°C and incubated at 37°C for 30 minutes to allow matrigel to set. Chemo-invasion was assessed and counted as described in section 4.3.5.1.

4.3.5.3 Proliferation assays

Proliferation assays are frequently performed in biological studies. There are a number of ways to determine cell proliferation. These methods can be grouped as either direct or indirect methods of quantification. Direct methods include cell counting using a microscope or an electronic particle counter. Indirect methods are more frequently used and these often include incorporation of radioactive precursors such as thymidine or the use of chromogenic dyes to quantify the cells metabolic activity.

Proliferation was determined using the CellTiter 96® Non-radioactive cell proliferation assay (Promega). Because this assay utilises the levels of by-product produced during a cell metabolism, it can be used to determine cell viability or the proliferation rate of cells. The principle behind this assay and protocol has been previously described in section 4.3.3, however, in this scenario, cells which are proliferating at a faster rate will produce greater levels of by-product and, therefore, the level of proliferation will be directly proportional to the intensity of the formazan product and thus the change in colour.

4.3.5.4 Cell cycle analysis

Cell cycle analysis was performed for cell lines using flow cytometry. When cells are fixed and permeabilised, they can be stained with a fluorescent dye which intercalates with DNA. The fluorescence intensity of the stained cells at specific wavelengths will directly correlate with the amount of DNA they contain. During the cell cycle, DNA duplicates during the S phase, therefore, the relative amount of cells within each phase (G₀/G₁ phase, S phase, and G₂/M phase) can be determined as the amount of fluorescence of cells in the G₂/M phase will be twice as high as the fluorescence from cells which are in G₀/G₁ phase, thus producing two distinct peaks.

Cells (5×10^5) were fixed and permeabilised using an intracellular staining buffer kit as previously described in section 2.5.4.2. To prevent the dye from interacting with RNA, cells were treated for 30 minutes with 0.1mg/ml RNaseA (Sigma-Aldrich) at room temperature in the dark. Cells were washed and resuspended in buffer with 0.05mg/ml propidium iodide (PI) (Sigma-Aldrich) and incubated at room temperature for 2 hours and analysed using FACS canto II on a low flow rate. Results were interpreted using Modfit software *LT* (Verity Software House, Maine, USA).

4.3.6 QuantumTM Simply Cellular[®] Beads

QuantumTM Simply Cellular[®] beads (Bangs Laboratories, Indianapolis, USA) are a set of microspheres which are used to quantitatively assess the expression of a cellular antigen. The beads come in a set of five, where each bead population has its own capacity to binding antigen. One set of beads consists of five populations, one blank and four which have increasing levels of Fc-specific capture antibody. When these beads are stained with the same antibody and analysed within the same suspension solution, at the same instrument settings as cell samples, a standard curve of antigen binding capacity (ABC) versus bead median fluorescence intensity (MFI) can be plotted to draw a standard curve. The MFI of each sample can then be plotted on this graph and the ABC of the cells can be interpolated.

4.4 Results

4.4.1 Construction of a *FOXP3*-expressing plasmid

One of the major aspects of this study was to investigate the effects following the re-introduction of a wild type *FOXP3* vector into an invasive breast cancer cell line. As demonstrated in chapter 3, *FOXP3* within MDA-MB-231 was significantly downregulated and predominately restricted to the cytoplasm. These cells are also known to be a more aggressive cell line as they have a greater invasive capacity than MCF-7. On this basis, it was deemed that MDA-MB-231 would be the most appropriate cell line to investigate the effects of *FOXP3*-overexpression.

In order to generate *FOXP3*-overexpressing MDA-MB-231, a plasmid containing *FOXP3* DNA was firstly constructed. This was done by cloning *FOXP3* DNA into a pcDNA3.1/Zeo(+) backbone as described below.

FOXP3 DNA, which was provided by Prof Sakaguchi (Kayoto, Japan), was sent for sequencing (Source Bioscience) using T7 Forward and BGH reverse primers to determine which restriction sites were present and compatible with sites within the multiple cloning region of the pcDNA3.1/Zeo(+) backbone.

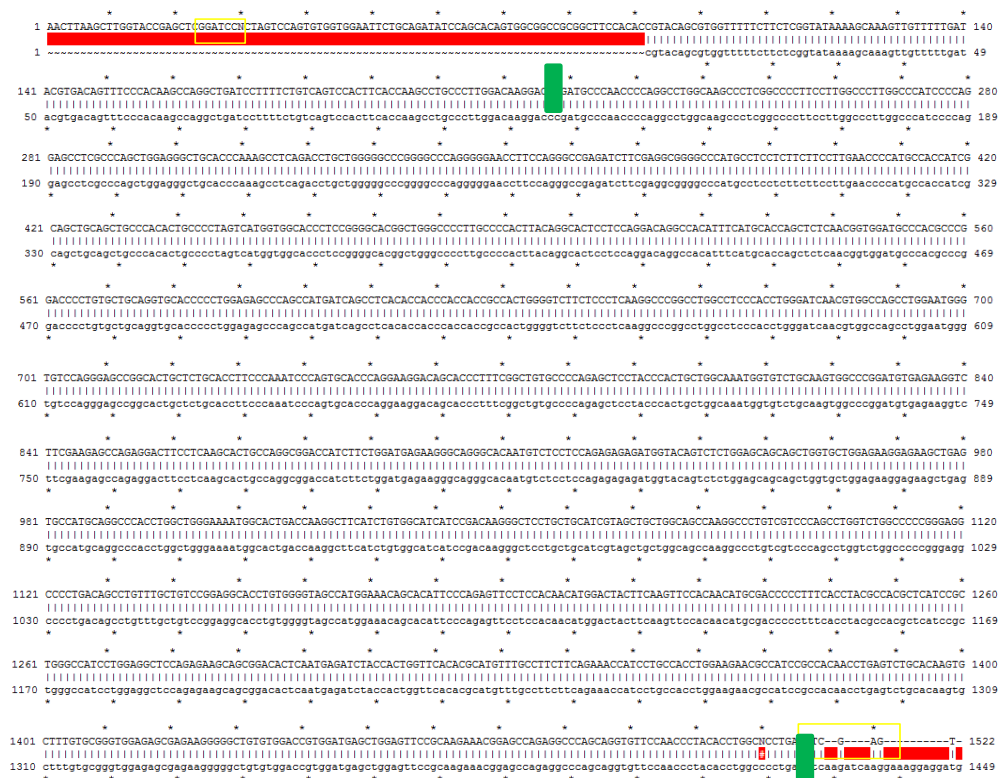
Sequencing results revealed two sites which were compatible with the multiple cloning region of pcDNA3.1/Zeo(+). *Bam*HI was present towards the beginning and *Xho*I was present at the end of the gene. Importantly, these sites are outside of the protein coding domain and therefore should not jeopardise protein production (**figure 4.2 panel A**).

FOXP3 and plasmid DNA were digested with the restriction enzymes *Bam*HI and *Xho*I. The digested products were separated on a 1.2% agarose gel at 90V. After confirming the bands produced were the correct size, they were extracted from the gel and ligated by incubating overnight at 37°C with a T4 ligase enzyme (promega). The following day, the culture containing *FOXP3* DNA which was ligated into the pcDNA3.1/Zeo(+) backbone was transformed into competent *E.coli* cells. The culture was then spread onto LB agar plates containing ampicillin (100µg/ml), and grew overnight at 37°C. The pcDNA3.1/Zeo(+) plasmid contains a gene which encodes ampicillin resistance, therefore, colonies which grew had successfully taken up the plasmid as they survived in the presence of the selection antibiotic.

Individual colonies were picked and grown overnight in LB with ampicillin (100µg/ml) in a 37°C heated shaker. The following day, plasmid DNA was extracted from the bacterial culture. To check *FOXP3* DNA was successfully inserted into the pcDNA3.1/Zeo(+) backbone, the newly constructed plasmid was double-digested with *Bam*HI and *Xho*I then run on a 1.2% agarose gel alongside undigested plasmid DNA (**figure 4.2 panel B**). The lane containing the double digested plasmid contained three bands. The 1.5kbp band represented the *FOXP3* insert, whereas, the band at 5kbp was the pcDNA3.1/Zeo(+) backbone. A final band at 6.5kbp demonstrated the remnants of undigested plasmid and appeared parallel to the undigested plasmid.

The new *FOXP3* plasmid is referred to as pcDNA3.1/Zeo-*FOXP3*. A map of pcDNA3.1/Zeo(+) (referred to as an empty vector) and pcDNA3.1/Zeo-*FOXP3* (referred to as a *FOXP3* vector) is provided in **figure 4.3**.

A



B

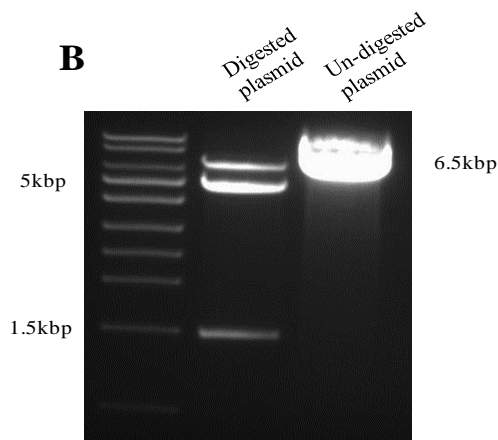


Figure 4-2 - Construction of pcDNA3.1/Zeo-FOXP3 vector

(A) The *FOXP3* DNA was sequenced to determine which restriction sites were compatible with the sites within the pcDNA3.1/Zeo(+) plasmid cloning region. Sequencing revealed *Bam*H1 and *Xho*I sites (highlighted in yellow boxes) within the *FOXP3* DNA. Green lines represent the limits of the protein coding domain of *FOXP3*. Sequences were aligned using ApE software where the upper row represents *FOXP3* DNA provided by Prof Sakaguchi and lower row represents wild type *FOXP3* (accession number NM_014009.3). Red regions represent regions of hang-over from the forward and reverse primer sequences (B) 1µg of pcDNA3.1/Zeo-FOXP3 was digested with *Bam*H1 and *Xho*I and ran on a 1.2% agarose gel alongside undigested plasmid. Bands at 5kbp and 1.5kbp in the digested plasmid lane represents *FOXP3* DNA (1.5kbp) and pcDNA3.1/Zeo(+) backbone (5kbp). A third band at 6.5kbp represents some undigested plasmid.

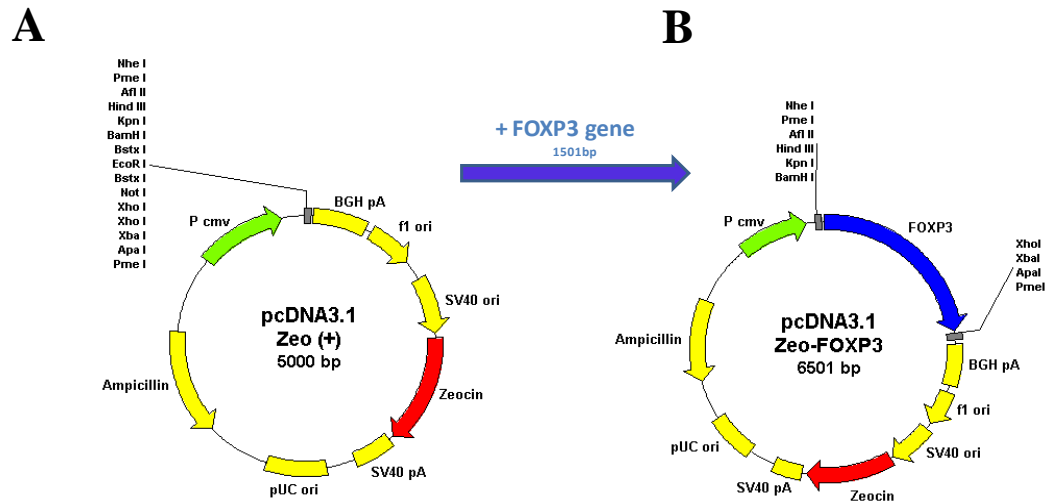


Figure 4-3 - Schematic representation of *FOXP3* insertion into the pcDNA3.1/Zeo(+)-vector

FOXP3 was cloned into the pcDNA3.1/Zeo(+) backbone (**A**) by double digestion using the restriction enzymes *BamHI* and *XhoI*. Digested *FOXP3* and pcDNA3.1/Zeo(+) DNA was ligated overnight at 37°C using T4 ligase enzyme. The new *FOXP3* expressing plasmid was named pcDNA3.1/Zeo-*FOXP3* (**B**).

4.4.2 Transient transfection of pcDNA3.1/Zeo-FOXP3 into HEK cells

After initially confirming that pcDNA3.1/Zeo-FOXP3 had successfully inserted the *FOXP3* DNA, the next step was to ensure that this plasmid was able to encode and produce FOXP3.

pcDNA3.1/Zeo-FOXP3 and the empty vector (pcDNA3.1/Zeo[+]), were transiently transfected into wild type HEK cells using the AmaxaTMNucleofectorTM program A-23. HEK cells are frequently used in transfection because they readily integrate and express exogenous DNA. 24 hours post-transfection, RNA was isolated, reverse transcribed and real-time PCR was used to assess *FOXP3* upregulation in the transfected cells. *FOXP3* was upregulated by a mean fold increase of approximately 96. This demonstrates the construct successfully induces high level *FOXP3* overexpression in cells (**Figure 4.4**).

4.4.3 Transient transfection of pmax GFP into MDA-MB-231 using AmaxaTMNucleofectorTM

MDA-MB-231 is a cell line known to be notoriously difficult to transfect. To ensure that the AmaxaTMNucleofectorTM is able to transfect these cells, pmaxGFP (supplied with the AmaxaTMNucleofectorTM) was transiently transfected into MDA-MB-231 with a program specific for these cells (X-013).

Results demonstrated that AmaxaTMNucleofectorTM can transfect MDA-MB-231 (**figure 4.5**). It should also be noted that due to the high voltage there was also a relatively high degree of cell death. However, when generating stable overexpressing cell lines, a large proportion of cell viability is not the most important aspect because stably transfected cells must be selected from single colonies.

After demonstrating that the pcDNA3.1/Zeo-FOXP3 plasmid is capable of overexpressing *FOXP3*, and the AmaxaTMNucleofectorTM is able to transfect MDA-MB-231, stable transfection of FOXP3 into MDA-MB-231 was begun.

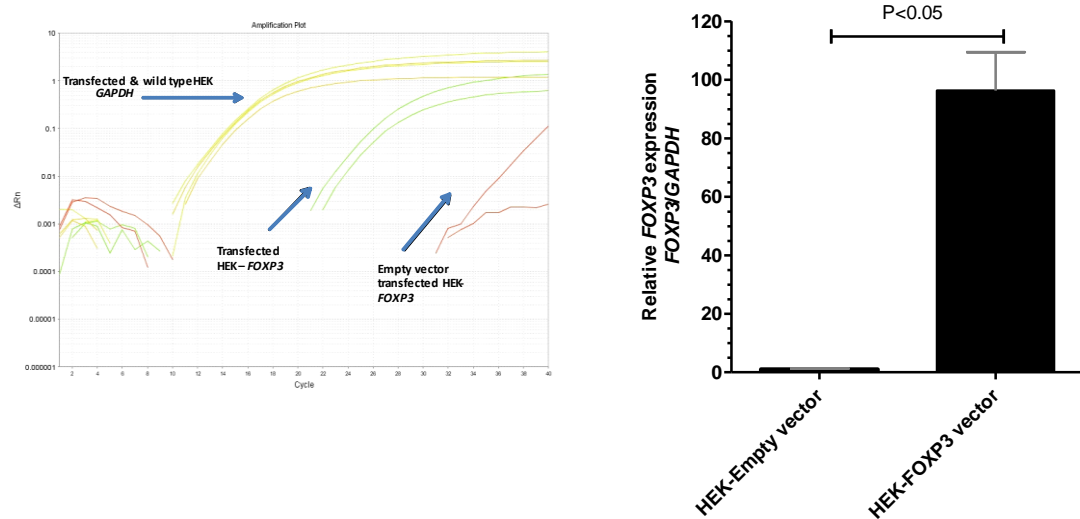


Figure 4-4 - Transient transfection of pcDNA3.1/Zeo-FOXP3 into HEK cells

Wild type HEK cells were transiently transfected with $2\mu\text{g}$ of pcDNA3.1/Zeo-FOXP3 or the empty vector using the AmaxaTMNucleofectorTM. 24 hours post-transfection, RNA was isolated from cells, reverse transcribed and real-time PCR was used to determine *FOXP3* expression. After normalising against endogenous *GAPDH* the amount of *FOXP3* transcripts from the HEK cells transfected with the FOXP3 vector was compared with the HEK cells transfected with an empty vector, which was arbitrarily set as 1.0. Data shown are means and SD of experiments performed in duplicate (n=2).

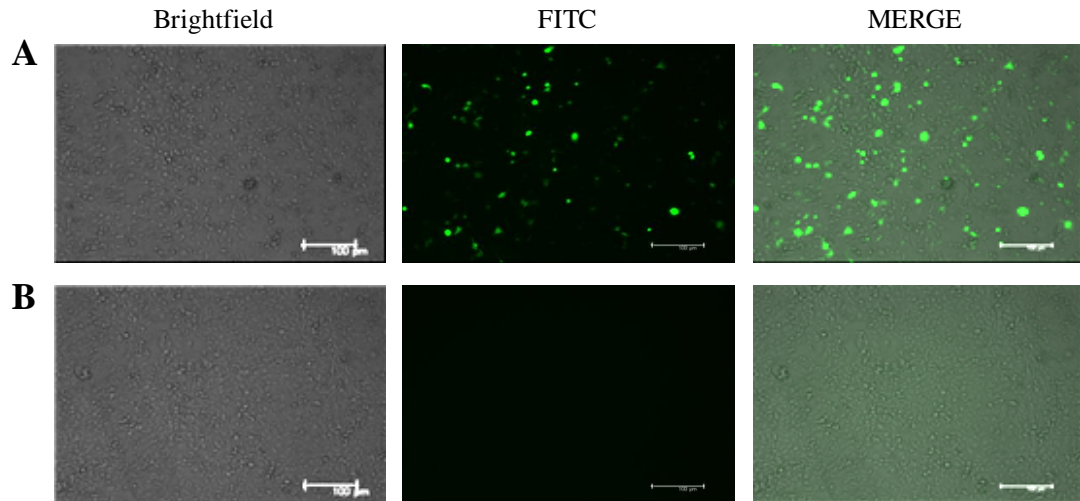


Figure 4-5 - Transient transfection of pmaxGFP into MDA-MB-231

(A) 2µg of highly purified pmaxGFP was combined with 1×10^6 MDA-MB-231 suspended in 100µl of AmaxaTMNucleofectorTM transfection solution from kit V. pmaxGFP was transfected into the cells using the AmaxaTMNucleofectorTM machine (program X-13). Successful uptake of DNA was determined by IF microscopy and compared with MDA-MB-231 transfected with no DNA (B).

4.4.4 ZeocinTM killing curve using MDA-MB-231

pcDNA3.1/Zeo-FOXP3 confers ampicillin resistance to *E.coli* and allows these cells to be grown in the presence of the antibiotic. pcDNA3.1/Zeo-FOXP3 and the empty vector also contain a sequence to transcribe resistance to ZeocinTM. Untransfected cells will not survive in the presence of ZeocinTM, which allows the successfully transfected cells to be selected by the presence of ZeocinTM in the culture media.

The vulnerability of cells to certain antibiotics ranges. Some cells are more sensitive to antibiotics and do not require high concentrations, whereas, others are less sensitive and can still grow despite the presence of an antibiotic. To determine the sensitivity of MDA-MB-231 to ZeocinTM, ensuring only stably transfected cells are able to survive, a killing curve was conducted using varying concentrations of ZeocinTM over 7 days to determine the minimum concentration required to kill non-transfected cells. Wild type MDA-MB-231 were seeded in to 96-well-plates and treated with concentrations of ZeocinTM ranging from 0-700µg/ml. The viability of the cells was measured each day for 7 days (**figure 4.6**).

MDA-MB-231 were sensitive to ZeocinTM as a relatively low concentration of the antibiotic was able to kill cells after 7 days. Approximately 40-60% of cells were killed after 4-5 days using 150µg/ml ZeocinTM and was therefore determined to be the optimum concentration to select stably transfected cells.

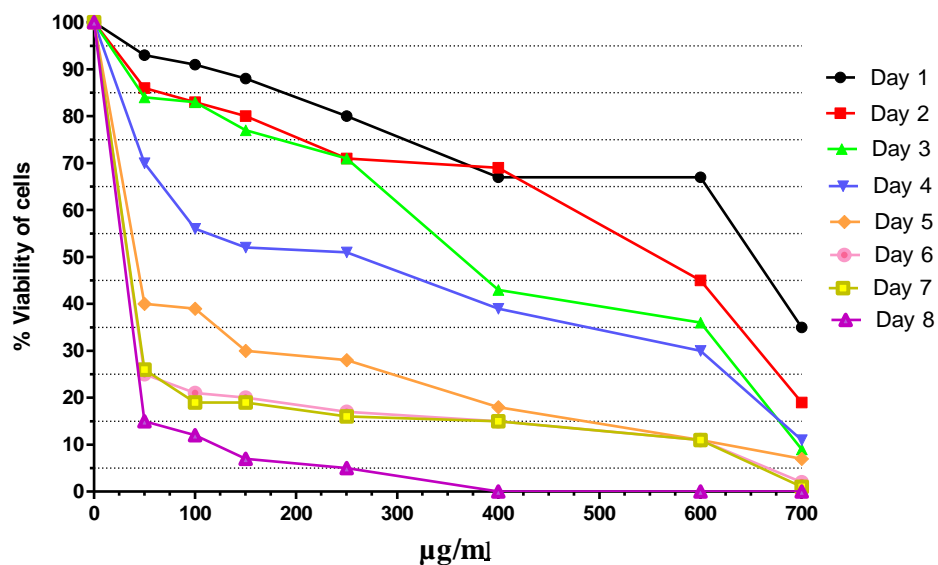


Figure 4-6 - Zeocin™ killing curve on MDA-MB-231

5×10^4 MDA-MB-231 were seeded into individual wells in a 96-well plate and incubated at 37°C with concentrations of Zeocin™ ranging from $0\mu\text{g/ml}$ to $700\mu\text{g/ml}$. The cell death was determined each day for a total of 7 days. Each day PMS and MTS (prepared to a 1:20 ratio) solutions were added to each well and incubated at 37°C for 2 hours. Cell death was determined by reading absorbance's at 540nm using a 96-well microplate reader at 540nm. Viability was recorded as a percentage of the absorbance of untreated cells. Results are plotted as mean absorbance from one experiment performed in triplicate.

4.4.5 Generation of stably transfected *FOXP3* overexpressing MDA-MB-231

Following the successful construction of a *FOXP3*-expressing plasmid, a number of essential parameters were optimised. Firstly, it was demonstrated that the newly constructed plasmid is capable of transcribing *FOXP3* in transfected cells (**figure 4.4**). It was then demonstrated that electroporation using AmaxaTMNucleofectorTM is a method capable of transfecting MDA-MD-231 (**figure 4.5**). And finally, the required concentration of ZeocinTM to select the transfected cells was determined (**figure 4.6**).

Random integration of the plasmid can often be an issue which results in cells integrating the plasmid DNA into the genome but failing to express the gene of interest. In order to minimise this risk, pcDNA3.1/Zeo-*FOXP3* was linearised prior to transfection using the restriction enzyme *ScaI*. Only one *ScaI* sequence is located within the pcDNA3.1/Zeo-*FOXP3* sequence and it is found within the region which confers ampicillin resistance (**figure 4.7 panel A**). It is a good area to digest the plasmid at this point as ampicillin resistance is only required in the growth and selection of competent *E.coli* cells. Following DNA isolation this ampicillin resistance is redundant.

FOXP3 was transfected into MDA-MB-231 using the AmaxaTMNucleofectorTM using the same methods as described in section 4.4.3. Following transfection, cells were placed into complete growth media and 24 hours post-transfection, fresh media containing 150µg/ml of ZeocinTM was added each day.

Many transfections were attempted over several months with most failing to result in the growth of any colonies. After one transfection, individual colonies became apparent. Some of these colonies gradually expanded, albeit at a slow pace. Unfortunately, many other colonies failed to expand, became gradually granular and eventually died. However, three colonies (colonies 4, 9 and 11) grew adequately, and were isolated and dispensed into separate culture flasks to expand further. Real-time PCR was used to determine the expression of *FOXP3* within each colony, including control cells transfected with an empty vector. From the 3 expanded colonies, only colony 4 significantly overexpressed *FOXP3* in comparison to the cells transfected with the empty vector (**figure 4.7 panels B and C**). Importantly, the level of

expression in colony 4 was also significantly greater than the levels of *FOXP3* found in HMEpC. This suggested that the generated cell line is a good model to demonstrate the effects of *FOXP3* overexpression in an invasive cancer cell line (**figure 4.7 panel D**).

Overexpression of FOXP3 was also validated at a protein level. As a transcription factor, the nuclear expression of FOXP3 is a prerequisite for effective functioning. Importantly, transfected MDA-MB-231 overexpressed FOXP3 predominately within the nucleus (**figure 4.8**).

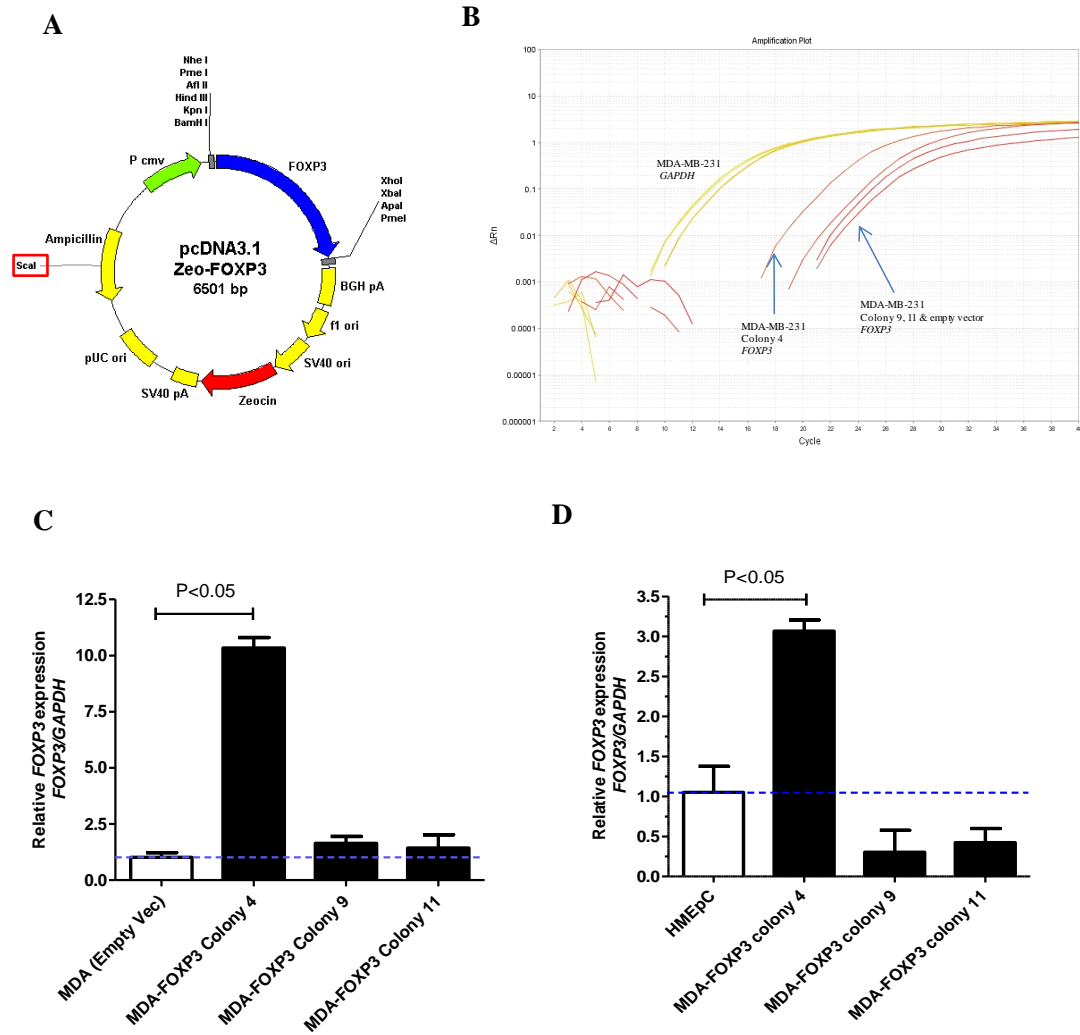


Figure 4-7 - Stable *FOXP3* overexpressing MDA-MB-231

(A) Prior to transfection, pcDNA3.1/Zeo-*FOXP3* was linearised by digesting with 1 unit of *ScaI*. pcDNA3.1/Zeo-*FOXP3* was transfected into MDA-MB-231 and cultured in the presence of 150 μ g/ml ZeocinTM until individual colonies were present and able to be selected. Following selection of stable clones, the relative expression of *FOXP3* in transfected MDA-MB-231 was determined using real-time PCR (B) and compared against MDA-MB-231 transfected with empty vector (C) and HMEpC (D) which were arbitrarily defined as 1.0. Results are means of SD in experiments performed in duplicate (n=2). Statistical analysis was determined using an unpaired t-test.

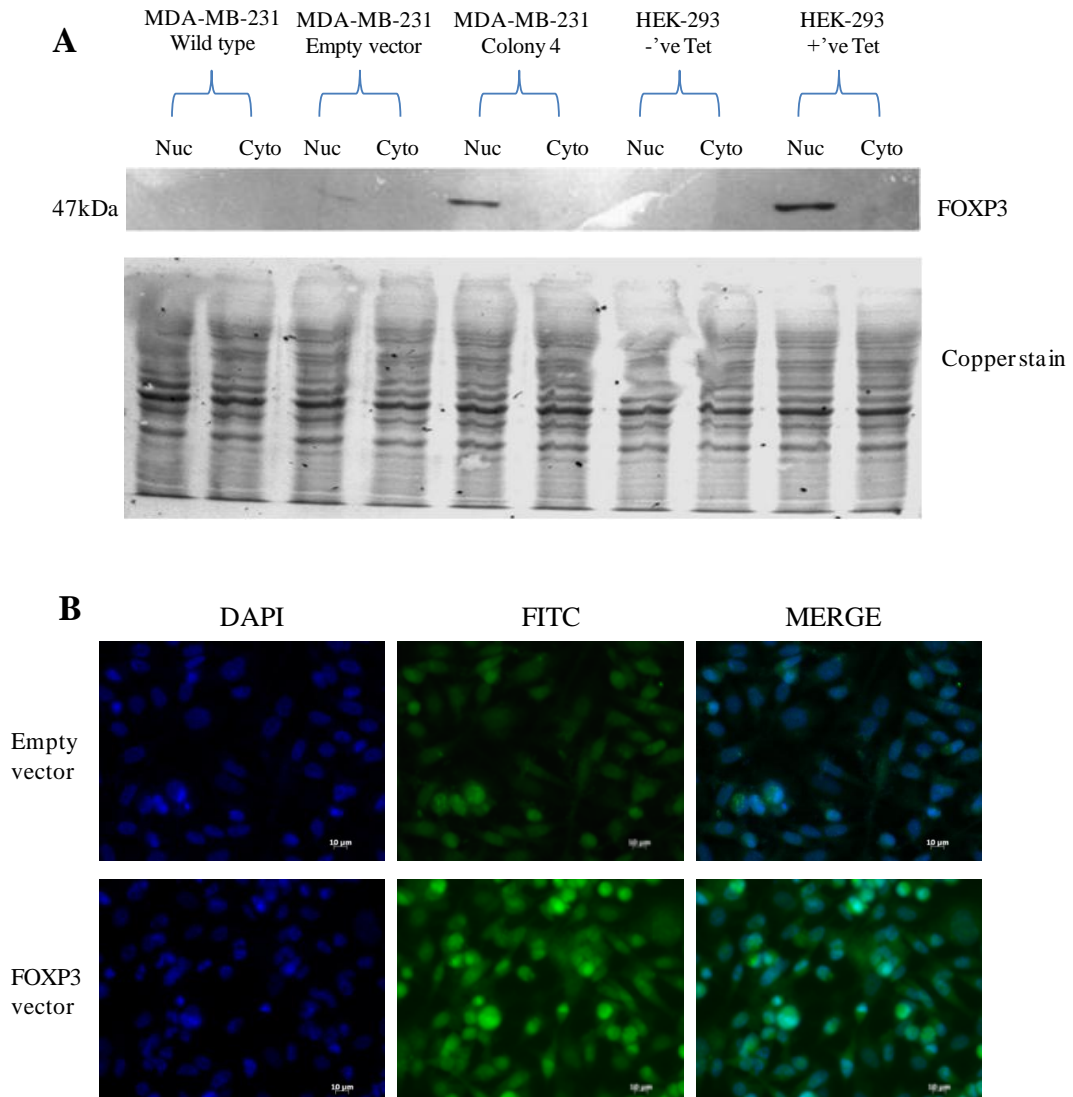


Figure 4-8 - Subcellular distribution of FOXP3 within stably transfected MDA-MB-231

(A) Nuclear (Nuc) and cytoplasmic (Cyto) domains of MDA-MB-231 were extracted using a NE-PER® fractionation kit. Protein from each domain was separated by SDS-PAGE, transferred onto PVDF membrane and immuno-probed using a human anti-FOXP3 antibody and developed onto X-ray film. Membrane was stained using copper phthalocyanine to ensure equal loading between lanes. (B) Empty vector transfected MDA-MB-231 and FOXP3 transfected MDA-MB-231 were seeded into chamber slides and left to grow overnight in normal growth conditions. The following day cells were fixed with 4% PFA and permeabilised using Triton X-100. Cells were stained using a human anti-FOXP3 primary antibody and a FITC-conjugated secondary antibody. Cells were counter stained with DAPI for nuclear visualisation.

4.4.6 Effects of stable FOXP3 overexpression in MDA-MB-231

Following confirmation that colony 4 stably and significantly overexpressed FOXP3 at transcript and protein levels in comparison to empty vector transfected MDA-MB-231 and HMEpC, the effects of this overexpression on gene regulation, and cell function were investigated.

4.4.6.1 Primer validation

TaqMan® real-time PCR primers were validated prior to investigation using a cDNA template which was serially diluted 5 times from 1µl to 0.0625µl (**figure 4.9**). A linear drop in Ct through each dilution represents primer specificity. The reaction efficiency of each primer was calculated and all were greater than 97% efficient.

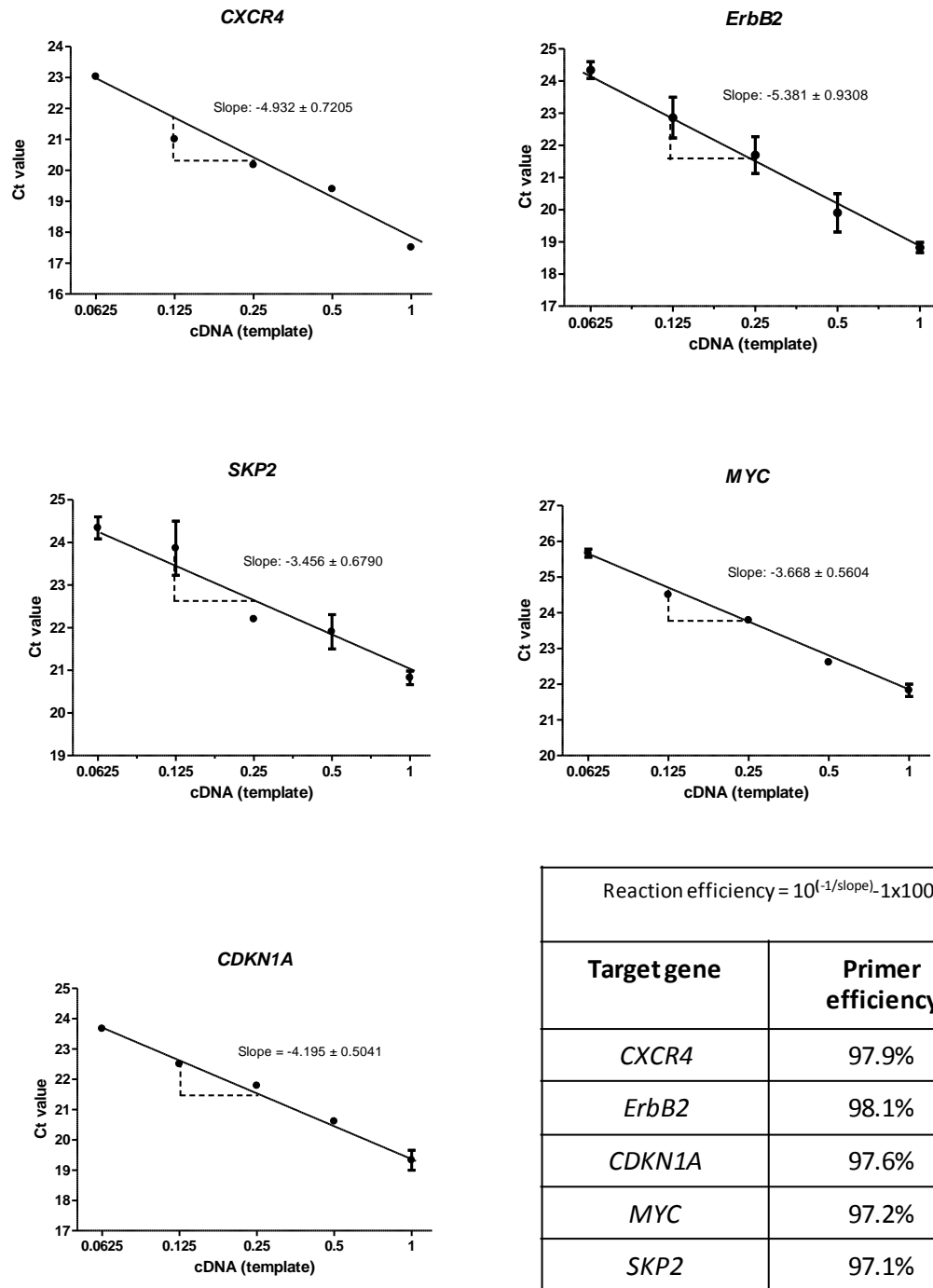


Figure 4-9 - Reaction efficiency of TaqMan® real-time PCR primers

cDNA was used to measure reaction efficiency of TaqMan® primers. cDNA was serially diluted and ran for 40 cycles. Ct values obtained were plotted against cDNA input in log2 format and represented as linear regression line plot of Ct value versus cDNA input. Reaction efficiency from each primer was calculated incorporating the slope of the linear regression into the equation: reaction efficiency = $10^{(-1/\text{slope})} \times 100$. PBMC cDNA was used as a template for *CXCR4*, SKBr3 cDNA was used for *ErbB2*, DMSO treated H69 cells was used for *CDKN1A*, MCF-7 cDNA was used for *MYC* and *SKP2*.

4.4.6.2 Relative expression of genes following stable FOXP3 integration in MDA-MB-231

FOXP3 has been widely reported as a transcriptional regulator of many genes in both Tregs and epithelial cells. The genes investigated in this study are all heavily implicated in cancer and have been previously reported as FOXP3 target genes (Zuo, Liu et al. 2007; Zuo, Wang et al. 2007; Liu, Wang et al. 2009; Wang, Liu et al. 2009).

Results demonstrated that *ErbB2*, *SKP2*, *MYC* and *CXCR4* were all expressed at higher levels in the empty vector transfected MDA-MB-231 in comparison to the HMEpC (**figure 4.10**). This, in accordance with the literature, demonstrates the importance of these genes in carcinogenesis.

Consistent with the literature, stable FOXP3-overexpression in MDA-MB-231 significantly repressed the expression of *ErbB2* ($p=0.0264$), *SKP2* ($p=0.0249$) and *MYC* ($p=0.0416$) (**figure 4.10 panels A-C**). Consistent with its role as an anti-cancer molecule, regulating proliferation and cell cycle progression, the expression of *CDKN1A* was significantly lower in MDA-MB-231 compared to HMEpC. FOXP3 has been demonstrated to directly increase the expression of p21 in MCF-7 (Frattini, Pisati et al. 2012) and glioblastoma cells (Liu, Wang et al. 2009). A 7-fold increase in *CDKN1A* transcripts was observed within the FOXP3-overexpressing MDA-MB-231 (**figure 4.10 panel D**). This further emphasises the ability of FOXP3 to act as either a transcriptional activator or repressor to specific genes.

Interestingly, out of five independent experiments, two experiments resulted in a decreased expression of *CXCR4*, however, three experiments failed to induce a change in expression of the same magnitude. Despite this, the combined change in expression was statistically significant ($p=0.0496$) (**figure 4.10 panel E**).

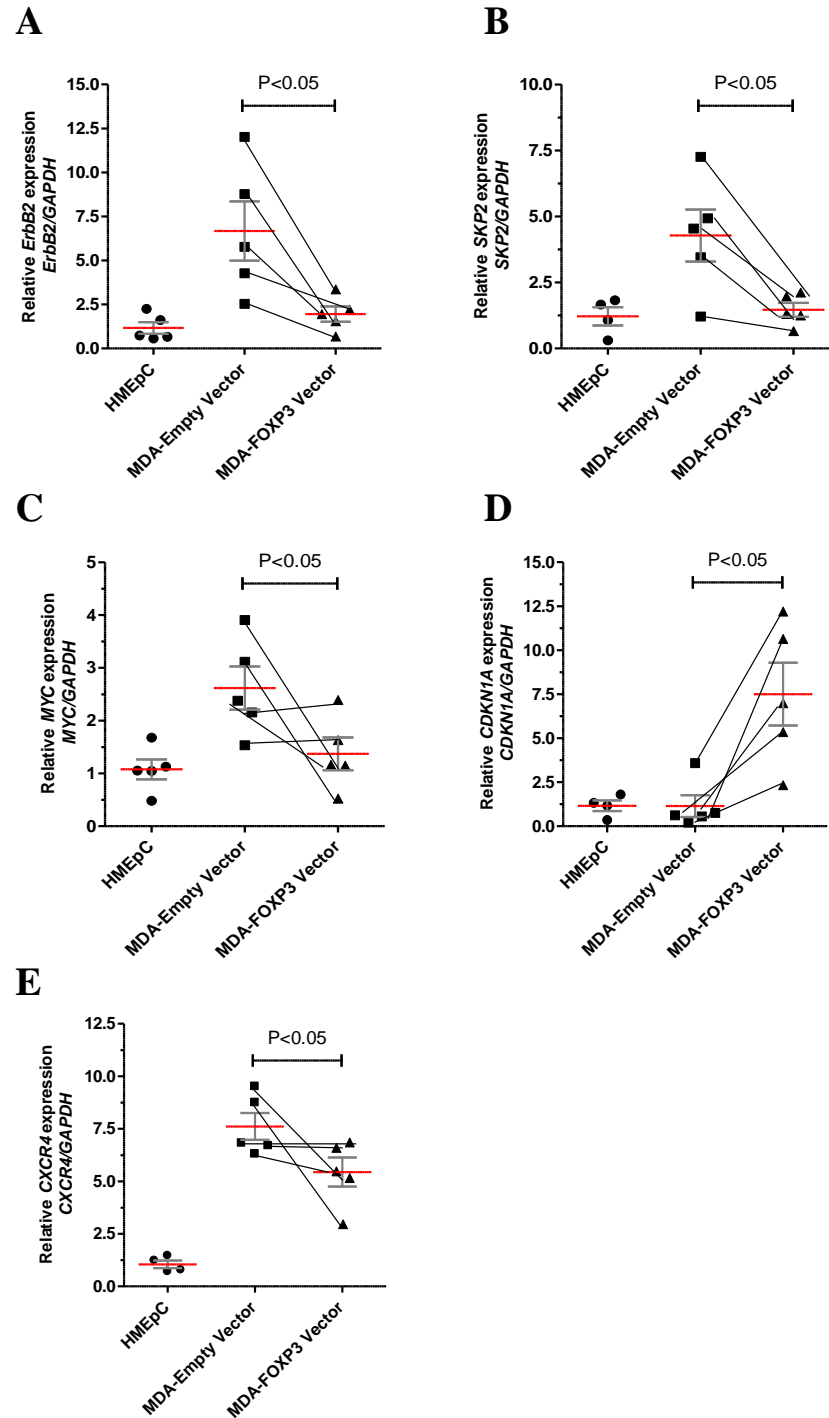


Figure 4-10 - Changes in oncogene expression following FOXP3 overexpression in MDA-MB-231

After normalising against endogenous *GAPDH*, the amount of transcripts in MDA-MB-231 cells transfected with a FOXP3 vector or the empty vector was compared to those from HMEpC which were arbitrarily defined as 1.0. Data shown are means and SD of at least 4 separate experiments performed in duplicate. (A) *ErbB2* transcripts, (B) *SKP2* transcripts, (C) *MYC* transcripts and (D) *CDKN1A* transcripts (E) *CXCR4* transcripts. HMEpC was included as direct comparison of transcript levels in normal mammary cells. An unpaired t-test was used to analyse MDA-Empty vector vs MDA-FOXP3 Vector columns.

4.4.6.3 Effects of FOXP3 overexpression on MDA-MB-231 proliferation

Whilst generating FOXP3 overexpressing MDA-MB-231, the process of expanding individual colonies was difficult as many colonies grew at slow rates. These colonies often became increasingly granular over time in comparison to empty vector transfected cells. Many colonies failed to be expanded and eventually died.

After confirming that colony 4 overexpressed FOXP3, a proliferation assay was used to investigate the effects of FOXP3 on the proliferation of MDA-MB-231 (**figure 4.11**). Wild type MDA-MB-231 and MDA-MB-231 transfected with an empty vector proliferated at a comparably quick rate, whereas, the FOXP3-transfected cells had a significantly reduced rate of growth. The incline of the line suggested that these cells were still growing, just at a very slow rate. In addition to this, data in section 4.4.6.2 demonstrated that following FOXP3-transfection, *CDKN1A* transcripts were significantly increased. *CDKN1A* encodes for p21 which is involved in cell cycle arrest at the G1 phase. On the basis of these results, cell cycle analysis was performed on MDA-MB-231 using PI to determine what proportion of cells were in each stage of the cell cycle (**figure 4.12**).

Approximately 58% of both wild type MDA-MB-231 and empty vector transfected MDA-MB-231 cells were within G1, whereas, approximately 69% of the FOXP3-overexpressing MDA-MB-231 was within G1.

This data, along with findings in the current literature, suggest that FOXP3 is able to increase the expression of p21 when overexpressed in breast cancer cells. Moreover, this expression may impair cell growth by inducing cell cycle arrest. It could be proposed that the failure to expand these cells further could be due to the presence of FOXP3 contributing to increased cellular senescence.

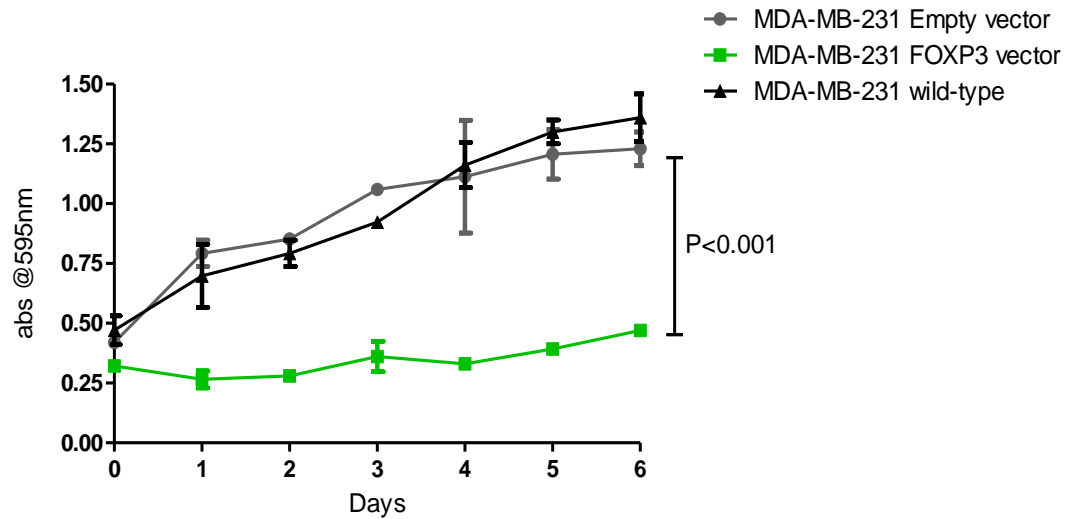


Figure 4-11 – Effects of FOXP3 overexpression on the proliferation of MDA-MB-231

Wild type MDA-MB-231 and MDA-MB-231 transfected with a FOXP3 or empty vector were dispensed into 96-well plates and proliferation was determined each day for 6 days using a non-radioactive cell proliferation assay kit. Statistical analysis was performed using a one way ANOVA. (n=2)

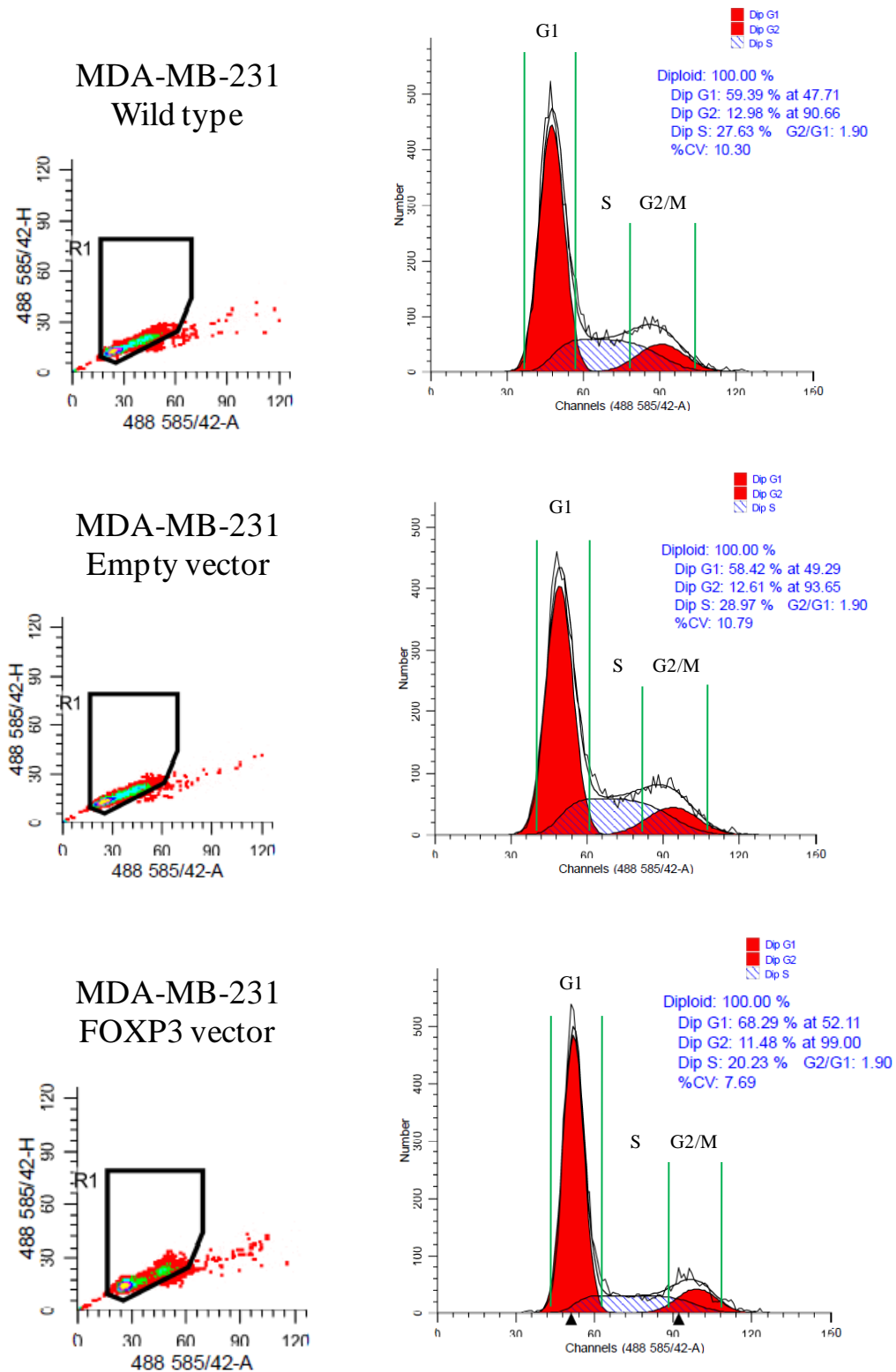


Figure 4-12 – Cell cycle analysis of MDA-MB-231 following FOXP3 overexpression

Wild type MDA-MB-231 and MDA-MB-231 stably transfected with FOXP3 or an empty vector were fixed and permeabilised then treated with 0.1mg/ml RNase A. Cells were then stained with 0.05mg/ml PI. Cell cycle analysis was conducted using ModFit *LT* software (n=2).

4.4.7 Optimising transient transfection of MDA-MB-231 using pmaxGFP

After failing to expand stably transfected FOXP3 overexpressing MDA-MB-231, further experiments investigating FOXP3 overexpression in these cells were attempted using transient transfections.

As demonstrated in section 4.4.3, electroporation using the AmaxaTMNucleofectorTM achieved moderate transient transfection of pmaxGFP into MDA-MB-231. However, because of the extreme conditions the cells were exposed to during electroporation, the process frequently resulted in low cell viability. Although this is acceptable in generating stably transfected cells, cell viability is as crucial as the transfection efficiency for functional assays and is therefore not a suitable option for transient transfections. Therefore, a range of lipid-based transfection reagents were attempted for transient transfections.

Conditions to transfect MDA-MB-231 using Lipofectamine®2000 were optimised using pmaxGFP with ratios of DNA to reagent ranging from 1:1 to 1:3 over 24 hours (**figure 4.13**) and 48 hours (**figure 4.14**).

Low transfection efficiencies were witnessed after 24 hours. Even after using a higher content of reagent, transfection efficiencies failed to increase. The increase in reagent also produced a greater proportion of cell death without causing an acceptable level of transfection. As expected, after 48 hours, there was an increase in the apparent transfection efficiency, with the greatest efficiency being witnessed using a 1:2 ratio of DNA to reagent. Because of the extended exposure to the transfection complexes, the cell viability was extremely low.

These results indicate that Lipofectamine®2000 cannot be used to transiently transfect MDA-MB-231 whilst maintaining good cell viability.

GenJetTM is a reagent specifically marketed to transfect MDA-MB-231 with a pre-optimised protocol. According to the manufacturers, this protocol is able to generate transfection efficiencies of 70% using eGFP. Disappointingly, this reagent also induced high cell death with no transfection, even after extended exposure to complexes and increased reagent ratios (**figure 4.15**).

Similar optimisation experiments were attempted using JetPRIME™, TurboFect™ and GeneJuice®. However, results consistently produced high levels of cytotoxicity and very low transfection efficiencies. Representative images from lipid-based transient transfections are included in **appendices 3 to 6**.

Unfortunately, because none of the lipid-based transfection reagents were able to achieve acceptable transfection efficiencies, and electroporation caused high levels of cell death, it was not deemed possible to transiently transfect MDA-MB-231 with FOXP3 to a level consistent with functional investigations.

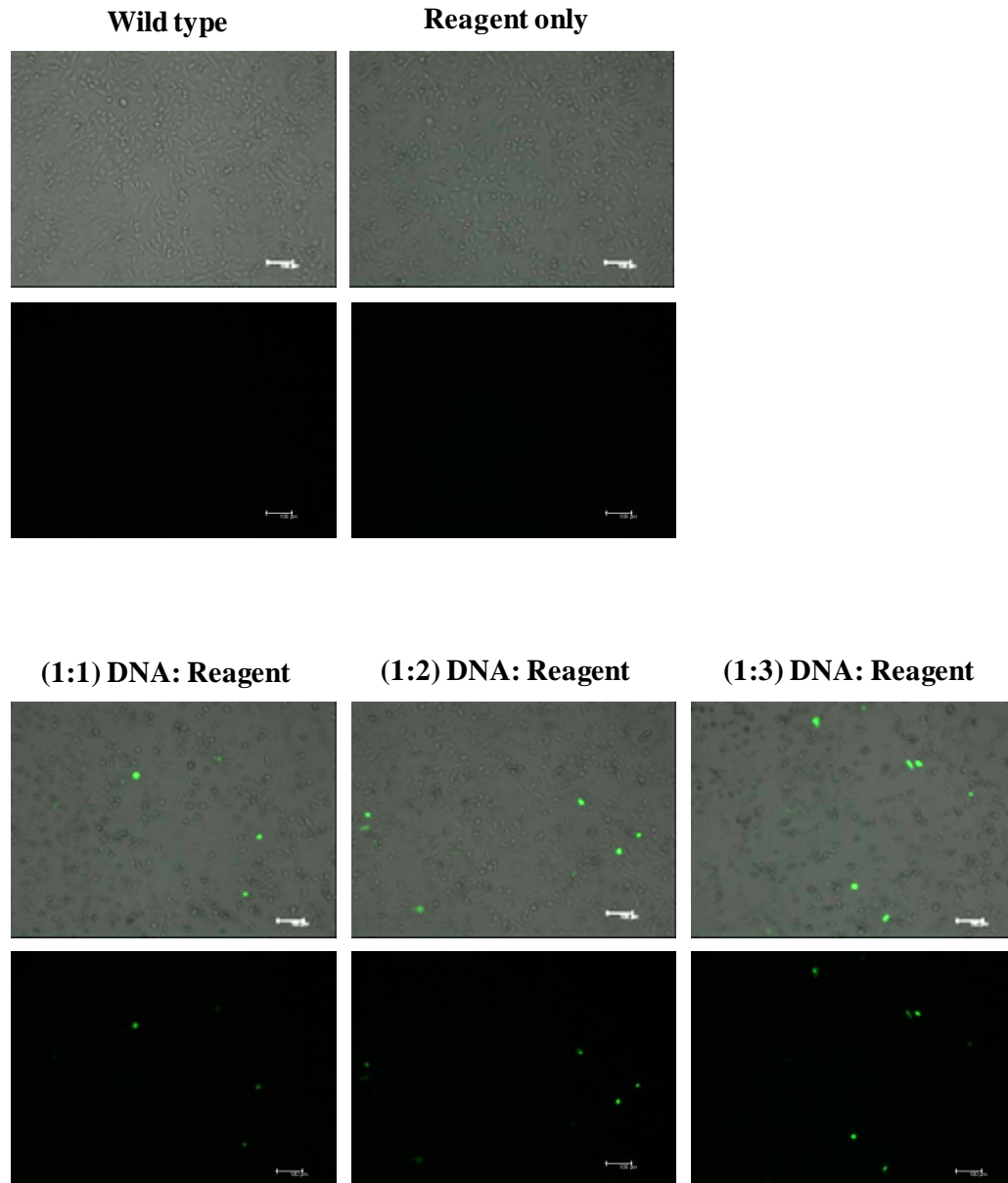


Figure 4-13 - Optimisation of pmaxGFP transfection into MDA-MB-231 using Lipofectamine®2000 after 24 hours

MDA-MB-231 were transfected with 4 μ g of pmaxGFP plasmid using varying ratios of Lipofectamine®2000 reagent ranging from 1:1 to 1:3 (μ g of DNA: μ l of reagent). Transfection efficiency was determined by IF microscopy after 24 hours. Wild type MDA-MB-231 and MDA-MB-231 treated with 4 μ l of Lipofectamine®2000 were used as negative controls (n=3). Upper panels represent FITC+brightfield merge and lower panels represent FITC only.

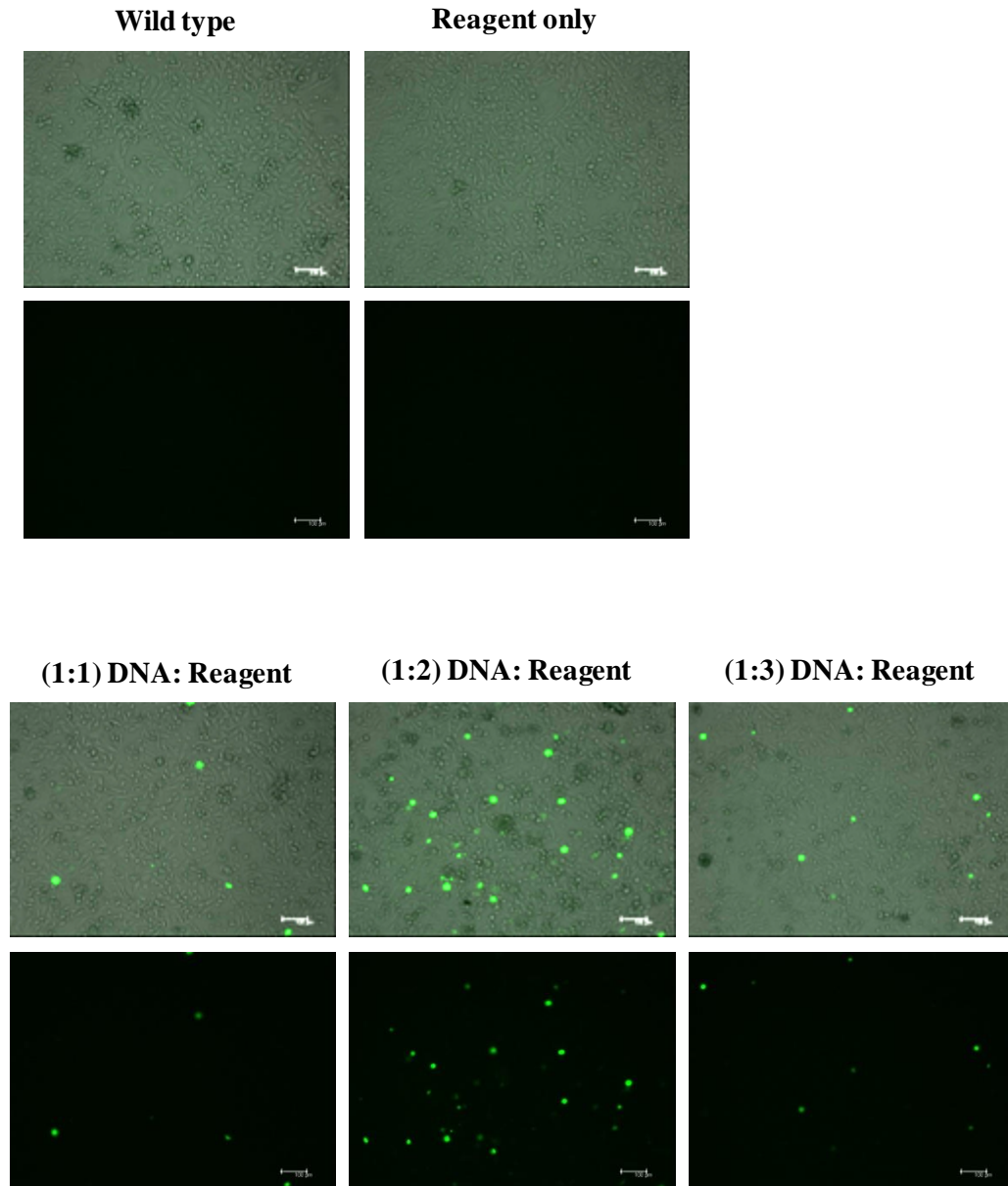


Figure 4-14 - Optimisation of pmaxGFP transfection into MDA-MB-231 using Lipofectamine®2000 after 48 hours

MDA-MB-231 were transfected with 4 μ g of pmaxGFP plasmid using varying ratios of Lipofectamine®2000 reagent ranging from 1:1 to 1:3 (μ g of DNA: μ l of reagent). Transfection efficiency was determined by IF microscopy after 48 hours. Wild type MDA-MB-231 and MDA-MB-231 treated with 4 μ l of Lipofectamine®2000 were used as negative controls (n=3). Upper panels represent FITC+brightfield merge and lower panels represent FITC only.

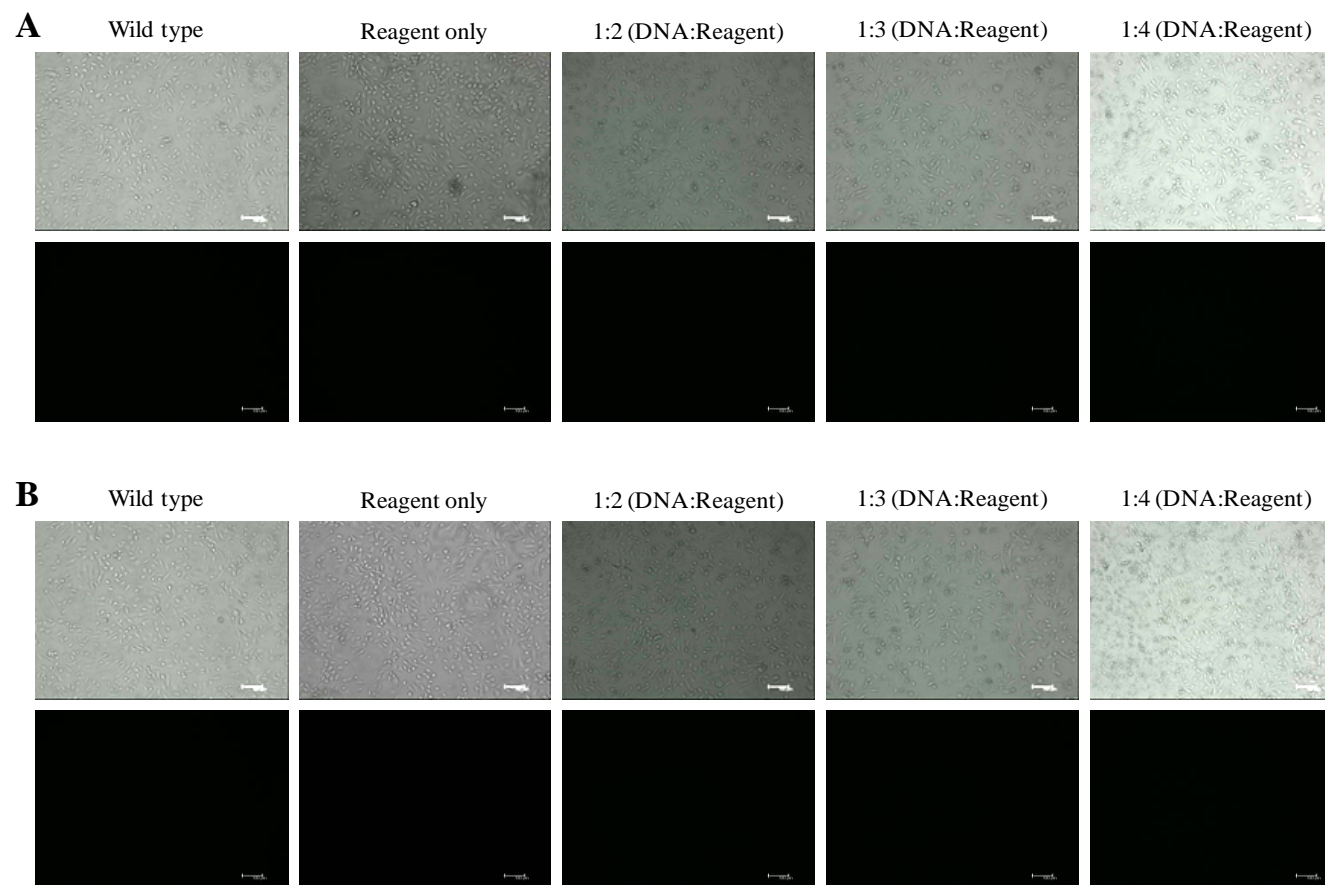


Figure 4-15 - Optimisation of pmaxGFP transfection into MDA-MB-231 using GenJet™

MDA-MB-231 cells transfected with pmaxGFP using ratios of DNA:GenJet™ reagent from 1:2 to 1:4 were assessed by fluorescent microscopy after 24 hours post-transfection (**A**) and 48 hours post-transfection (**B**).

4.4.8 Optimisation of FOXP3 knockdown in HMEpC using FOXP3 specific siRNA sequences

Having previously demonstrated that HMEpC do express nuclear FOXP3, another aspect of this chapter was to investigate the effects of FOXP3 knockdown in HMEpC.

4.4.8.1 Choice of transfection reagent to knockdown FOXP3 in HMEpC

Although the transfection efficiency with pmaxGFP was low in MDA-MB-231 using Lipofectamine®2000, it did provide the greatest success. Lipofectamine®2000 can also be used to transfect siRNA into cells. Mainly because of the size, transfecting siRNA is generally considered easier than transfecting plasmids.

siPORT™NeoFX™ is another lipid-based transfection reagent which is specifically designed for the delivery of siRNA. HMEpC were transfected with GAPDH-Cy³ siRNA using Lipofectamine®2000 and siPORT™NeoFX™. The transfection efficiency was determined by flow cytometry 24 hours post-transfection. The Cy³ fluorochrome fluoresces at 570nm and after excitation at approximately 550nm. This allows Cy³ to be detected on the same channel as PE on flow cytometers.

After 24 hours, both Lipofectamine®2000 and siPORT™NeoFX™ delivered high levels of GAPDH-Cy³ siRNA (**figure 4.16**). However, because the efficiency was higher and the reagent was less cytotoxic, siPORT™NeoFX™ was determined to be the best reagent to transfect HMEpC.

4.4.8.2 Choice of FOXP3 siRNA

Three FOXP3 *silencer*® select siRNAs were available and purchased from Ambion. HMEpC were transfected with 5nM of each FOXP3 siRNA or control siRNA. Relative transcript expression was determined by real-time PCR (**figure 4.17**), whereas, protein expression was determined by flow cytometry (**figure 4.18**) 24

hours post-transfection. Each individual FOXP3 siRNA caused greater than 70% knockdown of FOXP3 compared to the HMEpC transfected with control siRNA which remained constitutive. Importantly, the degree of downregulation was also less than that witnessed in wild type MDA-MB-231 which makes the knockdown a good model to investigate the effects of FOXP3 downregulation in normal mammary cells.

The fact that all three individual FOXP3 siRNA produced a similar degree of knockdown demonstrates the specificity of each primer to FOXP3, and downregulation is not as a result of other downstream effects in cells.

FOXP3 siRNA 2 was selected to be used for subsequent experiments

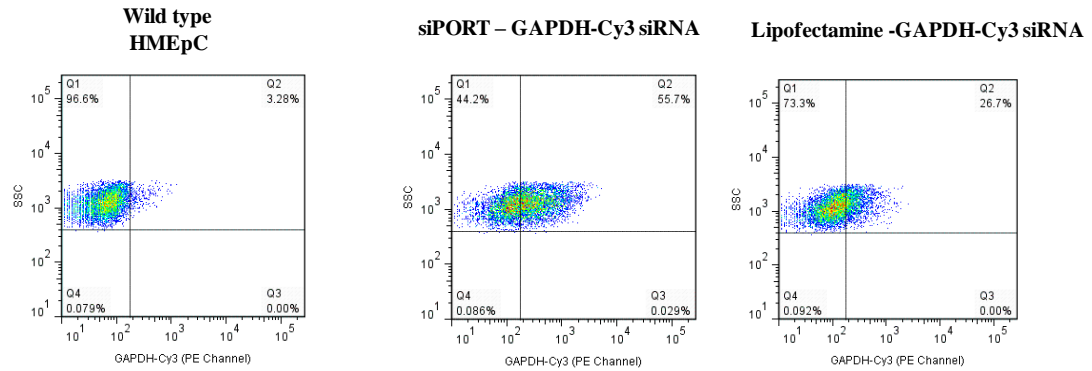


Figure 4-16 - Transfection of GAPDH-Cy³ siRNA into HMEpC using Lipofectamine®2000 and siPORTTMNeoFXTM

HMEpC were transfected with either 5nM of GAPDH-Cy³ primers or control siRNA using either Lipofectamine®2000 or siPORTTMNeoFXTM and incubated in normal growth conditions. 24 hours post-transfection, the transfection efficiencies were determined by flow cytometry.

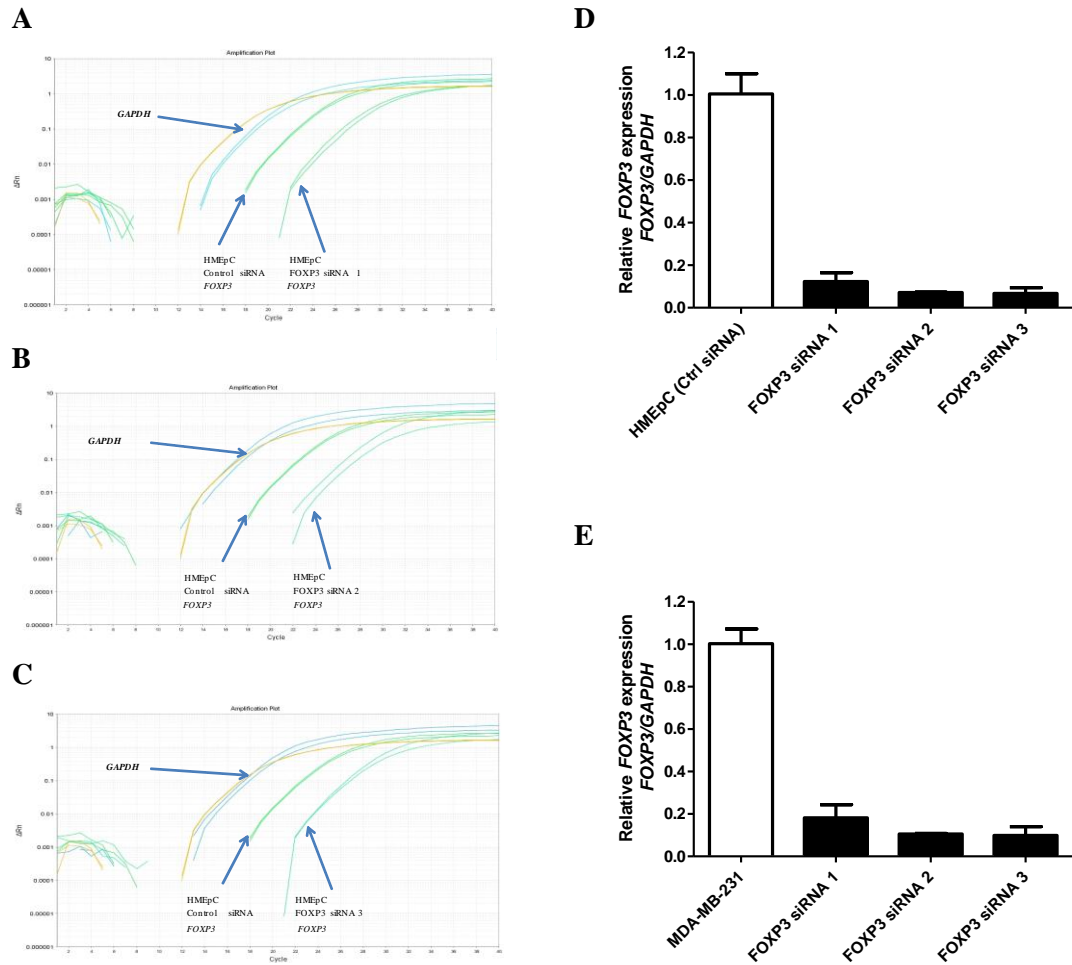


Figure 4-17 - Determination of *FOXP3* knockdown in HMEpC using *FOXP3* specific siRNA

HMEpC were transfected with 5nM of *FOXP3* siRNA or control siRNA using siPORTTMNeoFXTM and cultured in normal growth conditions without serum. After 24 hours, RNA was isolated and reverse transcribed into cDNA. Real-time PCR was used to determine the expression of *FOXP3*. **Panel A-C** are representative amplification plots demonstrating *FOXP3* knockdown using *FOXP3* siRNA 1 (**A**), *FOXP3* siRNA 2 (**B**) and *FOXP3* siRNA 3 (**C**). After normalising against endogenous *GAPDH*, the amount of *FOXP3* transcripts were compared to those from HMEpC transfected with control siRNA (**D**) and MDA-MB-231 (**E**) which were arbitrarily defined as 1.0. Data shown are means and SD of experiments performed in duplicates (n=2).

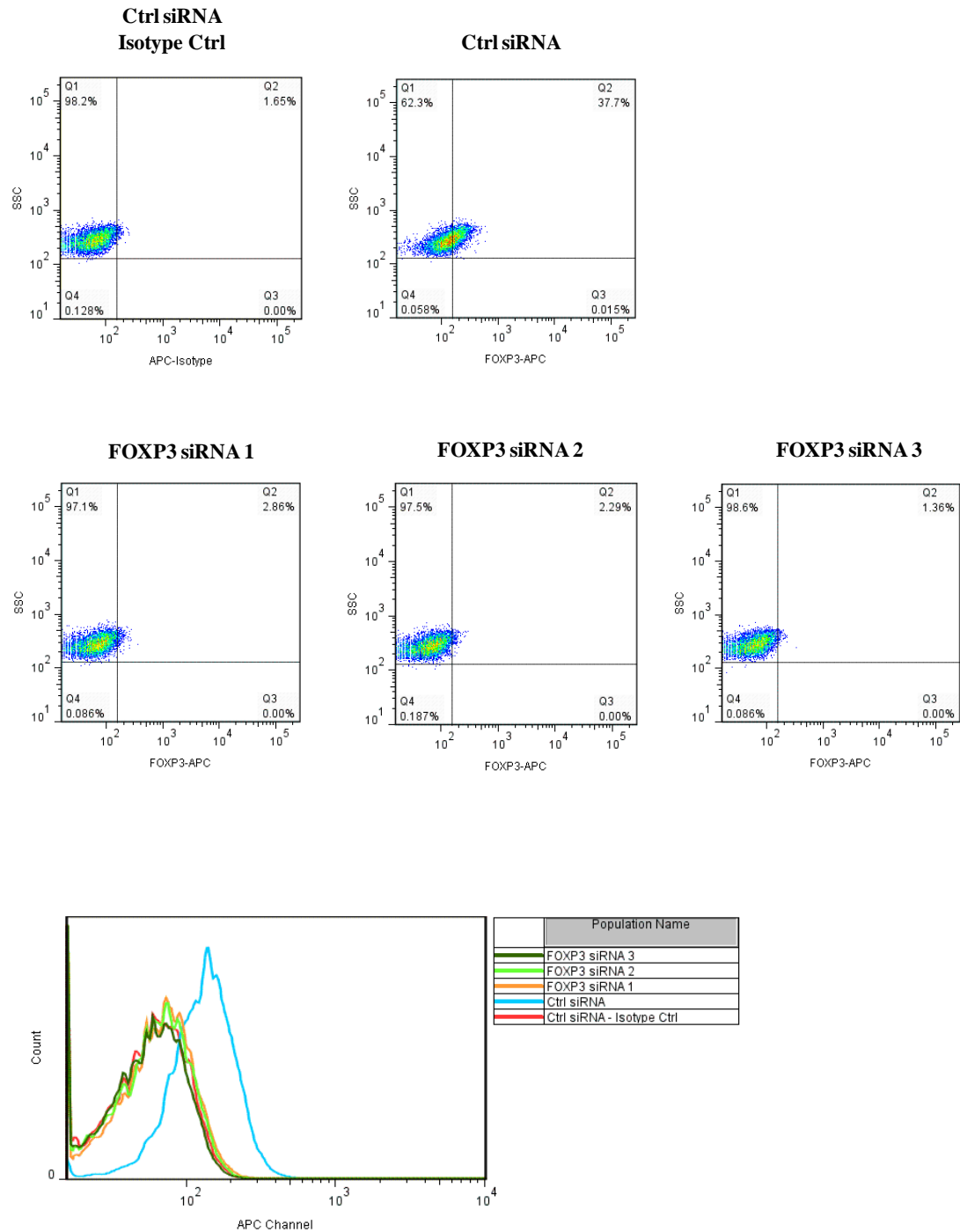


Figure 4-18 - Determination of FOXP3 in HMEpC following transfection of FOXP3 specific siRNA

HMEpC were transfected with either 5nM of FOXP3 siRNA or control siRNA using siPORT™ NeoFX™. Cells were left to incubate in normal growth conditions without serum. After 24 hours, cells were fixed, permeabilised and stained using a FOXP3-APC antibody or a matched isotype control. Images are representative of two experiments performed in duplicate.

4.4.9 Effects of FOXP3 knockdown in HMEpC

After investigating the effects of FOXP3-overexpression in MDA-MB-231, a further series of experiments was performed to investigate the transcriptional, proteomic and functional consequences of FOXP3 knockdown in HMEpC.

4.4.9.1 Relative expression of genes following FOXP3 knockdown in HMEpC

Following confirmation that FOXP3 could be knocked down in HMEpC, the effects of this knockdown on *ErbB2*, *SKP2*, *MYC*, *CDKN1A* and *CXCR4* was examined by real-time PCR (**figure 4.19**).

Levels of *ErbB2* and *SKP2* were moderately expressed within MDA-MB-231 and low in HMEpC. However, following *FOXP3* knockdown, these transcripts both significantly increased between 4- and 6-fold (**figure 4.19 panels A and B**).

Interestingly, FOXP3 knockdown failed to cause a significant increase in *MYC* or *CDKN1A* transcripts (**figure 4.19 panels C and D**). However, a clear trend was observed within *CDKN1A* ($p=0.0534$). A moderate expression of *CXCR4* was observed in MDA-MB-231, whereas, HMEpC expressed low levels which were barely detectable. Following FOXP3 knockdown, the levels of *CXCR4* increased in three experiments, whereas the other three experiments failed to induce an observable change in *CXCR4* expression. Nonetheless, taken together, this represented a mean fold increase of approximately 2, which was a significant increase in *CXCR4* expression ($p=0.0479$) (**figure 4.19 panel E**).

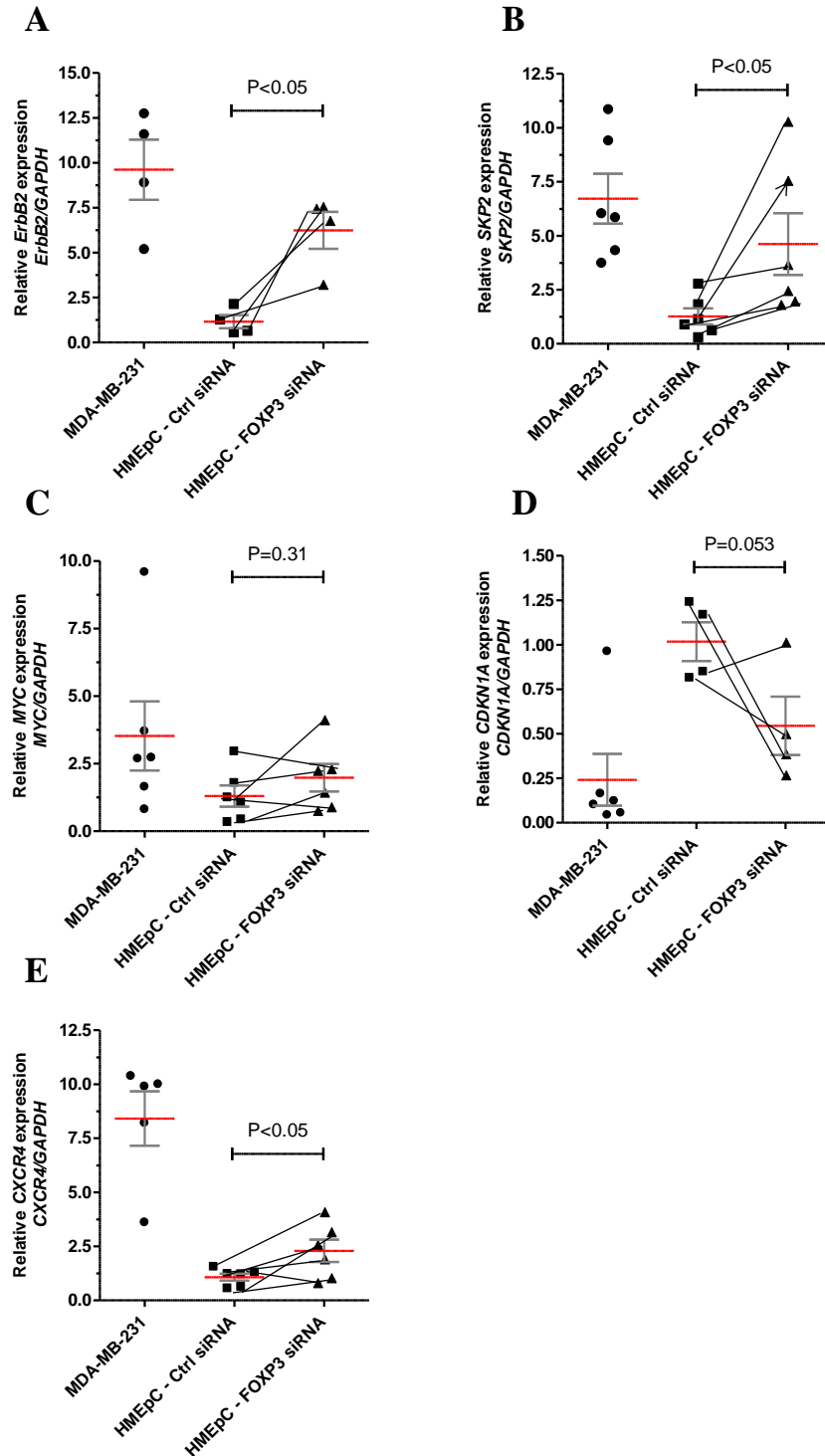


Figure 4-19 - Changes in oncogene expression following FOXP3 knockdown in HMEpC

After normalising against endogenous *GAPDH*, the amount of transcripts from HMEpC transfected with FOXP3 siRNA sequences were compared to those from HMEpC transfected with control siRNA cells which were arbitrarily defined as 1.0. Data shown are means and SD of experiments performed in duplicates. **(A)** *ErbB2*/HER-2 transcripts, **(B)** *SKP2* transcripts, **(C)** *MYC* transcripts and **(D)** *CDKN1A* transcripts **(E)** *CXCR4* transcripts. MDA-MB-231 was included as direct comparisons to an invasive cancer cell line. Unpaired t-tests were used to analyse HMEpC Ctrl siRNA vs HMEpC-FOXP3 siRNA columns.

4.4.9.2 Changes in CXCR4 following FOXP3 knockdown in HMEpC

After observing a significant increase in *CXCR4* transcripts following *FOXP3* knockdown in HMEpC, it was next determined whether the increase in transcript numbers translated to the protein level. Briefly, HMEpC were transfected with control siRNA or *FOXP3* siRNA sequences. After 24 and 48 hours post-transfection, cells were released from the culture flask and were fixed and permeabilised using an intracellular staining kit. HMEpC were stained for *FOXP3* and *CXCR4*. Changes in *CXCR4* and *FOXP3* expression were then determined by flow cytometry. Representative data from a 48 hour post-transfection is included in **figure 4.20**.

Consistent with the literature, flow cytometric dot plots showed that wild type HMEpC failed to express membrane *CXCR4*, whereas, *FOXP3* was detectable at low levels. These levels of expression remained constant after transfection with control siRNA which demonstrates that the control siRNA does not affect the cell phenotype.

The effects of *FOXP3* knockdown fluctuated, as some experiments resulted in an increase in *CXCR4*, whereas some experiments failed to induce any changes. These results were slightly ambiguous as discussed in section 1.4.10.1.

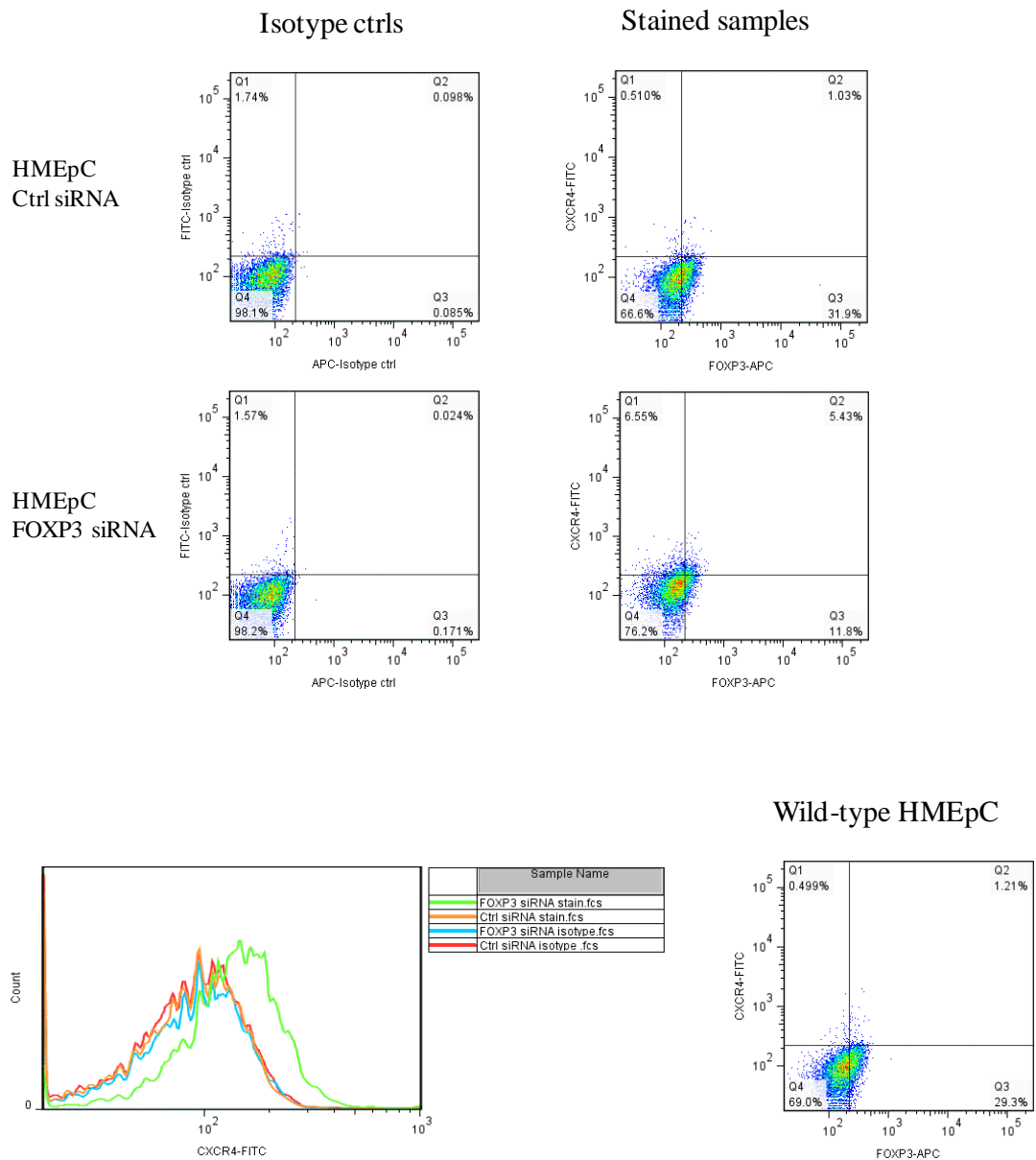


Figure 4-20 - Effects on CXCR4 expression following FOXP3 knockdown in HMEpC

Wild type HMEpC and HMEpC transfected with either FOXP3 siRNA or control siRNA sequences were stained for FOXP3 and CXCR4 48 hours post-transfection. HMEpC transfected with either FOXP3 siRNA or control siRNA were also each stained with a matched APC or FITC isotype control to determine staining specificity. Representative images of 48 hour post-transfection from 5 experiments.

4.4.10 Cytometric bead assay to determine anti-CXCR4 antibody binding capacity (ABC)

To determine the changes in anti-CXCR4 ABC following FOXP3 knockdown, QuantumTM Simply Cellular[®] beads were used to quantitatively analyse the membrane expression of CXCR4 on test samples. A standard curve was produced by plotting the MFI of an anti-CXCR4 antibody from each bead population versus the known ABC of each bead population. Therefore, the total CXCR4 binding capacity of each cell sample can be determined by interpolating the CXCR4 MFI from each sample, minus the background CXCR4 MFI (isotype controls) from the standard curve.

If monovalent antibody-to-surface receptor is presumed, the antigen binding capacity is directly proportional to the number of cell surface receptors.

Five sets of beads were stained with the same concentration of anti-CXCR4 antibody, incubated for the same length of time and ran on the same instrument with the same settings as test samples. The MFI of each bead population produced a linear increase in MFI as each bead has an increased capacity to bind antigen (**figure 4.21**).

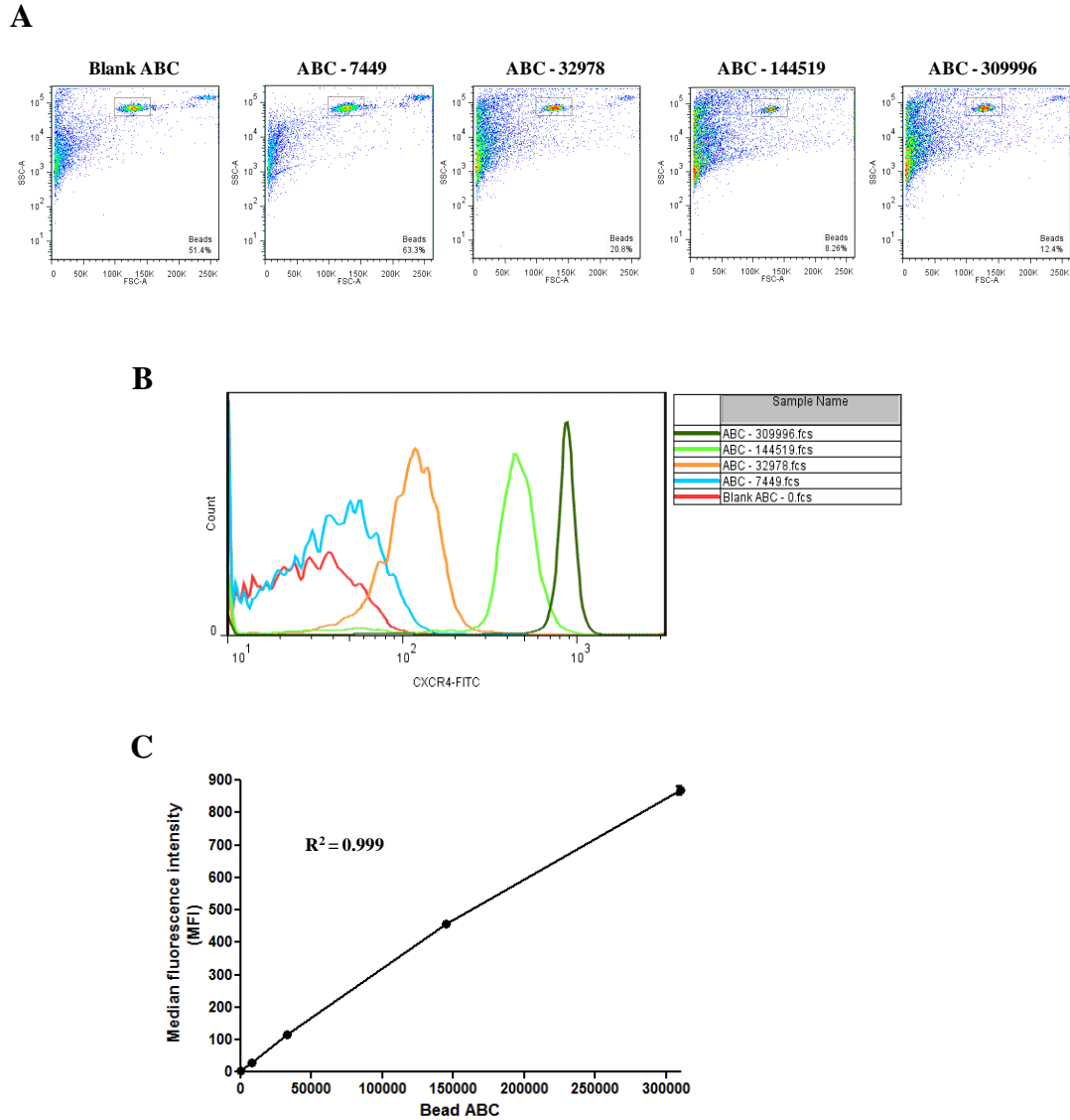


Figure 4-21 - Cytometric bead assay to determine ABC of the anti-CXCR4 antibody

Each population of bead was dispensed into FACS tubes and stained with anti-CXCR4-FITC antibody. Bead populations were gated using forward and side scatter dot plots (**A**). Representative histogram of fluorescence intensity from each bead population demonstrates an increase in fluorescence as the bead population also increases (**B**). MFI from each bead sample was plotted against the antigen binding capacity from each sample to produce a linear standard curve to be used in determining CXCR4 ABC in test samples (**C**) (n=2).

4.4.10.1 Changes in CXCR4 ABC following FOXP3 knockdown in HMEpC

The MFI of CXCR4 in fresh HMEpC following transfection of either control siRNA or FOXP3 siRNA sequences after 24 and 48 hours was measured by flow cytometry. ABC of CXCR4 in each sample was determined and plotted after subtracting the ABC of the isotope control (**figure 4.22**).

Interestingly, despite CXCR4 barely being detectable by dot plots and histograms, the QuantumTM Simply Cellular® beads suggested that HMEpC do contain low levels of CXCR4.

Two independent 24 hour post-transfection FOXP3 knockdown experiments showed an increase in CXCR4, whereas, one experiment resulted in a slight decrease (**figure 4.22 panel A**). Similar findings were witnessed 48 hours post-transfection. However, three experiments resulted in increases in CXCR4 of variable magnitude, whereas, CXCR4 decreased in two other experiments (**figure 4.22 panel B**). Overall findings from 24 hour ($p=0.33$) and 48 hour ($p=0.52$) post-transfections did not represent a significant increase in CXCR4 protein expression.

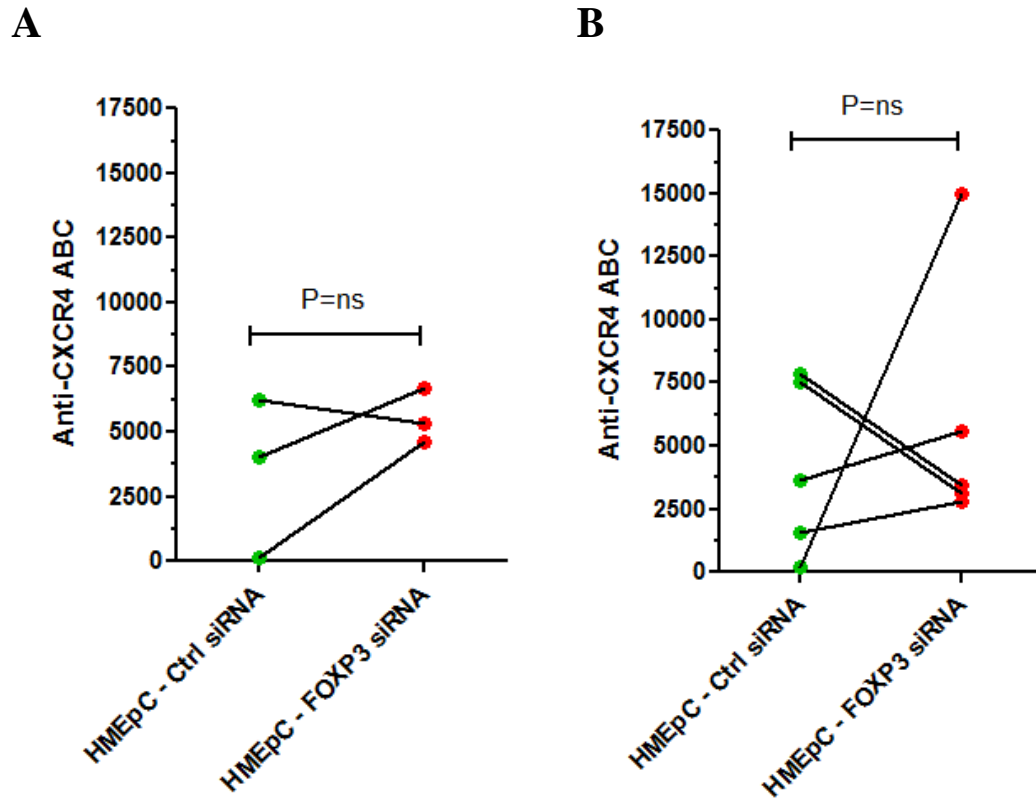


Figure 4-22 - Changes in CXCR4 ABC following FOXP3 knockdown in HMEpC

The CXCR4 antigen ABC was determined in HMEpC transfected with either control siRNA or FOXP3 siRNA sequences by measuring MFI of CXCR4 off a standard curve. Data was plotted after subtracting the CXCR4 ABC of each isotype (background) from the test sample. **Panel A** represents data 24 hours post-transfection. **Panel B** represents data 48 hours post transfection.

4.4.11 Optimisation of chemoinvasion towards CXCL12 using MDA-MB-231

As a chemokine receptor, the primary function of CXCR4 is to direct cell migration towards CXCL12. However, it is also well established that the expression of CXCR4 and subsequent interaction with CXCL12 induces signals which aid the invasion of cells (discussed in section 1.6.2). During metastasis, after excessive tumour growth, the initial stage is the ability to invade beyond the basement epithelial-coated membrane into the adjacent breast tissue. This is followed by the invasion into lymphatic vessels, and finally migration towards new secondary sites.

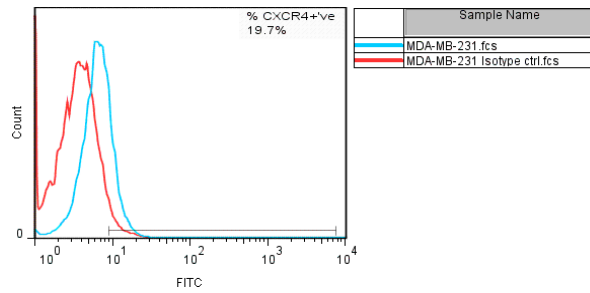
Next, the potential migration and invasive functional changes in HMEpC following FOXP3 knockdown was investigated.

MDA-MB-231 is a cell line known to express CXCR4 and respond to CXCL12 (Muller, Homey et al. 2001). Before determining whether the changes in CXCR4 on HMEpC represent a functional change, the concentration of chemokine and incubation period was optimised using MDA-MB-231.

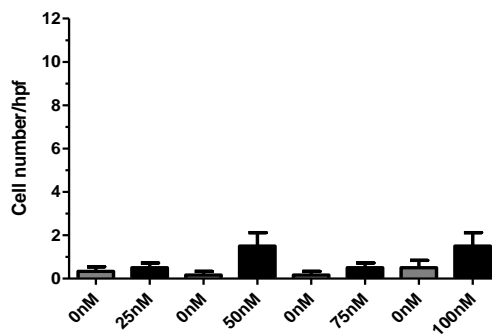
Chemoinvasion assays were set up using CXCL12 concentrations ranging from 0nM to 100nM with incubation periods ranging from 24 hours to 96 hours. Despite demonstrating that MDA-MB-231 express CXCR4 (**figure 4.23 panel A**) and reports frequently using the cells as positive controls in invasion assays, these cells did not invade to the levels reported in previous studies (Muller, Homey et al. 2001). However, using 75nM and 100nM of CXCL12, MDA-MB-231 did significantly penetrate a matrigel coated membrane after 72 hours and 96 hours incubation (**figure 4.23 panels B-E**).

It was decided that the optimum chemokine and incubation periods for assays were between 75nM and 100nM for 72 hours and 96 hours.

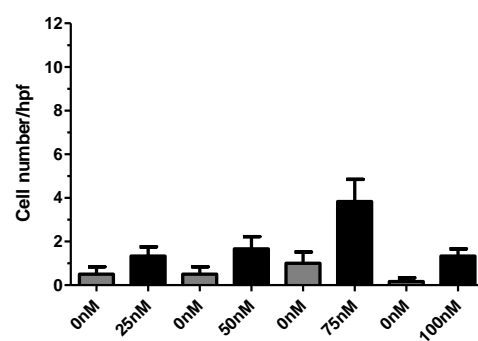
A



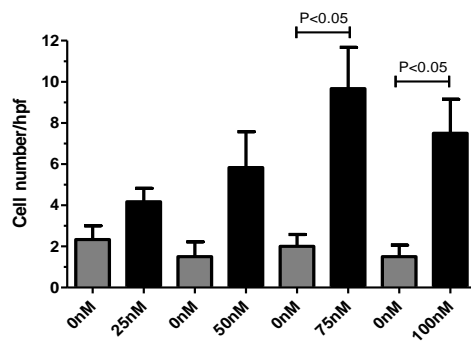
B



C



D



E

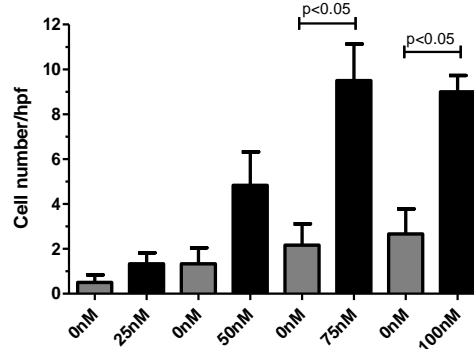


Figure 4-23 - Optimisation of chemoinvasion towards CXCL12 using MDA-MB-231

CXCR4 expression was determined using flow cytometry by staining MDA-MB-231 with a CXCR4-FITC antibody and a matched FITC-isotype control (A). Prior to invasion, chemo-invasion plates were blocked using chemotaxis buffer. 8 μ M pore filters were firstly coated in a thin layer of matrigel inside the filter, followed by 2.5 μ g/ml of fibronectin. MDA-MB-231 was then incubated for 24 hours (B), 48 hours (C), 72 hours (D) and 96 hours (E) with increasing amounts of CXCL12. Data shown are means and SD of experiments performed in duplicates. Statistitcal analysis between columns was done using a paired t-test.

4.4.12 Effects of FOXP3 knockdown on invasiveness of HMEpC

After optimising the chemokine concentration and incubation time, the invasive potential of HMEpC was investigated following FOXP3 knockdown.

Using 75nM of CXCL12, neither wild type nor control siRNA transfected HMEpC was able to penetrate a matrigel coated filter after 72 hours incubation. HMEpC transfected with FOXP3 siRNA also failed to significantly invade after 72 hours. Even after an extended incubation of 96 hours, neither wild type, control siRNA transfected HMEpC nor FOXP3 siRNA transfected HMEpC significantly invaded (**figure 4.24**).

Results after 72 hours and 96 hours incubation also showed no significant change in invasiveness after increasing the CXCL12 concentration to 100nM (**figure 4.25**).

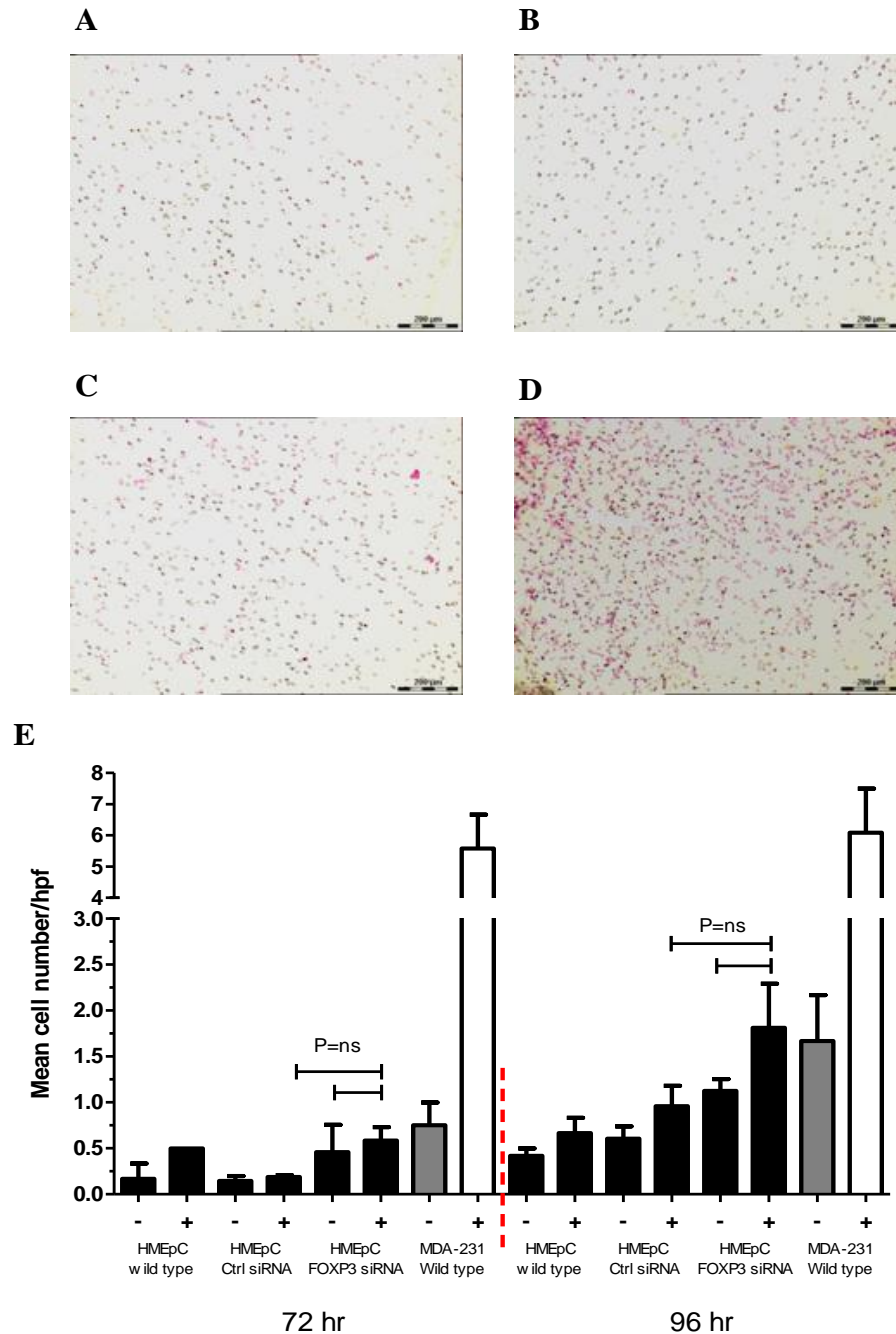


Figure 4-24 - Chemoinvasion of HMEpC in response to 75nM of CXCL12 following transfection of FOXP3 siRNA

Wild type HMEpC and HMEpC transfected with either control siRNA or FOXP3 siRNA sequences and incubated in normal growth conditions with 75nM of CXCL12 for 72 hours and 96 hours. As a negative control, each cell line was also cultured in the absence of chemokine. MDA-MB-231 was used as a positive control. **Panels A-D** are representative images 72 hours post transfection of the following conditions: **(A)** HMEpC transfected with control siRNA with 75nM of CXCL12, **(B)** HMEpC transfected with FOXP3 siRNA with no chemokine **(C)** HMEpC transfected with FOXP3 siRNA with 75nM of CXCL12 **(D)** Wild-type MDA-MB-231 with 75nM of CXCL12. **Panel E** shows data from 72 hour and 96 hour post transfections which are means and SD of experiments performed in duplicates (n=3).

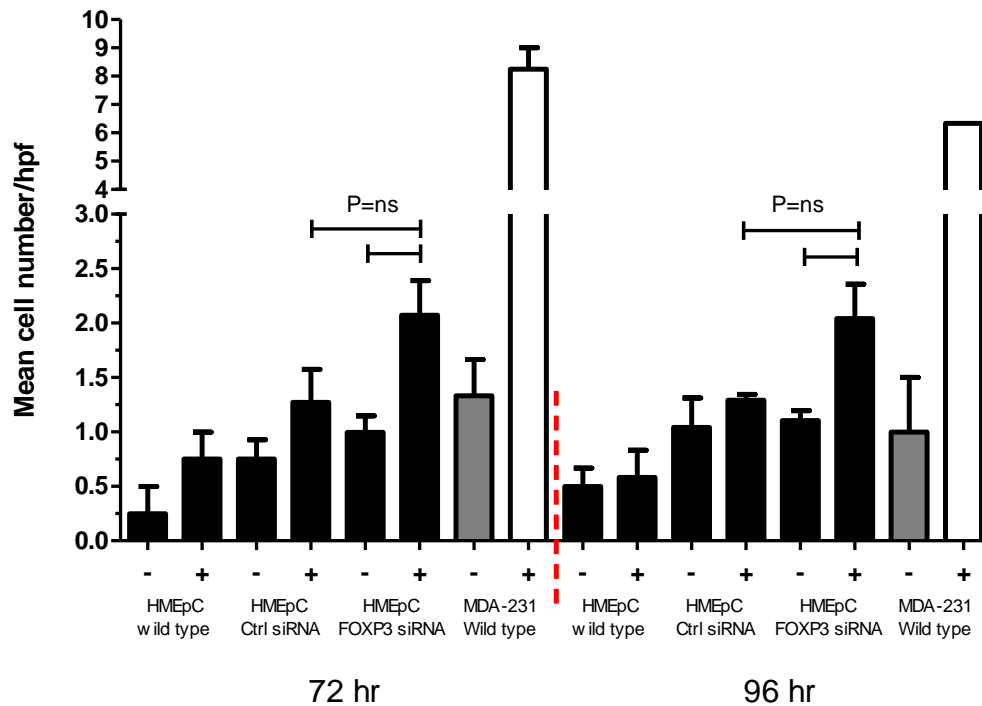


Figure 4-25 - Chemoinvasion of HMEpC in response to 100nM of CXCL12 following transfection of FOXP3 siRNA

Wild type HMEpC and HMEpC transfected with either control siRNA or FOXP3 siRNA and incubated in normal growth conditions with 100nM of CXCL12 for 72 hours and 96 hours. As a negative control, each cell line was also cultured in the absence of chemokine. MDA-MB-231 was used as a positive control. Data shown from 72 hours and 96 hours post transfections which are means and SD of experiments performed in duplicates (n=3)

4.4.13 Optimisation of chemotaxis assays towards CXCL12 using MDA-MB-231

As described, the main role of chemokine receptors, such as CXCR4, is to direct cell migration. Therefore, chemotaxis assays were used to determine whether FOXP3 knockdown is able to increase the migratory ability of HMEpC.

Initially, the concentration of CXCL12 was optimised. MDA-MB-231 were incubated in normal growth conditions, with chemotaxis buffer, for 24 hours with doubling concentrations of CXCL12 from 0nM to 50nM (**figure 4.26 panels A and B**). After 24 hours, filters were removed and cells were fixed, stained and mounted onto chamber slides.

MDA-MB-231 is a highly motile cell line and migrated even in the absence of CXCL12. In line with the literature, MDA-MB-231 expressing CXCR4 also responded strongly to CXCL12. As the chemokine concentration increased, the migration of MDA-MB-231 also increased. However, the maximum migration was witnessed using 25nM CXCL12. Doubling this concentration to 50nM failed to increase the migration of MDA-MB-231 any further, therefore, 25nM CXCL12 was considered the optimum concentration.

Next, the length of incubation was optimised between 6 hours and 36 hours using 25nM CXCL12 (**figure 4.26 panel C**).

Once again, even in absence of CXCL12, MDA-MB-231 migrated strongly after as little as 6 hours incubation. A statistically significant increase in migration was observed after 16, 24 and 36 hours. Although the cells potently migrated in the presence of 25nM CXCL12, as the length of incubation increased, so did the background number of cells cultured in the absence of CXCL12. The optimum length of incubation was 24 hours.

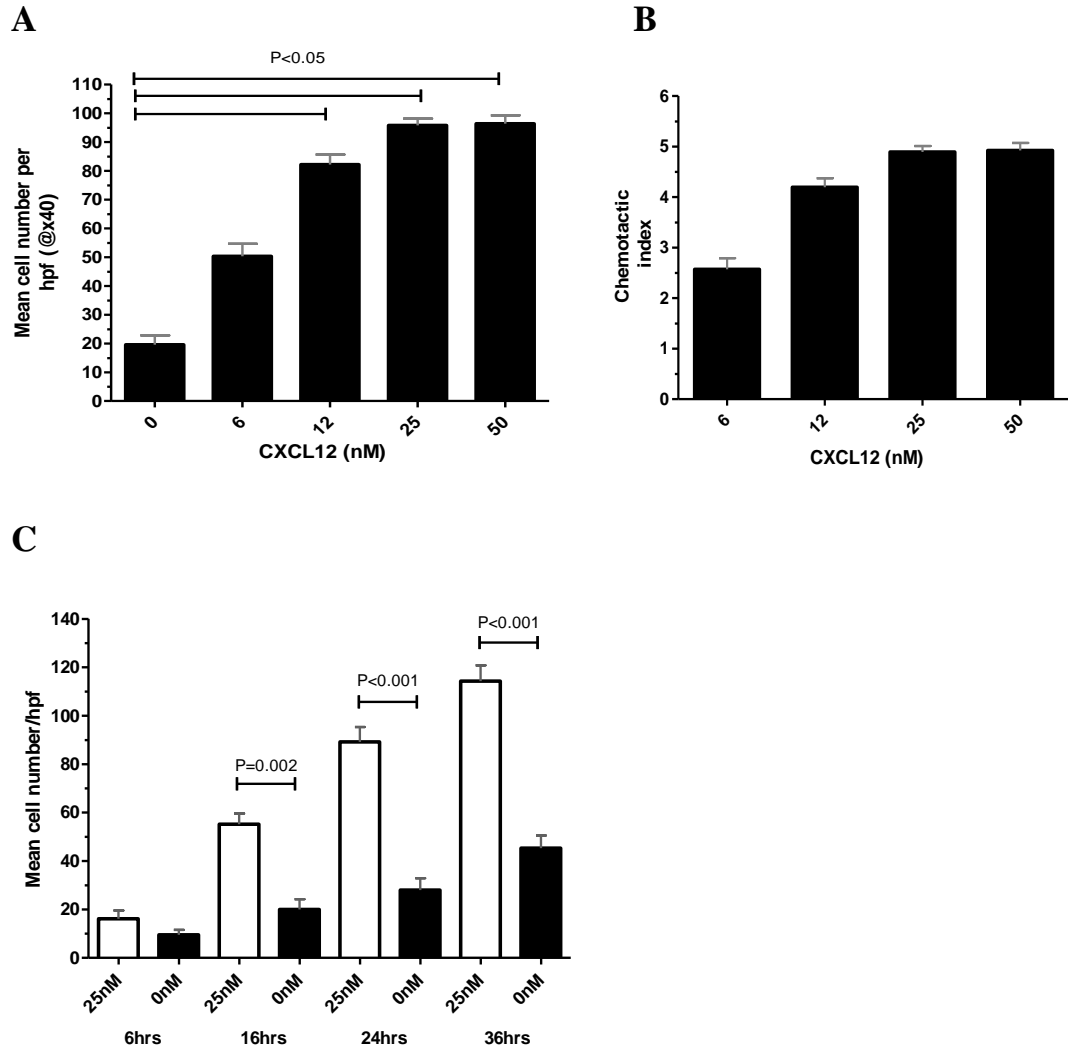


Figure 4-26 - Optimisation of chemotaxis assays towards CXCL12 using MDA-MB-231

Prior to migration, chemotaxis plates were blocked using 0.1% BSA in chemotaxis buffer. Firstly, 8 μ M pores filters were coated with 2.5 μ g/ml of fibronectin and MDA-MB-231 were then incubated for 24 hours with increasing concentrations of CXCL12 (**A**). Chemotaxis index represents the fold change in the migration of MDA-MB-231 cultured in the presence of CXCL12 over the migration of MDA-MB-231 with no chemokine (background). Chemotactic index demonstrates a significant dose dependant increase in migratory response to CXCL12 by MDA-MB-231 (**B**). The length of incubation to allow migration was optimised by incubating MDA-MB-231 with 25nM of CXCL12 for 6, 16, 24 and 36 hours (**C**), each time point contained a no chemokine control to measure background. Data shown are means and SD of a single experiment performed in duplicate. Statistical analysis between columns was performed using a paired t-test.

4.4.14 Effects of FOXP3 knockdown on migration of HMEpC

Wild type HMEpC and HMEpC transfected with either control siRNA or FOXP3 siRNA sequences were incubated in normal growth conditions for 24 hours and 48 hours with 25nM CXCL12.

Wild type HMEpC and control siRNA transfected HMEpC failed to migrate towards CXCL12 after 24 hours. No significant changes were witnessed in HMEpC transfected with FOXP3 siRNA after 24 or 48 hours with 25nM CXCL12 (**figure 4.27**).

Because MDA-MB-231 express CXCR4 (**figure 4.24 panel A**) and also migrate potently towards CXCL12 (**figure 4.26**), it was deemed that perhaps HMEpC (which undoubtedly express less CXCR4 than MDA-MB-231) may require a greater concentration of CXCL12. On this basis, another chemotaxis assay was set up using double the concentration of CXCL12. Similar to previous results, 24 hours incubation with 50nM CXCL12 failed to significantly induce migration, however, when HMEpC transfected with FOXP3 siRNA sequences were left to migrate for 48 hours in response to 50nM CXCL12 there was a significant increase in migration in comparison to cells cultured with no chemokine ($p=0.048$), and also in comparison to cells treated with control siRNA and incubated with 50nM CXCL12 ($p=0.041$) (**figure 4.28**). This demonstrates a chemotactic response which is dependent on the presence of CXCL12.

Interestingly, particularly in assays using 50nM CXCL12, the migration was also increased in HMEpC transfected with control siRNA with chemokine in comparison to wild type HMEpC. In addition to this, HMEpC transfected with FOXP3 siRNA sequences also had an increased migration in the absence of chemokine. This suggests the possibility that FOXP3 knockdown not only increases the migration towards CXCL12 but also makes cells more motile in general. This has been reported within the literature (Zhang and Sun 2010; Frattini, Pisati et al. 2012)

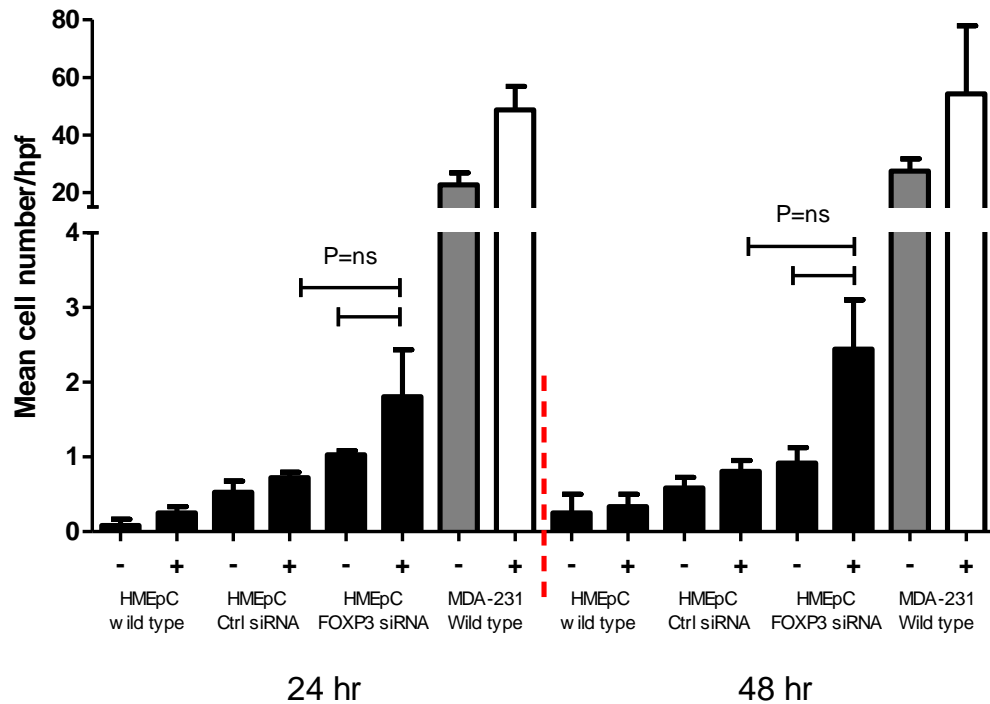


Figure 4-27 - Chemotaxis of HMEpC in response to 25nM of CXCL12 following FOXP3 knockdown in HMEpC

Wild type HMEpC and HMEpC transfected with either control siRNA or FOXP3 siRNA sequences and incubated in normal growth conditions with 25nM of CXCL12 for 24 hours and 48 hours. As a negative control, each cell line was also cultured in the absence of chemokine. MDA-MB-231 was used as a positive control. Data shown are means and SD of experiments performed in duplicates (n=3).

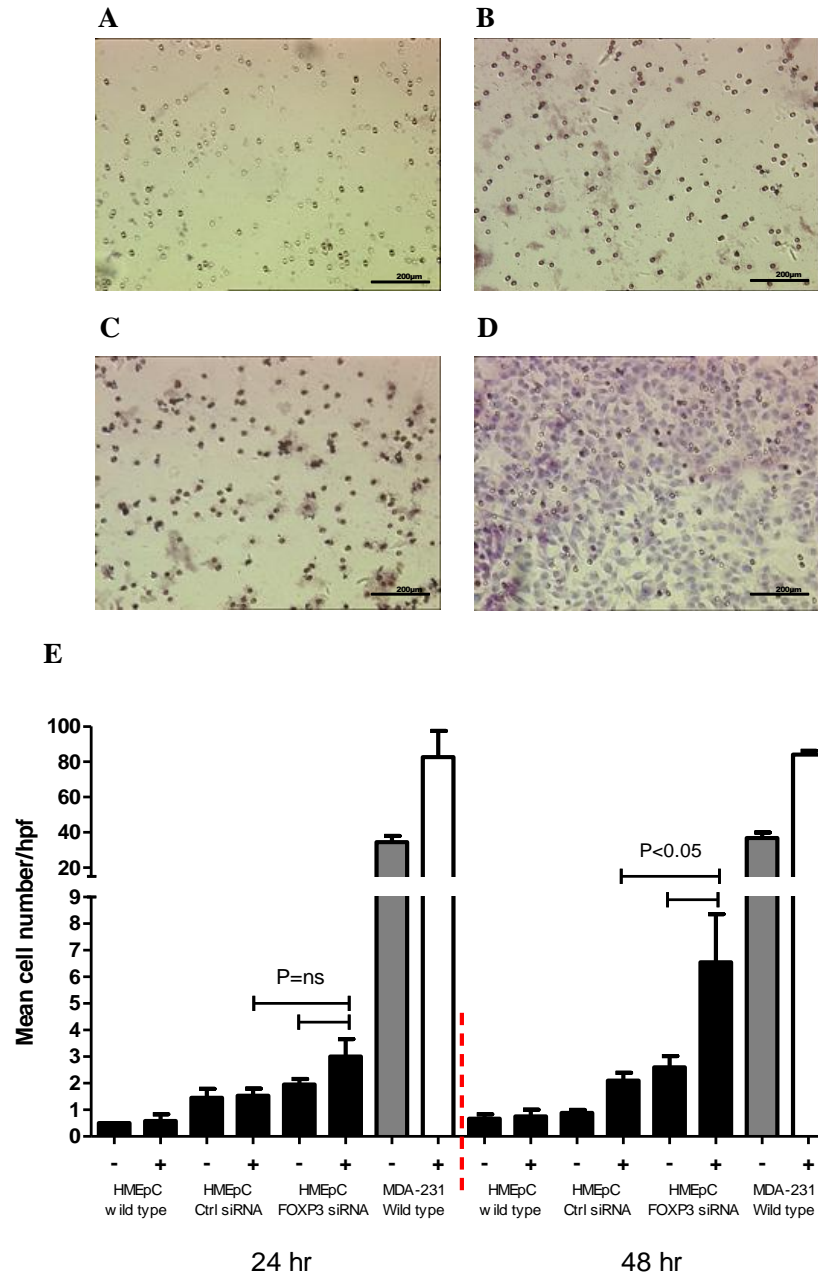


Figure 4-28 - Chemotaxis of HMEpC in response to 50nM of CXCL12 following FOXP3 knockdown in HMEpC

Wild type HMEpC and HMEpC transfected with either control siRNA or FOXP3 siRNA sequences and incubated in normal growth conditions with 50nM of CXCL12 for 24 hours and 48 hours. As a negative control, each cell line was also cultured in the absence of chemokine. MDA-MB-231 was used as a positive control. **Panels A-D** are representative images 48 hours post transfection (except D which was 24 hours) of the following conditions: (A) HMEpC transfected with control siRNA with 50nM of CXCL12, (B) HMEpC transfected with FOXP3 siRNA with no chemokine, (C) HMEpC transfected with FOXP3 siRNA with 50nM of CXCL12, (D) Wild-type MDA-MB-231 with 25nM of CXCL12. **Panel E** shows data from 24 hours (n=3) and 48 hours (n=5) post-transfection which are means and SD of experiments performed in duplicate. Paired t-test was used to statistically analyse the HMEpC FOXP3 siRNA 0nM vs 50nM, whereas, unpaired t-test was used to compare HMEpC Ctrl siRNA 50nM vs HMEpC FOXP3 siRNA 50nM.

4.5 Summary of chapter 4 results

- ✓ Successfully constructed a FOXP3-expressing plasmid
- ✓ Successfully generated stably transfected FOXP3 into MDA-MB-213, which significantly overexpressed FOXP3 in comparison to MDA-MB-231 transfected with the empty vector, and HMEpC
- ✓ The following was observed after stable FOXP3 transfection into MDA-MB-231:
 - Significantly reduced *ErbB2*, *SKP2*, *MYC* and *CXCR4* transcripts
 - Significantly increased *CDKN1A*
 - Significantly inhibited proliferation and an increased proportion of cells in the G1 phase of cell cycle
- ✓ Stably transfected MDA-MB-231 were difficult to continuously expand with many colonies eventually dying. Transient transfections were attempted using Lipofectamine®2000, GenJet™, Turbofect™, GeneJuice® and JetPRIME™ were not able to successfully transfect MDA-MB-231. Therefore, the effect of FOXP3 overexpression on migration and invasion was not assessed.
- ✓ FOXP3 was effectively knocked down at both transcript and protein level after 24 hours using three separate FOXP3-specific siRNA
- ✓ The following was observed after FOXP3 knockdown in HMEpC:
 - Significantly increased *ErbB2*, *SKP2* and *CXCR4* transcripts
 - CXCR4 protein expression was not significantly altered after FOXP3 knockdown 24 hours and 48 hours post transfection

- MDA-MB-231 were capable of penetrating matrigel coated filters in response to CXCL12, however, FOXP3 knockdown in HMEpC failed to induce an invasive capacity to these cells
- MDA-MB-231 potently migrated towards CXCL12, whereas, HMEpC did not. FOXP3 knockdown in HMEpC significantly increased the migratory response of HMEpC in response to 50nM of CXCL12 after 48 hours incubation.

4.6 Discussion

FOXP3 is a transcription factor capable of binding and influencing the expression of many genes (Zheng, Josefowicz et al. 2007). Much of the literature describing the functions of FOXP3 is reported for Tregs where FOXP3 is regarded as the master regulator of the development and function of these cells by controlling the high level expression of CD25 and CTLA-4 whilst preventing the production of IL-2 (Chen, Rowell et al. 2006).

The ability of FOXP3 to influence gene expression has also been demonstrated within epithelial cells where it influences *ErbB2* (Zuo, Wang et al. 2007), *SKP2* (Zuo, Liu et al. 2007), p21 (Liu, Wang et al. 2009; Frattini, Pisati et al. 2012), *c-MYC* (Wang, Liu et al. 2009; Frattini, Pisati et al. 2012) and *LATS2* (Li, Wang et al. 2011), *MMP9* and *VEGF* (Nakahira, Morita et al. 2013).

As well as regulating these genes, FOXP3 has also been shown to control proliferation, migration and invasion of cancer cells (Liu, Wang et al. 2009; Wang, Liu et al. 2009; Zhang and Sun 2010; Li, Wang et al. 2011; Frattini, Pisati et al. 2012; Nakahira, Morita et al. 2013). This demonstrates that FOXP3 is more than just an immune regulator but is also a protein important in preventing carcinogenesis.

FOXP3 is often dysregulated in breast cancer cases; this contributes to the increased expression of oncogenes as previously mentioned (Zuo, Liu et al. 2007; Zuo, Wang et al. 2007; Merlo, Casalini et al. 2009). On the other hand, it is now well established that CXCR4 plays an important role in breast cancer by influencing a number of processes involved with cancer progression (Chang and Karin 2001; Fresno Vara, Casado et al. 2004; Luker and Luker 2006; Liang, Brooks et al. 2007).

Although CXCR4, and another gene implicated in breast cancer, CCR7, have both been reported as FOXP3 target genes in thymic T-cells (Zheng, Josefowicz et al. 2007), to this date no reports have demonstrated links between FOXP3 and CXCR4 regulation in breast epithelial cells. Therefore, the aim of this chapter was to investigate the role of FOXP3 in epithelial cell homeostasis using *in vitro* techniques with a novel insight to its ability to influence CXCR4 expression.

In attempts to answer this question, two model systems were selected to study the effects of FOXP3. After the initial demonstration of the dysregulated expression of

FOXP3 within MDA-MB-231 and normal FOXP3 expression in HMEpC, experiments were designed to investigate the effects of overexpressing FOXP3 in MDA-MB-231, and knocking down wild type FOXP3 in HMEpC.

FOXP3 DNA was cloned into a pcDNA3.1/Zeo(+) backbone. The DNA contained the entire *FOXP3* protein coding domain and will therefore encode FOXP3 FL and not the $\Delta 3$ isoform. The ability of this plasmid to express *FOXP3* was tested by transiently transfecting the plasmid DNA into wild type HEK cells. *FOXP3* was highly upregulated after transfection demonstrating that this plasmid is capable of expressing FOXP3.

4.6.1 Generation of stable FOXP3 overexpressing MDA-MB-231

The stable transfection of MDA-MB-231 with FOXP3 was a challenging aspect of the project. Most researchers who have used MDA-MB-231 agree that it is a notoriously difficult cell line to transfect. Indeed many reagents are optimised for this “difficult-to-transfect” cell line. Nonetheless, MDA-MB-231 transfection has been reported in the literature (Chen, Kang et al. 2001; Wu, Chan et al. 2005).

Despite this difficulty, three colonies were expanded in the presence of ZeocinTM. However, only one of these, colony 4, stably overexpressed FOXP3. Because FOXP3 was overexpressed in comparison to MDA-MB-231 transfected with the empty vector and HMEpC, this was a good model to investigate the effects of re-introducing FOXP3 into an invasive breast cancer cell line.

As a transcription factor, a nuclear location is imperative to effective functioning. Previous results, in chapter 3, suggested that despite low level expression of FOXP3 within MDA-MB-231, the protein was predominately restricted to the cytoplasm. MDA-MB-231 which stably overexpressed FOXP3, expressed the protein predominately within the nucleus, which proposes that these cells have retained the processes required for normal nuclear translocation of the FOXP3 protein. This suggests that nuclear localisation of FOXP3 may depend on other factors which are maintained in MDA-MB-231.

Indeed, FOXP3 frequently works by cooperating with other transcription factors and proteins such as NFAT (Wu, Borde et al. 2006). NFAT is highly expressed in MDA-MB-231 and is associated with an aggressive phenotype (Yiu and Toker 2006). The expression of NFAT is generally located within the cytoplasm and then actively transported to the nucleus following dephosphorylation (Danesh, Newton et al. 1999). Few papers have investigated FOXP3 nuclear transport with many describing different mechanisms and often contradicting each other (Lopes, Torgerson et al. 2006; Hancock and Ozkaynak 2009). This suggests that the exact factors involved with FOXP3 transport remain inconclusive. On this basis, it is reasonable to hypothesise that FOXP3 may be actively transported to the nucleus in cooperation with other transcription factors such as NFAT. Since MDA-MB-231 express low levels of FOXP3, it may be that these levels are not sufficient to allow interaction with these factors and transfecting high levels of FOXP3 may restore this ability.

4.6.2 Effects of FOXP3 overexpression in MDA-MB-231

FOXP3 overexpressing MDA-MB-231 showed a reduction in relative expression of *ErbB2* and *SKP2* to levels similar to those observed in HMEpC. These findings are consistent with those described in the literature (Zuo, Liu et al. 2007; Zuo, Wang et al. 2007). In contrast to this, the expression of *CDKN1A* was significantly upregulated, which is also consistent with reports in the literature (Liu, Wang et al. 2009).

Constant expansion of the FOXP3 overexpressing MDA-MB-231 was almost as difficult as generating the colonies. Over time these cells seldom grew which was demonstrated by a proliferation assay showing a significantly reduced rate of proliferation. Interestingly, the overexpression of FOXP3 in cancer cell lines has also been demonstrated to significantly inhibit proliferation by several other groups (Zhang and Sun 2010; Frattini, Pisati et al. 2012).

CDKN1A is a gene responsible for encoding the cell cycle inhibitor p21, which is responsible for inducing cell cycle arrest at the G1 stage. Along with Ki67, p21 is now also considered as one of the most reliable markers of senescence (Kang, Kim et al. 2009; Jia, Li et al. 2011; Baker, Weaver et al. 2013).

Because there was approximately a 7-fold increase in *CDKN1A*, it could be that FOXP3 transfection resulted in the induction of cellular senescence of MDA-MB-231. The significant increase in *CDKN1A* expression in FOXP3 overexpressing MDA-MB-231 could be a factor which contributed to the reduced proliferation. Cell cycle analysis demonstrated an increased proportion of FOXP3-overexpressing MDA-MB-231 in the G1 stage of cell cycle. A report by Zhang and Sun (Zhang and Sun 2010) also demonstrated that FOXP3-transfection into a malignant cell line caused an increased proportion of cells within the G1 phase. However, because the number of cells arrested within the G1 phase was only approximately 11% greater than wild type and empty vector transfected MDA-MB-231, the reduced rate of proliferation in these cells is unlikely to be solely responsible for the increased expression in *CDKN1A*. It seems more likely that the increase in *CDKN1A* is merely one factor to consider for the reduced proliferation with a reduction in other genes responsible for cell growth also contributing to this result. Indeed the expression of *HER2* (Wolf-Yadlin, Kumar et al. 2006; Johnson, Seachrist et al. 2010), *SKP2*, (Wang, Wu et al. 2009; Inuzuka, Gao et al. 2012; Zhang, Ji et al. 2013) and *MYC* (Alfano, Votta et al. 2010; Liu, Radisky et al. 2012; Zhao, Jian et al. 2013) are all well known to increase the proliferation of cancer cells. Therefore, the significant reduction in these genes is likely to have a major influence on the proliferation of these cells.

In addition to reductions in the expression of *ErbB2*, *SKP2* and *MYC* by FOXP3 overexpressing cells, the expression of *CXCR4* was also reduced. Although the overall change in the expression in *CXCR4* transcripts ($p=0.0496$) was not as striking as the changes observed for *ErbB2* ($p=0.0264$) and *SKP2* ($p=0.0249$), which are both reported to be directly repressed by FOXP3 in breast cancer cells, the reduction in *CXCR4* was still statistically significant. Because the changes observed were small and of variable magnitude, the data may suggest that FOXP3 does not directly bind *CXCR4* like it does to the aforementioned genes, but possibly relies on other downstream effectors to influence *CXCR4* expression.

Data from chapter 3 suggested that MDA-MB-231 were deficient in the natural FOXP3 $\Delta 3$ isoform but despite reduced levels, still expressed the full length variant.

Interestingly, because the FOXP3 DNA cloned into the plasmid encoded only the full length isoform, the effects observed following overexpression were still a result of FOXP3FL and not FOXP3Δ3 variant.

4.6.3 Effects of FOXP3 knockdown in HMEpC

To further validate the role of FOXP3 in breast epithelial cells, the normal expression of FOXP3 by HMEpC was knocked down using commercial siRNA. Three FOXP3 specific *silencer*® select siRNA sequences were validated by comparing against HMEpC transfected with control siRNA sequences. In all cases, a reduction was observed in FOXP3 expression at both a transcript and protein level 24 hours post-transfection. Because the half-life of FOXP3 is approximately 21 minutes (Lee, Gao et al. 2008), this reduction in FOXP3 within a relatively short period of time is, therefore, perhaps expected. Following transfection with siRNA sequences, *FOXP3* transcripts fell below the levels within HMEpC and MDA-MB-231, and thus provided a good model to investigate the effects of FOXP3 knockdown.

The HMEpC with reduced FOXP3 showed a significant increase in *ErbB2* and *SKP2* transcripts. However, the level of *MYC* was not significantly increased. Because the potential of FOXP3 to directly repress *MYC* has only been demonstrated for prostate epithelia (Wang, Liu et al. 2009) and glioblastoma cells (Frattini, Pisati et al. 2012) it is possible that FOXP3 does not influence *MYC* in breast epithelia as potently as it does in other epithelial cells. In addition to this, FOXP3 knockdown failed to cause a significant decrease in *CDKN1A* transcripts (p=0.0534), however, a clear trend was observed. FOXP3 knockdown in HMEpC also resulted in a significant increase in *CXCR4* transcripts (p=0.0479). Although, in a similar manner to the changes witnessed after FOXP3-overexpression in MDA-MB-231, the magnitude of the increase observed and reproducibility was not as compelling as the effects witnessed in other FOXP3 target genes. This again supports the theory that FOXP3 may not directly influence *CXCR4* expression.

Following FOXP3 knockdown, there was no significant change in level of CXCR4 protein in comparison to HMEpC transfected with control siRNA sequences.

Although the changes of *CXCR4* at a transcript level were significant, the changes were not large which could explain the lack of significant changes observed at a protein level.

It is known that MDA-MB-231 are extremely motile and invasive in response to CXCL12 both *in vivo* and *in vitro*, whereas their normal HMEpC counterparts are incapable of these actions (Muller, Homey et al. 2001). MDA-MB-231 were capable of penetrating matrigel coated membranes using *in vitro* invasion assays, however the extent of invasion was not as great as reported in other studies (Muller, Homey et al. 2001). Some reports use MDA-MB-231 as positive controls for invasion (Muller, Homey et al. 2001). However, in this study, concentrations of up to 75nM of chemokine, and incubation periods of 72 hours were required before MDA-MB-231 significantly invaded.

On the other hand, migration assays using MDA-MB-231 demonstrated they potently responded, and migrated towards 12nM of CXCL12 after 16 hours. In accordance with the literature, HMEpC did not migrate or invade in response to CXCL12. On the contrary, although results from flow cytometry suggested no CXCR4 expression was present on wild type and control siRNA transfected HMEpC, the results using the cytometric beads suggested that HMEpC did have CXCR4 present on the cell surface. This would suggest that, perhaps, either the number of CXCR4 detected is too low to respond to CXCL12, or, the CXCR4 receptors present on the cell surface are not functionally active.

FOXP3 knockdown was unable to create an invasive phenotype in HMEpC. However, after doubling the period of incubation and the concentration of CXCL12 from the optimised protocol, it did significantly increase the migratory potential of HMEpC. Interestingly, although FOXP3 knockdown increased the migratory response in HMEpC when the levels of CXCL12 were doubled, there was also an observable increase in the background motility of these cells, as well as an increase in the migration of cells transfected with control siRNA. The cytometric bead assay suggested that HMEpC transfected with control siRNA also had increased levels of CXCR4.

Two aspects must be considered when determining the validity of these findings. Firstly, control siRNA primer sequences used were unknown. Firstly, these were purchased from Ambion who do not allow their control siRNA primer sequences to be released. Despite these sequences not affecting FOXP3 expression, we cannot rule out the possibility that these primers do bind elsewhere in the genome and the increase in CXCR4 may be the result of indirect off-target binding of control siRNA. Secondly, it is well reported, and discussed in this report (section 1.6.3.2), that CXCR4 can be influenced from factors within cells, such as HER2 (Li, Pan et al. 2004) and NF- κ B (Helbig, Christopherson et al. 2003), but also factors within the microenvironment, such as hypoxia and various stress inducing elements (Schioppa, Uranchimeg et al. 2003; Ishikawa, Nakashiro et al. 2009). Therefore, it should also be considered that treatment with a cytotoxic transfection reagent, such as siPORT, may induce cellular stress and increase CXCR4 expression in response to this reagent.

Taken together, this data suggests that although the cells may be responding to the CXCR4 ligand, CXCL12, firstly, an increase in CXCR4 may not be due to FOXP3 knockdown, and secondly, an increase in CXCR4 may not be the sole reason for the increase in migration. In fact, previous studies have shown that FOXP3 knockdown is associated with increased migration of ovarian epithelial cells, whereas FOXP3-overexpression can reduce migration of glioblastoma in the absence of chemokines (Zhang and Sun 2010; Frattini, Pisati et al. 2012). This suggests that FOXP3 is able to regulate the general motility of cells. Indeed, this study and other reports have provided strong evidence suggesting that FOXP3 knockdown is able to increase the expression of certain oncogenes such as *HER2*, *SKP2* and *MYC*. Interestingly, all these factors have been demonstrated to increase the migration of cells (Wolf-Yadlin, Kumar et al. 2006; Wang, Wu et al. 2009; Alfano, Votta et al. 2010; Johnson, Seachrist et al. 2010; Inuzuka, Gao et al. 2012; Liu, Radisky et al. 2012; Zhang, Ji et al. 2013; Zhao, Jian et al. 2013)..

In addition to this, although they were not investigated in this study, FOXP3 has been demonstrated to repress the expression of *MMP2* (Zhang and Sun 2010), *MMP9* (Zhang and Sun 2010; Nakahira, Morita et al. 2013), *LATS2* (Li, Wang et al. 2011) and *VEGFA* (Nakahira, Morita et al. 2013), as well as NF- κ B and mTOR signalling (Zhang and Sun 2010) in cancer cells. Interestingly, all of these factors

have been frequently reported to be involved in regulating the migration and invasion of cancer cells and the role these factors may also play should not be easily dismissed (Rak, Mitsuhashi et al. 1995; Andela, Schwarz et al. 2000; Chang and Karin 2001; Zhang, Rodriguez-Aznar et al. 2012; An, Kang et al. 2013; Nakahira, Morita et al. 2013).

4.7 Conclusion

FOXP3 is a transcription factor recently implicated in a number of malignancies where it is able to influence not only oncogene expression but also cell proliferation, migration and invasion of breast, prostate, ovarian cancers and glioblastomas (Zuo, Liu et al. 2007; Zuo, Wang et al. 2007; Liu, Wang et al. 2009; Wang, Liu et al. 2009; Zhang and Sun 2010; Li, Wang et al. 2011; Frattini, Pisati et al. 2012; Li, Katoh et al. 2013). On the other hand, the profound importance of CXCR4 in driving breast cancer is well documented within the literature (Muller, Homey et al. 2001; Luker and Luker 2006).

The aim of this chapter was to investigate the effects that FOXP3 has in a breast cancer cell line and also a normal mammary epithelial cell line using *in vitro* models. In line with the literature, data in this study suggests that FOXP3 is able to regulate the expression of *ErbB2*, *SKP2*, *c-MYC* and *CDKN1A*. Findings from this study are consistent with existing literature and suggest that FOXP3 may play a role in limiting the proliferation and migration of normal mammary cells, thereby preventing breast cancer progression. However, it should also be noted that these effects are most likely not driven by a single molecule and are probably due to an accumulation of changes involving FOXP3.

FOXP3 has already been reported to act on oncogenes which are implicated in cell proliferation, migration, and invasion, however, the effects on CXCR4 are unreported. Data suggests that FOXP3 may be able to influence the expression of *CXCR4* at low levels. However, in comparison to the effects witnessed in oncogenes already reported as direct FOXP3 target genes, due to the reproducibility and magnitude of the changes regarding this aspect of the study, they suggest that *CXCR4* may not be directly influenced by FOXP3, and more likely to be a consequence of other factors affected by alternative signalling pathways involved with FOXP3. On the other hand, several potential mechanisms do exist within the literature which proposes how FOXP3 may be able to influence the expression of *CXCR4* through the actions of other molecules. This is discussed further in chapter 6.

After investigating the influence of FOXP3 *in vitro*, the transcript and protein levels of FOXP3 and CXCR4 within breast cancer patients of opposing lymph node involvement will be investigated in the next chapter.

	Chapter
General introduction	1
General materials and methods	2
Study of FOXP3 expression in normal and malignant breast cell lines	3
<i>In vitro</i> modelling of FOXP3 expression in normal and malignant breast cell lines	4
<i>In vivo</i> levels of FOXP3 and CXCR4 expression in breast cancer samples	5
Discussion	6
List of references	7
Appendices	8

5 *In vivo* levels of FOXP3 and CXCR4 expression in breast cancer patient samples

5.1 Introduction

Several studies have investigated the expression of FOXP3 within breast cancer patients. Although the majority of studies have reported a dysregulation of FOXP3 expression in cancer (Chen, Chen et al. 2008; Merlo, Casalini et al. 2009; Wang, Liu et al. 2009), there remains a degree of ambiguity. For instance, Hinz et al (Hinz, Pagerols-Raluy et al. 2007) reported a lack of FOXP3 in normal pancreatic cells, but a marked increase in the malignant counterparts. A similar study by Ebert et al (Ebert, Tan et al. 2008) reported that FOXP3 was present within melanoma cells but not in normal melanocytes, whilst a recent study by Lal et al (Lal, Chan et al. 2013) described an increase in epithelial cell FOXP3 as breast cancer progresses.

Although the involvement of FOXP3 in epithelial cells and carcinogenesis is a relatively new area of cancer research, the involvement of CXCR4 is much more defined as it is consistently upregulated in a number of malignancies, including breast cancer (Muller, Homey et al. 2001; Luker and Luker 2006; Mukherjee and Zhao 2013), melanoma (Kim, Koh et al. 2010; O'Boyle, Swidenbank et al. 2013), ovarian cancer (Ray, Lewin et al. 2011; Wang, Cai et al. 2011), and prostate cancer (Gladson and Welch 2008).

Although CXCR4 and FOXP3 have been investigated either individually, or in correlation with other proteins, their expression has never been investigated simultaneously in the same study.

5.1.1 Tumour microenvironment

Many diseases which produce chronic inflammation are associated with a high risk of cancer. Tumours not only contain cancer cells, but also a wide variety of other cell types including stromal cells, fibroblasts, endothelial cells and most importantly,

inflammatory cells (Balkwill and Mantovani 2001; Coussens and Werb 2002). Experimental, clinical and epidemiological studies have revealed that malignant tumours not only exist at sites of chronic inflammation, but inflammation also contributes to cancer progression. The first link between cancer and inflammation was observed approximately 150 years ago by Rudolf Virchow (Balkwill and Mantovani 2001) who reported that many cancers tend to occur at sites which are in states of chronic inflammation. Inflammatory breast cancer is one of the most aggressive forms of breast cancer and is characterised by very high levels of inflammation. Inflammatory cytokines such as TNF- α , IL-1, and chemokines such as CCL2 and CXCL8 are key mediators in tissue remodelling and neo-angiogenesis (Conti and Rollins 2004; Condeelis and Pollard 2006; Varney, Johansson et al. 2006) in cancer.

There are many components that contribute to a tumours growth, invasion and metastasis. These include the extracellular matrix, fibroblasts, endothelial cells, inflammatory cells and a network of chemokines and promoters of angiogenesis (Ali and Lazennec 2007; Harvey, Mellor et al. 2007; Mellor, Harvey et al. 2007). Reports indicate that TAMs are key regulators involved in the link between inflammation and cancer (Leek and Harris 2002; Medrek, Ponten et al. 2012; Quatromoni and Eruslanov 2012).

The importance of macrophages in the tumour microenvironment is well documented as they are one of the predominate leukocytes in the tumour mass (Balkwill, Charles et al. 2005). Macrophages play an indispensable role in innate and adaptive immunity. They are activated by a number of stimuli which allows them to differentiate into multiple subtypes displaying various phenotypes which are dependent on the microenvironment. Two main states of polarised activation for macrophages have been described: the classically activated M1 macrophage and the alternatively activated M2 macrophage. M1 macrophages are activated following stimulation with IFN- γ , a number of cytokines and TNF- α . Once activated, these cells then secrete high levels of IL-12 and IL-23, but low levels of IL-10 (Gordon and Taylor 2005; Mantovani, Sica et al. 2005; Solinas, Germano et al. 2009). On the other hand, once M2 macrophages are activated by secrete high levels of IL-10 and low levels of IL-12 and IL-23 (Mantovani, Sica et al. 2005; Solinas, Germano et al. 2009).

Mainly because of their opposing cytokine profiles, the phenotypes of the polarized macrophages are reported to have differing roles within the cancer environment and tumour growth. Because the classically activated M1 macrophages express a number of pro-inflammatory cytokines, this allows them to act in an anti-tumour manner, whereas, the majority of TAMs exhibit M2 phenotypes which express a variety of anti-inflammatory molecules. These M2 macrophages are now associated with a worse prognosis as they provide an immunosuppressive environment for the tumour to grow. Moreover, TAM infiltration has been linked to the interaction with cancer-stem cells leading to not only tumorigenesis and metastasis, but also drug resistance and increased risk of relapse (Rosen and Jordan 2009).

Despite the importance of macrophages in the inflammatory environment, research has also suggested that they do not work alone and other infiltrating leukocytes including neutrophils, mast cells, eosinophils and activated T-cells also release chemokines, proteases and angiogenic factors which contribute to malignancy (Coussens, Raymond et al. 1999; Coussens, Tinkle et al. 2000; Di Carlo, Forni et al. 2001).

5.1.1.1 T-cell infiltration

Infiltration of lymphocytes around the tumour is the main contributor to chronic inflammation. These cells may be recruited to the region with the intention of combating tumour cells.

Interestingly, the specific subtype of these T-cells is thought to be important in predicting patient survival. Breast cancer patients with high levels of CD4⁺ and/or CD8⁺ T-cells within the tumour have a better outcome as they are responsible for the production of IFN- γ (Mahmoud, Paish et al. 2011; Liu, Lachapelle et al. 2012; Gu-Trantien, Loi et al. 2013). On the other hand, alternative reports have also suggested that some patients with high levels of CD4⁺ and CD8⁺ T-cell infiltration have a worse overall survival (Matkowski, Gisterek et al. 2009).

The immunoregulatory CD3⁺CD4⁺CD25^{hi} subset, Tregs, are the body's main peripheral defence. Tregs are responsible for suppressing the actions of autoreactive T-cells within the peripheral blood. These cells are often reported to be significantly

more abundant in the peripheral blood of cancer patients than healthy individuals (Liyanage, Moore et al. 2002; Ye, Ma et al. 2013). In particular, Tregs are most commonly found around lymphoid-rich areas around tumours (Mizukami, Kono et al. 2008). This is thought to be a mechanism of immune evasion and, as a result, is associated with an unfavourable clinical prognosis (Hinz, Pagerols-Raluy et al. 2007; Mohos, Sebestyen et al. 2013; Sisirak, Faget et al. 2013). Although the majority of reports suggest a strong link between Tregs and a poor patient survival, an alternative study opposed this theory and suggested that cancer patients have fewer Tregs than healthy individuals (Okita, Saeki et al. 2005).

The exact mechanism responsible for the infiltration of Tregs into the tumour environment is unknown. However, several plausible theories have been described and reviewed by Zou (Zou 2006). Tregs are known to express CCR4, whereas, tumour cells and TAMs have been shown to secrete the CCR4 ligand, CCL22 (Curiel, Coukos et al. 2004; Miller, Lundberg et al. 2006). Therefore, the chemokine-chemokine receptor axis of CCR4/CCL22 could provide a mechanism of Tregs homing to tumour environment. Another theory is that the high levels of TGF- β present within tumours could contribute to the conversion of CD4⁺ T-cells into induced Tregs (Zou 2006). A similar scenario has been reported by Dumitriu et al (Dumitriu, Dunbar et al. 2009) who reported that human lung cancer cell lines can prompt dendritic cells to release TGF- β which subsequently transformed CD4⁺ T-cells into Tregs.

5.1.2 Breast cancer classification

At the time of diagnosis, breast cancer is divided into several categories which define the stage of the tumour, the grade of the tumour, and whether the tumour cells overexpress specific growth factor and hormone receptors.

The aim of this classification is to describe each individual case in order to select the most appropriate treatment.

5.1.2.1 Tumour grade

The tumour grade is often assessed using a light microscope. The pathologist examines the appearance of malignant cells in comparison to normal healthy cells. Tumours are graded as follows; if the cells are well differentiated and still resemble normal cells, they are considered as low grade (grade I). If the cells are moderately differentiated, they are considered as intermediate grade (grade II) and if the cells are poorly differentiated they are considered to be high grade (grade III). Higher grades suggest a worse prognosis because undifferentiated cells divide more rapidly and have an increased risk of metastasis, whereas, low grade tumour cells closely resemble healthy cells and grow more slowly (Hatteville, Mahe et al. 2002).

The grade is calculated on three criteria (Hatteville, Mahe et al. 2002); tubule formation, nuclear pleomorphism, and the frequency of mitosis. Each of these criteria is scored between one and three points and the final score is the sum of the individual scores (**table 5.1**). Each criterion is discussed briefly below:

Tubule formation: During tumorigenesis the tissue structures, such as the tubules, become less orderly as the cancer breaks down mechanisms the cells use to attach to each other. Points in this parameter are defined by the percentage of the tumour forming normal duct structures. If the tumour has more than 75% tubule formation it is scored one point. If tubule formation is between 10-75% of the tumour it is scored two points, and if tubule formation is less than 10%, three points are scored.

Nuclear pleomorphism: A common trait of cancer is dysregulated control over various genes. These changes can often result in irregularities in the appearance of the nucleus which becomes larger and darker. The pathologist scores this parameter by the appearance of the tumour cells nuclei in comparison to that of normal healthy cells. A minimal change in the size and shape of the nuclei is scored one point, moderate changes are scored two points, whereas, marked variations are scored three points. The more pleomorphic the nuclei, the worse the prognosis.

Mitotic frequency: As previously described in section 1.4.3, one of the hallmarks of cancer cells is the ability to divide uncontrollably. The final parameter the pathologist scores is the number of dividing cells in a specific number of microscopic fields of view (depending on the microscope used). The scoring system

described below is based on the Leitz Ortholux microscope at x25 magnification. 0-9 mitotic counts are scored 1 point. Mitotic counts between 10 and 19 are scored 2 points, whereas more than 19 mitotic counts are scored 3 points.

Grade	Points range
Grade I	3 – 5 points
Grade II	6 – 7 points
Grade III	8– 9 points

Table 5-1 - Scoring system used for tumour grading

Breast tumours are scored by calculating total points regarding tubular formation, nuclear pleomorphism and mitotic frequency when assessing tumour. The total points from each category are combined and the points range can define the tumour as a specific grade.

5.1.2.2 Tumour stage

When pathologists stage breast cancer, they determine the size of the tumour and whether it has spread or not. Determination of the stage of cancer once again helps the specialist decide on the best course of treatment for the patient.

Once the stage has been assessed, clinicians use a formula called the Nottingham prognostic index (NPI) to help predict the effectiveness of the treatment.

$$NPI = (0.2 \times \text{Tumour diameter size [cm]}) + \text{Lymph node stage} + \text{Tumour grade}$$

This formula was originally devised in 1982 (Haybittle, Blamey et al. 1982) and revised ten years later (Galea, Blamey et al. 1992); however, treatments have continued to improve so the true implication of this index is often questioned. After calculating the NPI, patients are subcategorised into four groups. This helps to predict the prognosis of the patient. The four subcategories are summarised in **table 5.2**.

Breast cancer is most commonly staged using the TNM system which takes into account the tumour size (**T**-tumour), whether the lymph nodes are involved (**N**-node) and finally whether the tumour has spread beyond the lymph nodes to any other regions in the body (**M**-metastases). **Table 5.3** summarises a slightly simplified version of the TNM system (Singletary and Greene 2003).

NPI category (based on calculated prognosis)	NPI score
Excellent	Equal to or less than 2.4
Good	From 2.5 - 3.4
Moderate	3.5 - 5.4
Poor	Greater than 5.5

Table 5-2 - Table for Nottingham prognostic index ranges

The NPI is a system utilising a calculation based on the tumour size, grade and lymph node status to predict the prognosis of a patient.

A

Tumour status (T)	Description
Tx	Tumour cannot be assessed
T0	No evidence of primary tumour
Tis	Tumour <i>in situ</i> . This can also refer to Paget's disease with no tumour mass
T1	Tumour smaller than 2cm in size
T2	Tumour between 2-5cm in size
T3	Tumour greater than 5cm in size
T4	Tumour is affecting chest wall and skin. Inflammatory cancer can also be scored T4

B

Lymph node status (N)	Description
Nx	Lymph node cannot be assessed
N0	No regional lymph nodes involved
N1	Between 1-3 regional lymph nodes involved
N2	Between 4-9 regional lymph nodes
N3	More than 10 lymph nodes involved

C

Metastasis (M)	Description
Mx	Presence of distant metastasis cannot be assessed
M0	No distant metastasis detected
M1	Presence of distant metastasis

D

Stage	Sub-stage	Definition by TNM score				
0	-	Tis, N0, M0	-	-	-	-
I	-	T1, N0, M0	-	-	-	-
II	IIa	T0, N1, M0	T1, N1, M0	T2, N0, M0	-	-
	IIb	T2, N1, M0	T3, N0, M0	-	-	-
III	IIIa	T0, N2, M0	T1, N2, M0	T2, N2, M0	T3, N1, M0	T3, N2, M0
	IIIb	T4, N0, M0	T4, N1, M0	T4, N2, M0	-	-
	IIIc	Any T, N3, M0	-	-	-	-
IV	-	Any T, any N, M1	-	-	-	-

Table 5-3 - Classification of the tumour-node-metastasis (TNM) system

Pathologists diagnose tumours relying on the size of the tumour (T), the number of lymph nodes which are involved (N) and whether the tumour has metastasised to distant sites (M). Table (A) demonstrates the criteria for the scoring of the tumour size. Table (B) demonstrates the criteria for scoring the number of lymph nodes involved. Table (C) demonstrates the criteria for scoring the presence of metastases. **Table D** demonstrates possible combinations from the TNM score and the stage of the tumour (Singletary and Greene 2003).

5.2 Aims and objectives

- Measure the transcript and protein levels of CXCR4 and FOXP3 from epithelial cells within breast cancer samples from lymph node negative, lymph node positive patients and sections from normal tissue.

- Investigate the potential correlation between the expression of FOXP3 and CXCR4 in breast cancer samples.

- Investigate the potential prognostic implications of FOXP3 and CXCR4 expression in breast cancer samples.

5.3 Specific materials and methods

5.3.1 Ethical approval

Ethical approval for the use of paraffin-embedded and frozen human breast tissue sections were submitted to the Newcastle and North Tyneside Local Research Ethics Committee. Approval was granted for the use of anonymised paraffin-embedded sections (REC reference number: 06/Q0906/12) and the use of anonymised frozen tissue for RNA isolation in the study (REC reference number: 10/H0906/26).

5.3.2 Selection of patient samples

Breast cancer samples, isolated at the Queen Elizabeth (QE) Hospital (Gateshead, UK) were selected based on the patient's lymph node involvement and NPI score. Ten patients were selected with no nodal involvement (referred to as LN-negative) and, and nine patients with high nodal involvement (referred to as LN-positive). All samples were derived from patients with IDC of NST. In addition, tissues from two separate patients who had undergone breast reduction surgery were used as normal breast tissue (referred to as normal #1 and normal #2). To ensure patient anonymity, the ten LN-negative breast cancer patients were referred to as cases #1 to #10, whereas, the nine LN-positive patients were referred to as cases #11 to #19. The details of individual breast cancer patients selected, including the lymph node status (and percentage positivity), the NPI, the date of the operation and the post-operative follow up status' are included in **table 5.4**.

All frozen tumour samples were stored at -80°C in accordance with the Human Tissue Act (HTA). Frozen tumours were used for RNA isolation, whereas, the matched paraffin-embedded sections were used for IHC.

It should also be noted that three LN-negative paraffin tissue samples (cases #1, #5 and #8) had previously been used by the QE Hospital as control material and were not available to be stained using IHC. This information was discovered late in the study and alternative tissues were not able to be selected in time. Therefore, only seven LN-negative tissues were investigated using IHC.

A

Patient number	Lymph node involvement	NPI	Date of operation	Post-op follow up status
#1	0/7	3.23 (Good)	2005	Alive and well (Discharged 2010)
#2	0/10	3.36 (Good)	1998	Alive and well (Discharged -2007)
#3	0/8	3.3 (Good)	1998	Alive and well (Discharged -2003)
#4	0/12	3.3 (Good)	1998	Deceased Liver mets (2010)
#5	0/5	3.3 (Good)	2005	Alive and well (Discharged - 2010)
#6	0/4	3.12 (Good)	1997	Alive and well (Discharged - 2004)
#7	0/7	3.28 (Good)	2005	Alive but suffering metastasis (2013)
#8	0/6	3.2 (Good)	2005	Alive and well (Discharged - 2010)
#9	0/8	3.4 (Moderate)	2004	Alive and well (Discharged - 2010)
#10	0/13	3.22 (Good)	2001	Alive and well (Discharged - 2006)

B

Patient number	Lymph node involvement (%)	NPI	Date of operation	Post-op follow up status
#11	13/16 (81%)	N/A	1996	Deceased - 1997
#12	7/8 (88%)	6.6 (Poor)	1998	Deceased - 2000
#13	10/12 (83%)	7.2 (Poor)	1999	Alive and well (2013)
#14	20+	5.5 (Poor)	1998	Deceased - 1998
#15	5/5 (100%)	5.3 (Moderate)	2000	Deceased - 2009
#16	18	6.8 (Poor)	1998	Deceased - 1999
#17	22/22 (100%)	6.6 (Poor)	1999	Deceased - 2005
#18	8/13 (61%)	5.5 (Poor)	1998	Deceased - 1998
#19	13/14 (92%)	5.5 (Poor)	2000	Deceased - 2000

Table 5-4 - Patient histories of selected breast cancer samples

Details of breast cancer samples from LN-negative patients (A) and LN-positive patients (B)

5.3.3 RNA isolation from frozen patient samples using GentleMACS™ dissociator

The GentleMACS™ dissociator (Milentyi Biotec, Surrey, UK) is an automated bench top instrument (**figure 5.1 panel A**) used to dissociate tissues into single cell suspensions using a number of specific pre-optimised applications. This instrument was used to dissociate frozen tissue sections for flow cytometric analysis and RNA isolation.

Prior to dissociation, tissues were weighed and partially thawed on ice. Tissues to be used for flow cytometry or to be used with RNeasy spin columns (QIAGEN) were thawed in 2ml of basal DMEM media with 100µg/ml DNase (Sigma-Aldrich), whereas, tissues to be used with TRI reagent were homogenised in 2ml of TRI reagent. Whilst thawing at room temperature in media, the tissues were cut into small sections using fresh sterile scalpels for each section. This prevents the machine from becoming blocked due to the size of the sections. The sections and media were then dispensed into C-tubes (Miltenyi Biotec) and placed into the GentleMACS™ dissociator and homogenised using program (H_Tumour RNA). After dissociation, the homogenised tissue was strained through a 40µm filter and dispensed into appropriate tubes (depending on experiment to be continued with) and washed in PBS by centrifugation at 500xg. After centrifugation the supernatant was removed and cell pellet was used for future experiments.

5.3.4 RNeasy mini spin columns

RNeasy (QIAGEN) is a silica-based column method of isolating RNA from cells or tissue sections. After the initial homogenisation described in section 5.3.3, cells were dispensed into 1.5ml Eppendorf tubes and centrifuged to pellet. The cells were lysed by the addition of 1ml buffer RLT and vortexed. Next, 500µl of 70% ethanol was added and mixed by pipetting. The mixture was dispensed into an RNeasy mini spin column 700µl at a time. The column was centrifuged for 15 seconds at 8000xg and the flow through was discarded. 700µl of buffer RW1 was added to the spin column and centrifuged for 15 seconds at 8000xg. The flow-through was discarded and the column was washed twice in buffer RPE at 8000xg, firstly for 15 seconds, followed

by a 2 minute spin. Finally, the RNeasy spin column was placed into a fresh, sterile, 1.5ml collection tube and RNA was eluted from the column by the addition of 50µl RNase-free water and centrifuged for 1 minute at 8000xg

5.3.5 IHC staining of breast tissue

IHC is a technique used in laboratories for localisation of proteins in tissue sections using specific primary antibodies directed against the antigen. Once the antibody is bound, it is visualised using a coloured reaction which is observable by light microscope.

Direct methods of IHC are when the primary antibody itself carries the signal generating molecules that provide the method of visualisation. However, the most common methods of IHC are indirect. These methods require additional steps to locate the antigen-bound primary antibody and subsequently generate the signal.

5.3.5.1 CD3 and CXCR4 staining

All CD3 and CXCR4 staining was performed by senior biomedical scientist, Ms Denise Woolley, within the Pathology Department within QE Hospital. All staining was performed using the autostainer link 48 (DAKO, Cambridge, UK) (**figure 5.1 panel B**) with the EnVision™ FLEX⁺ mouse detection kit (DAKO). All equipment described in this section was provided by DAKO unless specified. The procedure used to stain the slides can be broken down into the following subsections: Dewaxing of sections, antigen retrieval, and finally, the automated staining protocol. These are described in the following paragraphs.

Dewaxing: Paraffin-embedded breast tissue on slides were dewaxed by submerging in xylene for 5 minutes, followed by rehydrating the tissues by passing through decreasing levels of ethanol (100%-90%-75%-50%). Sections were then placed into water to remove xylene and ethanol from slides.

Antigen retrieval: Antigen retrieval was performed using the PT-Link (DAKO) (**figure 5.1 panel C**) with a 1:50 ratio of EnVision™ FLEX Target Retrieval

Solution (High pH) with distilled water. The pre-treatment solution was heated to 65°C in the PT-link, then slides were placed into the solution and incubated for 40 minutes at 97°C. Slides were cooled back to 65°C in the PT-link and washed in EnVision™ FLEX wash buffer for 5 minutes before being loaded into the autostainer link 48 for staining.

Staining protocol: CD3 and CXCR4 staining was carried using the following automated protocol. Primary antibodies were diluted in EnVision™ FLEX antibody diluent. All steps were performed at room temperature, whereas, all wash steps were performed using the EnVision™ FLEX wash buffer (prepared using a 1:20 ratio with deionised water). Slides were washed in buffer for 5 minutes before the addition of 200µl EnVision™ FLEX Peroxidase-Blocking Reagent for 15 minutes. Slides were washed in buffer for 20 minutes before being treated with 200µl of solution containing specific dilutions of primary antibody (anti-CXCR4/anti-CD3) + FLEX for 50 minutes. CD3 staining is regarded as an “in-house” stain within pathology departments and is frequently used so did not require optimising (1:150 dilution). However, because CXCR4 staining required optimising, the antibody dilutions varied between tests. For this reason, the specific antibody dilution used is described within the appropriate figure legends. Slides were washed in buffer and received 200µl of EnVision™ FLEX⁺ mouse secondary antibody for 15 minutes. The slides were washed again, before 200µl of EnVision™ FLEX/HRP was added and left to incubate for 20 minutes. The slides were washed twice in buffer for 20 minutes before having 200µl of the substrate working solution added and left to incubate for 10 minutes. The slides were washed for 20 minutes in buffer before being counter-stained in 200µl EnVision™ FLEX Haematoxylin for 5 minutes. Slides received two final 15 minute washes before being passed through increasing amount of alcohol (50%-75%-90%-100%) to dehydrate slides before being mounted in DPX. Slides were left to air dry for 2-3 hours before being viewed.

5.3.5.2 FOXP3 staining

FOXP3 staining was attempted using two automated staining protocols (which were amended appropriately), and one pre-optimised protocol used by previous members of this group. Each is described below:

All FOXP3 staining was carried out by Ms Denise Woolley within the Pathology Department in the QE Hospital using the same protocol as described in section 5.3.5.1. Antibody dilutions required optimising, therefore, the specific antibody dilution used in each test is described in the figure legend.

FOXP3 staining was also performed by specialist biomedical scientist, Ms Anna Long, within the Pathology Department in the Royal Victoria Infirmary (RVI) (Newcastle-Upon-Tyne, UK). All steps were performed using the BenchMark ULTRA (Ventana, Tucson, AZ, USA) (**figure 5.1 panel D**), with all equipment described in this section provided by Ventana unless stated.

A number of protocols were attempted using Ventana machines, including two separate detection kits, three antigen retrieval methods and a range of antibody dilutions. Each detection kit and antigen retrieval method is described below and the conditions used in each test are described within the figure legends.

Dewaxing: Slides stained within the RVI were dewaxed using EZ prep solution by pre-heating slides to 72°C for 4 minutes followed by 3 washes, where EZ prep solution was applied for 4 minutes, rinsed off and reapplied.

Antigen retrieval: Antigen retrieval using the cell conditioning solutions were performed using the BenchMark ULTRA. Cell conditioning-1 is a high pH solution (set at pH 8.0), whereas, cell conditioning-2 is a low pH solution (set at pH6.0). Antigen retrieval was carried out according to the manufacturers protocol. Briefly, slides were warmed to 95°C and incubated in the appropriate cell conditioning solution for total of 1 hour with fresh solution being added approximately every 15 minutes.

Retrieval was also attempted manually with a pressure cooker using Tris/EDTA (pH9.0) and citrate (pH6.0) buffers. Briefly, the temperature of the pressure cooker was heated to 65°C, followed by the addition of the slides which were incubated for 1 minute when the cooker reached 100°C. The cooker was then cooled back down to 65°C before being cooled rapidly in water. Following retrieval, staining was commenced.

Detection kits and staining protocols: The optiview and *ultra*VIEW detection kits were used in the FOXP3 staining in this study. Both kits are compatible for use with

the BenchMark ULTRA and are indirect, biotin-free systems for detecting primary antibodies.

The ultraVIEW detection kit, is a 2-step method which uses a cocktail of secondary antibodies conjugated to HRP that locates the primary antibody. The complex of primary and secondary antibody is then visualised by precipitating the enzyme product by the addition of H₂O₂ and 3,3'Diaminobenzidine tetrahydrochloride (DAB) (**figure 5.2**).

The optiview detection kit, is a 3-step method. This technique uses a cocktail of secondary (linker) antibodies to detect the primary antibody, followed by a tertiary antibody which is directly conjugated to HRP. Again, this visualisation is performed by the addition of H₂O₂ and DAB (**figure 5.3**).

Manual FOXP3 staining, was carried by myself using a pre-optimised protocol developed by previous members of the group. FOXP3 staining was performed using the ABC Vectashield mouse staining detection kit (Vector laboratories). This kit utilises avidin-biotinylated peroxidase complexes which then develops DAB into a brown coloured substrate (**figure 5.4**). Because the Avidin-biotinylated peroxidase complexes are stable at room temperature for several hours, these complexes were prepared prior to staining. Complexes were prepared by diluting avidin reagent with the biotinylated peroxidase reagent at a ratio of 1:100 (avidin:biotinylated peroxidase). All wash steps were done with tris-based-saline (TBS) at pH7.6. All steps were performed at room temperature.

Sections were dewaxed as described in section 5.3.5.1. Antigens were retrieved using 1.5L of Tris/EDTA at pH8.0 in the pressure cooker. The pressure cooker was brought to 100°C then slides were incubated for 1 minute before the pan was rapidly cooled in cold water. Slides were removed and staining was commenced. Briefly, sections were washed for 5 minutes before blocking endogenous peroxidase by the addition of a blocking serum for 10 minutes which was provided by the company. This was then replaced with the primary antibody (at a dilution of 1:50 [diluted in TBS]) and incubated for 60 minutes at 4°C. Slides were then washed twice for 5 minutes before being covered in the biotinylated secondary antibody for 30 minutes. 5 minute wash steps were performed twice before the addition of the avidin-biotinylated peroxidase complexes which were then incubated for 30 minutes.

Another two wash steps were performed before the DAB substrate solution was added for approximately 2 minutes before being washed well in water. Slides were then counter stained in haematoxylin for 30 seconds, washed in water, and then washed Scott's tap water to help develop the blue colour. Slides received a final wash in water before being dehydrated through increasing ethanol (50%-75%-90%-100%) and mounted in DPX.

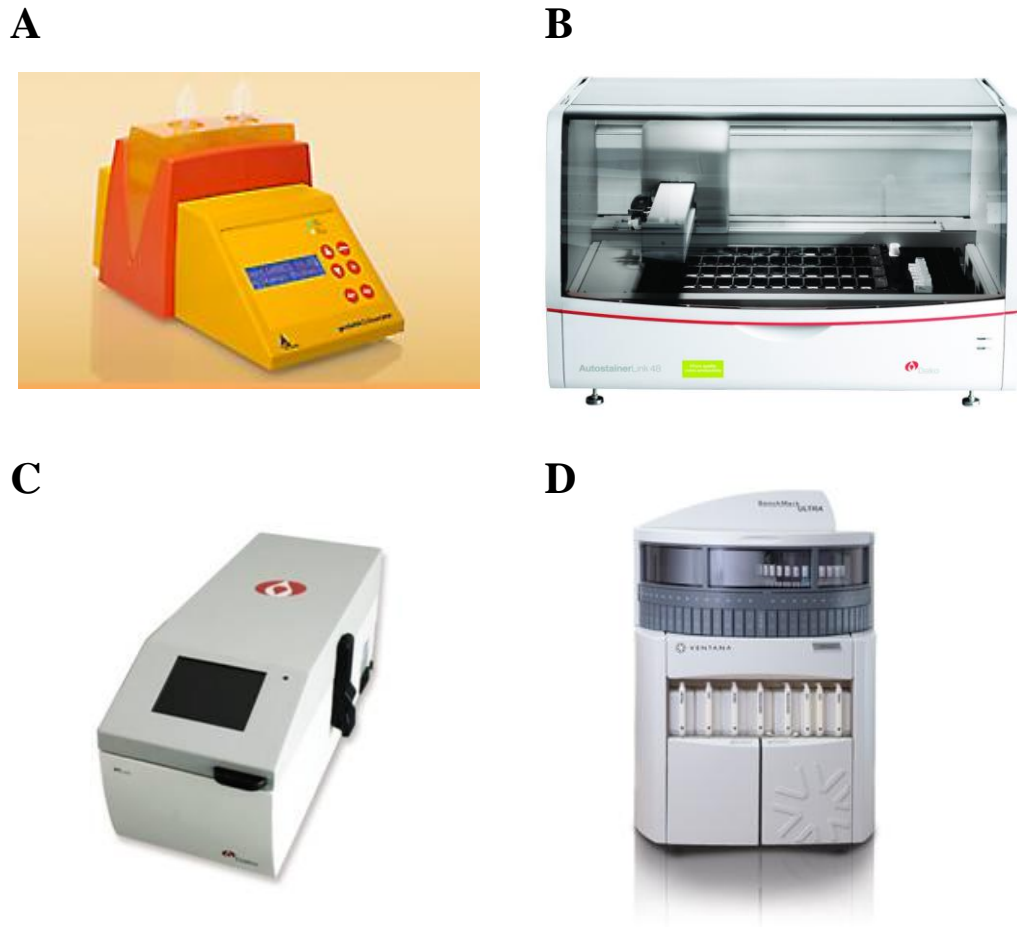


Figure 5-1 - Automated equipment used in frozen tissue homogenisation and paraffin embedded tissue IHC

(A) The GentleMACS™ dissociator was used to dissociate frozen breast tissue sections. (B) The autostainer link 48 was used to stain paraffin embedded tissue for FOXP3, CXCR4, and CD3 in the QE Hospital. (C) The PT link was used to retrieve antigens before IHC in the QE Hospital. (D) The BenchMark ULTRA was used by the RVI Hospital, for antigen retrieval and IHC staining for FOXP3. Images were taken from DAKO and Ventana websites.

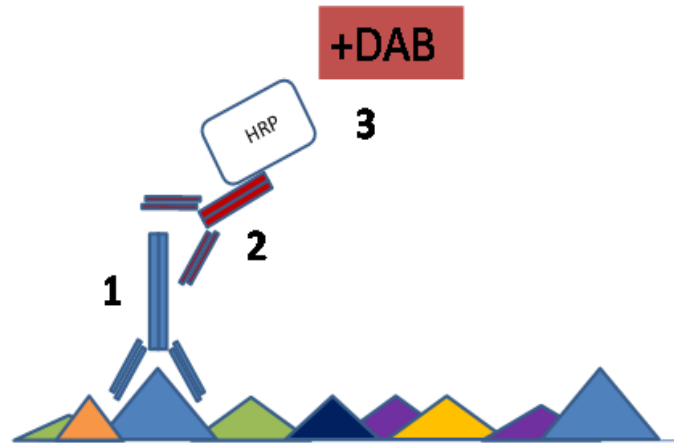


Figure 5-2 - Schematic representation of the *ultra*VIEW detection kit

Following dewaxing and antigen retrieval stages, slides were incubated with a primary antibody specific for the target antigen (1). The primary antibody is then located by the addition of a secondary antibody which is directly conjugated to HRP (2). The complex is then visualised by the addition of H_2O_2 and DAB which produces a brown precipitate which is detectable by light microscopy (3).

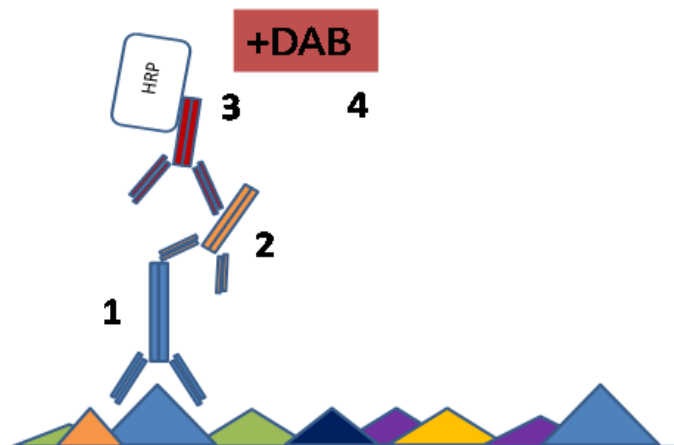


Figure 5-3 - Schematic representation of the optiview detection kit

Following dewaxing and antigen retrieval stages, slides were incubated with a primary antibody specific for the target antigen (1). The primary antibody is then located by the addition of a secondary (linker) antibody (2). A tertiary antibody which is directly conjugated to HRP (3) is added then the complex is then visualised by the addition of H_2O_2 and DAB which produces a brown precipitate which is detectable by light microscopy (4).

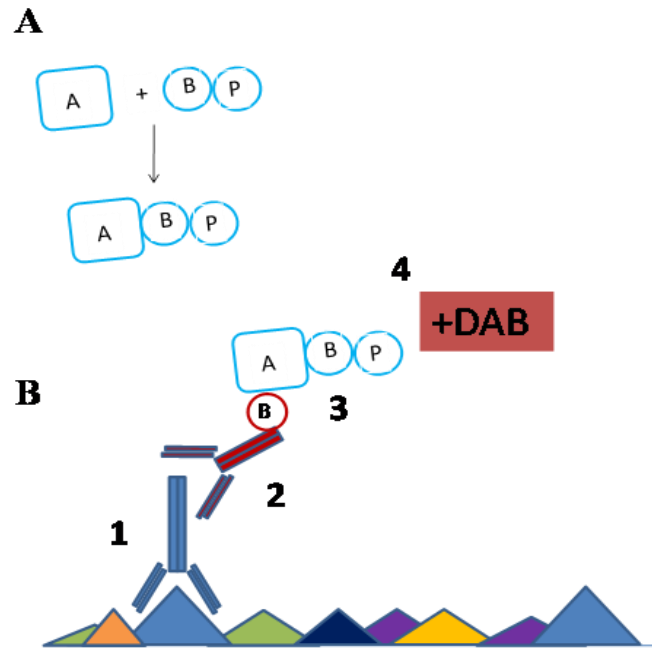


Figure 5-4 - Schematic representation of the ABC Vectashield detection kit

- (A) Prior to staining, the avidin-biotinylated peroxidase complexes were prepared by the addition of avidin (labelled as A) with biotinylated peroxidase (labelled as B-P).
- (B) After the antigen retrieval process, the addition of the primary antibody is able to bind to the specific antigen (1). A biotinylated secondary antibody which has specificity towards the primary antibody is able to locate the antigen (2). Because of the high affinity avidin has towards biotin the addition of the avidin-biotinylated peroxidase complexes (3) is able to bind directly to the secondary antibody. Finally the addition of H_2O_2 and DAB is able to produce a brown colour which is detectable by microscope (4).

5.3.5.3 List of antibodies used for IHC

Antibodies used for IHC staining are provided in **table 5.5**.

5.3.6 Quick score algorithm used for IHC staining

The scoring of patient samples was done blindly by trained pathologist, Dr John Brain (RVI, Newcastle, UK). Scoring used Allred quick score which focuses on the proportion of cells stained (0 = no nuclear staining, 1 = less than 1% nuclear staining, 2 = 1-10% nuclear staining, 3 = 11-33% nuclear staining, 4 = 34-65% nuclear staining, 5 = 66-100% nuclear staining) and the intensity of staining (0 = no staining, 1 = weak staining, 2 = moderate staining, 3 = strong staining). The score for the proportion of cells stained and the score for the intensity of staining were added to get the total score, which ranged from 0 to 8 (Mudduwa 2009).

Antibody target	Clone	Species raised in	Company
Human Anti-FOXP3	259D	Mouse	BioLegend
Human Anti-FOXP3	236A/E7	Mouse	Abcam
Human Anti-CXCR4	44716	Mouse	R&D systems
Human Anti-CD3	F7.2.38	Mouse	DAKO

Table 5-5 - List of antibodies used for IHC

All antibodies used for IHC along with antibody clones, species raised in and the manufacturers.

5.4 Results

5.4.1 Separation of T-cells from frozen breast tumours

As described in section 5.1.1, the tumour microenvironment often contains a large number of infiltrating leukocytes. A relatively high percentage of these T-cells are known to express *FOXP3* and *CXCR4*. Because this study is focused on measuring the levels of *FOXP3* and *CXCR4* derived from epithelial cells within the tumour section, the strategy was developed to exclude infiltrating T-cells by staining with a human anti-CD3 antibody and use FACS.

Because the breast tissues were not fresh and had been frozen for several years, they were not in good condition. To test whether the frozen breast cancer cells could be successfully stained, sections were homogenised into single-cell suspensions using the GentleMACS™ dissociator, then stained with an anti-CD3 antibody and analysed by flow cytometry (**figure 5.5 panel A**). As a positive control, and also to locate CD3⁺ cells on the FACS dot plot, half of the homogenised sample was spiked with PBMC. Tumour samples spiked with PBMC had high levels of CD3⁺ cells, whereas, all of the homogenised breast tumours tested appeared to have less than 6% of CD3⁺ cells (**figure 5.5 panel B**).

Because T-cell infiltration in breast cancer is common, the results suggesting that each breast cancer had very few infiltrating T-cells is most likely not a true reflection of the tumour, but a consequence of poor tissue quality. On this basis, it is more plausible that a combination of the age, condition, and the process of homogenising the tissue left the cells in a state where they could not be adequately stained. Therefore, potential T-cells could not be isolated from the sections using FACS.

To continue the investigation of *CXCR4* and *FOXP3* transcripts in frozen breast tumours, whole tumour sections were analysed and the extent of tumour infiltrating T-cells was determined in each tumour section using real-time PCR with *CD3* specific primers and CD3 IHC on the matched paraffin-embedded sections. This is demonstrated in section 5.4.4.

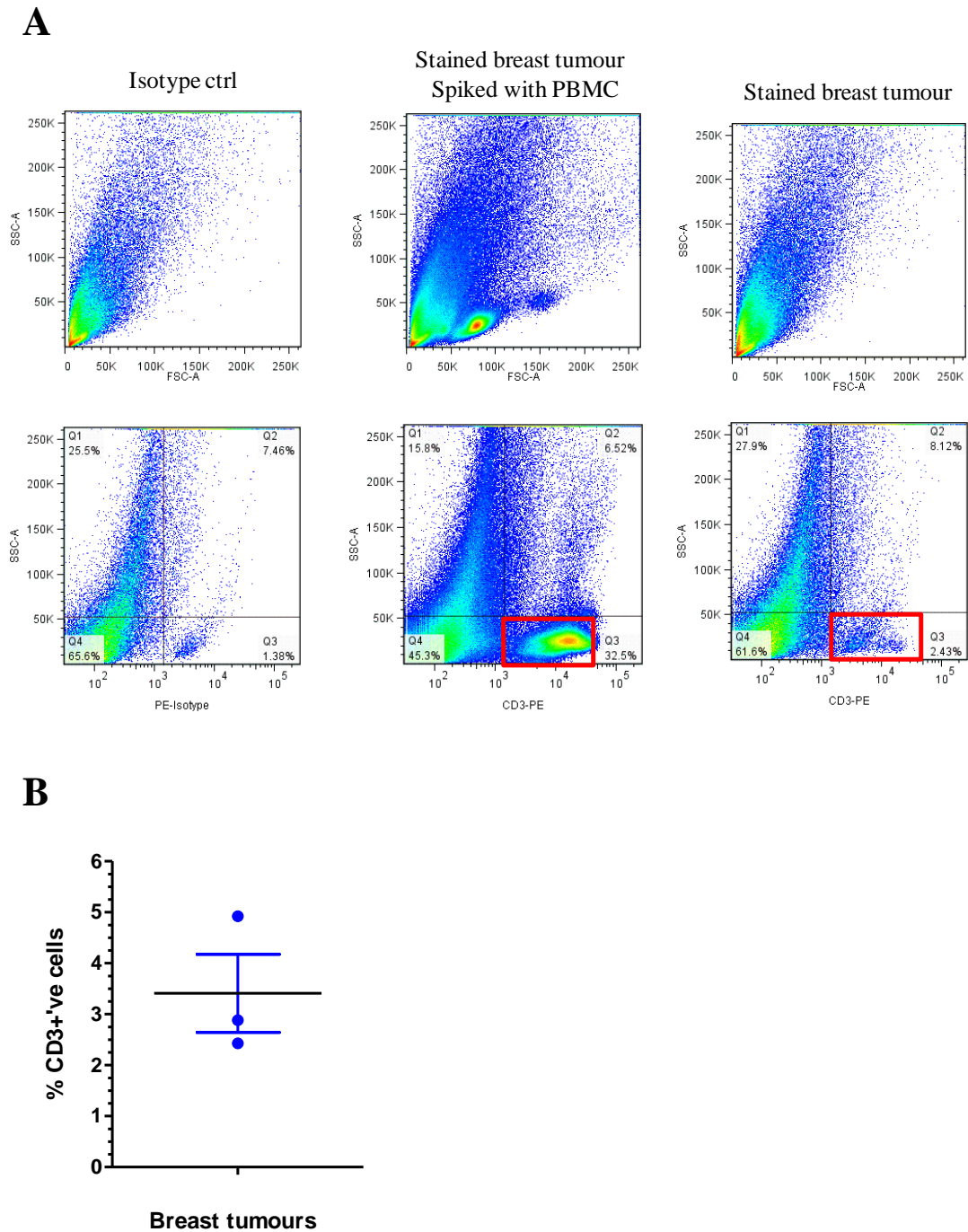


Figure 5-5 – Determination of infiltrating CD3⁺ cells in dissociated breast tumours by flow cytometry

Frozen breast tumours were partially thawed on ice and dissociated in serum free media supplemented with 100µg/ml DNase to reveal a single cell suspension. Cells were strained through 40µm filters and washed 3 times in FACS buffer. Cells were stained with human anti-CD3-PE antibody or an isotype control and analysed by flow cytometry. Red boxes indicate regions of CD3⁺ cells. **Panel A** is a representative image of three experiments. **Panel B** demonstrates the percentage of CD3⁺ cells within each tumour section assessed.

5.4.2 Optimisation of RNA isolation from frozen tumour sections

Isolating good quality RNA from tissue sections is considered by many a difficult prospect, especially when the tissue is not fresh and cell viability is low. In addition to this, since we only had one frozen tumour per patient, RNA isolation could only be attempted once. On this basis, RNA extraction from tumours was practised and optimised using TRI reagent and RNeasy spin columns to determine the best method.

TRI reagent has been used previously in the study to extract RNA from cell lines with success (chapters 3 and 4). However, TRI reagent can also be used to isolate RNA from frozen tissue sections. Unlike TRI reagent, which is based around phenol:chloroform and phase separation, RNeasy spin columns use silica-based columns to isolate and purify RNA.

RNA isolation was optimised using frozen breast tumours of differing sizes. One sample weighed in excess of 100mg (referred to as ‘large tumour’) and the other was less than 100mg (referred to as ‘small tumour’). Each tumour was cut into two equal sections, with one half being used for each isolation method. This ensures that results are not tissue specific and are dependent solely on the extraction process.

The tissues were homogenised into a single-cell suspension using a GentleMACS™ dissociator as described in section 5.3.3. Once homogenised, RNA was extracted from the tumour in accordance with the manufacturers protocol. Following isolation, RNA purity was determined using a nanodrop spectrophotometer, and the integrity was determined by running a small sample on an agarose gel.

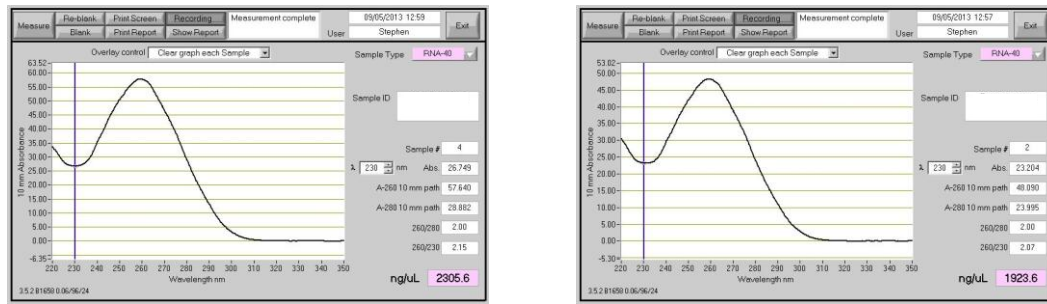
As demonstrated by the Nanodrop spectrophotometer, RNA isolation using TRI reagent produced high RNA concentrations of approximately 2µg/µl from both the large and small tumours (**figure 5.6 panel A**). The 260/280 and the 230/260 ratios were both between 2.00 and 2.15, which demonstrate that the RNA isolated from both tumour sizes was of good quality with little contamination by proteins or organic solvents such as phenol or ethanol. Despite the high levels of pure RNA isolated using TRI reagent, when the integrity was examined by agarose gel electrophoresis, the RNA bands were smeared suggesting degradation (**figure 5.6**

panel B). This was commonly observed, implying the condition of the tumours is most likely the problem rather than the technique. This was further validated as RNA isolated from wild type HEK cells was far less degraded. Despite this, 28S and 18S bands were still visible and it was possible to be reverse transcribed and amplified by real-time PCR (**figure 5.6 panel C**). It should also be noted that the Ct values of *GAPDH* were approximately 22 which is quite high for a housekeeping gene which are abundantly expressed in the cells. This again suggests poor RNA quality.

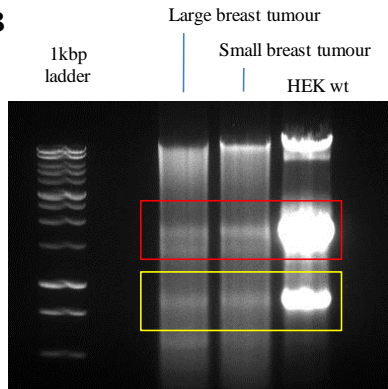
Results from the RNeasy spin columns demonstrated the concentration of RNA isolated from both tumours was approximately 5-fold less than that using TRI reagent (**figure 5.7 panel A**). The 260/280 ratios demonstrated that the quality of RNA was good, although, the poorer 260/230 ratios demonstrated greater risk of contamination. In addition to this, the integrity of RNA on the agarose gel was poorer (**figure 5.7 panel B**). However, real-time PCR results demonstrated that the template could still be amplified to a similar level as cDNA templates produced from RNA isolated using TRI reagent (**figure 5.7 panel C**).

Hence, the TRI reagent was judged superior to spin columns and was deemed the optimal method for use in subsequent experiments.

A



B



C

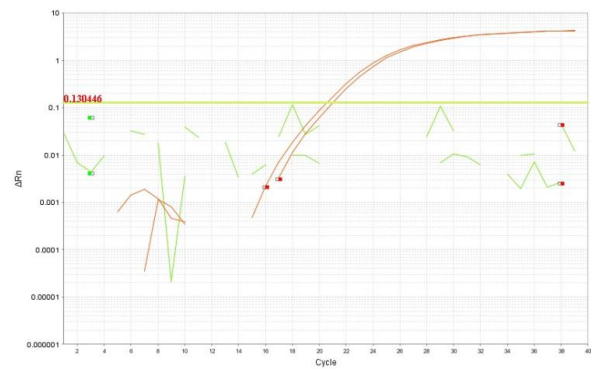
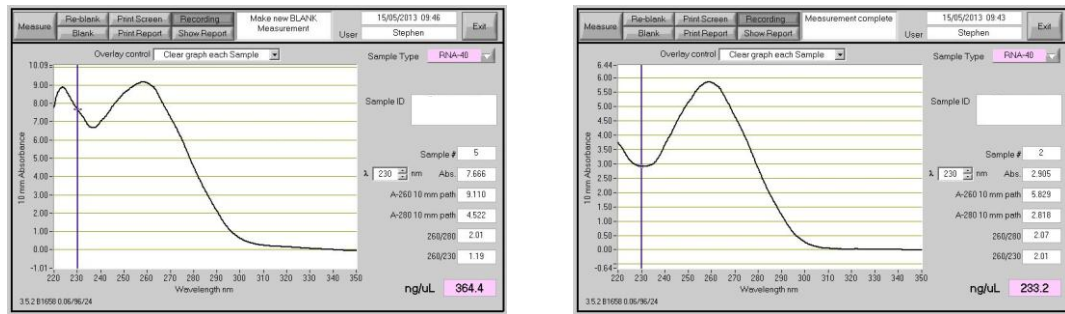


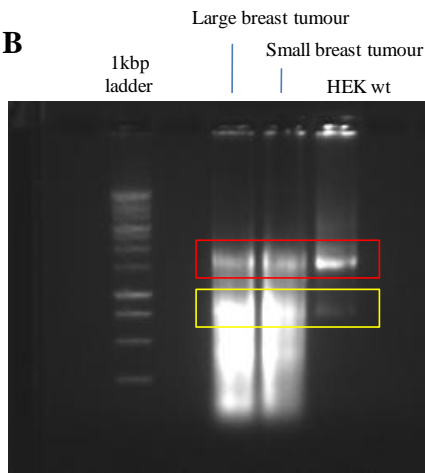
Figure 5-6 - Confirmation of RNA integrity following isolation from frozen cells using TRI reagent

RNA was isolated from two separate frozen breast tumours separate using TRI reagent. Following isolation, RNA was quantified and the purity was checked using the Nanodrop spectrophotometer. Left panel represents RNA isolated from small sized tumour, whereas, the right panel represents large sized tumour (**A**). Integrity of RNA was determined by running total RNA isolated from frozen breast tissues on 1.2% agarose gels. Red and yellow boxes represent the ribosomal RNA subunits 28S (red box) and 18S (yellow box) (**B**). RNA was reverse transcribed into cDNA and *GAPDH* was amplified using Taqman® real-time PCR primers (**C**). Data is representative of four independent experiments.

A



B



C

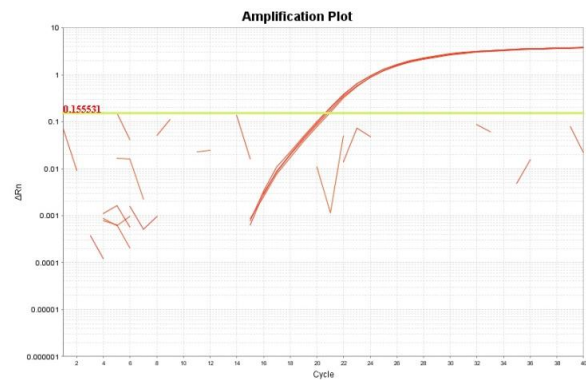


Figure 5-7 - Confirmation of RNA integrity following isolation from frozen cells using RNeasy spin columns reagent

RNA was isolated from two separate frozen breast tumours using RNeasy spin columns. Following isolation, RNA was quantified and the purity was checked using the Nanodrop spectrophotometer. Left panel represents RNA isolated from small sized tumour, whereas, the right panel represents large sized tumour (**A**). Integrity of RNA was determined by running total RNA isolated from frozen breast tissues on 1.2% agarose gels. Red and yellow boxes represent the ribosomal RNA subunits 28S (red box) and 18S (yellow box) (**B**). RNA was reverse transcribed into cDNA and *GAPDH* was amplified using Taqman® real-time PCR primers (**C**). Data is representative of two independent experiments

5.4.3 Selection of suitable housekeeping genes

After isolating RNA from all test samples, the most appropriate housekeeping gene was determined. Housekeeping genes are endogenously expressed within most normal and pathological cells. Uniform expression of these genes between samples allows them to be used as a reference to measure the relative expression of a test gene.

The three housekeeping genes tested were: *GAPDH*, β -*Actin*, and β -*Tubulin*. These are all commonly used as housekeeping genes in real-time PCR.

Probably due to the poor RNA integrity from the samples, results demonstrated the amplification of all three genes was fairly low with most samples. All genes were relatively similar in their expression across the breast cancer samples (*GAPDH*: mean Ct 22.66 ± 3.65 SD, β -*Actin*: mean Ct 24.11 ± 2.758 SD, β -*Tubulin*: mean Ct 25.19 ± 1.36 SD) (**figure 5.8**). *GAPDH* was selected as the housekeeping gene to be used in subsequent experiments.

Because cDNA template from cancer case #19 failed to amplify sufficiently with any of the housekeeping genes tested, it was excluded from further analysis

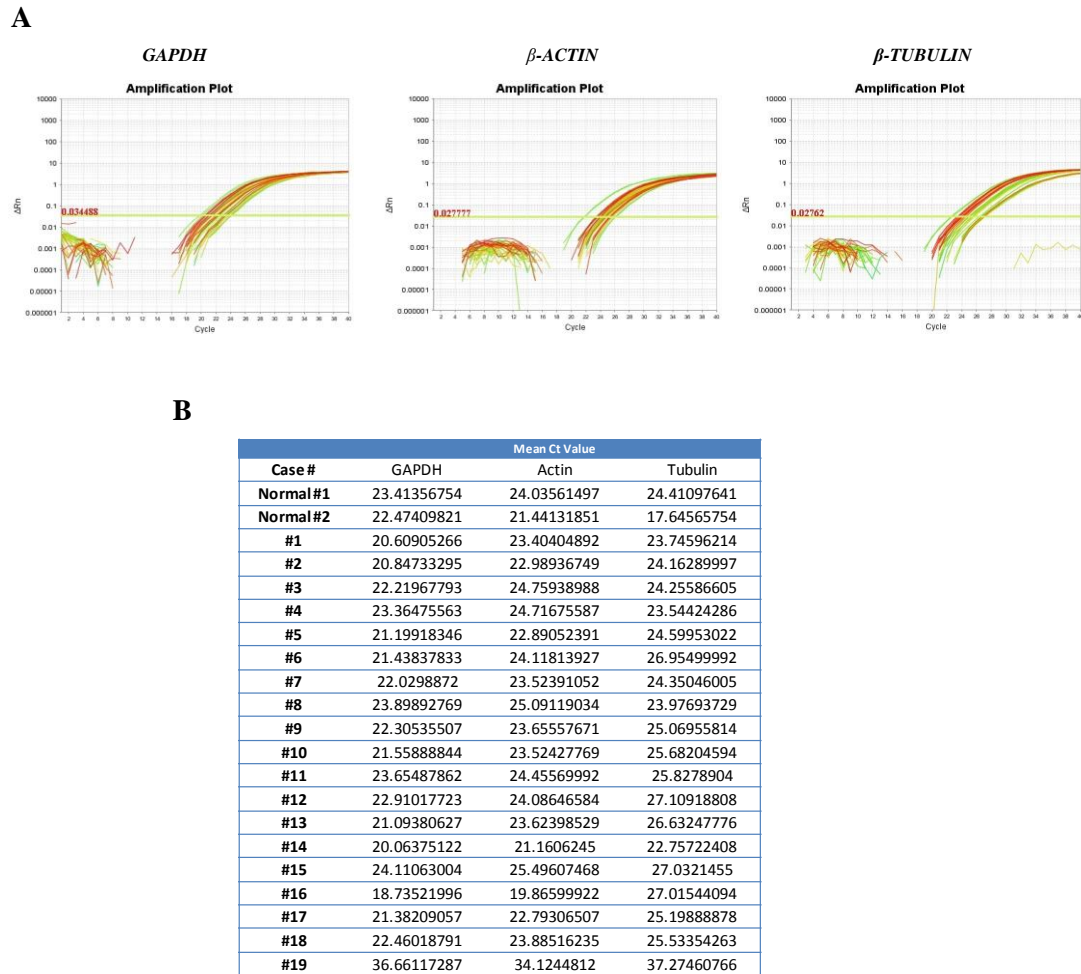


Figure 5-8 - Determining the most compatible housekeeping gene in frozen breast cancer tissues

RNA was isolated from each breast tumour using TRI reagent and reverse transcribed into cDNA. cDNA was then amplified using Taqman® primers for *GAPDH*, *β-Actin* and *β-Tubulin*. **Panel A** represents amplification plots produced from each sample. **Panel B** is the mean Ct value produced from each sample for each housekeeping gene tested. Data is the mean of a single experiment performed in duplicate.

5.4.4 Determination of T-cell infiltration in breast samples

Because T-cells could not be excluded from the frozen tissue samples and could potentially mask the level of *FOXP3* and *CXCR4* expressed by epithelial cells, CD3 infiltration was determined at both transcript and protein levels within each sample.

The level of *CD3* transcripts in breast cancer was compared to the level in two normal mammary tissue samples (**figure 5.9 panel A**). *CD3* was only expressed at a low level in normal mammary tissues, whereas, the majority of cancer samples showed higher levels of *CD3* expression. However, despite a clear trend, *CD3* was not significantly increased in either LN-negative or LN-positive samples in comparison to normal tissues ($p>0.05$; **figure 5.9 panel B**).

These findings were further validated at a protein level by performing IHC. Each sample also had a NPA stain included which was clean, demonstrating the specificity of the anti-CD3 antibody. The results were similar to those observed at transcript level, as the two normal mammary tissues had few CD3⁺ cells present (**figure 5.10**), whereas, strong CD3⁺ staining was observed within most LN-negative (**figure 5.11 panel A**) and LN-positive (**figure 5.11 panel B**) breast cancer samples. This demonstrates that breast cancer samples do frequently show T-cell infiltration into the tumour environment.

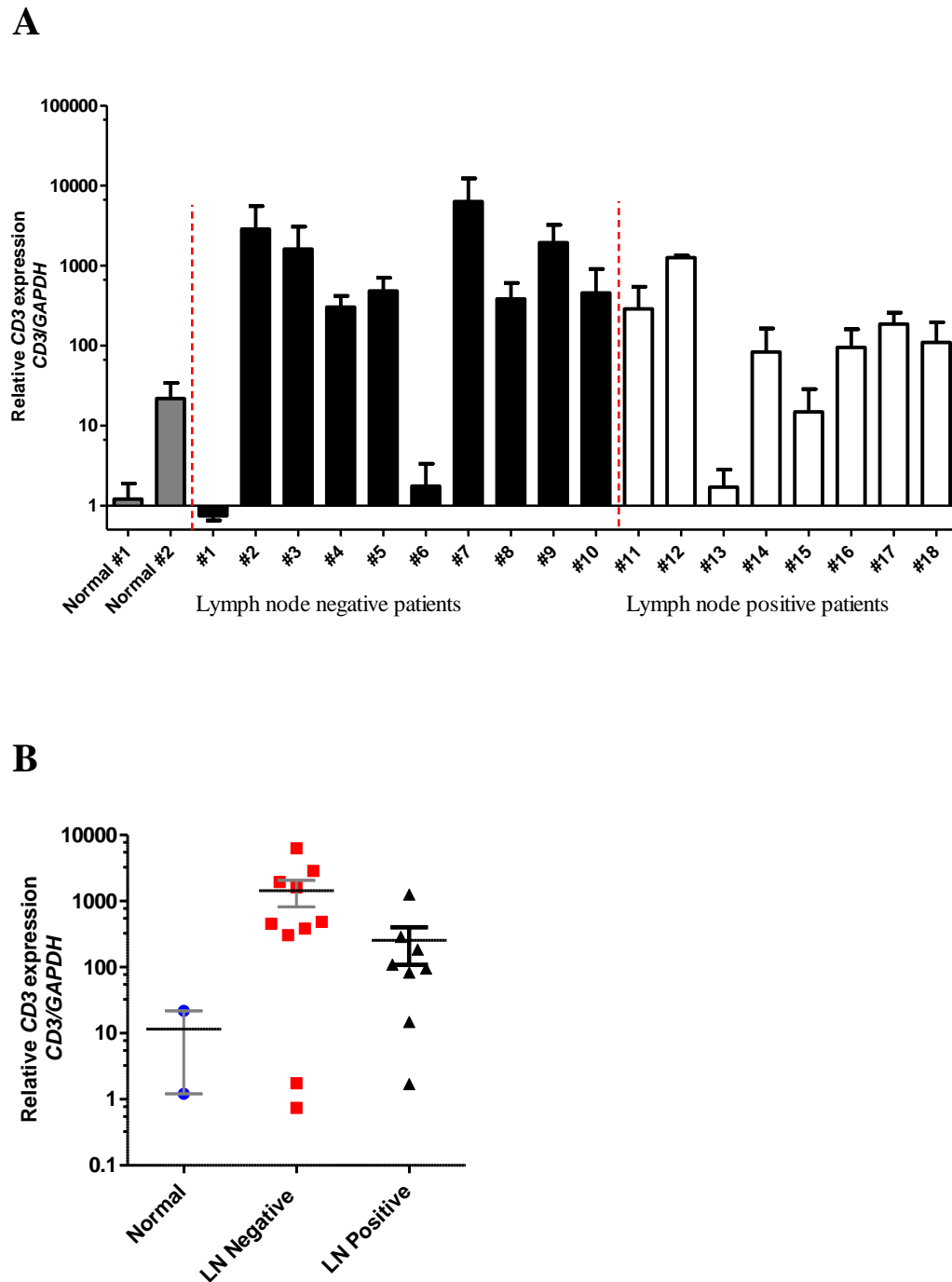


Figure 5-9 - Determination of *CD3* transcripts in normal and breast cancer tissues

CD3 transcripts within each breast sample were determined using real-time PCR. (A) After normalising against endogenous *GAPDH*, the amount of *CD3* transcripts were compared to those from normal breast tissue. Expression from normal #1 was arbitrarily defined as 1.0. Data was plotted in a log10 format which data points representing means and SD of experiments performed in duplicates (n=2). (B) The mean relative expression levels from each sample were grouped into their lymph node status and compared to normal breast tissue.

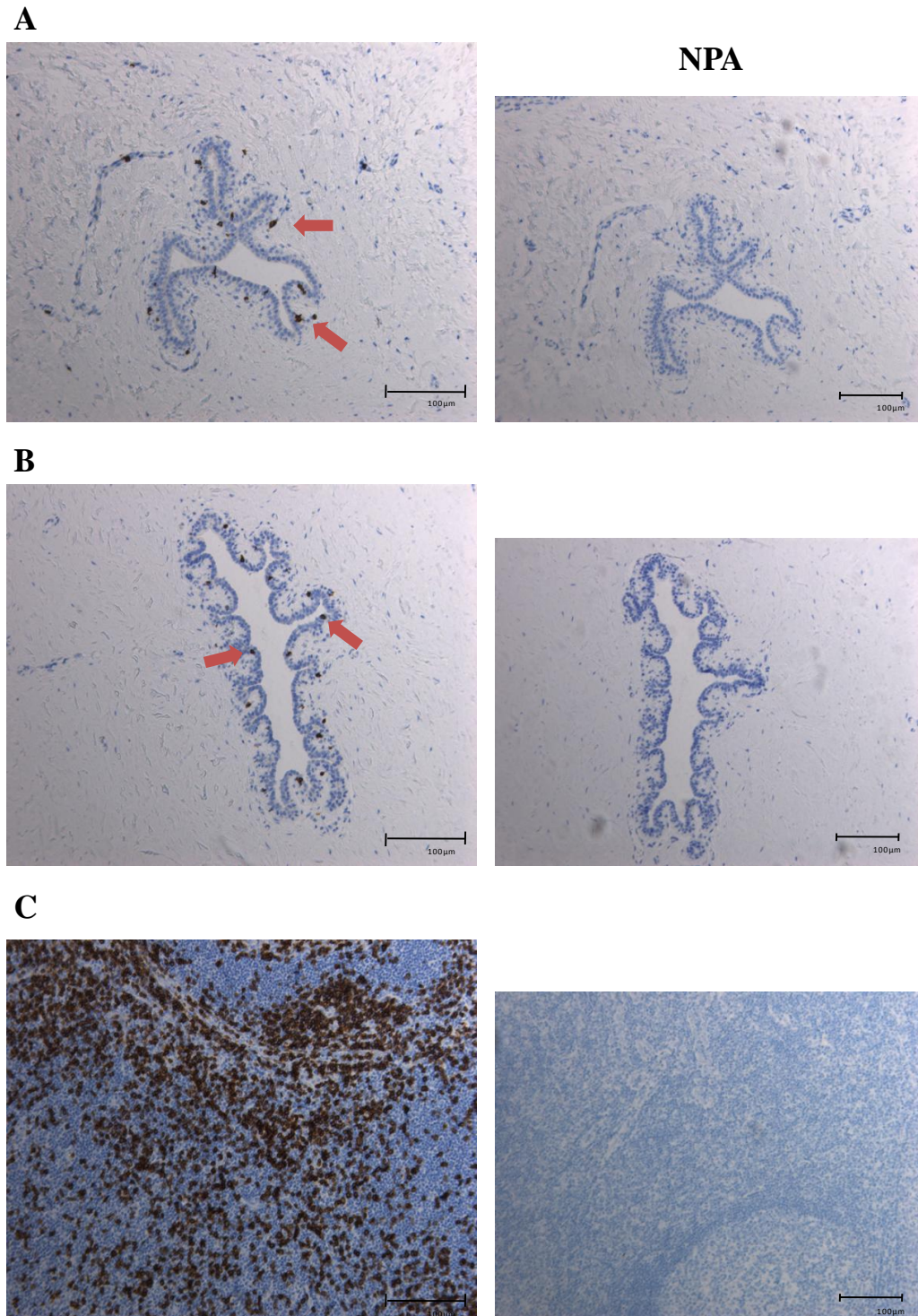


Figure 5-10 - IHC staining of CD3 in normal mammary breast tissue

Normal mammary breast tissue isolated from reduction surgery was stained by Ms Denise Woolley in the QE Hospital. CD3 staining using a pre-optimised protocol with the autostainer link 48. Red arrows demonstrate the presence of CD3⁺ positive cells within duct epithelial cells. (A) Represents normal mammary tissue #1 (normal #1). (B) Represents normal mammary tissue #2 (normal #2). Tonsil was used as a positive control (C), whereas each sample tested also had a control NPA as a negative control

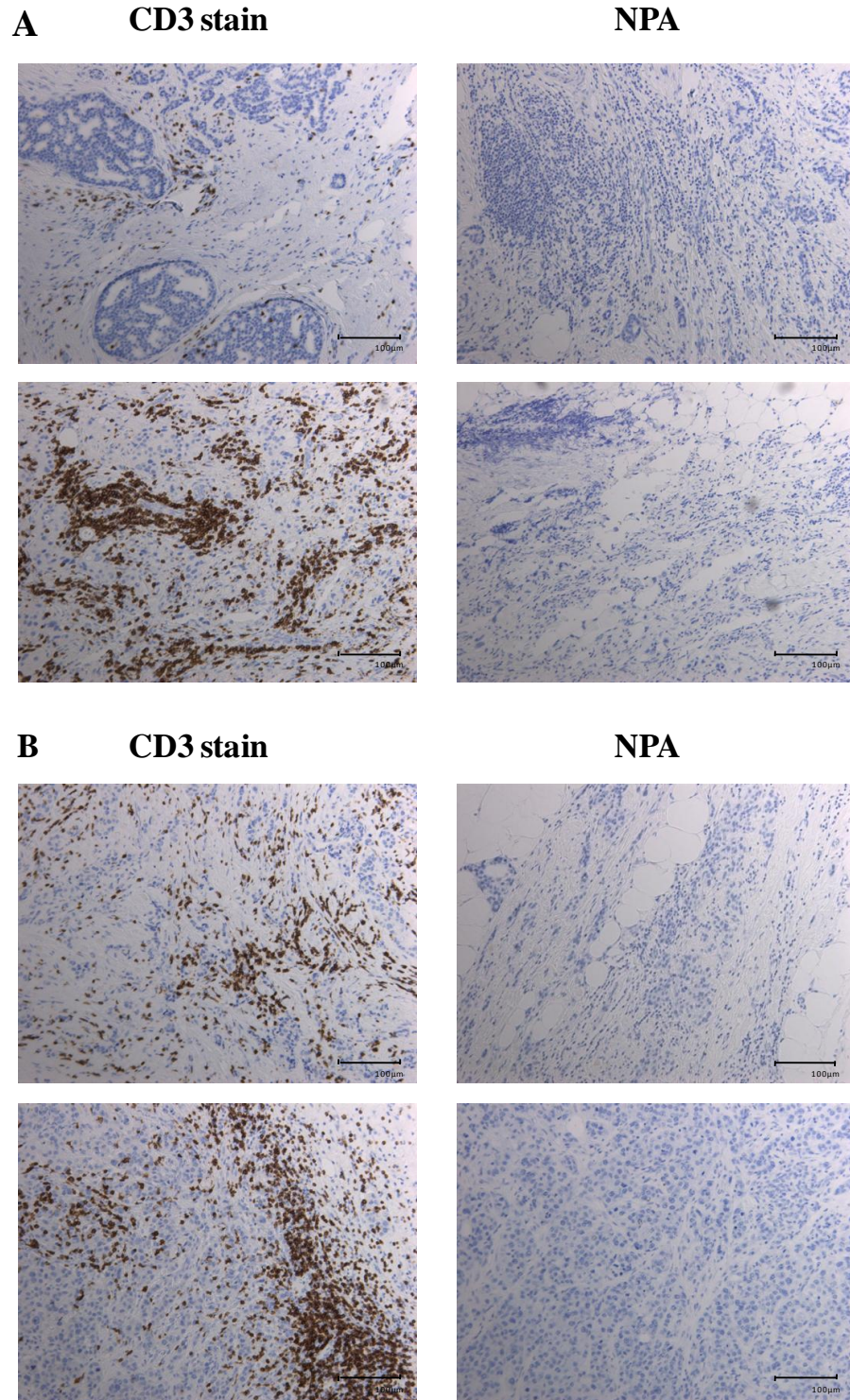


Figure 5-11 - IHC staining of CD3 in breast cancer samples

Representative images of CD3 staining on breast cancer samples were stained for CD3 by Ms Denise Woolley using a pre-optimised protocol with the autostainer link 48 in the QE Hospital. **Panel A** represents images from two LN-negative breast cancer patients (upper panel shows case #6, lower panel shows case #7). **Panel B** represents images from two LN-positive breast cancer patients (upper panel shows case #13, lower panel shows case #12). NPA stains were included as individual negative controls. A tonsil positive control is included in **figure 5.10** as all sections were stained together.

5.4.5 Measurement of *CXCR4* transcripts in breast samples

CXCR4 transcripts were determined in each sample using Taqman® primers specific for *CXCR4*. In line with the literature, neither of the normal mammary tissues expressed *CXCR4* (Muller, Homey et al. 2001). However, *CXCR4* was increased in all breast cancer samples (**figure 5.12 panel A**). Although, as determined in the previous section, due to the high levels of infiltrating T-cells, the cell specific origin of *CXCR4* expression could not be determined.

CXCR4 was significantly increased in the LN-negative samples in comparison to the normal breast tissue samples, however, despite a clear increase in *CXCR4* in the LN-positive samples, the expression was not significant when compared to the normal tissues, although a clear trend was observed ($p=0.076$; **figure 5.12 panel B**).

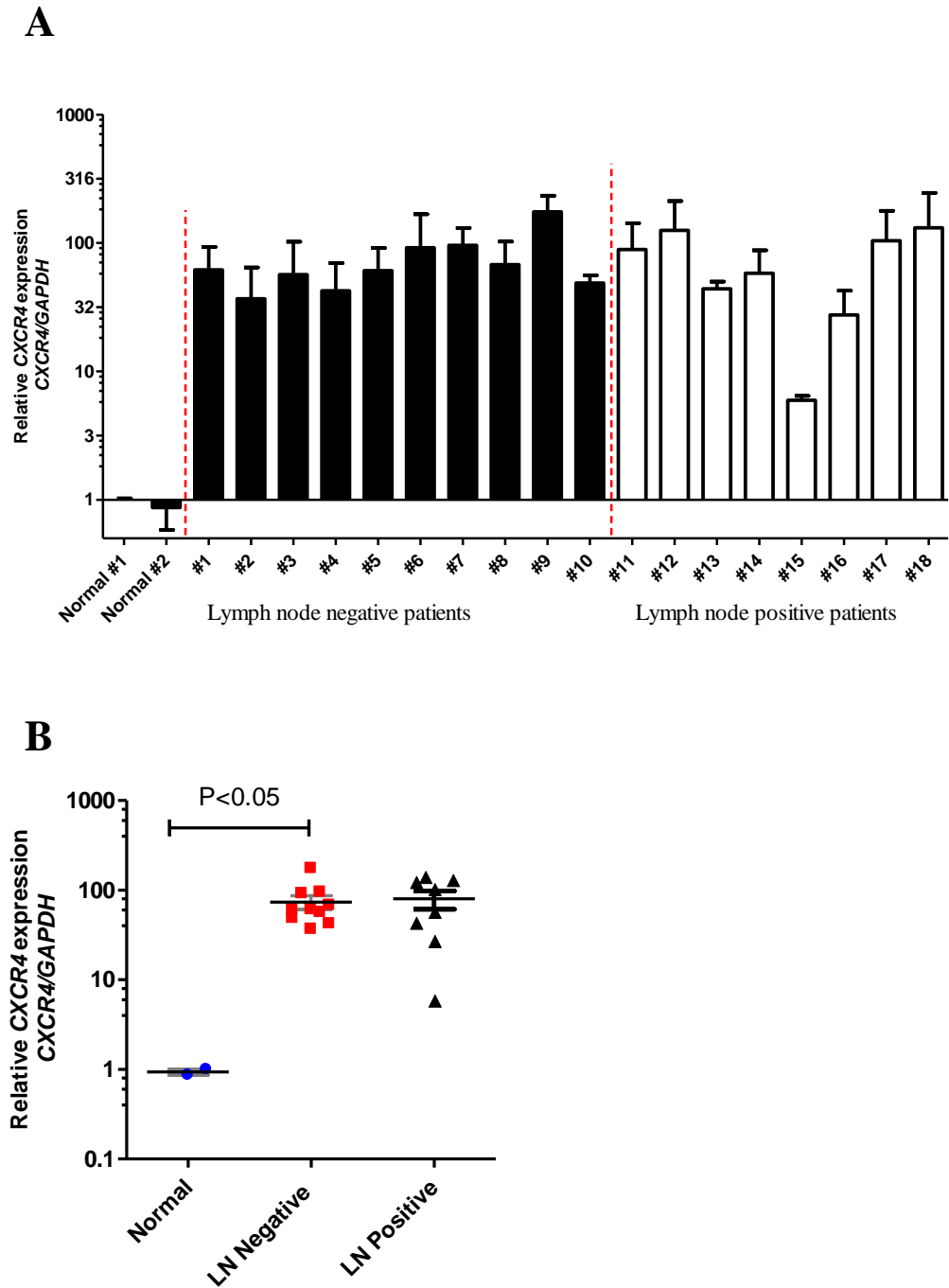


Figure 5-12 - Determination of *CXCR4* transcripts in normal and breast cancer tissues

CXCR4 transcripts within each breast sample were determined using real-time PCR. (A) After normalising against endogenous *GAPDH*, the amount of *CXCR4* transcripts were compared to those from normal breast tissue. Expression from normal #1 was arbitrarily defined as 1.0. Data was plotted in a log10 format which data points representing means and SD of experiments performed in duplicate (n=2). (B) The mean relative expression levels from each sample were grouped into their lymph node status and compared to normal breast tissue. Statistical analysis was performed using an unpaired t-test.

5.4.6 Optimisation of CXCR4 IHC staining

Before staining the test tissue, the optimum antibody dilution was determined by staining human tonsil. Staining was performed within the QE Hospital using the autostainer link 48.

The optimised dilutions ranged from between 1:100 and 1:500 (**figure 5.13**). Each test also contained a NPA stain as negative controls. Negative controls contained no staining which demonstrates the specificity of the primary antibody. The results demonstrated that the antibody produced a dilution-dependent response. As the dilution increased, the intensity of the stain diminished. Strong staining was observed using 1:100 (**figure 5.13 panel A**). The 1:150 dilution (**figure 5.13 panel B**) still detected the expression of CXCR4, however, the 1:300 (**figure 5.13 panel C**) and 1:500 dilutions (**figure 5.13 panel D**) did not detect CXCR4 and was similar to the NPA controls.

Because the 1:150 dilution was the lowest dilution to detect CXCR4, this was determined as the optimum dilution to stain the breast samples.

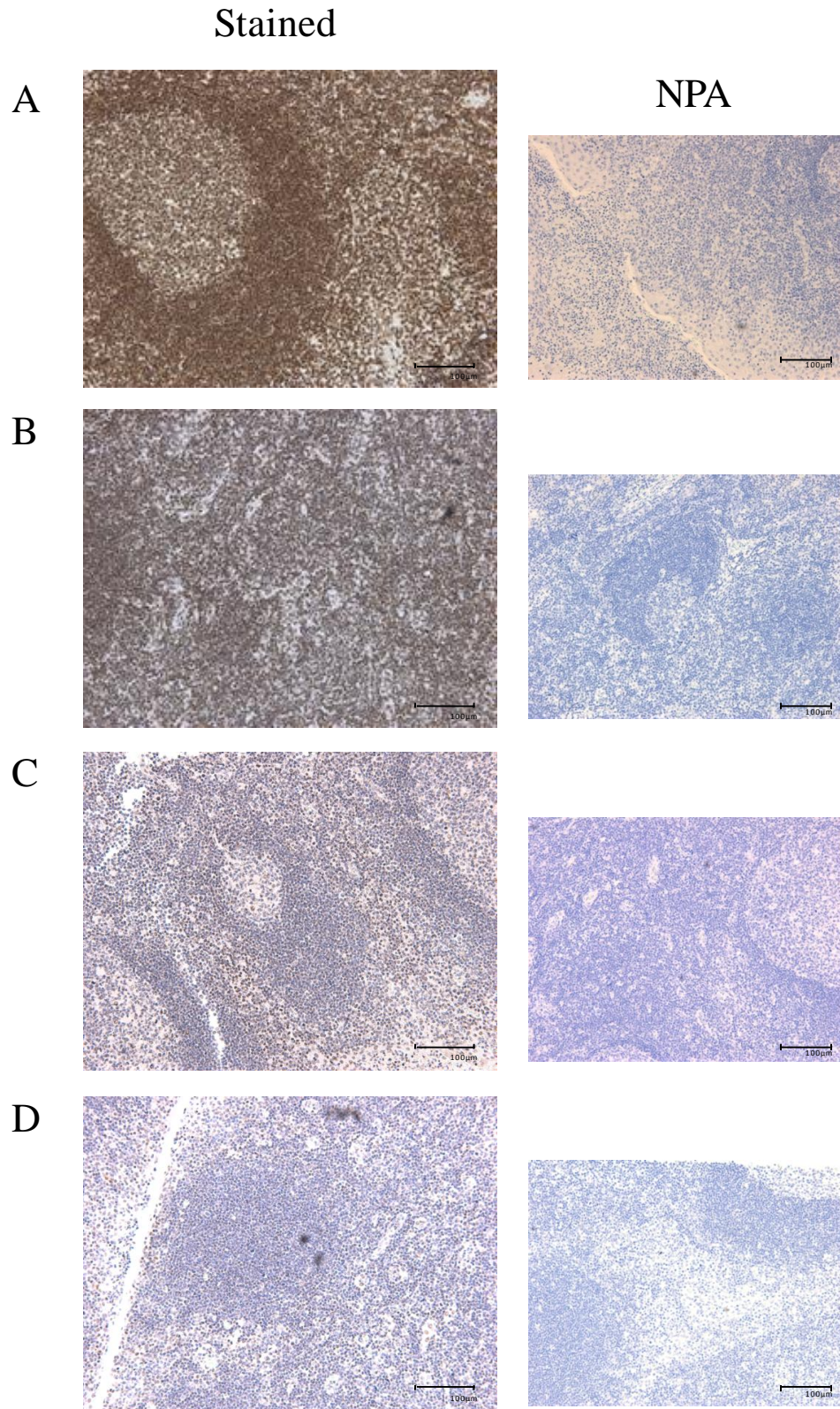


Figure 5-13 – Optimisation of CXCR4 IHC staining using human tonsil

Sections of human tonsil were sourced from the QE Hospital. CXCR4 staining was performed by Ms Denise Woolley using the autostainer link 48 with the following dilutions 1:100 (**A**), 1:150 (**B**), 1:300 (**C**), 1:500 (**D**).

5.4.7 Measurement of CXCR4 protein expression in breast samples

After determining the optimum dilution to stain the breast tissue, the levels of CXCR4 protein were determined within the LN-negative and LN-positive cancer cases.

The normal mammary tissue had no detectable CXCR4 associated with epithelial cells of the ducts and lobules (**figure 5.14 panels A and B**). Low levels of CXCR4 were detected within the stroma but this might be associated with T-cell infiltration.

Interestingly, the source of the normal tissue appears to be important. Although the normal tissue taken from breast reduction surgeries (used in previous experiments) did not show CXCR4 expression, ‘normal’ tissue taken adjacent to a breast tumour expressed CXCR4 (**figure 5.14 panel C**). This suggests that although areas peripheral to breast cancers are often described as cancer-free or non-malignant, they may still exhibit features different from tissue with no underlying pathology. Following this result only tissue from breast reduction surgeries were defined as normal.

CXCR4 was highly expressed in LN-negative (**figure 5.15**) and LN-positive samples (**figure 5.16**). Staining of epithelial cells and T-cells could be determined from IHC by a pathologist based on the size and location of cells. As described by the pathologist, CXCR4 positive lymphocytes were clearly present. However, the epithelial cells within the ductal tumours had also upregulated CXCR4.

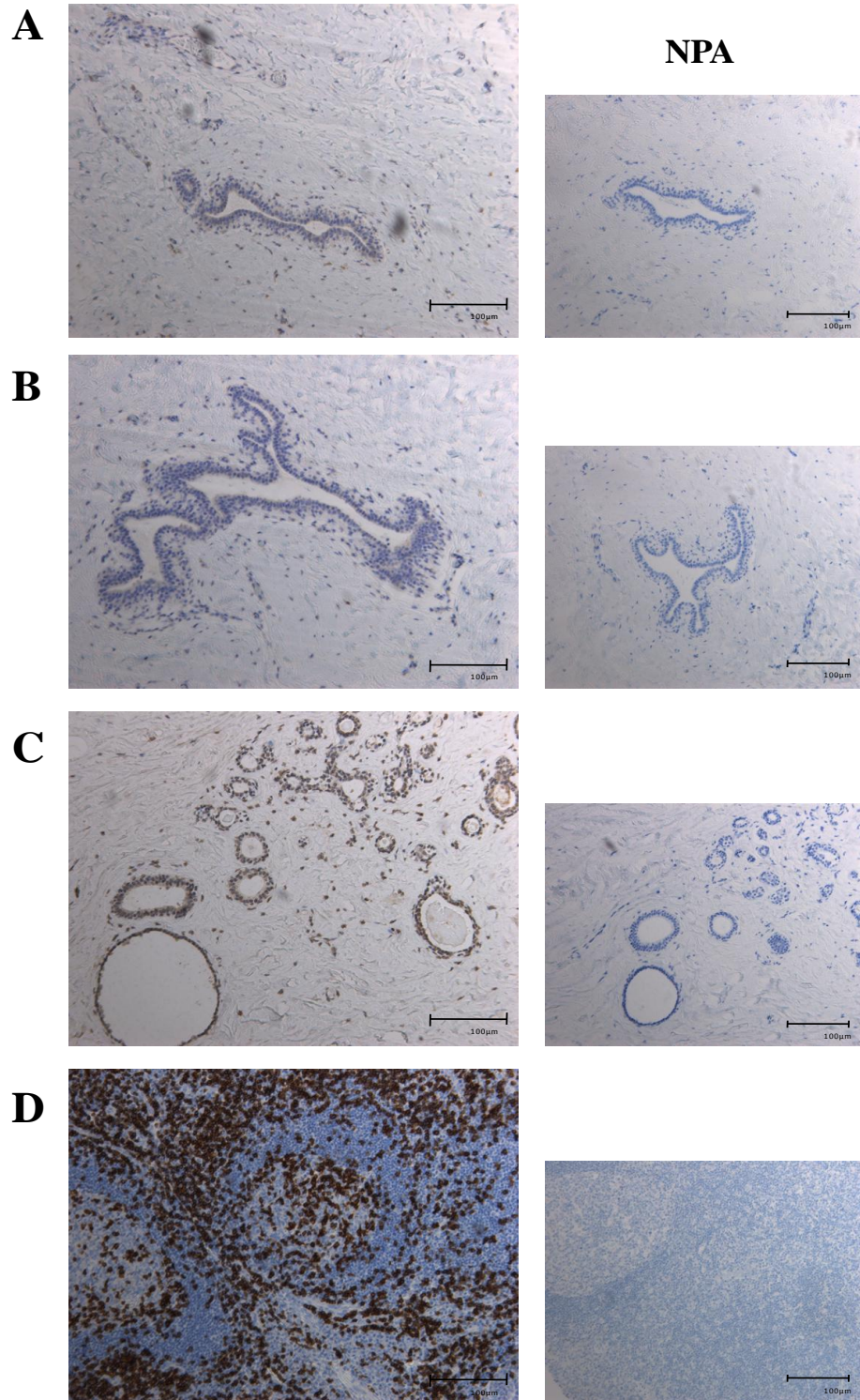


Figure 5-14 - IHC staining of CXCR4 in normal breast tissue

Normal mammary breast tissue isolated from reduction surgery ([A] –Normal #1, [B] – Normal #2) were stained for CXCR4 by Ms Denise Woolley using the autostainer link 48 in the QE Hospital. Alternatively, a region of non-malignant tissue from a breast cancer case (case #6) was also stained using the same protocol as previously described (C). Tonsil was used as a positive control (D), whereas each sample tested also had a NPA as a negative control.

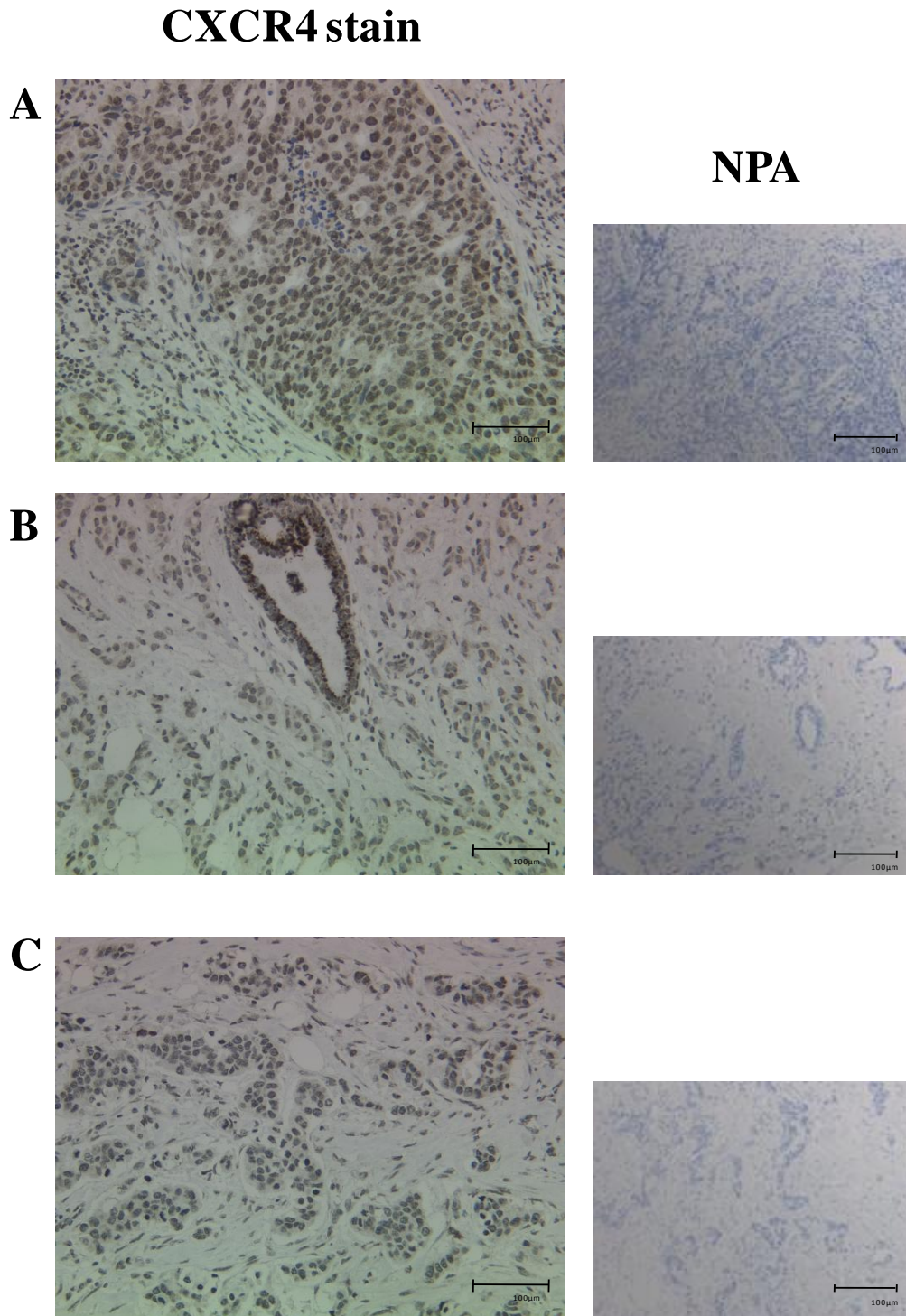


Figure 5-15 - IHC staining of CXCR4 in LN-negative breast cancer samples

Breast cancer tissue from patients with no lymph node involvement was stained for CXCR4 by Ms Denise Woolley with a pre-optimised protocol (1:150 dilution) using the autostainer link 48 in the QE Hospital. Tonsil was used as a positive control which is included in **figure 5.14** as samples were ran together. Each sample tested also had a NPA as a negative control. Representative images are of cases; **Panel A** shows case #7, **panel B** shows case #8 and **panel C** shows case #10. Each sample was stained in duplicates which produced similar findings

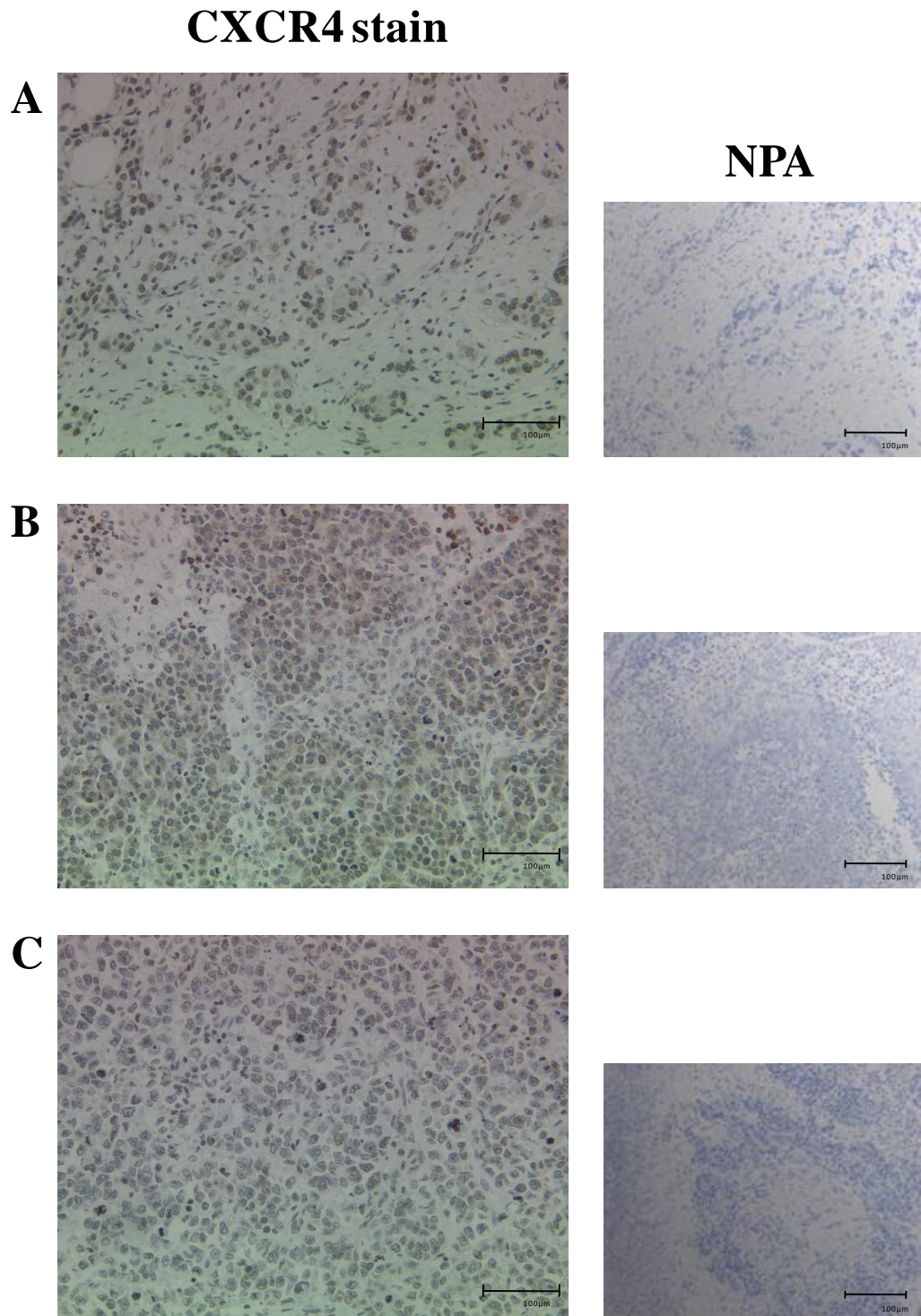


Figure 5-16 - IHC staining of CXCR4 in LN-positive breast cancer samples

Breast cancer tissue from patients with high lymph node involvement was stained for CXCR4 by Ms Denise Woolley with a pre-optimised protocol (1:150 dilution) using the autostainer link 48 in the QE Hospital. Tonsil was used as a positive control which is included in **figure 5.14** as samples were ran together. Each sample tested also had a NPA as a negative control. Representative images are of cases; **Panel A** shows case #11, **panel B** shows case #13 and **panel C** shows case #15. Each sample was stained in duplicates which produced similar findings.

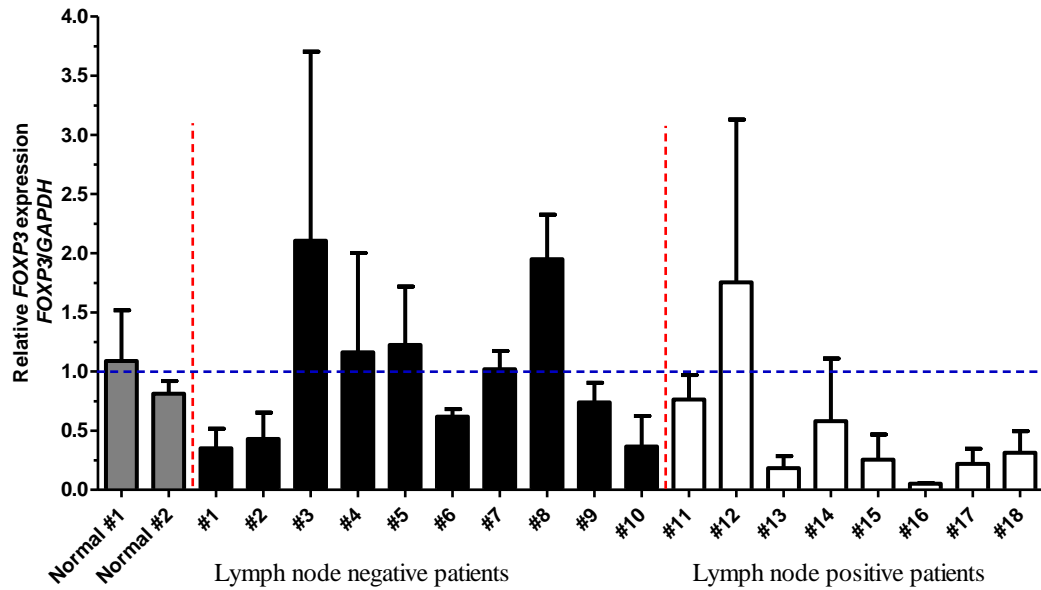
5.4.8 Measurement of *FOXP3* transcripts in breast samples

FOXP3 transcripts were determined in each breast sample using Taqman® primers specific for *FOXP3*.

Relatively low levels of *FOXP3* were detected within both normal mammary samples. However, variable results were found for both the LN-negative and LN-positive cancer samples (**figure 5.17 panel A**). Although there was no statistical change in either LN-negative ($p=0.92$) or LN-positive tissues ($p=0.31$), four of the LN-negative samples (cases #1, #2, #6 and #10) expressed less *FOXP3* than the normal mammary tissue, whereas, majority of LN-negative tissues (cases #3, #4, #5, #7, #8, and #9) expressed *FOXP3* at a similar or higher level compared to the normal mammary tissues. Six LN-positive patients (cases #13, #14, #15, #16, #17, and #18) had lower levels of *FOXP3* compared to the normal mammary tissue.

The varied distribution of *FOXP3* in the LN-negative patients is best demonstrated by **figure 5.17 panel B**, which shows that the overall mean distribution of *FOXP3* is similar to the level in the two normal tissues tested (mean expression of normal tissue 0.95 ± 0.194 SD, mean expression of LN-negative tissue 0.99 ± 0.629 SD). On the other hand, the distribution of *FOXP3* in the LN-positive patients (mean expression 0.51 ± 0.55 SD) was decreased compared to the LN-negative breast cancer samples, and also the normal breast tissues.

A



B

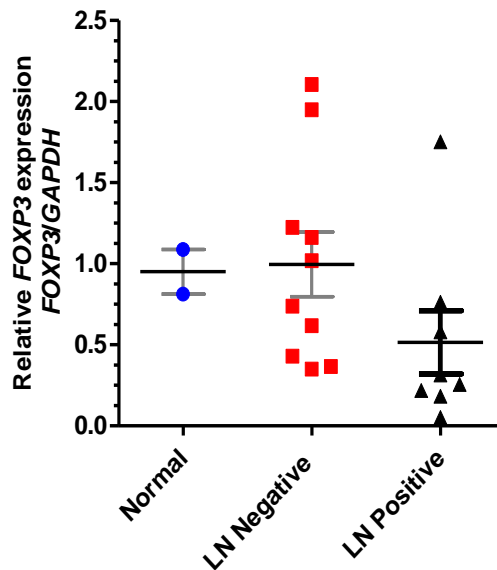


Figure 5-17 - Measurement of *FOXP3* transcripts in normal and breast cancer frozen tissues

FOXP3 transcripts within each breast sample were determined using real-time PCR. (A) After normalising against endogenous *GAPDH*, the amount of *FOXP3* transcripts were compared to those from normal breast tissue. Expression from normal #1 was arbitrarily defined as 1.0. Data representing means and SD of experiments performed in duplicate (n=2). (B) The mean relative expression levels from each sample were grouped into their lymph node status and compared to normal breast tissue

5.4.9 Optimisation of FOXP3 IHC staining and measurement in patient samples

The expression of FOXP3 in normal breast tissue has been demonstrated by several research groups using IHC (Zuo, Wang et al. 2007; Chen, Chen et al. 2008; Merlo, Casalini et al. 2009). These groups have consistently shown that the expression of this protein in these tissues is low. Indeed, results using Western blot (**figure 3.10 panel A**), IF (**figure 3.10 panel B**) and ELISA (**figure 3.11**) in this study have suggested that the expression of FOXP3 is low within the normal mammary epithelial cell line, HMEpC.

In line with this notion, two FOXP3 antibody clones were tested for their reactivity in normal breast tissue. Because the majority of reports demonstrate that FOXP3 is most frequently downregulated in malignant tissue in comparison to normal tissue, the method best able to stain FOXP3 in normal tissue was considered optimal for testing the malignant tissues.

Initial attempts to stain FOXP3 in normal breast samples were made using the 236A/E7 (Abcam) and 259D (BioLegend) human anti-FOXP3 antibody clones. The 236A/E7 antibody was used with the DAKO automated staining equipment within the Pathology Department in the QE Hospital, whereas, the 259D antibody was used with the Ventana equipment in Pathology Department of the RVI Hospital.

Because of the low level expression of FOXP3 in normal tissue, all samples tested in the QE Hospital underwent antigen retrieval with a high pH solution and received 4 minutes amplification (referred to as FLEX in the DAKO protocols). Initially, a number of antibody dilutions ranging from 1:25, to 1:150 (1:50 increments) were used with the autostainer link 48. Unfortunately, despite strong staining within the positive tonsil control, methods using this machine were not able to detect FOXP3 within the breast epithelial cells (**representative images of FOXP3 staining with each antibody dilution and NPA included in appendix 7**).

A member of this research group has developed a protocol for detection of FOXP3 in T-cells using the BenchMark ULTRA machines in the RVI Hospital with the 259D antibody. However, because the level of FOXP3 in Tregs is considerably higher than the expression in epithelial cells, further optimisation was carried out using a total of

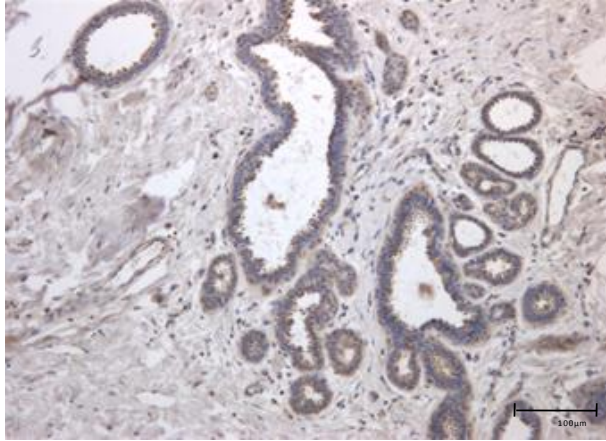
four antigen retrieval techniques (Cell Conditioning solution-1 [high pH], Cell Conditioning solution-2 [low pH], pressure cooker with Tris/EDA [pH 9] and also with citrate buffer [pH 6]), two antigen detection kits (*ultraview* and *optiview*), a range of antibody dilutions and increased amplification times. Unfortunately, none of the techniques was able to detect FOXP3 in normal breast epithelia (representative images of all conditions attempted are included in **appendices 8 to 10** with descriptions of each method labelled in the figure legend).

It was deemed that the automated protocols were not sensitive enough to detect FOXP3 in epithelial cells. Previous members of this research have manually stained and detected FOXP3 in normal breast samples using a pre-optimised protocol. Using this method, FOXP3 was detectable within the epithelial cells of both normal breast tissues tested (**figure 5.18 panels A and B**). The antibody specificity was validated as individual NPA controls for each sample were negative. Staining was also validated using tonsil as a positive control, which also showed a clean NPA control (**figure 5.18 panel C**).

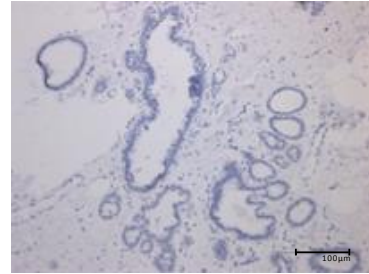
After confirming that this protocol was able to detect FOXP3 within normal mammary tissue, the cancer sections were all stained.

Despite the majority of the literature describing downregulation of FOXP3 in breast cancer, results in this study demonstrated strong FOXP3 positive staining in all breast cancer samples. Representative images of LN-negative samples are included as **figure 5.19**, whereas representative images of LN-positive samples are included as **figure 5.20**.

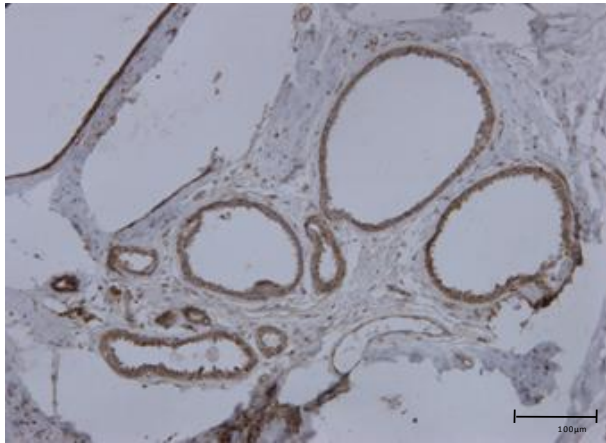
A



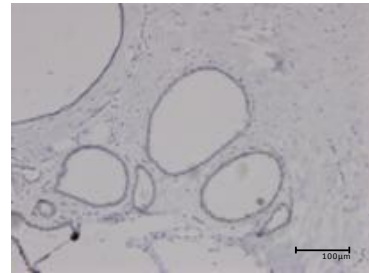
NPA



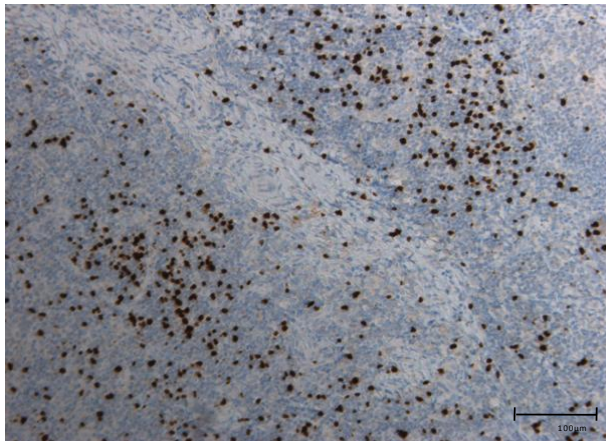
B



NPA



C



NPA

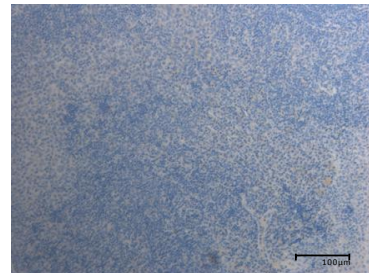


Figure 5-18 - Manual IHC staining of FOXP3 in normal breast tissue using FOXP3 clone 259D

Normal mammary breast tissue isolated from reduction surgery ([A] –Normal #1, [B] – Normal #2) were stained for FOXP3 manually using a pre-optimised protocol. (C) Tonsil was used as a positive control. Each sample tested also had a NPA control.

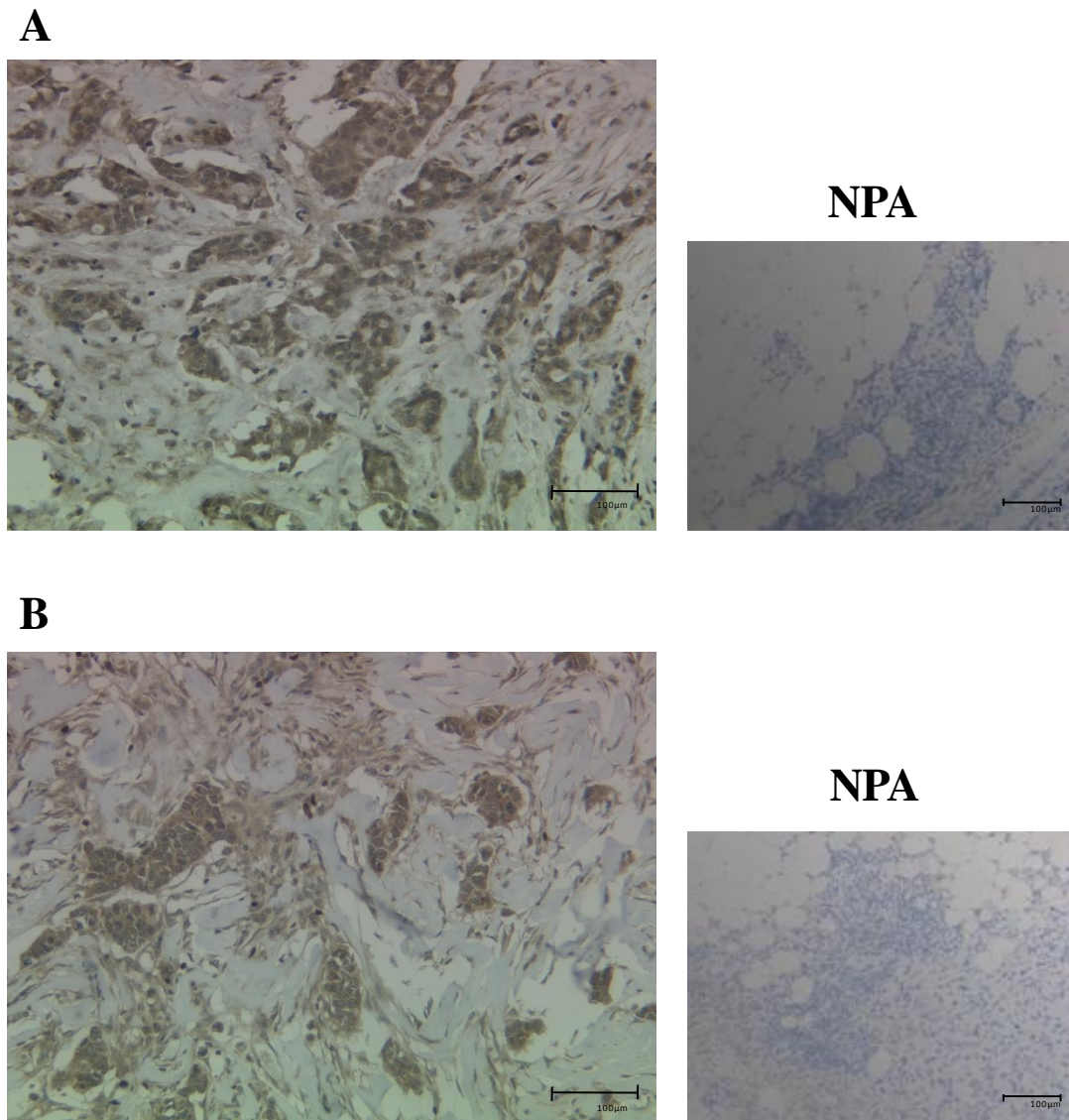


Figure 5-19 - FOXP3 staining in LN-negative breast cancer samples

Breast cancer tissue from patients with no lymph node involvement was manually stained for FOXP3 with an optimised protocol. Each sample tested also had a NPA control. Representative images are of cases; **Panel A** shows case #6, **panel B** shows case #10. Each sample was stained in duplicates which produced similar findings

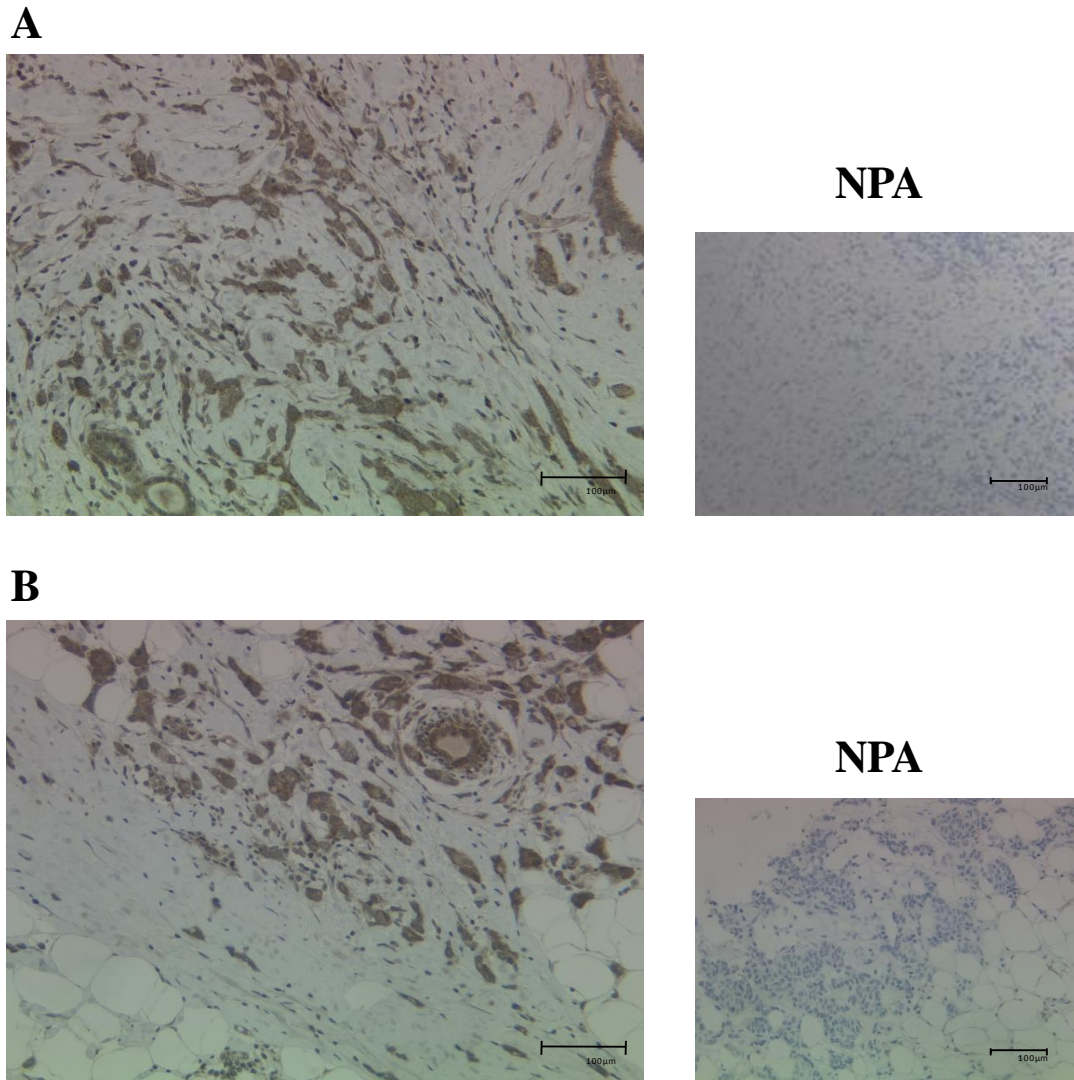


Figure 5-20 - FOXP3 staining in LN-positive breast cancer samples

Breast cancer tissue from patients with no lymph node involvement was manually stained for FOXP3 with an optimised protocol. Each sample tested also had a NPA control. Representative images are of cases; **Panel A** shows case #13, **panel B** shows case #17. Each sample was stained in duplicates which produced similar findings

5.4.10 Correlation of FOXP3 and CXCR4 protein expression in breast samples

The levels of FOXP3 and CXCR4 expression in the IHC stained breast samples were scored blindly and individually by a trained Pathologist using the allred quick score method (**figure 5.21 panel A**).

As previously described, both normal breast reduction samples expressed FOXP3 within the epithelial cells. The same tissues also showed no observable CXCR4 expression in the epithelial cells.

When the breast cancer samples were scored, results suggested that although CXCR4 was clearly upregulated in the cancer samples, there was no observable difference in the expression between the LN-negative and LN-positive samples (**figure 5.21 panel B**).

On the other hand, both the LN-negative and LN-positive cases still expressed FOXP3 at similar levels to those observed in normal breast tissues. In addition, there was no change in the expression between the LN-negative and LN-positive samples (**figure 5.21 panel C**).

These data sets suggest there is a marked increase in the expression of CXCR4 within breast cancer cases. However, the relative constant expression of FOXP3 by normal and cancerous breast samples suggests that FOXP3 is not frequently downregulated in breast cancer, which disagrees with many reports within the literature.

Due to the strong staining of FOXP3 and CXCR4 in all breast cancer samples, this finding also suggests there is no link between FOXP3 downregulation and CXCR4 upregulation in breast cancer *in vivo*.

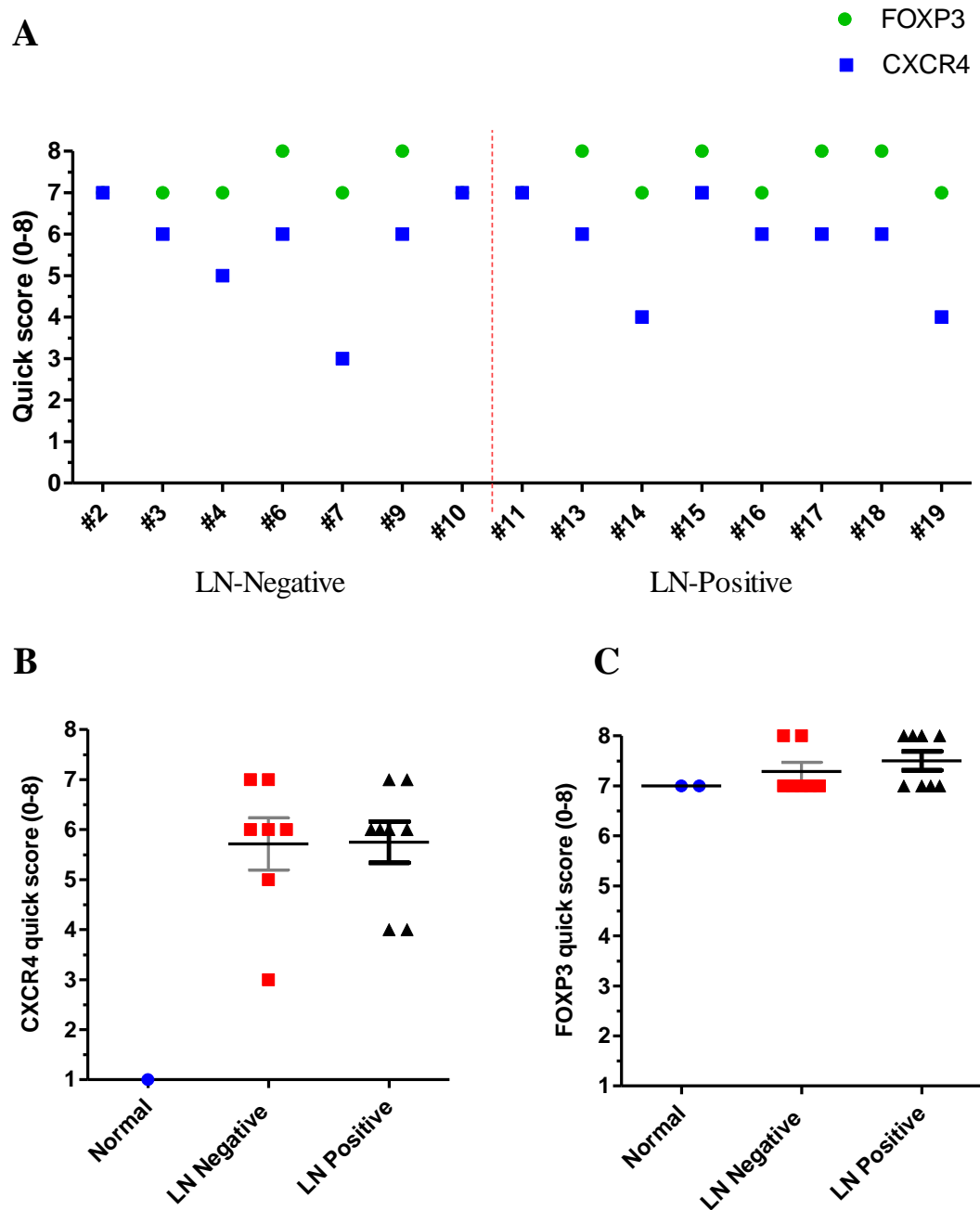


Figure 5-21 - Quick scores for FOXP3 and CXCR4 expression in breast tissue

After IHC staining, the expression of FOXP3 and CXCR4 were blind scored by a trained pathologist. **Panel A** demonstrates the expression of FOXP3 and CXCR4 within individual LN-negative cases (#2 - #10) and LN-positive cases (#11 - #19). Individual blue point represents an equal score of FOXP3 and CXCR4. **Panel B** and **C** represent a comparison between the LN-negative and LN-positive expression of CXCR4 (**panel B**) and FOXP3 (**panel C**).

5.5 Summary of chapter 5 results

- ✓ T-cells could not be excluded from digested frozen tissues by FACS.
- ✓ TRI reagent was used to isolate RNA from frozen tumour sections as it provided a greater yield of purer RNA.
- ✓ Normal breast tissue showed very low levels of infiltration by T-cells. However, the level of T-cells present within both LN-negative and LN-positive breast cancer samples was clearly increased.
- ✓ *FOXP3* transcripts within LN-negative cancer samples were comparable to levels observed in normal breast tissue. However, there was a marked decrease in the level in LN-positive cancer samples.
- ✓ *FOXP3* protein was difficult to detect within normal tissues using the autostainer link 48 and the BenchMark ULTRA automated machines. However, *FOXP3* was detectable using a manual staining protocol.
- ✓ There was no difference in *FOXP3* protein expression between normal breast tissue, LN-negative and LN-positive cancer samples.
- ✓ The source of normal breast tissue is important as non-malignant regions of tissue from cancer samples were positive for *CXCR4*, but normal breast tissue from reduction surgery was *CXCR4* negative

- ✓ CXCR4 was increased at transcript and protein levels within both LN-negative and LN-positive cancer samples in comparison to normal breast tissue

- ✓ No apparent correlation was observed between FOXP3 and CXCR4 in LN-negative or LN-positive cancer samples from this study.

5.6 Discussion

Since the discovery that FOXP3 is the first X-chromosome linked TSG, research is continuously producing data suggesting it is much more than just a protein involved in the function and development of Tregs (Douglass, Ali et al. 2012).

Few studies have investigated the prognostic implications of FOXP3 expression in epithelial cells *in vivo*. On the other hand, CXCR4 is a relatively well established molecule involved with breast cancer metastasis (Muller, Homey et al. 2001; Luker and Luker 2006). Therefore, the final aspect of this study had two main aims; firstly, to investigate any potential correlation between FOXP3 and CXCR4 expression *in vivo*, and secondly, to investigate the potential prognostic implications of FOXP3 and CXCR4 expression in breast cancer patients with opposing lymph node involvement and survival outcomes.

5.6.1 Correlation of lymph node status in selected patients and overall survival

Patients with no or high lymph node involvement were selected to study aggressive and less-aggressive breast cancer. The selection of patients on the basis of their lymph node involvement was validated by the patients NPI scores mostly being ‘good’ (for LN-negative samples) or ‘poor’ (for the LN-positive samples).

Because there has been a recent increase in more innovative and successful therapies, the current prognostic relevance of the NPI has been questioned. However, when the follow-up data was examined, the majority of LN-negative patients had been discharged and were alive and well after five years, whereas, the majority of the LN-positive patients were deceased due to metastasis. This suggests that the NPI was a successful basis to select patients for investigating FOXP3 and CXCR4 expression in aggressive and less aggressive breast cancers.

Interestingly, 6 out of the 10 LN-negative samples were dissected post-2000, whereas, only 2 out of the 9 LN-positive samples were dissected post-2000. This proposes the argument that perhaps the more aggressive LN-positive samples were more historic, whereas the LN-negative samples were more recent. Because the

screening procedures, methods of diagnosis and treatments for breast cancer are always improving, it would have been more ideal to select LN-negative and LN-positive samples from approximately the same year would eradicate this.

5.6.2 The impact of T-cell infiltrates on real-time PCR results

One of the most common symptoms associated with breast cancer is the onset of chronic inflammation. The cells responsible for this inflammation are a range of leukocytes, but most commonly lymphocytes. Both *FOXP3* and *CXCR4* are expressed by a number of these infiltrating leukocytes. However, this study was designed to investigate the expression of *FOXP3* and *CXCR4* specifically in epithelial cells.

Specific selection of epithelial cells from the tumour was attempted by FACS. This aimed to prevent the infiltrating leukocytes from obscuring epithelial cell expression of *FOXP3* and *CXCR4*. Results consistently suggested that frozen breast tumours had very low levels of CD3⁺ T-cell infiltration contradicting many reports within the literature (Liyanage, Moore et al. 2002; Liu, Wong et al. 2007; Matkowski, Gisterek et al. 2009). The tissues used in this study were extremely old, and in a poor condition. This and a combination of the initial freezing process (snap-frozen) led to the RNA isolated from the cells being heavily degraded as tumour cells in the frozen sections were dead.

This left no options available to remove potential T-cells from the frozen tissues. Therefore, real-time PCR was performed using whole tumour blocks and the extent of T-cell infiltration was determined by quantifying *CD3* transcripts and performing CD3 IHC.

Real-time PCR and IHC for CD3 suggested that all but three breast cancer samples (cases #1, #6 and #13) had high levels of CD3⁺ T-cell infiltration. Since the cell-specific origin of transcripts cannot be determined, this leaves the significance of the real-time PCR data of limited value, as *FOXP3* and *CXCR4* are well known to be expressed by leukocytes, as well as epithelial cells.

Both LN-negative and LN-positive breast cancer cases had high levels of infiltrating CD3⁺ T-cells in comparison to the normal tissue. Because of the opposing outcomes between LN-negative and LN-positive cases, data from this study would suggest that there was no correlation between CD3⁺ T-cell infiltration and patient prognosis.

5.6.3 Source of normal tissue for CXCR4 staining

One the strengths of this chapter was the care taken to find ‘normal’ breast tissue. Often, when investigating the changes from normal and cancerous tissue, the peritumoural tissue is taken adjacent from the tumour and used as normal control breast tissue. Because these regions of tissue show no overt signs of malignancy they are considered as good control tissue. However, this study suggests that the peritumoural tissue is affected by changes associated with the tumour microenvironment. Regions of peritumoural tissue described as non-malignant by a Pathologist were stained for CXCR4. This tissue was CXCR4-positive. However, tissue from two independent breast reduction surgeries, which were both completely free from malignancy, was CXCR4-negative.

The presence of a tumour mass, which has considerable growth advantages compared to normal tissue, changes the levels of nutrients, and oxygen, supplied to cells, inducing a hypoxic environment. Interestingly, epithelial cells are known to upregulate CXCR4 when exposed to hypoxia. This is driven by HIF-1 α (Ishikawa, Nakashiro et al. 2009; Liu, Xue et al. 2010; Melchionna, Romani et al. 2010) which is discussed in section 1.6.3.1. This suggests that the stresses placed on the normal epithelial cells by the presence of the tumour are able to induce CXCR4, potentially through induction of hypoxia.

Although the tissue taken from the reduction surgery was deemed as the best tissue to use as “normal”, it could also be questioned to how normal this tissue is as reduction surgeries are generally performed due to abnormally large breasts or obesity. Interestingly, when the tissue from the reduction surgery was observed, it contained a great detail of adipose tissue, suggesting the patients may have been clinically overweight. As mentioned in section 1.4.1, risk factors associated with an increased risk of breast cancer development include weight and diet. Although these samples

were considered as the best source of control tissue available, using tissue from breast resection surgeries should also be approached with caution.

5.6.4 FOXP3 IHC staining in normal tissue

As discussed, the source of the normal tissue was important, but it should also be noted that tissue chosen for optimising FOXP3 staining was also important.

Because of the different expression levels of FOXP3 in specific cells, staining must be optimised for the specific cell type which is targeted. Normal breast resection tissue was used to optimise FOXP3 staining. The expression of *FOXP3* is estimated to be approximately 100-fold lower than the expression observed in Tregs (Wang, Liu et al. 2009). Therefore, if staining was optimised using a positive control, such as Tregs, then the conditions might not be sensitive enough to detect the protein in cells where the expression is considerably lower. Several studies suggest that *FOXP3* is frequently downregulated amongst breast cancer cases in comparison to their normal counterparts (Zuo, Liu et al. 2007; Merlo, Casalini et al. 2009). Therefore, a protocol optimised to detect FOXP3 in normal breast cells acts as a benchmark to measure potential increases or decreases of FOXP3 in breast cancer samples.

CD3 and CXCR4 were successfully stained by the QE Hospital using the automated staining equipment within the Pathology Department. However, because of the low level expression of FOXP3, the automated machinery within the QE Hospital and RVI Hospital was not able to detect FOXP3 in these tissues. This notion is consistent with other studies which have reported similar difficulties with extended antigen retrieval steps and antibody incubations being required to stain normal breast tissue (Wang, Liu et al. 2009).

Previous members of this research group have stained FOXP3 in normal breast tissue manually. This protocol led to the detection of FOXP3 within epithelial cells of normal breast samples.

5.6.5 FOXP3 and CXCR4 IHC staining in breast cancer patients

Following FOXP3 and CXCR4 staining in breast cancer samples, each slide was blind scored by a pathologist using the allred quick scoring system. When scored, only epithelial cells within regions demonstrating clear malignancy were graded.

Ideally, this element of the study would have been improved by dual staining of FOXP3 and CXCR4 on each patient sample. This would have allowed a more direct comparison of FOXP3 and CXCR4 expression in individual epithelial cells. IF staining of FOXP3 and CXCR4 with separate fluorescent probes may have provided a clearer, more quantitative, method of determining the expression levels of each protein. This also would have made the subcellular distribution of each protein easier to distinguish. However, due to the low levels of FOXP3 expression, and the difficulty in achieving the required staining intensity, it was deemed that staining for FOXP3 and CXCR4 on separate slides was the best method to use.

Although CXCR4 was not detectable in the normal breast reduction tissues, it was upregulated on all LN-negative and LN-positive samples. The expression of CXCR4 is correlated with an increased risk of lymph node metastasis and an overall poor prognosis (Salvucci, Bouchard et al. 2006; Parker, Kim et al. 2012; Xu, Shen et al. 2013). However, this study showed no apparent difference between the CXCR4 staining in the LN-negative and LN-positive breast cancer patients. This data could suggest that CXCR4 is upregulated within the early stages of carcinogenesis, a notion in accordance within the literature which have reported that CXCR4 is upregulated as early as ADH with the expression of CXCR4 increasing as cancer becomes more aggressive (Schmid, Rudas et al. 2004). Data in this study shows that FOXP3 was clearly observable within the LN-negative and LN-positive breast cancer cases. In addition to this, there was no observable difference in FOXP3 expression in the cancerous tissues in comparison to the normal breast tissues which suggest that FOXP3 has no prognostic significance in breast cancer.

Many reports suggest that FOXP3 is downregulated in breast cancer, and that this dysregulated expression of FOXP3 is correlated with a poor prognosis (Zuo, Wang et al. 2007; Merlo, Casalini et al. 2009). However, several recent reports have

opposed these findings by suggesting that FOXP3 expression increases in cancer cells as the disease stage progresses (Kim, Koo et al. 2013; Lal, Chan et al. 2013).

Wang et al (Wang, Liu et al. 2009) reported that FOXP3 downregulation occurred with epithelial neoplasia in prostate cancer suggesting FOXP3 inactivation occurs within early stages of carcinogenesis. Interestingly, Merlo et al (Merlo, Casalini et al. 2009) reported that FOXP3 which was absent or restricted to the cytoplasm of breast epithelial cells, represented a worse overall survival than patients who had nuclear FOXP3. This suggests that despite its presence, the distribution of FOXP3 is equally important.

5.7 Conclusion

In conclusion, the aim of this study was to assess the potential correlation between the expression of *FOXP3* and *CXCR4* in breast cancer *in vivo*.

Due to the condition of the frozen tumours available epithelial cells were unable to be selected using FACS. Normal breast tissue showed little infiltration by CD3⁺ T-cells, however, the number of these cells is greatly increased in breast cancer. Regrettably, since the cell specific origin of *FOXP3* and *CXCR4* in the frozen tumours cannot be determined, the transcript results are of limited value.

Due to the different sizes of lymphocytes and epithelial cells, IHC staining allows of lymphocytes and epithelial cells to be discriminated. The expression of *CXCR4* is present in increased levels in breast cancer. The expression of *CXCR4* was similar between LN-negative and LN-positive breast cancer samples. *CXCR4* was not detected in epithelial cells from normal breast tissue, however, the presence of *CXCR4* on normal epithelial cells peripheral to areas of cancer suggests that the expression of *CXCR4*, to some extent, may be a non-specific consequence of breast cancer.

IHC protocols to detect *FOXP3* expression in normal breast tissue required extensive optimisation. This demonstrates that *FOXP3* is expressed at low levels in these tissues. This technique showed little difference in *FOXP3* expression between normal and breast cancer tissues. Moreover, these results suggest that *CXCR4* upregulation in breast cancer is not directly correlated with *FOXP3* downregulation.

	Chapter
General introduction	1
General materials and methods	2
Study of FOXP3 expression in normal and malignant breast cell lines	3
<i>In vitro</i> modelling of FOXP3 expression in normal and malignant breast cell lines	4
<i>In vivo</i> levels of FOXP3 and CXCR4 expression in breast cancer samples	5
Discussion	6
List of references	7
Appendices	8

6 Discussion

6.1 The role of FOXP3 in breast cancer

The main aim of this project was to investigate the impact of FOXP3 on breast cancer. Until recently, FOXP3 was considered to be a marker of Tregs and restricted to the lymphocyte lineage. However, low levels of FOXP3 have now been identified within the epithelial cells of some organs (Chen, Chen et al. 2008; Merlo, Casalini et al. 2009; Wang, Liu et al. 2009; Zhang and Sun 2010; Frattini, Pisati et al. 2012; Lal, Chan et al. 2013). Since the discovery of FOXP3 in these cells is a relatively recent area of research, the full function of FOXP3 in epithelial cells has not been fully elucidated.

Normal human epithelial cells contain both natural FOXP3 isoforms within the nucleus in approximately equal proportions (Zuo, Wang et al. 2007). However, it is frequently downregulated, mutated, completely absent or predominately restricted to the cytoplasm in malignant cells (Zuo, Wang et al. 2007; Merlo, Casalini et al. 2009; Wang, Liu et al. 2009; Zhang and Sun 2010; Frattini, Pisati et al. 2012). Despite recent studies describing an increase in epithelial FOXP3 as cancer progresses (Kim, Koo et al. 2013; Lal, Chan et al. 2013), FOXP3 is generally considered to have strong anti-cancer properties and acts as a potent TSG by directly repressing the expression of many key oncogenes including *ErbB2*, *SKP2*, *c-Myc*, *LATS2* whilst increasing the expression of p21 (Zuo, Liu et al. 2007; Zuo, Wang et al. 2007; Liu, Wang et al. 2009; Wang, Liu et al. 2009; Zhang and Sun 2010; Li, Wang et al. 2011; Frattini, Pisati et al. 2012; Li, Katoh et al. 2013; Nakahira, Morita et al. 2013).

Despite never being identified as direct FOXP3 targets, transfection of a FOXP3 expression plasmid into ovarian and breast cancer cell lines led to the repression of several molecules including *MMP2* and *uPA* (Zhang and Sun 2010) and *MMP9* and *VEGFA* (Nakahira, Morita et al. 2013). FOXP3 is also involved in inhibiting the activation of NF- κ B and mTOR signalling (Zhang and Sun 2010). In a similar manner to p21, FOXP3 can also regulate the expression of p18, which is also a

molecule involved in cell cycle arrest at the G₁ phase (Liu, Wang et al. 2009). Therefore, FOXP3 has the capacity to influence a number of important downstream pathways involved in carcinogenesis

Reports have not only demonstrated that FOXP3 is able to regulate the expression of oncogenes, *in vitro* and *in vivo* studies have suggested it is also able to mediate the proliferation (Zuo, Liu et al. 2007; Zuo, Wang et al. 2007; Liu, Wang et al. 2009; Wang, Liu et al. 2009; Zhang and Sun 2010; Li, Wang et al. 2011; Frattini, Pisati et al. 2012), migration (Zhang and Sun 2010; Frattini, Pisati et al. 2012), invasion (Zhang and Sun 2010; Nakahira, Morita et al. 2013) and survival of cancer cells (Zuo, Wang et al. 2007; Wang, Liu et al. 2009; Frattini, Pisati et al. 2012; Li, Katoh et al. 2013).

Wang et al (Wang, Liu et al. 2009) used a system to generate mice with a floxed-*FOXP3* gene specific to the prostate epithelial cells. These authors demonstrated that a *FOXP3* deletion was able to generate the onset of prostate cancer in new born mice. This emphasises that FOXP3 is not just a molecule which becomes dysregulated as cancer progresses, but it may also be involved in the initial carcinogenic transformation of cells. By contrast, a report investigating Foxp3 in murine glioblastoma cells demonstrated that Foxp3 was still present in early stages of tumour development but diminished through tumorigenesis (Frattini, Pisati et al. 2012).

Few mechanisms have been identified which control the expression of FOXP3 in epithelial cells. However, a report by Jung et al (Jung, Jin et al. 2010) used chIP to demonstrate that p53 directly upregulated FOXP3 in cancer cells. Because p53 is mutated in more than 50% of cancers (Hollstein, Rice et al. 1994), this would suggest that the frequency of FOXP3 also being dysregulated in these cells is equally high.

Based on data from the current study, the importance of FOXP3 can be discussed from two separate angles. Much of the *in vitro* data agrees that FOXP3 acts as a potent TSG, whereas, *in vivo* data implies the involvement of FOXP3 in breast cancer may be limited.

Initial experiments focused on the expression of FOXP3 in two breast cancer cell lines. Within both these cell lines FOXP3 was significantly downregulated at both protein and transcript levels. Interestingly, the non-invasive, MCF-7 contained both natural isoforms which were predominately located within the nucleus. This finding was similar to HMEpC, although these cells expressed higher levels of FOXP3. On the other hand, in the invasive MDA-MB-231, FOXP3 was predominately restricted to the cytoplasm and the natural *FOXP3Δ3* isoform was not expressed. This isoform has been recently reported to be important in preventing migration and invasion of cells *in vitro* (Frattoni, Pisati et al. 2012).

The function of FOXP3 in MDA-MB-231 and HMEpC was investigated by *in vitro* modelling. Stable overexpression of FOXP3 in MDA-MB-231 led to a significant reduction in *HER2*, *SKP2*, *MYC* and *CXCR4* transcripts. By contrast, the expression of p21 was increased. FOXP3-overexpression also inhibited proliferation and increased the proportion of cells within the G₁ phase of the cell cycle. Conversely, when FOXP3 was knocked down in HMEpC, there was almost an exact inverse of the profile witnessed when FOXP3 was transfected into MDA-MB-231. FOXP3 knockdown also increased the migratory capacity of HMEpC. This does not prove that FOXP3 limits the potential of breast cancer invasiveness but it does suggest that FOXP3 can influence a number factors frequently implicated in cancer progression and acts in an ‘anti-tumour’ manner.

On the other hand, the *in vivo* data from FOXP3 IHC on breast cancer patient samples showed that none of the cancer samples, regardless of LN-involvement or survival, had observably downregulated FOXP3 in comparison to normal mammary tissue.

6.2 The role of FOXP3 on CXCR4 expression

Because FOXP3 is a transcription factor, the main role it has in cancer is the ability to regulate the expression of specific genes. As reviewed by Douglass et al (Douglass, Ali et al. 2012), and data from this study, have suggested that FOXP3 has the ability to regulate a number of oncogenes, however, the ability of FOXP3 to

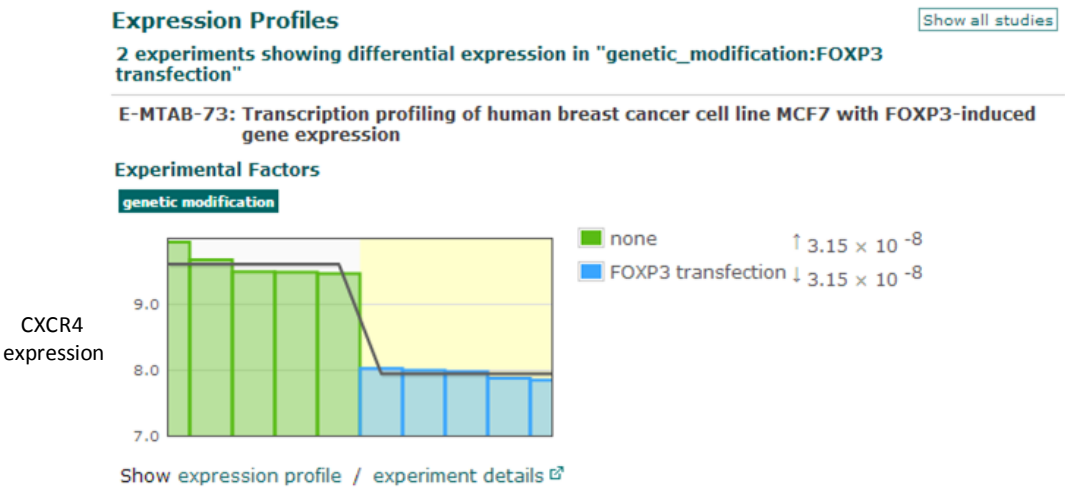
influence the expression of *CXCR4* is unreported. This makes the investigation of a FOXP3-*CXCR4* interaction the most novel aspect of this study.

Unlike FOXP3, *CXCR4* is a well established molecule involved in breast cancer (Li, Pan et al. 2004; Smith, Luker et al. 2004; Luker and Luker 2006; Liang, Brooks et al. 2007). *CXCR4* is a chemokine receptor which was first identified as a lymphocyte homing receptor. It is now also known that *CXCR4* is a key mediator in the site-specific metastasis of breast cancer (Muller, Homey et al. 2001). As well as the expression profile of *CXCR4* and *CXCL12*, the signalling pathways involved with these molecules demonstrate their importance in breast cancer as they regulate far more than just the ability to direct cell migration, including increased survival, invasion and proliferation of cancer cells (Murakami, Maki et al. 2002; Allinen, Beroukhi et al. 2004; Orimo, Gupta et al. 2005; Luker and Luker 2006).

Although it would appear that the functions of FOXP3 in lymphocytes and epithelial cells are not similar, potential links between FOXP3 and *CXCR4* may exist in T-cells. For instance, naive T-cells have negligible levels of FOXP3, and detectable levels of *CXCR4*. However, following T-cell activation, the levels of FOXP3 transiently increase (Pekalski, Jenkinson et al. 2013) whilst the expression of *CXCR4* is reduced (Newton, O'Boyle et al. 2009).

The European Bioinformatics Institute recently performed a meta-analysis to investigate the potential of FOXP3 to regulate *CXCR4* expression in MCF-7. Their analysis suggested that FOXP3 transfection into MCF-7, results in a significant decrease in the expression of *CXCR4*, thus suggesting FOXP3 is able to regulate *CXCR4* in breast cancer cells (**figure 6.1 panel A**) (EMBL-EBI 2013). On the other hand, despite FOXP3 being reported to be a TSG in prostate epithelial cells, and *CXCR4* also reported to be overexpressed in prostate cancer (Singh, Singh et al. 2004; Chinni, Yamamoto et al. 2008; Wang, Liu et al. 2009), the same company reported that FOXP3 transfection into the human prostate cancer cell line (LNCaP) would increase *CXCR4* expression (**figure 6.1 panel B**) (EMBL-EBI 2013). This suggests that the regulatory function of FOXP3 on *CXCR4* expression may not be consistent between epithelial cells.

A



B

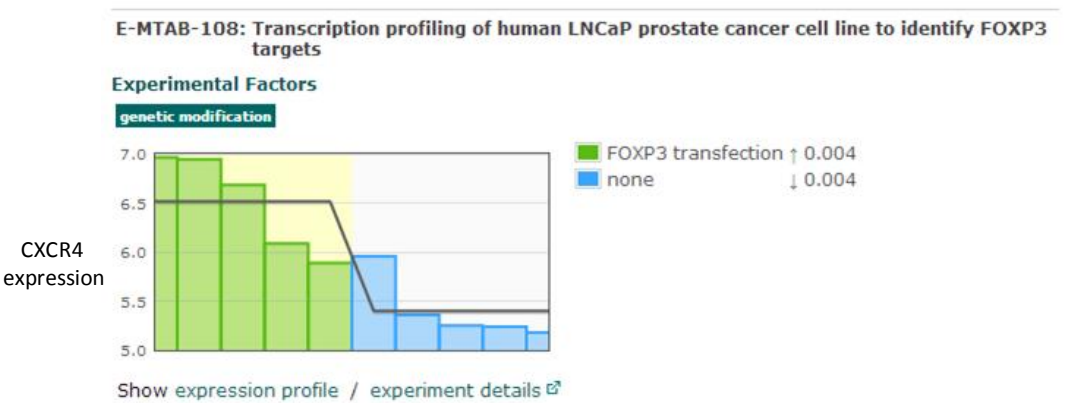


Figure 6-1 - Effects of CXCR4 expression following FOXP3 transfection into malignant breast and prostate cell lines

Meta-analysis results produced from EMBL-EBI suggested that following FOXP3 transfection into MCF-7 would significantly decrease the expression of CXCR4 (A) whereas, if FOXP3 was transfected into the prostate cancer cell lines, LNCaP, it increases the expression of CXCR4 (B). Screen shot image from webpage (EMBL-EBI 2013).

Cancer is a complex genetic disease, and the dysregulation reported in the signalling pathways within malignant cells is often difficult to comprehend. Due to the complexity of these pathways, and the number of molecules able to regulate them, the fact that specific cancers commonly overexpress certain molecules makes it unlikely that the factors responsible for the overexpression are consistent between the cells.

The network involved in regulating the expression of CXCR4 is equally complex. There are many reports describing a number of factors involved with several mechanisms which can regulate the expression CXCR4, suggesting it can be influenced downstream of many pathways (Luker and Luker 2006). This wide spread ability to increase CXCR4 is most likely one key reason why it is so frequently expressed in a number of malignancies.

6.3 Concluding thoughts

This project was designed primarily to investigate the impact of FOXP3 expression in breast cancer progression. I believe that results from this study have provided strong evidence to suggest that FOXP3 is able to regulate the expression of several important oncogenes and the function of epithelial cells *in vitro*. FOXP3 can be considered an important factor involved in breast cancer development.

Another direction the project took was to investigate the potential of FOXP3 to regulate CXCR4. The complexity of the signalling pathways and the multitude of factors involved in CXCR4 regulation make it very conceivable that there will be cross talk between FOXP3 and CXCR4 in breast epithelia at a molecular level. Indeed some of the data from this project suggests that FOXP3 is able to influence the expression of CXCR4 at low levels in breast cancer cell lines.

However, from these results, the ability of FOXP3 to directly influence CXCR4 in a similar manner to *ErbB2* and *SKP2* seems unlikely and probably relies on a number of other pathways downstream from FOXP3. Therefore, because any changes in CXCR4 expression are probably dependent on several other factors, it's difficult to conclude that FOXP3 regulates CXCR4, but is probably more accurate to suggest that it has the potential to be influenced at a modest level and FOXP3 represents a

small part of a much larger puzzle involving the upregulation of CXCR4 in breast cancer.

A few possible downstream signalling pathways of FOXP3 which could contribute to CXCR4 expression are discussed in the next section

6.4 Potential FOXP3 - CXCR4 mechanisms

The literature describes a number of pathways by which functional FOXP3 can modify CXCR4 expression in breast epithelial cells (**figure 6.2 panel A**).

Although direct links between FOXP3 and CXCR4 in epithelial cells have never been published in the literature, evidence suggests that FOXP3 can regulate *CXCR4* in T-cells. Zheng et al (Zheng, Josefowicz et al. 2007) performed a genome-wide analysis of FOXP3 target genes in Tregs. They reported that in naive thymic T-cells, *CXCR4* was a FOXP3 target gene. This suggests that the CXCR4 promoter may contain FOXP3 binding sites allowing FOXP3 to directly regulate the expression of CXCR4. However, as mentioned, it remains controversial how translatable the roles of FOXP3 and CXCR4 are in lymphocytes and epithelial cells. A number of indirect mechanisms also exist which are discussed below:

The ability of FOXP3 to directly repress HER2 in breast epithelia has been demonstrated by Zou et al (Zuo, Wang et al. 2007) using several strong lines of evidence where a loss in FOXP3 subsequently resulted in an increased expression of HER2. By contrast, the overexpression of HER2 on breast cancer cells has been demonstrated to increase the expression of CXCR4 (Li, Pan et al. 2004). It is thought that this HER2-mediated increase in CXCR4 occurs via the PI3K/Akt/mTOR pathway (Li, Pan et al. 2004).

A further pathway can be proposed which is mediated through NF- κ B signalling. FOXP3 has been shown to repress NF- κ B in a number of reports (Grant, Oh et al. 2006; Zhang and Sun 2010; Loizou, Andersen et al. 2011). Loizou et al (Loizou, Andersen et al. 2011) published data suggesting that FOXP3 is able to repress the expression of NF- κ B through the c-Rel domain. This report suggested that the N-terminal region of FOXP3 was required for c-Rel interaction, whereas, the forkhead box domain was not associated with c-Rel interaction. A separate report by Grant et

al (Grant, Oh et al. 2006) also demonstrated that FOXP3 was able to inhibit the expression of NF- κ B, however, the regions of FOXP3 responsible for this repression opposed the finding from Loizou et al (Loizou, Andersen et al. 2011). Grant et al (Grant, Oh et al. 2006) demonstrated that deletion of the FOXP3 forkhead domain abrogated the ability of FOXP3 to suppress NF- κ B in HEK cells (the same cell line used by Liouzhou et al (Loizou, Andersen et al. 2011)). Interestingly, the forkhead domain was not required for NF- κ B repression in primary CD4⁺ T-cells or Jurkats. This suggests that although the ability of FOXP3 to repress NF- κ B is consistent, the mechanisms responsible for this repression differ between cell types. A report investigating the role of FOXP3 in ovarian cancer cells by Zhang and Sun (Zhang and Sun 2010) demonstrated that following FOXP3 transfection into SKOV3 cells, there was a subsequent decrease in NF- κ B. This suggests that FOXP3 is also able to inhibit NF- κ B in epithelial cells.

A report by Helbig et al (Helbig, Christopherson et al. 2003) produced comprehensive data demonstrating that NF- κ B is able to bind directly to the promoter of *CXCR4* leading to increased expression. The increase in CXCR4 was of functional importance as the cells were able to migrate significantly more in response to CXCL12, demonstrating the importance of NF- κ B in CXCR4-mediated breast cancer metastasis (Helbig, Christopherson et al. 2003). Interestingly, research groups have also reported that NF- κ B is able to regulate the expression of MMP2, MMP9 (Ogawa, Chen et al. 2004; Lin, Lu et al. 2010), uPA (Reuning, Wilhelm et al. 1995; Zhang and Sun 2010; Moreau, Mourah et al. 2011) and a number of cytokines in highly metastatic breast cancer cell lines (Karin and Greten 2005; Karin 2009), further contributing to the potential downstream effects of FOXP3.

Although Li et al (Li, Pan et al. 2004) demonstrated the ability of HER2 to increase CXCR4, suggesting the PI3K/Akt/mTOR pathway was responsible for this, a study by a separate group suggests that an alternative pathway signalling through NF- κ B may exist. Merkhofer et al (Merkhofer, Cogswell et al. 2010) suggested that HER2 is able to activate NF- κ B using a completely Akt-independent pathway, utilising a canonical pathway involving IKK α . The importance of this signalling pathway in breast cancer was emphasised by the ability of this signalling pathway to inhibit breast cancer invasion (Merkhofer, Cogswell et al. 2010). The influence of increased NF- κ B signalling appears to be a key mediator of many breast cancer signalling

pathways. Its effects on breast cancer progression can be expanded further by also regulating the expression of VEGF (Shibata, Nagaya et al. 2002; Ramanathan, Pinhal-Enfield et al. 2007). Interestingly, a recent study by Nakahira et al (Nakahira, Morita et al. 2013) reported that upregulation of FOXP3 by LCK in MCF-7 resulted in a significant reduction in *VEGFA* expression. Moreover, the subsequent expression of VEGF has also been shown to regulate the expression of CXCR4 (Kijowski, Baj-Krzyworzeka et al. 2001; Zagzag, Lukyanov et al. 2006) therefore, providing another pathway.

As well as the potential mechanisms of FOXP3-mediated CXCR4 expression previously discussed, a number of reports have also suggested possible feedback loops which can accentuate CXCR4 expression (**figure 6.2 pathways labelled B**).

Upon binding of CXCL12 to CXCR4, a number of processes are activated. CXCL12-CXCR4 signalling is able to transactivate HER2 in breast (Cabioglu, Summy et al. 2005) and prostate (Chinni, Yamamoto et al. 2008) cancer cells, subsequently increasing the ability of cells to migrate and metastasise. CXCR4 signalling is also able to increase the expression of VEGF (Liang, Brooks et al. 2007). This CXCR4-mediated VEGF regulation was reported to be dependent on the PI3K/Akt pathway (Liang, Brooks et al. 2007).

Finally, studies on oral cancer have demonstrated that CXCL12 is able to activate NF- κ B which is able to promote cell invasion through the Carma3/bc110.Malt1 complex (Rehman and Wang 2009).

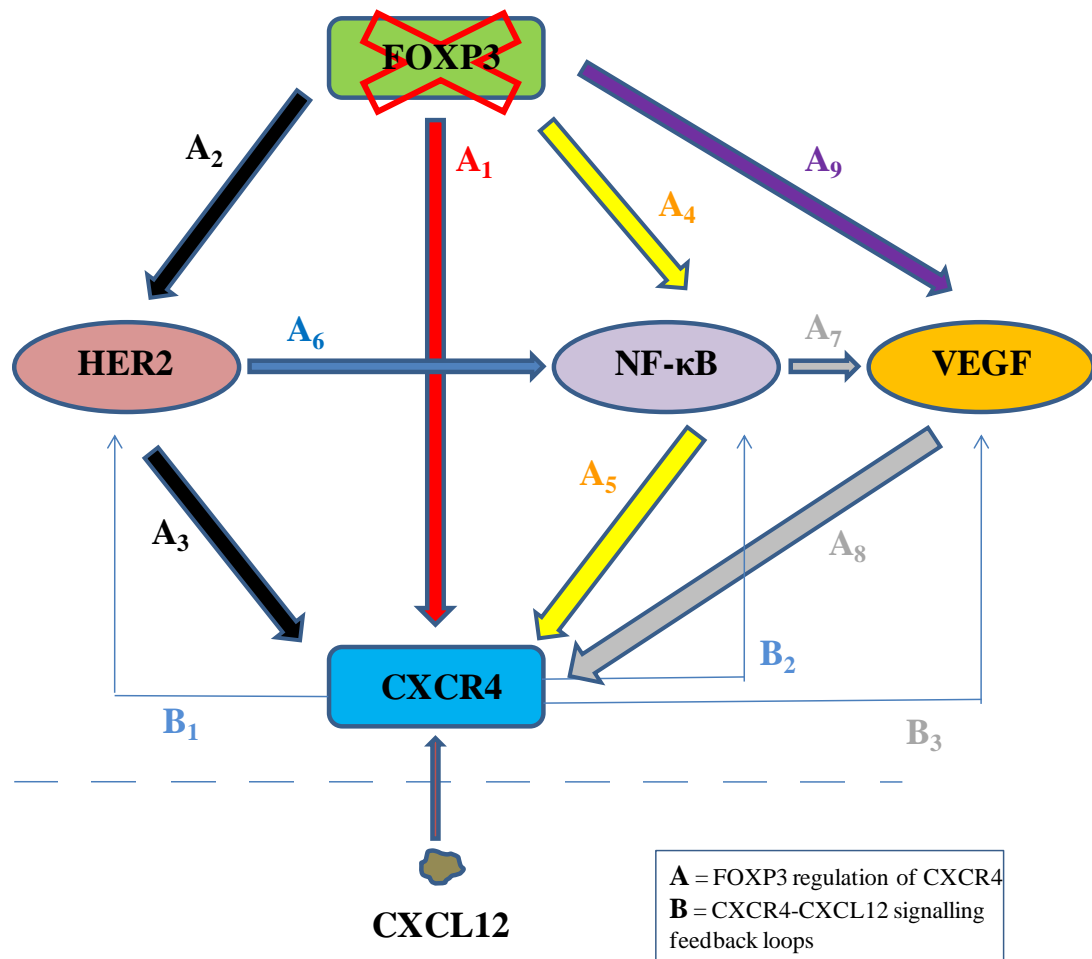


Figure 6-2 - Potential mechanisms of FOXP3 influencing CXCR4 expression

Should FOXP3 functioning be lost in epithelial cells, a number of possible pathways could increase CXCR4 expression.

(A₁) CXCR4 has been identified as a FOXP3 target gene in developing thymic T-cells, therefore, suggesting CXCR4 could be directly regulated by FOXP3. Alternatively, (A₂) FOXP3 acts as a direct repressor to HER2 in breast epithelial cells, whereas, (A₃) increased expression of HER2 is able to increase the expression of CXCR4 through the PI3K/Akt/mTOR pathway. (A₄) FOXP3 has been demonstrated by a number of research groups to interact and regulate the activation of NF-κB, which is then (A₅) able to upregulate CXCR4 by directly binding in the promoter region. (A₆) An alternative route via HER2 can be proposed as HER2 is able to activate NF-κB expression, independent of the PI3K/Akt/mTOR pathway, through the canonical pathway. (A₇) NF-κB is able to increase the expression of VEGF, which in turn (A₈) is able to increase the expression of CXCR4. (A₉) FOXP3 has recently been identified as a factor which is able to repress the expression of VEGF-A.

A number of feedback loops signalling through CXCR4 could potentially continue the increased expression of the chemokine receptor. (B₁) Upon binding of the CXCR4 ligand, CXCL12, it has been reported in prostate and breast epithelial that HER2 becomes transactivated. (B₂) CXCR4 signalling has also been demonstrated to increase the activation and signalling of NF-κB and also (B₃) VEGF.

6.5 Therapeutic implications

Both the emergence of FOXP3, and the established role of CXCR4 in breast cancer have been acknowledged by a number of research groups who have investigated the potential to possibly treat cancer by targeting FOXP3 restoration and inhibiting CXCR4 *in vitro* and *in vivo*. A number of these are discussed.

6.5.1 FOXP3 therapies

Many papers have now demonstrated on several lines of evidence that FOXP3 is a potent tumour suppressor regulating a number of oncogenes. Because FOXP3 is reported to be dysregulated in many malignant tissues, this suggests the potential for FOXP3-based therapies. Many of these therapies have been discussed by Douglass et al (Douglass, Ali et al. 2012).

The majority of breast cancers with *FOXP3* mutations have demonstrated that these mutations are heterozygous with transcripts of the gene originating from the mutant alleles. Similarly, all cases which describe deletions of *FOXP3* are also heterozygous. This leaves the wild type allele silenced within the tumour cell whilst emphasising that a single hit is enough to inactivate *FOXP3*.

Some reports have focused on the concept of re-activating wild type *FOXP3* to normalise the biology of cancer cells which lack the wild type protein. Because one of the alleles of the X-linked genes has not undergone selection during carcinogenesis, it will remain unaffected; therefore, the prospect of re-activating X-linked TSGs as a cancer therapy would be appealing. Despite our knowledge of the how X-chromosome inactivation is induced, how this inactivation is maintained is far less defined. In addition to this, the concept of re-activating the function of an inactivated TSG is one of the most challenging aspects in cancer therapy. However, even if this became a possibility, it should be emphasised that the re-activation of X-linked genes must be approached with considerable care due to the potential of side effects. Naturally, any potential side effects could be minimised, or avoided, if specific genes could be selectively reactivated.

As of yet, there are no pharmaceutical companies which have designed drugs to reactivate X-linked TSGs; however, a number of studies have well-constructed research models which induce the expression of FOXP3 in cancer cells.

The TSG p53 is able to upregulate the expression of FOXP3 in breast and prostate cell lines, whereas, doxorubicin is able to activate p53 which leads to increased transcription of FOXP3 (Jung, Jin et al. 2010). Alternatively, administration of anisomycin to several human breast cancer cell lines led to increased expression of FOXP3. Moreover, this increase in FOXP3 was able to induce apoptosis and reduce the growth rate of pre-established tumours in murine models of breast cancer. This upregulation was reported to be due to activating c-Jun and AFT2 heterodimers (Liu, Wang et al. 2009).

Recently, gene therapy has become a popular method of restoring normal expression of dysfunctional genes. However, these methods have often had technical challenges which result in a poor outcome. Alternatively to gene therapy, reasonable success has been highlighted using antibody-mediated protein therapy of FOXP3 in numerous *in vitro* and *in vivo* models (Heinze, Baldwin et al. 2009). When the Fv region of a monoclonal antibody tagged with a FOXP3 fusion protein was able to induce a dose-dependent cell death of breast, ovarian and colon cancer cells *in vitro* (Heinze, Baldwin et al. 2009). *In vivo* administration of this antibody in Balb/c mice was able to reduce the metastasis of colon tumours to the liver (Heinze, Baldwin et al. 2009).

Not only do these reports provide the early signs of exciting innovative techniques to overcome cancer, they also propose that FOXP3-based therapies have real potential as a novel therapeutic. However, the requirement to fully understand the molecular mechanisms involved in these techniques cannot be underestimated and the need to validate whether the re-introduction of FOXP3 can be explored as a safe cancer therapy.

6.5.2 CXCR4 inhibitors

Unlike FOXP3, which is still a relatively emerging molecule in cancer research, CXCR4 is a well established chemokine receptor in a number of malignancies which potentially makes it a good target for cancer.

Several research groups have now investigated whether inhibition of CXCR4 expression can potentially prevent tumour growth. Plerixafor, also known as AMD3100, is a molecule which is able to block CXCR4. Because CXCR4 acts a co-receptor for certain HIV virus strains, it was later used as a drug for HIV treatment (Davies 2007).

Because CXCR4 is heavily involved in cancer, it has also recently been hypothesised as a potent drug for cancer treatment. This hypothesis has been validated by a number of *in vitro* and *in vivo* cancer studies. For instance, treatment with AMD3100 was able to reduce the growth of both the primary and metastatic breast tumours in mice (Smith, Luker et al. 2004). However, despite this reported success with AMD3100, 70% of the drug is excreted within 24 hours meaning the pharmacokinetics of this drugs have made the clinical translation of AMD3100 difficult. A recent report by O'Boyle et al (O'Boyle, Swidenbank et al. 2013) demonstrated that an alternative CXCR4 inhibitor, AMD11070, is not only able to reduce the migration of melanoma cells, but the reduced migration was also significantly more effective than AMD3100. Because AMD11070 can be taken orally and has a more favourable pharmacokinetic profile in comparison to AMD3100, if the prospect of using CXCR4 inhibitors to treat breast cancer progressed, the use of AMD11070 may be the better choice to use.

On the other hand, because CXCR4 is expressed by a number of lymphocytes and is involved in lymphocyte homing, unless the CXCR4 actions could be targeted directly towards epithelial cells, chronic blockage of CXCR4 may result in adverse immunological side effects

6.6 Limitations and future directions for the study

A number of factors limited the progress of this research. These are described below together with strategies for their mitigation or circumvention. Novel areas for investigation suggested by the study are also described.

- One of the main aims of this project was to investigate the impact of restoring FOXP3 into MDA-MB-231. Initially, the project set out to generate MDA-MB-231 stably transfected with FOXP3. Although this was achieved, it proved technically challenging to transfect these “hard-to-transfect” cells. Following successful transfection, an increase in p21 expression was observed which led to a reduction in cell proliferation and the suggestion of FOXP3-induced senescence. Although this was not formally a “limitation”, studies of cell function were not possible.

One method to address this is by use of a tetracycline-inducible FOXP3 system in MDA-MB-231. Tetracycline induction of FOXP3 expression by HEK cells was used successfully in this study. Other groups have reported use of tetracycline-inducible FOXP3 in MCF-7 (Zuo, Liu et al. 2007; Liu, Wang et al. 2009; Li, Wang et al. 2011). This system would avoid the induction of FOXP3-mediated senescence, as FOXP3 expression could be regulated when required.

Alternatively, viral transduction has become a very popular method of transfection as it appears to have greater transfection efficiencies and cell viability than lipofection or electroporation. This technique uses viruses as carriers of the plasmid DNA to infect cells and causes a very reproducible and high level of transfection efficiency. Unfortunately, permission to use viral transduction is only granted when the laboratories have the specific safety measures in place. During this phase of the project, our laboratory was not permitted to perform viral transduction.

- The final aspect of the study aimed to investigate the expression of FOXP3 and CXCR4 at transcript and protein levels in patient samples. Although a range of frozen cancer samples was available for this study, the condition of the preserved tissue made it impossible to separate T-cells expressing FOXP3

and CXCR4 from breast cancer cells. This meant that transcript findings were of limited value as heavy T-cell infiltration was observed in almost all tumour samples.

A further study using fresh tissue would eliminate this problem. Combination with either laser microdissection or *in situ* hybridisation would allow specific quantification of cancer cell-associated *FOXP3* and *CXCR4*.

- *FOXP3* is expressed at very low levels in normal mammary epithelial cells. Protocols to detect this protein by automated IHC all failed as a consequence of inadequate sensitivity. A manual protocol developed by previous members of this group to detect *FOXP3* in normal mammary epithelial cells was more successful but the resolution did not allow discrimination between nuclear and cytoplasmic staining. A number of research groups have reported the subcellular distribution of *FOXP3* to be important in cancer (Hinz, Pagerols-Raluy et al. 2007; Merlo, Casalini et al. 2009; Wang, Liu et al. 2009). In order to generate more useful data the IHC method will require further development to enhance its spatial resolution.
- Although results regarding *FOXP3*-*CXCR4* interactions are slightly ambiguous in this study, some aspects do suggest that *FOXP3* is able to influence the expression of *CXCR4* at a modest level. Section 6.4 has discussed a number of potential mechanisms by which *FOXP3* could regulate *CXCR4* expression indirectly. However, because *FOXP3* is a transcription factor which is able to directly repress a number of genes, a chIP assay would confirm whether *FOXP3* is able to directly bind and regulate *CXCR4* in a similar manner to how *ErbB2*, *SKP2*, *c-Myc*, *LATS2*, and *p21*, are regulated.
- As a transcription factor, it is perhaps unsurprising that the majority of reports, including this study, have focused specifically on factors which can be influenced downstream of *FOXP3*. However, because *FOXP3* is commonly reported to be dysregulated which can then lead to an

accumulation of other dysregulated factors, it would be of interest to investigate the factors which are able to regulate the expression of FOXP3. This would represent a very novel direction of research as few studies have reported factors able to regulate FOXP3 in epithelial cells.

Recently, p53 (Jung, Jin et al. 2010) and LCK (Lal, Chan et al. 2013) have been identified as factors able to upregulate FOXP3 in cancer cells, whereas, the methylation status of CpG motifs and protein phosphorylation of FOXP3 are both reported to be important in FOXP3 activation (Lee, Fitzpatrick et al. 2001; Lal, Chan et al. 2013).

	Chapter
General introduction	1
General materials and methods	2
Study of FOXP3 expression in normal and malignant breast cell lines	3
<i>In vitro</i> modelling of FOXP3 expression in normal and malignant breast cell lines	4
<i>In vivo</i> levels of FOXP3 and CXCR4 expression in breast cancer samples	5
Discussion	6
List of references	7
Appendices	8

7 List of references

- Ahmadzadeh, M., A. Felipe-Silva, et al. (2008). "FOXP3 expression accurately defines the population of intratumoral regulatory T cells that selectively accumulate in metastatic melanoma lesions." *Blood* **112**(13): 4953-4960.
- Ahmadzadeh, M. and S. A. Rosenberg (2006). "IL-2 administration increases CD4+ CD25(hi) Foxp3+ regulatory T cells in cancer patients." *Blood* **107**(6): 2409-2414.
- Alfano, D., G. Votta, et al. (2010). "Modulation of cellular migration and survival by c-Myc through the downregulation of urokinase (uPA) and uPA receptor." *Mol Cell Biol* **30**(7): 1838-1851.
- Ali, S. and G. Lazennec (2007). "Chemokines: novel targets for breast cancer metastasis." *Cancer Metastasis Rev* **26**(3-4): 401-420.
- Allan, S. E., S. Q. Crome, et al. (2007). "Activation-induced FOXP3 in human T effector cells does not suppress proliferation or cytokine production." *Int Immunol* **19**(4): 345-354.
- Allan, S. E., L. Passerini, et al. (2005). "The role of 2 FOXP3 isoforms in the generation of human CD4+ Tregs." *J Clin Invest* **115**(11): 3276-3284.
- Allinen, M., R. Beroukhi, et al. (2004). "Molecular characterization of the tumor microenvironment in breast cancer." *Cancer Cell* **6**(1): 17-32.
- Altundag, K., P. Morandi, et al. (2005). "Possible role of CXCR4-mediated chemotaxis in breast cancer patients with central nervous system metastases." *Breast Cancer Res Treat* **89**(3): 317.
- An, Y., Q. Kang, et al. (2013). "Lats2 modulates adipocyte proliferation and differentiation via hippo signaling." *PLoS One* **8**(8): e72042.
- Anastasi, E., A. F. Campese, et al. (2003). "Expression of activated Notch3 in transgenic mice enhances generation of T regulatory cells and protects against experimental autoimmune diabetes." *J Immunol* **171**(9): 4504-4511.
- Andela, V. B., E. M. Schwarz, et al. (2000). "Tumor metastasis and the reciprocal regulation of prometastatic and antimetastatic factors by nuclear factor kappaB." *Cancer Res* **60**(23): 6557-6562.
- Andersson, J., D. Q. Tran, et al. (2008). "CD4+ FoxP3+ regulatory T cells confer infectious tolerance in a TGF-beta-dependent manner." *J Exp Med* **205**(9): 1975-1981.
- Aplin, A. E., A. Howe, et al. (1998). "Signal transduction and signal modulation by cell adhesion receptors: the role of integrins, cadherins, immunoglobulin-cell adhesion molecules, and selectins." *Pharmacol Rev* **50**(2): 197-263.
- Aronowitz, R. A. (2007). *Unnatural history : breast cancer and American society*. Cambridge ; New York, Cambridge University Press.
- Asano, N., T. Watanabe, et al. (2008). "Notch1 signaling and regulatory T cell function." *J Immunol* **180**(5): 2796-2804.
- Aydin, F., T. Akagun, et al. (2011). "Clinicopathologic characteristics and BRCA-1/BRCA-2 mutations of Turkish patients with breast cancer." *Bratisl Lek Listy* **112**(9): 521-523.
- Bacchetta, R., L. Passerini, et al. (2006). "Defective regulatory and effector T cell functions in patients with FOXP3 mutations." *J Clin Invest* **116**(6): 1713-1722.

- Bachelder, R. E., M. A. Wendt, et al. (2002). "Vascular endothelial growth factor promotes breast carcinoma invasion in an autocrine manner by regulating the chemokine receptor CXCR4." *Cancer Res* **62**(24): 7203-7206.
- Bachman, K. E., P. Argani, et al. (2004). "The PIK3CA gene is mutated with high frequency in human breast cancers." *Cancer Biol Ther* **3**(8): 772-775.
- Baeuerle, P. A. and T. Henkel (1994). "Function and activation of NF-kappa B in the immune system." *Annu Rev Immunol* **12**: 141-179.
- Baggiolini, M. (2001). "Chemokines in pathology and medicine." *J Intern Med* **250**(2): 91-104.
- Baguley, B. and E. Leung (2011). "Heterogeneity of Phenotype in Breast Cancer Cell Lines, Breast Cancer - Carcinogenesis, Cell Growth and Signalling Pathways,."
- Baker, D. J., R. L. Weaver, et al. (2013). "p21 both attenuates and drives senescence and aging in BubR1 progeroid mice." *Cell Rep* **3**(4): 1164-1174.
- Balabanian, K., B. Lagane, et al. (2005). "The chemokine SDF-1/CXCL12 binds to and signals through the orphan receptor RDC1 in T lymphocytes." *J Biol Chem* **280**(42): 35760-35766.
- Balkwill, F. (2004). "Cancer and the chemokine network." *Nat Rev Cancer* **4**(7): 540-550.
- Balkwill, F. (2004). "The significance of cancer cell expression of the chemokine receptor CXCR4." *Semin Cancer Biol* **14**(3): 171-179.
- Balkwill, F., K. A. Charles, et al. (2005). "Smoldering and polarized inflammation in the initiation and promotion of malignant disease." *Cancer Cell* **7**(3): 211-217.
- Balkwill, F. and A. Mantovani (2001). "Inflammation and cancer: back to Virchow?" *Lancet* **357**(9255): 539-545.
- Banham, A. H., L. Lyne, et al. (2009). "Monoclonal antibodies raised to the human FOXP3 protein can be used effectively for detecting Foxp3(+) T cells in other mammalian species." *Vet Immunol Immunopathol* **127**(3-4): 376-381.
- Bardin, A., N. Boulle, et al. (2004). "Loss of ERbeta expression as a common step in estrogen-dependent tumor progression." *Endocr Relat Cancer* **11**(3): 537-551.
- Bargou, R. C., F. Emmerich, et al. (1997). "Constitutive nuclear factor-kappaB-RelA activation is required for proliferation and survival of Hodgkin's disease tumor cells." *J Clin Invest* **100**(12): 2961-2969.
- Baumgartner, J., C. Wilson, et al. (2007). "Melanoma induces immunosuppression by up-regulating FOXP3(+) regulatory T cells." *J Surg Res* **141**(1): 72-77.
- Bayer, A. L., J. Y. Lee, et al. (2008). "A function for IL-7R for CD4+CD25+Foxp3+ T regulatory cells." *J Immunol* **181**(1): 225-234.
- Beadling, C. and K. A. Smith (1993). "Tactics for the isolation of interleukin-2-induced immediate-early genes." *Semin Immunol* **5**(5): 365-373.
- Beadling, C. and K. A. Smith (2002). "DNA array analysis of interleukin-2-regulated immediate/early genes." *Med Immunol* **1**(1): 2.
- Beckmann, M. W., D. Niederacher, et al. (1997). "Multistep carcinogenesis of breast cancer and tumour heterogeneity." *J Mol Med (Berl)* **75**(6): 429-439.
- Begg, A. C., F. A. Stewart, et al. (2011). "Strategies to improve radiotherapy with targeted drugs." *Nat Rev Cancer* **11**(4): 239-253.
- Bendre, M., D. Gaddy, et al. (2003). "Breast cancer metastasis to bone: it is not all about PTHrP." *Clin Orthop Relat Res*(415 Suppl): S39-45.
- Berger, C. L., R. Tigelaar, et al. (2005). "Cutaneous T-cell lymphoma: malignant proliferation of T-regulatory cells." *Blood* **105**(4): 1640-1647.

- Bertani, G. (2004). "Lysogeny at mid-twentieth century: P1, P2, and other experimental systems." *J Bacteriol* **186**(3): 595-600.
- Bettelli, E., M. Dastrange, et al. (2005). "Foxp3 interacts with nuclear factor of activated T cells and NF-kappa B to repress cytokine gene expression and effector functions of T helper cells." *Proc Natl Acad Sci U S A* **102**(14): 5138-5143.
- Beyer, M., M. Kochanek, et al. (2005). "Reduced frequencies and suppressive function of CD4+CD25hi regulatory T cells in patients with chronic lymphocytic leukemia after therapy with fludarabine." *Blood* **106**(6): 2018-2025.
- Bhide, S. A. and C. M. Nutting (2010). "Recent advances in radiotherapy." *BMC Med* **8**: 25.
- Bottazzi, B., N. Polentarutti, et al. (1983). "Regulation of the macrophage content of neoplasms by chemoattractants." *Science* **220**(4593): 210-212.
- Boumil, R. M. and J. T. Lee (2001). "Forty years of decoding the silence in X-chromosome inactivation." *Hum Mol Genet* **10**(20): 2225-2232.
- Breastcancer.org. (2013). "Breastcancer.org." Retrieved 01/07/2013, 2013, from <http://www.breastcancer.org/>.
- Breastcancerbgone.com. (2012, 1-7-2013). "Breastcancerbgone.com." Retrieved 2013, 2012, from <http://www.breastcancerbgone.com/tag/anatomy-of-breast-2/>.
- Brouet, J. C., C. Rabian, et al. (1984). "Clinical and immunological study of non-Hodgkin T-cell lymphomas (cutaneous and lymphoblastic lymphomas excluded)." *Br J Haematol* **57**(2): 315-327.
- Broxmeyer, H. E., L. Kohli, et al. (2003). "Stromal cell-derived factor-1/CXCL12 directly enhances survival/antiapoptosis of myeloid progenitor cells through CXCR4 and G(alpha)i proteins and enhances engraftment of competitive, repopulating stem cells." *J Leukoc Biol* **73**(5): 630-638.
- Burger, J. A., M. Burger, et al. (1999). "Chronic lymphocytic leukemia B cells express functional CXCR4 chemokine receptors that mediate spontaneous migration beneath bone marrow stromal cells." *Blood* **94**(11): 3658-3667.
- Burns, J. M., B. C. Summers, et al. (2006). "A novel chemokine receptor for SDF-1 and I-TAC involved in cell survival, cell adhesion, and tumor development." *J Exp Med* **203**(9): 2201-2213.
- Cabioglu, N., J. Summy, et al. (2005). "CXCL-12/stromal cell-derived factor-1alpha transactivates HER2-neu in breast cancer cells by a novel pathway involving Src kinase activation." *Cancer Res* **65**(15): 6493-6497.
- Cailleau, R., R. Young, et al. (1974). "Breast tumor cell lines from pleural effusions." *J Natl Cancer Inst* **53**(3): 661-674.
- Campeau, P. M., W. D. Foulkes, et al. (2008). "Hereditary breast cancer: new genetic developments, new therapeutic avenues." *Hum Genet* **124**(1): 31-42.
- cancerresearchuk.org. (2012, 7-11-2012). "cancerresearchuk.org." Retrieved 1-7-2013, 2013, from <http://www.cancerresearchuk.org/cancer-info/cancerstats/keyfacts/breast-cancer/cancerstats-key-facts-on-breast-cancer>.
- Cardones, A. R., T. Murakami, et al. (2003). "CXCR4 enhances adhesion of B16 tumor cells to endothelial cells in vitro and in vivo via beta(1) integrin." *Cancer Res* **63**(20): 6751-6757.

- Carnero, A., C. Blanco-Aparicio, et al. (2008). "The PTEN/PI3K/AKT signalling pathway in cancer, therapeutic implications." Curr Cancer Drug Targets **8**(3): 187-198.
- Caudy, A. A., S. T. Reddy, et al. (2007). "CD25 deficiency causes an immune dysregulation, polyendocrinopathy, enteropathy, X-linked-like syndrome, and defective IL-10 expression from CD4 lymphocytes." J Allergy Clin Immunol **119**(2): 482-487.
- Cayrol, C., M. Knibiehler, et al. (1998). "p21 binding to PCNA causes G1 and G2 cell cycle arrest in p53-deficient cells." Oncogene **16**(3): 311-320.
- Chae, W. J., O. Henegariu, et al. (2006). "The mutant leucine-zipper domain impairs both dimerization and suppressive function of Foxp3 in T cells." Proc Natl Acad Sci U S A **103**(25): 9631-9636.
- Chakravarty, D., S. S. Nair, et al. (2010). "Extranuclear functions of ER impact invasive migration and metastasis by breast cancer cells." Cancer Res **70**(10): 4092-4101.
- Chang, L. and M. Karin (2001). "Mammalian MAP kinase signalling cascades." Nature **410**(6824): 37-40.
- Chatila, T. A., F. Blaeser, et al. (2000). "JM2, encoding a fork head-related protein, is mutated in X-linked autoimmunity-allergic dysregulation syndrome." J Clin Invest **106**(12): R75-81.
- Chavey, C., F. Bibeau, et al. (2007). "Oestrogen receptor negative breast cancers exhibit high cytokine content." Breast Cancer Res **9**(1): R15.
- Chen, C., E. A. Rowell, et al. (2006). "Transcriptional regulation by Foxp3 is associated with direct promoter occupancy and modulation of histone acetylation." J Biol Chem **281**(48): 36828-36834.
- Chen, C. R., Y. Kang, et al. (2001). "Defective repression of c-myc in breast cancer cells: A loss at the core of the transforming growth factor beta growth arrest program." Proc Natl Acad Sci U S A **98**(3): 992-999.
- Chen, G. S., H. S. Yu, et al. (2006). "CXC chemokine receptor CXCR4 expression enhances tumorigenesis and angiogenesis of basal cell carcinoma." Br J Dermatol **154**(5): 910-918.
- Chen, G. Y., C. Chen, et al. (2008). "Cutting edge: Broad expression of the FoxP3 locus in epithelial cells: a caution against early interpretation of fatal inflammatory diseases following in vivo depletion of FoxP3-expressing cells." J Immunol **180**(8): 5163-5166.
- Chen, S. and G. Parmigiani (2007). "Meta-analysis of BRCA1 and BRCA2 penetrance." J Clin Oncol **25**(11): 1329-1333.
- Chen, W., W. Jin, et al. (2003). "Conversion of peripheral CD4+CD25- naive T cells to CD4+CD25+ regulatory T cells by TGF-beta induction of transcription factor Foxp3." J Exp Med **198**(12): 1875-1886.
- Chinni, S. R., H. Yamamoto, et al. (2008). "CXCL12/CXCR4 transactivates HER2 in lipid rafts of prostate cancer cells and promotes growth of metastatic deposits in bone." Mol Cancer Res **6**(3): 446-457.
- Ciacchi, C., Y. R. Mahida, et al. (1993). "Functional interleukin-2 receptors on intestinal epithelial cells." J Clin Invest **92**(1): 527-532.
- Clark, K. L., E. D. Halay, et al. (1993). "Co-crystal structure of the HNF-3/fork head DNA-recognition motif resembles histone H5." Nature **364**(6436): 412-420.
- Coffer, P. J. and B. M. Burgering (2004). "Forkhead-box transcription factors and their role in the immune system." Nat Rev Immunol **4**(11): 889-899.

- Cogswell, P. C., D. C. Guttridge, et al. (2000). "Selective activation of NF-kappa B subunits in human breast cancer: potential roles for NF-kappa B2/p52 and for Bcl-3." *Oncogene* **19**(9): 1123-1131.
- Condeelis, J. and J. W. Pollard (2006). "Macrophages: obligate partners for tumor cell migration, invasion, and metastasis." *Cell* **124**(2): 263-266.
- Conti, I. and B. J. Rollins (2004). "CCL2 (monocyte chemoattractant protein-1) and cancer." *Semin Cancer Biol* **14**(3): 149-154.
- Coussens, L. M., W. W. Raymond, et al. (1999). "Inflammatory mast cells up-regulate angiogenesis during squamous epithelial carcinogenesis." *Genes Dev* **13**(11): 1382-1397.
- Coussens, L. M., C. L. Tinkle, et al. (2000). "MMP-9 supplied by bone marrow-derived cells contributes to skin carcinogenesis." *Cell* **103**(3): 481-490.
- Coussens, L. M. and Z. Werb (2002). "Inflammation and cancer." *Nature* **420**(6917): 860-867.
- Crump, M. P., J. H. Gong, et al. (1997). "Solution structure and basis for functional activity of stromal cell-derived factor-1; dissociation of CXCR4 activation from binding and inhibition of HIV-1." *EMBO J* **16**(23): 6996-7007.
- Cunningham, H. D., L. A. Shannon, et al. (2010). "Expression of the C-C chemokine receptor 7 mediates metastasis of breast cancer to the lymph nodes in mice." *Transl Oncol* **3**(6): 354-361.
- Curiel, T. J., G. Coukos, et al. (2004). "Specific recruitment of regulatory T cells in ovarian carcinoma fosters immune privilege and predicts reduced survival." *Nat Med* **10**(9): 942-949.
- Danesh, J., R. Newton, et al. (1999). "The bacteria craze." *Lancet* **353**(9162): 1447.
- Darce, J., D. Rudra, et al. (2012). "An N-terminal mutation of the Foxp3 transcription factor alleviates arthritis but exacerbates diabetes." *Immunity* **36**(5): 731-741.
- Davies, S. L. S., N. Bolós, J. Bayés, M (2007). "Plerixafor Hydrochloride." *Drugs of the future* **32**(2): 123.
- De Placido, S., C. Carlomagno, et al. (1998). "c-erbB2 expression predicts tamoxifen efficacy in breast cancer patients." *Breast Cancer Res Treat* **52**(1-3): 55-64.
- Delaney, G. (2005). "Recent advances in the use of radiotherapy to treat early breast cancer." *Curr Opin Obstet Gynecol* **17**(1): 27-33.
- Delaney, G., S. Jacob, et al. (2005). "The role of radiotherapy in cancer treatment: estimating optimal utilization from a review of evidence-based clinical guidelines." *Cancer* **104**(6): 1129-1137.
- Delgado, M. B., I. Clark-Lewis, et al. (2001). "Rapid inactivation of stromal cell-derived factor-1 by cathepsin G associated with lymphocytes." *Eur J Immunol* **31**(3): 699-707.
- Derynck, R., Y. Zhang, et al. (1998). "Smads: transcriptional activators of TGF-beta responses." *Cell* **95**(6): 737-740.
- DeVries, M. E., A. A. Kelvin, et al. (2006). "Defining the origins and evolution of the chemokine/chemokine receptor system." *J Immunol* **176**(1): 401-415.
- Dhillon, A. S., S. Hagan, et al. (2007). "MAP kinase signalling pathways in cancer." *Oncogene* **26**(22): 3279-3290.
- Di Carlo, E., G. Forni, et al. (2001). "The intriguing role of polymorphonuclear neutrophils in antitumor reactions." *Blood* **97**(2): 339-345.
- Dillon, R. L., D. E. White, et al. (2007). "The phosphatidyl inositol 3-kinase signaling network: implications for human breast cancer." *Oncogene* **26**(9): 1338-1345.

- Ding, G. X., C. C. Feng, et al. (2012). "Paraneoplastic symptoms: Cachexia, polycythemia, and hypercalcemia are, respectively, related to vascular endothelial growth factor (VEGF) expression in renal clear cell carcinoma." Urol Oncol.
- Ding, L., X. Chen, et al. (2006). "Inhibition of the VEGF expression and cell growth in hepatocellular carcinoma by blocking HIF-1alpha and Smad3 binding site in VEGF promoter." J Huazhong Univ Sci Technolog Med Sci **26**(1): 75-78.
- Dong, G., Z. Chen, et al. (1999). "The host environment promotes the constitutive activation of nuclear factor-kappaB and proinflammatory cytokine expression during metastatic tumor progression of murine squamous cell carcinoma." Cancer Res **59**(14): 3495-3504.
- Dore, J. J., Jr., M. Edens, et al. (1998). "Heteromeric and homomeric transforming growth factor-beta receptors show distinct signaling and endocytic responses in epithelial cells." J Biol Chem **273**(48): 31770-31777.
- Douglass, S., S. Ali, et al. (2012). "The role of FOXP3 in the development and metastatic spread of breast cancer." Cancer Metastasis Rev **31**(3-4): 843-854.
- Downward, J. (2003). "Targeting RAS signalling pathways in cancer therapy." Nat Rev Cancer **3**(1): 11-22.
- Du, J., C. Huang, et al. (2008). "Isoform-specific inhibition of ROR alpha-mediated transcriptional activation by human FOXP3." J Immunol **180**(7): 4785-4792.
- Du, J., C. Sun, et al. (2010). "Lysophosphatidic acid induces MDA-MB-231 breast cancer cells migration through activation of PI3K/PAK1/ERK signaling." PLoS One **5**(12): e15940.
- Dulic, V., W. K. Kaufmann, et al. (1994). "p53-dependent inhibition of cyclin-dependent kinase activities in human fibroblasts during radiation-induced G1 arrest." Cell **76**(6): 1013-1023.
- Dumble, M., C. Gatz, et al. (2004). "Insights into aging obtained from p53 mutant mouse models." Ann N Y Acad Sci **1019**: 171-177.
- Dumitriu, I. E., D. R. Dunbar, et al. (2009). "Human dendritic cells produce TGF-beta 1 under the influence of lung carcinoma cells and prime the differentiation of CD4+CD25+Foxp3+ regulatory T cells." J Immunol **182**(5): 2795-2807.
- Ebert, L. M., B. S. Tan, et al. (2008). "The regulatory T cell-associated transcription factor FoxP3 is expressed by tumor cells." Cancer Res **68**(8): 3001-3009.
- Einama, T., Y. Kagata, et al. (2006). "High-level Skp2 expression in pancreatic ductal adenocarcinoma: correlation with the extent of lymph node metastasis, higher histological grade, and poorer patient outcome." Pancreas **32**(4): 376-381.
- el-Deiry, W. S., T. Tokino, et al. (1993). "WAF1, a potential mediator of p53 tumor suppression." Cell **75**(4): 817-825.
- Elbendary, A. A., F. D. Cirisano, et al. (1996). "Relationship between p21 expression and mutation of the p53 tumor suppressor gene in normal and malignant ovarian epithelial cells." Clin Cancer Res **2**(9): 1571-1575.
- Elston, C. W. and I. O. Ellis (1998). The Breast. Edinburgh ; New York, Churchill Livingstone.
- EMBL-EBI (2013). "Expression atlas - CXCR4."
- Fattorossi, A., A. Battaglia, et al. (2004). "Lymphocyte composition of tumor draining lymph nodes from cervical and endometrial cancer patients." Gynecol Oncol **92**(1): 106-115.

- Feil, C. and H. G. Augustin (1998). "Endothelial cells differentially express functional CXC-chemokine receptor-4 (CXCR-4/fusin) under the control of autocrine activity and exogenous cytokines." Biochem Biophys Res Commun **247**(1): 38-45.
- Fernandez, E. J. and E. Lolis (2002). "Structure, function, and inhibition of chemokines." Annu Rev Pharmacol Toxicol **42**: 469-499.
- Fernandis, A. Z., A. Prasad, et al. (2004). "Regulation of CXCR4-mediated chemotaxis and chemoinvasion of breast cancer cells." Oncogene **23**(1): 157-167.
- Fidler, I. J. (2001). "Seed and soil revisited: contribution of the organ microenvironment to cancer metastasis." Surg Oncol Clin N Am **10**(2): 257-269, vii-viii.
- Fidler, I. J. (2003). "The pathogenesis of cancer metastasis: the 'seed and soil' hypothesis revisited." Nat Rev Cancer **3**(6): 453-458.
- Floess, S., J. Freyer, et al. (2007). "Epigenetic control of the foxp3 locus in regulatory T cells." PLoS Biol **5**(2): e38.
- Fontenot, J. D., M. A. Gavin, et al. (2003). "Foxp3 programs the development and function of CD4+CD25+ regulatory T cells." Nat Immunol **4**(4): 330-336.
- Forsythe, J. A., B. H. Jiang, et al. (1996). "Activation of vascular endothelial growth factor gene transcription by hypoxia-inducible factor 1." Mol Cell Biol **16**(9): 4604-4613.
- Frank, D. A., M. J. Robertson, et al. (1995). "Interleukin 2 signaling involves the phosphorylation of Stat proteins." Proc Natl Acad Sci U S A **92**(17): 7779-7783.
- Franke, T. F., C. P. Hornik, et al. (2003). "PI3K/Akt and apoptosis: size matters." Oncogene **22**(56): 8983-8998.
- Frattini, V., F. Pisati, et al. (2012). "FOXP3, a novel glioblastoma oncosuppressor, affects proliferation and migration." Oncotarget **3**(10): 1146-1157.
- Frattini, V., F. Pisati, et al. (2012). "FOXP3, a novel glioblastoma oncosuppressor, affects proliferation and migration." Oncotarget.
- Fresno Vara, J. A., E. Casado, et al. (2004). "PI3K/Akt signalling pathway and cancer." Cancer Treat Rev **30**(2): 193-204.
- Friedenson, B. (2007). "The BRCA1/2 pathway prevents hematologic cancers in addition to breast and ovarian cancers." BMC Cancer **7**: 152.
- Galea, M. H., R. W. Blamey, et al. (1992). "The Nottingham Prognostic Index in primary breast cancer." Breast Cancer Res Treat **22**(3): 207-219.
- Garcia-Tunon, I., M. Ricote, et al. (2004). "Interleukin-2 and its receptor complex (alpha, beta and gamma chains) in in situ and infiltrative human breast cancer: an immunohistochemical comparative study." Breast Cancer Res **6**(1): R1-7.
- Gartler, S. M. (1967). "Genetic markers as tracers in cell culture." Natl Cancer Inst Monogr **26**: 167-195.
- Garton, K. J., P. J. Gough, et al. (2001). "Tumor necrosis factor-alpha-converting enzyme (ADAM17) mediates the cleavage and shedding of fractalkine (CX3CL1)." J Biol Chem **276**(41): 37993-38001.
- Gavin, M. A., T. R. Torgerson, et al. (2006). "Single-cell analysis of normal and FOXP3-mutant human T cells: FOXP3 expression without regulatory T cell development." Proc Natl Acad Sci U S A **103**(17): 6659-6664.
- Gerber, A. L., A. Munst, et al. (2013). "High Expression Of Foxp3 In Primary Melanoma Is Associated With Tumour Progression." Br J Dermatol.

- Ghiringhelli, F., N. Larmonier, et al. (2004). "CD4+CD25+ regulatory T cells suppress tumor immunity but are sensitive to cyclophosphamide which allows immunotherapy of established tumors to be curative." Eur J Immunol **34**(2): 336-344.
- Giai, M., R. Roagna, et al. (1994). "Prognostic and predictive relevance of c-erbB-2 and ras expression in node positive and negative breast cancer." Anticancer Res **14**(3B): 1441-1450.
- Gladson, C. L. and D. R. Welch (2008). "New insights into the role of CXCR4 in prostate cancer metastasis." Cancer Biol Ther **7**(11): 1849-1851.
- Godfrey, V. L., J. E. Wilkinson, et al. (1991). "Fatal lymphoreticular disease in the scurfy (sf) mouse requires T cells that mature in a sf thymic environment: potential model for thymic education." Proc Natl Acad Sci U S A **88**(13): 5528-5532.
- Goetze, K., M. Scholz, et al. (2010). "Tumor cell migration is not influenced by p21 in colon carcinoma cell lines after irradiation with X-ray or (12)C heavy ions." Radiat Environ Biophys **49**(3): 427-435.
- Gordon, S. and P. R. Taylor (2005). "Monocyte and macrophage heterogeneity." Nat Rev Immunol **5**(12): 953-964.
- Grandori, C., S. M. Cowley, et al. (2000). "The Myc/Max/Mad network and the transcriptional control of cell behavior." Annu Rev Cell Dev Biol **16**: 653-699.
- Grant, C., U. Oh, et al. (2006). "Foxp3 represses retroviral transcription by targeting both NF-kappaB and CREB pathways." PLoS Pathog **2**(4): e33.
- Gu-Trantien, C., S. Loi, et al. (2013). "CD4(+) follicular helper T cell infiltration predicts breast cancer survival." J Clin Invest **123**(7): 2873-2892.
- Guleng, B., K. Tateishi, et al. (2005). "Blockade of the stromal cell-derived factor-1/CXCR4 axis attenuates in vivo tumor growth by inhibiting angiogenesis in a vascular endothelial growth factor-independent manner." Cancer Res **65**(13): 5864-5871.
- Gupta, R., J. S. Babb, et al. (2011). "The numbers of FoxP3+ lymphocytes in sentinel lymph nodes of breast cancer patients correlate with primary tumor size but not nodal status." Cancer Invest **29**(6): 419-425.
- Gupta, S. K., P. G. Lysko, et al. (1998). "Chemokine receptors in human endothelial cells. Functional expression of CXCR4 and its transcriptional regulation by inflammatory cytokines." J Biol Chem **273**(7): 4282-4287.
- Han, E. S., F. L. Muller, et al. (2008). "The in vivo gene expression signature of oxidative stress." Physiol Genomics **34**(1): 112-126.
- Han, Y., J. Wang, et al. (2001). "TNF-alpha down-regulates CXCR4 expression in primary murine astrocytes." Brain Res **888**(1): 1-10.
- Hanahan, D. and R. A. Weinberg (2000). "The hallmarks of cancer." Cell **100**(1): 57-70.
- Hancock, W. W. and E. Ozkaynak (2009). "Three distinct domains contribute to nuclear transport of murine Foxp3." PLoS One **4**(11): e7890.
- Hansen, S. K., P. A. Baeuerle, et al. (1994). "Purification, reconstitution, and I kappa B association of the c-Rel-p65 (RelA) complex, a strong activator of transcription." Mol Cell Biol **14**(4): 2593-2603.
- Hartmann, T. N., J. A. Burger, et al. (2005). "CXCR4 chemokine receptor and integrin signaling co-operate in mediating adhesion and chemoresistance in small cell lung cancer (SCLC) cells." Oncogene **24**(27): 4462-4471.

- Hartmann, T. N., V. Grabovsky, et al. (2008). "A crosstalk between intracellular CXCR7 and CXCR4 involved in rapid CXCL12-triggered integrin activation but not in chemokine-triggered motility of human T lymphocytes and CD34+ cells." *J Leukoc Biol* **84**(4): 1130-1140.
- Harvey, J. R., P. Mellor, et al. (2007). "Inhibition of CXCR4-mediated breast cancer metastasis: a potential role for heparinoids?" *Clin Cancer Res* **13**(5): 1562-1570.
- Hatteville, L., C. Mahe, et al. (2002). "Prediction of the long-term survival in breast cancer patients according to the present oncological status." *Stat Med* **21**(16): 2345-2354.
- Haybittle, J. L., R. W. Blamey, et al. (1982). "A prognostic index in primary breast cancer." *Br J Cancer* **45**(3): 361-366.
- Heinze, E., S. Baldwin, et al. (2009). "Antibody-mediated FOXP3 protein therapy induces apoptosis in cancer cells in vitro and inhibits metastasis in vivo." *Int J Oncol* **35**(1): 167-173.
- Helbig, G., K. W. Christopherson, 2nd, et al. (2003). "NF-kappaB promotes breast cancer cell migration and metastasis by inducing the expression of the chemokine receptor CXCR4." *J Biol Chem* **278**(24): 21631-21638.
- Hernandez, L., M. A. Magalhaes, et al. (2011). "Opposing roles of CXCR4 and CXCR7 in breast cancer metastasis." *Breast Cancer Res* **13**(6): R128.
- Hinz, S., L. Pagerols-Raluy, et al. (2007). "Foxp3 expression in pancreatic carcinoma cells as a novel mechanism of immune evasion in cancer." *Cancer Res* **67**(17): 8344-8350.
- Hollstein, M., K. Rice, et al. (1994). "Database of p53 gene somatic mutations in human tumors and cell lines." *Nucleic Acids Res* **22**(17): 3551-3555.
- Hong, H. K., J. K. Noveroske, et al. (2001). "The winged helix/forkhead transcription factor Foxq1 regulates differentiation of hair in satin mice." *Genesis* **29**(4): 163-171.
- Hori, S., T. Nomura, et al. (2003). "Control of regulatory T cell development by the transcription factor Foxp3." *Science* **299**(5609): 1057-1061.
- Huang, D. B., Y. Q. Chen, et al. (2001). "X-ray crystal structure of proto-oncogene product c-Rel bound to the CD28 response element of IL-2." *Structure* **9**(8): 669-678.
- Huang, X., J. Shen, et al. (2003). "Molecular dynamics simulations on SDF-1alpha: binding with CXCR4 receptor." *Biophys J* **84**(1): 171-184.
- Hudis, C. A. (2007). "Trastuzumab--mechanism of action and use in clinical practice." *N Engl J Med* **357**(1): 39-51.
- Huter, E. N., G. A. Punkosdy, et al. (2008). "TGF-beta-induced Foxp3+ regulatory T cells rescue scurfy mice." *Eur J Immunol* **38**(7): 1814-1821.
- Hwang, J. H., H. K. Chung, et al. (2003). "CXC chemokine receptor 4 expression and function in human anaplastic thyroid cancer cells." *J Clin Endocrinol Metab* **88**(1): 408-416.
- Iavarone, A. and J. Massague (1997). "Repression of the CDK activator Cdc25A and cell-cycle arrest by cytokine TGF-beta in cells lacking the CDK inhibitor p15." *Nature* **387**(6631): 417-422.
- Inuzuka, H., D. Gao, et al. (2012). "Acetylation-dependent regulation of Skp2 function." *Cell* **150**(1): 179-193.
- Ishikawa, T., K. Nakashiro, et al. (2009). "Hypoxia enhances CXCR4 expression by activating HIF-1 in oral squamous cell carcinoma." *Oncol Rep* **21**(3): 707-712.

- Janson, P. C., M. E. Winerdal, et al. (2008). "FOXP3 promoter demethylation reveals the committed Treg population in humans." *PLoS One* **3**(2): e1612.
- Jensen, E. V. and V. C. Jordan (2003). "The estrogen receptor: a model for molecular medicine." *Clin Cancer Res* **9**(6): 1980-1989.
- Jia, L., H. Li, et al. (2011). "Induction of p21-dependent senescence by an NAE inhibitor, MLN4924, as a mechanism of growth suppression." *Neoplasia* **13**(6): 561-569.
- Jiang, B. H. and L. Z. Liu (2009). "PI3K/PTEN signaling in angiogenesis and tumorigenesis." *Adv Cancer Res* **102**: 19-65.
- Jiang, Z., X. Li, et al. (2006). "Promoter hypermethylation-mediated down-regulation of LATS1 and LATS2 in human astrocytoma." *Neurosci Res* **56**(4): 450-458.
- Jimenez-Velasco, A., J. Roman-Gomez, et al. (2005). "Downregulation of the large tumor suppressor 2 (LATS2/KPM) gene is associated with poor prognosis in acute lymphoblastic leukemia." *Leukemia* **19**(12): 2347-2350.
- Johnson, E., D. D. Seachrist, et al. (2010). "HER2/ErbB2-induced breast cancer cell migration and invasion require p120 catenin activation of Rac1 and Cdc42." *J Biol Chem* **285**(38): 29491-29501.
- Jorgensen, J. T. (2010). "Targeted HER2 treatment in advanced gastric cancer." *Oncology* **78**(1): 26-33.
- Jorgensen, J. T. and M. Hersom (2012). "HER2 as a Prognostic Marker in Gastric Cancer - A Systematic Analysis of Data from the Literature." *J Cancer* **3**: 137-144.
- Jourdan, P., J. P. Vendrell, et al. (2000). "Cytokines and cell surface molecules independently induce CXCR4 expression on CD4+ CCR7+ human memory T cells." *J Immunol* **165**(2): 716-724.
- Jung, D. J., D. H. Jin, et al. (2010). "Foxp3 expression in p53-dependent DNA damage responses." *J Biol Chem* **285**(11): 7995-8002.
- Jung, P., A. Menssen, et al. (2008). "AP4 encodes a c-MYC-inducible repressor of p21." *Proc Natl Acad Sci U S A* **105**(39): 15046-15051.
- Kaestner, K. H., W. Knochel, et al. (2000). "Unified nomenclature for the winged helix/forkhead transcription factors." *Genes Dev* **14**(2): 142-146.
- Kang, H., R. E. Mansel, et al. (2005). "Genetic manipulation of stromal cell-derived factor-1 attests the pivotal role of the autocrine SDF-1-CXCR4 pathway in the aggressiveness of breast cancer cells." *Int J Oncol* **26**(5): 1429-1434.
- Kang, J. Y., J. J. Kim, et al. (2009). "The p53-p21(Cip1/WAF1) pathway is necessary for cellular senescence induced by the inhibition of protein kinase CKII in human colon cancer cells." *Mol Cells* **28**(5): 489-494.
- Karar, J. and A. Maity (2011). "PI3K/AKT/mTOR Pathway in Angiogenesis." *Front Mol Neurosci* **4**: 51.
- Karin, M. (2009). "NF-kappaB as a critical link between inflammation and cancer." *Cold Spring Harb Perspect Biol* **1**(5): a000141.
- Karin, M. and F. R. Greten (2005). "NF-kappaB: linking inflammation and immunity to cancer development and progression." *Nat Rev Immunol* **5**(10): 749-759.
- Karin, M. and A. Lin (2002). "NF-kappaB at the crossroads of life and death." *Nat Immunol* **3**(3): 221-227.
- Katoh, M. (2004). "Human FOX gene family (Review)." *Int J Oncol* **25**(5): 1495-1500.

- Kawaida, H., K. Kono, et al. (2005). "Distribution of CD4+CD25high regulatory T-cells in tumor-draining lymph nodes in patients with gastric cancer." J Surg Res **124**(1): 151-157.
- Kenemans, P., R. A. Verstraeten, et al. (2004). "Oncogenic pathways in hereditary and sporadic breast cancer." Maturitas **49**(1): 34-43.
- Key, T. J., P. K. Verkasalo, et al. (2001). "Epidemiology of breast cancer." Lancet Oncol **2**(3): 133-140.
- Kijima, T., G. Maulik, et al. (2002). "Regulation of cellular proliferation, cytoskeletal function, and signal transduction through CXCR4 and c-Kit in small cell lung cancer cells." Cancer Res **62**(21): 6304-6311.
- Kijowski, J., M. Baj-Krzyworzeka, et al. (2001). "The SDF-1-CXCR4 axis stimulates VEGF secretion and activates integrins but does not affect proliferation and survival in lymphohematopoietic cells." Stem Cells **19**(5): 453-466.
- Kim, H. P. and W. J. Leonard (2007). "CREB/ATF-dependent T cell receptor-induced FoxP3 gene expression: a role for DNA methylation." J Exp Med **204**(7): 1543-1551.
- Kim, M., Y. J. Koh, et al. (2010). "CXCR4 signaling regulates metastasis of chemoresistant melanoma cells by a lymphatic metastatic niche." Cancer Res **70**(24): 10411-10421.
- Kim, M. H., J. S. Koo, et al. (2013). "FOXP3 Expression Is Related to High Ki-67 Index and Poor Prognosis in Lymph Node-Positive Breast Cancer Patients." Oncology **85**(2): 128-136.
- Klug, A. and D. Rhodes (1987). "Zinc fingers: a novel protein fold for nucleic acid recognition." Cold Spring Harb Symp Quant Biol **52**: 473-482.
- Knudson, A. G., Jr. (1971). "Mutation and cancer: statistical study of retinoblastoma." Proc Natl Acad Sci U S A **68**(4): 820-823.
- Koshiba, T., R. Hosotani, et al. (2000). "Expression of stromal cell-derived factor 1 and CXCR4 ligand receptor system in pancreatic cancer: a possible role for tumor progression." Clin Cancer Res **6**(9): 3530-3535.
- Koster, A., S. Landgraf, et al. (1991). "Expression of oncogenes in human breast cancer specimens." Anticancer Res **11**(1): 193-201.
- Krishna, S. S., I. Majumdar, et al. (2003). "Structural classification of zinc fingers: survey and summary." Nucleic Acids Res **31**(2): 532-550.
- Kryczek, I., S. Wei, et al. (2007). "Stroma-derived factor (SDF-1/CXCL12) and human tumor pathogenesis." Am J Physiol Cell Physiol **292**(3): C987-995.
- Kwon, H. K., J. S. So, et al. (2008). "Foxp3 induces IL-4 gene silencing by affecting nuclear translocation of NFkappaB and chromatin structure." Mol Immunol **45**(11): 3205-3212.
- Lai, C. S., S. E. Fisher, et al. (2001). "A forkhead-domain gene is mutated in a severe speech and language disorder." Nature **413**(6855): 519-523.
- Lai, Y. L., B. L. Mau, et al. (2008). "PIK3CA exon 20 mutation is independently associated with a poor prognosis in breast cancer patients." Ann Surg Oncol **15**(4): 1064-1069.
- Lal, A., L. Chan, et al. (2013). "FOXP3-positive regulatory T lymphocytes and epithelial FOXP3 expression in synchronous normal, ductal carcinoma in situ, and invasive cancer of the breast." Breast Cancer Res Treat **139**(2): 381-390.
- Lal, G. and J. S. Bromberg (2009). "Epigenetic mechanisms of regulation of Foxp3 expression." Blood **114**(18): 3727-3735.

- Lal, G., N. Zhang, et al. (2009). "Epigenetic regulation of Foxp3 expression in regulatory T cells by DNA methylation." *J Immunol* **182**(1): 259-273.
- Lambeir, A. M., P. Proost, et al. (2001). "Kinetic investigation of chemokine truncation by CD26/dipeptidyl peptidase IV reveals a striking selectivity within the chemokine family." *J Biol Chem* **276**(32): 29839-29845.
- Langley, R. R. and I. J. Fidler (2011). "The seed and soil hypothesis revisited--the role of tumor-stroma interactions in metastasis to different organs." *Int J Cancer* **128**(11): 2527-2535.
- Laoui, D., K. Movahedi, et al. (2011). "Tumor-associated macrophages in breast cancer: distinct subsets, distinct functions." *Int J Dev Biol* **55**(7-9): 861-867.
- Lapteva, N., A. G. Yang, et al. (2005). "CXCR4 knockdown by small interfering RNA abrogates breast tumor growth in vivo." *Cancer Gene Ther* **12**(1): 84-89.
- Lee, G. R., S. T. Kim, et al. (2006). "T helper cell differentiation: regulation by cis elements and epigenetics." *Immunity* **24**(4): 369-379.
- Lee, J. M., I. S. Kim, et al. (2010). "RORalpha attenuates Wnt/beta-catenin signaling by PKCalpha-dependent phosphorylation in colon cancer." *Mol Cell* **37**(2): 183-195.
- Lee, P. P., D. R. Fitzpatrick, et al. (2001). "A critical role for Dnmt1 and DNA methylation in T cell development, function, and survival." *Immunity* **15**(5): 763-774.
- Lee, S. M., B. Gao, et al. (2008). "FoxP3 maintains Treg unresponsiveness by selectively inhibiting the promoter DNA-binding activity of AP-1." *Blood* **111**(7): 3599-3606.
- Leek, R. D. and A. L. Harris (2002). "Tumor-associated macrophages in breast cancer." *J Mammary Gland Biol Neoplasia* **7**(2): 177-189.
- Lesur, O., K. Arsalane, et al. (1997). "Functional IL-2 receptors are expressed by rat lung type II epithelial cells." *Am J Physiol* **273**(3 Pt 1): L495-503.
- Levine, A. J. (1997). "p53, the cellular gatekeeper for growth and division." *Cell* **88**(3): 323-331.
- Li, C. and P. W. Tucker (1993). "DNA-binding properties and secondary structural model of the hepatocyte nuclear factor 3/fork head domain." *Proc Natl Acad Sci U S A* **90**(24): 11583-11587.
- Li, J. K., L. Yu, et al. (2008). "Inhibition of CXCR4 activity with AMD3100 decreases invasion of human colorectal cancer cells in vitro." *World J Gastroenterol* **14**(15): 2308-2313.
- Li, L. and P. E. Shaw (2004). "A STAT3 dimer formed by inter-chain disulphide bridging during oxidative stress." *Biochem Biophys Res Commun* **322**(3): 1005-1011.
- Li, S., J. Weidenfeld, et al. (2004). "Transcriptional and DNA binding activity of the Foxp1/2/4 family is modulated by heterotypic and homotypic protein interactions." *Mol Cell Biol* **24**(2): 809-822.
- Li, W., H. Katoh, et al. (2013). "FOXP3 Regulates Sensitivity of Cancer Cells to Irradiation by Transcriptional Repression of BRCA1." *Cancer Res* **73**(7): 2170-2180.
- Li, W., L. Wang, et al. (2011). "Identification of a tumor suppressor relay between the FOXP3 and the Hippo pathways in breast and prostate cancers." *Cancer Res* **71**(6): 2162-2171.

- Li, X., J. Huang, et al. (2004). "Single-chain estrogen receptors (ERs) reveal that the ERalpha/beta heterodimer emulates functions of the ERalpha dimer in genomic estrogen signaling pathways." *Mol Cell Biol* **24**(17): 7681-7694.
- Li, Y. M., Y. Pan, et al. (2004). "Upregulation of CXCR4 is essential for HER2-mediated tumor metastasis." *Cancer Cell* **6**(5): 459-469.
- Liang, Z., J. Brooks, et al. (2007). "CXCR4/CXCL12 axis promotes VEGF-mediated tumor angiogenesis through Akt signaling pathway." *Biochem Biophys Res Commun* **359**(3): 716-722.
- Lin, M. L., Y. C. Lu, et al. (2010). "Down-regulation of MMP-2 through the p38 MAPK-NF-kappaB-dependent pathway by aloe-emodin leads to inhibition of nasopharyngeal carcinoma cell invasion." *Mol Carcinog* **49**(9): 783-797.
- Liu, H., D. C. Radisky, et al. (2012). "MYC suppresses cancer metastasis by direct transcriptional silencing of alphav and beta3 integrin subunits." *Nat Cell Biol* **14**(6): 567-574.
- Liu, H., W. Xue, et al. (2010). "Hypoxic preconditioning advances CXCR4 and CXCR7 expression by activating HIF-1alpha in MSCs." *Biochem Biophys Res Commun* **401**(4): 509-515.
- Liu, R., L. Wang, et al. (2009). "FOXP3 up-regulates p21 expression by site-specific inhibition of histone deacetylase 2/histone deacetylase 4 association to the locus." *Cancer Res* **69**(6): 2252-2259.
- Liu, S., J. Lachapelle, et al. (2012). "CD8+ lymphocyte infiltration is an independent favorable prognostic indicator in basal-like breast cancer." *Breast Cancer Res* **14**(2): R48.
- Liu, V. C., L. Y. Wong, et al. (2007). "Tumor evasion of the immune system by converting CD4+CD25- T cells into CD4+CD25+ T regulatory cells: role of tumor-derived TGF-beta." *J Immunol* **178**(5): 2883-2892.
- Liu, Y., S. R. Cox, et al. (1995). "Hypoxia regulates vascular endothelial growth factor gene expression in endothelial cells. Identification of a 5' enhancer." *Circ Res* **77**(3): 638-643.
- Liu, Y., L. Wang, et al. (2013). "Inhibition of p300 impairs Foxp3 T regulatory cell function and promotes antitumor immunity." *Nat Med*.
- Liu, Y., Y. Wang, et al. (2009). "Activating transcription factor 2 and c-Jun-mediated induction of FoxP3 for experimental therapy of mammary tumor in the mouse." *Cancer Res* **69**(14): 5954-5960.
- Liyanage, U. K., T. T. Moore, et al. (2002). "Prevalence of regulatory T cells is increased in peripheral blood and tumor microenvironment of patients with pancreas or breast adenocarcinoma." *J Immunol* **169**(5): 2756-2761.
- Loizou, L., K. G. Andersen, et al. (2011). "Foxp3 interacts with c-Rel to mediate NF-kappaB repression." *PLoS One* **6**(4): e18670.
- Long, S. A., K. Cerosaletti, et al. (2010). "Defects in IL-2R signaling contribute to diminished maintenance of FOXP3 expression in CD4(+)CD25(+) regulatory T-cells of type 1 diabetic subjects." *Diabetes* **59**(2): 407-415.
- Lopes, J. E., T. R. Torgerson, et al. (2006). "Analysis of FOXP3 reveals multiple domains required for its function as a transcriptional repressor." *J Immunol* **177**(5): 3133-3142.
- Luboshits, G., S. Shina, et al. (1999). "Elevated expression of the CC chemokine regulated on activation, normal T cell expressed and secreted (RANTES) in advanced breast carcinoma." *Cancer Res* **59**(18): 4681-4687.
- Luker, K. E. and G. D. Luker (2006). "Functions of CXCL12 and CXCR4 in breast cancer." *Cancer Lett* **238**(1): 30-41.

- Luo, H., B. H. Jiang, et al. (2008). "Inhibition of cell growth and VEGF expression in ovarian cancer cells by flavonoids." *Nutr Cancer* **60**(6): 800-809.
- Luo, J., B. D. Manning, et al. (2003). "Targeting the PI3K-Akt pathway in human cancer: rationale and promise." *Cancer Cell* **4**(4): 257-262.
- Luo, X., Q. Zhang, et al. (2008). "Cutting edge: TGF-beta-induced expression of Foxp3 in T cells is mediated through inactivation of ERK." *J Immunol* **180**(5): 2757-2761.
- Lynch, H. T., E. Silva, et al. (2008). "Hereditary breast cancer: part I. Diagnosing hereditary breast cancer syndromes." *Breast J* **14**(1): 3-13.
- Ma, Q., D. Jones, et al. (1998). "Impaired B-lymphopoiesis, myelopoiesis, and derailed cerebellar neuron migration in CXCR4- and SDF-1-deficient mice." *Proc Natl Acad Sci U S A* **95**(16): 9448-9453.
- Maheshwari, A., R. D. Christensen, et al. (2003). "ELR+ CXC chemokines in human milk." *Cytokine* **24**(3): 91-102.
- Mahmoud, S. M., E. C. Paish, et al. (2011). "Tumor-infiltrating CD8+ lymphocytes predict clinical outcome in breast cancer." *J Clin Oncol* **29**(15): 1949-1955.
- Maki, C. G. and P. M. Howley (1997). "Ubiquitination of p53 and p21 is differentially affected by ionizing and UV radiation." *Mol Cell Biol* **17**(1): 355-363.
- Maltzman, W. and L. Czyzyk (1984). "UV irradiation stimulates levels of p53 cellular tumor antigen in nontransformed mouse cells." *Mol Cell Biol* **4**(9): 1689-1694.
- Mantel, P. Y., N. Ouaked, et al. (2006). "Molecular mechanisms underlying FOXP3 induction in human T cells." *J Immunol* **176**(6): 3593-3602.
- Mantovani, A., A. Sica, et al. (2005). "Macrophage polarization comes of age." *Immunity* **23**(4): 344-346.
- Marchese, A. and J. L. Benovic (2001). "Agonist-promoted ubiquitination of the G protein-coupled receptor CXCR4 mediates lysosomal sorting." *J Biol Chem* **276**(49): 45509-45512.
- Marchese, A., C. Chen, et al. (2003). "The ins and outs of G protein-coupled receptor trafficking." *Trends Biochem Sci* **28**(7): 369-376.
- Massague, J. (2008). "TGFbeta in Cancer." *Cell* **134**(2): 215-230.
- Massague, J., S. W. Blain, et al. (2000). "TGFbeta signaling in growth control, cancer, and heritable disorders." *Cell* **103**(2): 295-309.
- Matkowski, R., I. Gisterek, et al. (2009). "The prognostic role of tumor-infiltrating CD4 and CD8 T lymphocytes in breast cancer." *Anticancer Res* **29**(7): 2445-2451.
- Matsuura, K., Y. Yamaguchi, et al. (2009). "FOXP3 expression of micrometastasis-positive sentinel nodes in breast cancer patients." *Oncol Rep* **22**(5): 1181-1187.
- Matteucci, E., M. Locati, et al. (2005). "Hepatocyte growth factor enhances CXCR4 expression favoring breast cancer cell invasiveness." *Exp Cell Res* **310**(1): 176-185.
- Mayack, S. R. and L. J. Berg (2006). "Cutting edge: an alternative pathway of CD4+ T cell differentiation is induced following activation in the absence of gamma-chain-dependent cytokine signals." *J Immunol* **176**(4): 2059-2063.
- Mazzucchelli, R., J. A. Hixon, et al. (2008). "Development of regulatory T cells requires IL-7Ralpha stimulation by IL-7 or TSLP." *Blood* **112**(8): 3283-3292.

- McQuibban, G. A., G. S. Butler, et al. (2001). "Matrix metalloproteinase activity inactivates the CXC chemokine stromal cell-derived factor-1." J Biol Chem **276**(47): 43503-43508.
- Medrek, C., F. Ponten, et al. (2012). "The presence of tumor associated macrophages in tumor stroma as a prognostic marker for breast cancer patients." BMC Cancer **12**: 306.
- Melchionna, R., M. Romani, et al. (2010). "Role of HIF-1alpha in proton-mediated CXCR4 down-regulation in endothelial cells." Cardiovasc Res **86**(2): 293-301.
- Mellor, P., J. R. Harvey, et al. (2007). "Modulatory effects of heparin and short-length oligosaccharides of heparin on the metastasis and growth of LMD MDA-MB 231 breast cancer cells in vivo." Br J Cancer **97**(6): 761-768.
- Merkhofer, E. C., P. Cogswell, et al. (2010). "Her2 activates NF-kappaB and induces invasion through the canonical pathway involving IKKalpha." Oncogene **29**(8): 1238-1248.
- Merlo, A., P. Casalini, et al. (2009). "FOXP3 expression and overall survival in breast cancer." J Clin Oncol **27**(11): 1746-1752.
- Miao, Z., K. E. Luker, et al. (2007). "CXCR7 (RDC1) promotes breast and lung tumor growth in vivo and is expressed on tumor-associated vasculature." Proc Natl Acad Sci U S A **104**(40): 15735-15740.
- Miettinen, P. J., R. Ebner, et al. (1994). "TGF-beta induced transdifferentiation of mammary epithelial cells to mesenchymal cells: involvement of type I receptors." J Cell Biol **127**(6 Pt 2): 2021-2036.
- Mikami, Y., T. Hori, et al. (2005). "The functional region of CENP-H interacts with the Nuf2 complex that localizes to centromere during mitosis." Mol Cell Biol **25**(5): 1958-1970.
- Miller, A. M., K. Lundberg, et al. (2006). "CD4+CD25high T cells are enriched in the tumor and peripheral blood of prostate cancer patients." J Immunol **177**(10): 7398-7405.
- Mizukami, Y., K. Kono, et al. (2008). "Localisation pattern of Foxp3+ regulatory T cells is associated with clinical behaviour in gastric cancer." Br J Cancer **98**(1): 148-153.
- Mohle, R., M. Schittenhelm, et al. (2000). "Functional response of leukaemic blasts to stromal cell-derived factor-1 correlates with preferential expression of the chemokine receptor CXCR4 in acute myelomonocytic and lymphoblastic leukaemia." Br J Haematol **110**(3): 563-572.
- Mohos, A., T. Sebestyen, et al. (2013). "Immune cell profile of sentinel lymph nodes in patients with malignant melanoma - FOXP3+ cell density in cases with positive sentinel node status is associated with unfavorable clinical outcome." J Transl Med **11**: 43.
- Moja, L., L. Tagliabue, et al. (2012). "Trastuzumab containing regimens for early breast cancer." Cochrane Database Syst Rev **4**: CD006243.
- Moller, C., T. Stromberg, et al. (2003). "Expression and function of chemokine receptors in human multiple myeloma." Leukemia **17**(1): 203-210.
- Moreau, M., S. Mourah, et al. (2011). "beta-Catenin and NF-kappaB cooperate to regulate the uPA/uPAR system in cancer cells." Int J Cancer **128**(6): 1280-1292.
- Moretti, R. M., M. Montagnani Marelli, et al. (2002). "Role of the orphan nuclear receptor ROR alpha in the control of the metastatic behavior of androgen-independent prostate cancer cells." Oncol Rep **9**(5): 1139-1143.

- Morgan, M. E., J. H. van Bilsen, et al. (2005). "Expression of FOXP3 mRNA is not confined to CD4+CD25+ T regulatory cells in humans." Hum Immunol **66**(1): 13-20.
- Moriuchi, M., H. Moriuchi, et al. (1997). "Cloning and analysis of the promoter region of CXCR4, a coreceptor for HIV-1 entry." J Immunol **159**(9): 4322-4329.
- Moser, B. and K. Willmann (2004). "Chemokines: role in inflammation and immune surveillance." Ann Rheum Dis **63 Suppl 2**: ii84-ii89.
- Mudduwa, L. K. (2009). "Quick score of hormone receptor status of breast carcinoma: correlation with the other clinicopathological prognostic parameters." Indian J Pathol Microbiol **52**(2): 159-163.
- Mukherjee, D. and J. Zhao (2013). "The Role of chemokine receptor CXCR4 in breast cancer metastasis." Am J Cancer Res **3**(1): 46-57.
- Mukhtar, R. A., O. Nseyo, et al. (2011). "Tumor-associated macrophages in breast cancer as potential biomarkers for new treatments and diagnostics." Expert Rev Mol Diagn **11**(1): 91-100.
- Muller, A., B. Homey, et al. (2001). "Involvement of chemokine receptors in breast cancer metastasis." Nature **410**(6824): 50-56.
- Mullis, K. B. (2013). "Nobel Lecture: The Polymerase Chain Reaction."
- Murakami, T., W. Maki, et al. (2002). "Expression of CXC chemokine receptor-4 enhances the pulmonary metastatic potential of murine B16 melanoma cells." Cancer Res **62**(24): 7328-7334.
- Murdoch, C. and A. Finn (2000). "Chemokine receptors and their role in inflammation and infectious diseases." Blood **95**(10): 3032-3043.
- Nakahira, K., A. Morita, et al. (2013). "Phosphorylation of FOXP3 by LCK Downregulates MMP9 Expression and Represses Cell Invasion." PLoS One **8**(10): e77099.
- Nakayama, K., H. Nagahama, et al. (2004). "Skp2-mediated degradation of p27 regulates progression into mitosis." Dev Cell **6**(5): 661-672.
- Nakayama, K. I. and K. Nakayama (2006). "Ubiquitin ligases: cell-cycle control and cancer." Nat Rev Cancer **6**(5): 369-381.
- Nakshatri, H., P. Bhat-Nakshatri, et al. (1997). "Constitutive activation of NF-kappaB during progression of breast cancer to hormone-independent growth." Mol Cell Biol **17**(7): 3629-3639.
- Neel, N. F., E. Schutyser, et al. (2005). "Chemokine receptor internalization and intracellular trafficking." Cytokine Growth Factor Rev **16**(6): 637-658.
- Nelson-Rees, W. A., R. R. Flandermeyer, et al. (1974). "Banded marker chromosomes as indicators of intraspecies cellular contamination." Science **184**(4141): 1093-1096.
- Newton, P., G. O'Boyle, et al. (2009). "T cell extravasation: demonstration of synergy between activation of CXCR3 and the T cell receptor." Mol Immunol **47**(2-3): 485-492.
- Nishihara, M., H. Ogura, et al. (2007). "IL-6-gp130-STAT3 in T cells directs the development of IL-17+ Th with a minimum effect on that of Treg in the steady state." Int Immunol **19**(6): 695-702.
- Norgauer, J., B. Metzner, et al. (1996). "Expression and growth-promoting function of the IL-8 receptor beta in human melanoma cells." J Immunol **156**(3): 1132-1137.
- O'Boyle, G., I. Swidenbank, et al. (2013). "Inhibition of CXCR4-CXCL12 chemotaxis in melanoma by AMD11070." Br J Cancer **108**(8): 1634-1640.

- O'Malley, B. W. (2006). "Molecular biology. Little molecules with big goals." *Science* **313**(5794): 1749-1750.
- Odemis, V., K. Boosmann, et al. (2010). "CXCR7 is an active component of SDF-1 signalling in astrocytes and Schwann cells." *J Cell Sci* **123**(Pt 7): 1081-1088.
- Ogawa, K., F. Chen, et al. (2004). "Suppression of matrix metalloproteinase-9 transcription by transforming growth factor-beta is mediated by a nuclear factor-kappaB site." *Biochem J* **381**(Pt 2): 413-422.
- Ohta, M., Y. Kitadai, et al. (2002). "Monocyte chemoattractant protein-1 expression correlates with macrophage infiltration and tumor vascularity in human esophageal squamous cell carcinomas." *Int J Cancer* **102**(3): 220-224.
- Okita, R., T. Saeki, et al. (2005). "CD4+CD25+ regulatory T cells in the peripheral blood of patients with breast cancer and non-small cell lung cancer." *Oncol Rep* **14**(5): 1269-1273.
- Ono, M., H. Yaguchi, et al. (2007). "Foxp3 controls regulatory T-cell function by interacting with AML1/Runx1." *Nature* **446**(7136): 685-689.
- Orimo, A., P. B. Gupta, et al. (2005). "Stromal fibroblasts present in invasive human breast carcinomas promote tumor growth and angiogenesis through elevated SDF-1/CXCL12 secretion." *Cell* **121**(3): 335-348.
- Ou-Yang, H. F., H. W. Zhang, et al. (2009). "Notch signaling regulates the FOXP3 promoter through RBP-J- and Hes1-dependent mechanisms." *Mol Cell Biochem* **320**(1-2): 109-114.
- Parker, C. C., R. H. Kim, et al. (2012). "The chemokine receptor CXCR4 as a novel independent prognostic marker for node-positive breast cancer patients." *J Surg Oncol* **106**(4): 393-398.
- Passerini, L., S. E. Allan, et al. (2008). "STAT5-signaling cytokines regulate the expression of FOXP3 in CD4+CD25+ regulatory T cells and CD4+CD25-effector T cells." *Int Immunol* **20**(3): 421-431.
- Payne, A. S. and L. A. Cornelius (2002). "The role of chemokines in melanoma tumor growth and metastasis." *J Invest Dermatol* **118**(6): 915-922.
- Pearson, G., F. Robinson, et al. (2001). "Mitogen-activated protein (MAP) kinase pathways: regulation and physiological functions." *Endocr Rev* **22**(2): 153-183.
- Pekalski, M., S. E. Jenkinson, et al. (2013). "Renal allograft rejection: examination of delayed differentiation of Treg and Th17 effector T cells." *Immunobiology* **218**(3): 303-310.
- Peled, A., I. Hardan, et al. (2002). "Immature leukemic CD34+CXCR4+ cells from CML patients have lower integrin-dependent migration and adhesion in response to the chemokine SDF-1." *Stem Cells* **20**(3): 259-266.
- Pharoah, P. D., N. E. Day, et al. (1997). "Family history and the risk of breast cancer: a systematic review and meta-analysis." *Int J Cancer* **71**(5): 800-809.
- Pinto, A. E., S. Andre, et al. (2005). "Correlations of cell cycle regulators (p53, p21, pRb and mdm2) and c-erbB-2 with biological markers of proliferation and overall survival in breast cancer." *Pathology* **37**(1): 45-50.
- Platet, N., A. M. Cathiard, et al. (2004). "Estrogens and their receptors in breast cancer progression: a dual role in cancer proliferation and invasion." *Crit Rev Oncol Hematol* **51**(1): 55-67.
- Porter, D. A., I. E. Krop, et al. (2001). "A SAGE (serial analysis of gene expression) view of breast tumor progression." *Cancer Res* **61**(15): 5697-5702.

- Powell, B. R., N. R. Buist, et al. (1982). "An X-linked syndrome of diarrhea, polyendocrinopathy, and fatal infection in infancy." J Pediatr **100**(5): 731-737.
- Powzaniuk, M., S. McElwee-Witmer, et al. (2004). "The LATS2/KPM tumor suppressor is a negative regulator of the androgen receptor." Mol Endocrinol **18**(8): 2011-2023.
- Prasad, A., A. Z. Fernandis, et al. (2004). "Slit protein-mediated inhibition of CXCR4-induced chemotactic and chemoinvasive signaling pathways in breast cancer cells." J Biol Chem **279**(10): 9115-9124.
- Press, M. F., L. Bernstein, et al. (1997). "HER-2/neu gene amplification characterized by fluorescence in situ hybridization: poor prognosis in node-negative breast carcinomas." J Clin Oncol **15**(8): 2894-2904.
- Price, B. D. and S. K. Calderwood (1993). "Increased sequence-specific p53-DNA binding activity after DNA damage is attenuated by phorbol esters." Oncogene **8**(11): 3055-3062.
- Qian, X. and R. H. Costa (1995). "Analysis of hepatocyte nuclear factor-3 beta protein domains required for transcriptional activation and nuclear targeting." Nucleic Acids Res **23**(7): 1184-1191.
- Qin, L., L. Liao, et al. (2008). "The AIB1 oncogene promotes breast cancer metastasis by activation of PEA3-mediated matrix metalloproteinase 2 (MMP2) and MMP9 expression." Mol Cell Biol **28**(19): 5937-5950.
- Quatromoni, J. G. and E. Eruslanov (2012). "Tumor-associated macrophages: function, phenotype, and link to prognosis in human lung cancer." Am J Transl Res **4**(4): 376-389.
- Radke, S., A. Pirkmaier, et al. (2005). "Differential expression of the F-box proteins Skp2 and Skp2B in breast cancer." Oncogene **24**(21): 3448-3458.
- Rak, J., J. Filmus, et al. (1995). "Oncogenes as inducers of tumor angiogenesis." Cancer Metastasis Rev **14**(4): 263-277.
- Rak, J., Y. Mitsushashi, et al. (1995). "Mutant ras oncogenes upregulate VEGF/VPF expression: implications for induction and inhibition of tumor angiogenesis." Cancer Res **55**(20): 4575-4580.
- Ramanathan, M., G. Pinhal-Enfield, et al. (2007). "Synergistic up-regulation of vascular endothelial growth factor (VEGF) expression in macrophages by adenosine A2A receptor agonists and endotoxin involves transcriptional regulation via the hypoxia response element in the VEGF promoter." Mol Biol Cell **18**(1): 14-23.
- Rao, A., C. Luo, et al. (1997). "Transcription factors of the NFAT family: regulation and function." Annu Rev Immunol **15**: 707-747.
- Ray, P., S. A. Lewin, et al. (2011). "Noninvasive imaging reveals inhibition of ovarian cancer by targeting CXCL12-CXCR4." Neoplasia **13**(12): 1152-1161.
- Rech, A. J., R. Mick, et al. (2010). "Homeostasis of peripheral FoxP3(+) CD4 (+) regulatory T cells in patients with early and late stage breast cancer." Cancer Immunol Immunother **59**(4): 599-607.
- Rehman, A. O. and C. Y. Wang (2009). "CXCL12/SDF-1 alpha activates NF-kappaB and promotes oral cancer invasion through the Carma3/Bcl10/Malt1 complex." Int J Oral Sci **1**(3): 105-118.
- Rempel, S. A., S. Dudas, et al. (2000). "Identification and localization of the cytokine SDF1 and its receptor, CXC chemokine receptor 4, to regions of

- necrosis and angiogenesis in human glioblastoma." Clin Cancer Res **6**(1): 102-111.
- Reuning, U., O. Wilhelm, et al. (1995). "Inhibition of NF-kappa B-Rel A expression by antisense oligodeoxynucleotides suppresses synthesis of urokinase-type plasminogen activator (uPA) but not its inhibitor PAI-1." Nucleic Acids Res **23**(19): 3887-3893.
- Ried, T. (2009). "Homage to Theodor Boveri (1862-1915): Boveri's theory of cancer as a disease of the chromosomes, and the landscape of genomic imbalances in human carcinomas." Environ Mol Mutagen **50**(8): 593-601.
- Righi, E., S. Kashiwagi, et al. (2011). "CXCL12/CXCR4 blockade induces multimodal antitumor effects that prolong survival in an immunocompetent mouse model of ovarian cancer." Cancer Res **71**(16): 5522-5534.
- Robledo, M. M., R. A. Bartolome, et al. (2001). "Expression of functional chemokine receptors CXCR3 and CXCR4 on human melanoma cells." J Biol Chem **276**(48): 45098-45105.
- Rosen, J. M. and C. T. Jordan (2009). "The increasing complexity of the cancer stem cell paradigm." Science **324**(5935): 1670-1673.
- Rossi, D. and A. Zlotnik (2000). "The biology of chemokines and their receptors." Annu Rev Immunol **18**: 217-242.
- Roy, V. and E. A. Perez (2009). "Beyond trastuzumab: small molecule tyrosine kinase inhibitors in HER-2-positive breast cancer." Oncologist **14**(11): 1061-1069.
- Rubin, J. B. (2009). "Chemokine signaling in cancer: one hump or two?" Semin Cancer Biol **19**(2): 116-122.
- Sakaguchi, S. (2005). "Naturally arising Foxp3-expressing CD25+CD4+ regulatory T cells in immunological tolerance to self and non-self." Nat Immunol **6**(4): 345-352.
- Salvucci, O., A. Bouchard, et al. (2006). "The role of CXCR4 receptor expression in breast cancer: a large tissue microarray study." Breast Cancer Res Treat **97**(3): 275-283.
- Santin, A. D., S. Bellone, et al. (2008). "Trastuzumab treatment in patients with advanced or recurrent endometrial carcinoma overexpressing HER2/neu." Int J Gynaecol Obstet **102**(2): 128-131.
- Sasada, T., M. Kimura, et al. (2003). "CD4+CD25+ regulatory T cells in patients with gastrointestinal malignancies: possible involvement of regulatory T cells in disease progression." Cancer **98**(5): 1089-1099.
- Schaefer, C., G. G. Kim, et al. (2005). "Characteristics of CD4+CD25+ regulatory T cells in the peripheral circulation of patients with head and neck cancer." Br J Cancer **92**(5): 913-920.
- Schioppa, T., B. Uranchimeg, et al. (2003). "Regulation of the chemokine receptor CXCR4 by hypoxia." J Exp Med **198**(9): 1391-1402.
- Schmid, B. C., M. Rudas, et al. (2004). "CXCR4 is expressed in ductal carcinoma in situ of the breast and in atypical ductal hyperplasia." Breast Cancer Res Treat **84**(3): 247-250.
- Schrader, A. J., O. Lechner, et al. (2002). "CXCR4/CXCL12 expression and signalling in kidney cancer." Br J Cancer **86**(8): 1250-1256.
- Schramm, C., S. Huber, et al. (2004). "TGFbeta regulates the CD4+CD25+ T-cell pool and the expression of Foxp3 in vivo." Int Immunol **16**(9): 1241-1249.
- Scotton, C. J., J. L. Wilson, et al. (2001). "Epithelial cancer cell migration: a role for chemokine receptors?" Cancer Res **61**(13): 4961-4965.

- Scotton, C. J., J. L. Wilson, et al. (2002). "Multiple actions of the chemokine CXCL12 on epithelial tumor cells in human ovarian cancer." Cancer Res **62**(20): 5930-5938.
- Sebolt-Leopold, J. S. (2008). "Advances in the development of cancer therapeutics directed against the RAS-mitogen-activated protein kinase pathway." Clin Cancer Res **14**(12): 3651-3656.
- Sereti, I., H. Imamichi, et al. (2005). "In vivo expansion of CD4CD45RO-CD25 T cells expressing foxP3 in IL-2-treated HIV-infected patients." J Clin Invest **115**(7): 1839-1847.
- Shibata, A., T. Nagaya, et al. (2002). "Inhibition of NF-kappaB activity decreases the VEGF mRNA expression in MDA-MB-231 breast cancer cells." Breast Cancer Res Treat **73**(3): 237-243.
- Shu, W., H. Yang, et al. (2001). "Characterization of a new subfamily of winged-helix/forkhead (Fox) genes that are expressed in the lung and act as transcriptional repressors." J Biol Chem **276**(29): 27488-27497.
- Signoret, N., J. Oldridge, et al. (1997). "Phorbol esters and SDF-1 induce rapid endocytosis and down modulation of the chemokine receptor CXCR4." J Cell Biol **139**(3): 651-664.
- Signoretti, S., L. Di Marcotullio, et al. (2002). "Oncogenic role of the ubiquitin ligase subunit Skp2 in human breast cancer." J Clin Invest **110**(5): 633-641.
- Singh, R. K., M. Gutman, et al. (1994). "Expression of interleukin 8 correlates with the metastatic potential of human melanoma cells in nude mice." Cancer Res **54**(12): 3242-3247.
- Singh, S., U. P. Singh, et al. (2004). "CXCL12-CXCR4 interactions modulate prostate cancer cell migration, metalloproteinase expression and invasion." Lab Invest **84**(12): 1666-1676.
- Singletary, S. E. and F. L. Greene (2003). "Revision of breast cancer staging: the 6th edition of the TNM Classification." Semin Surg Oncol **21**(1): 53-59.
- Sisirak, V., J. Faget, et al. (2013). "Plasmacytoid dendritic cells deficient in IFNalpha production promote the amplification of FOXP3 regulatory T cells and are associated with poor prognosis in breast cancer patients." Oncoimmunology **2**(1): e22338.
- Slamon, D. J., G. M. Clark, et al. (1987). "Human breast cancer: correlation of relapse and survival with amplification of the HER-2/neu oncogene." Science **235**(4785): 177-182.
- Slamon, D. J., W. Godolphin, et al. (1989). "Studies of the HER-2/neu proto-oncogene in human breast and ovarian cancer." Science **244**(4905): 707-712.
- Smith, E. L., H. M. Finney, et al. (2006). "Splice variants of human FOXP3 are functional inhibitors of human CD4+ T-cell activation." Immunology **119**(2): 203-211.
- Smith, M. C., K. E. Luker, et al. (2004). "CXCR4 regulates growth of both primary and metastatic breast cancer." Cancer Res **64**(23): 8604-8612.
- Snow, J. W., N. Abraham, et al. (2003). "Loss of tolerance and autoimmunity affecting multiple organs in STAT5A/5B-deficient mice." J Immunol **171**(10): 5042-5050.
- Solinas, G., G. Germano, et al. (2009). "Tumor-associated macrophages (TAM) as major players of the cancer-related inflammation." J Leukoc Biol **86**(5): 1065-1073.

- Somasundaram, K., H. Zhang, et al. (1997). "Arrest of the cell cycle by the tumour-suppressor BRCA1 requires the CDK-inhibitor p21WAF1/Cip1." *Nature* **389**(6647): 187-190.
- Somasundaram, R., L. Jacob, et al. (2002). "Inhibition of cytolytic T lymphocyte proliferation by autologous CD4⁺/CD25⁺ regulatory T cells in a colorectal carcinoma patient is mediated by transforming growth factor-beta." *Cancer Res* **62**(18): 5267-5272.
- Song, J. H., J. J. Waataja, et al. (2006). "Subcellular targeting of RGS9-2 is controlled by multiple molecular determinants on its membrane anchor, R7BP." *J Biol Chem* **281**(22): 15361-15369.
- Sonoda, H., H. Inoue, et al. (2006). "Significance of skp2 expression in primary breast cancer." *Clin Cancer Res* **12**(4): 1215-1220.
- Soriano, S. F., A. Serrano, et al. (2003). "Chemokines integrate JAK/STAT and G-protein pathways during chemotaxis and calcium flux responses." *Eur J Immunol* **33**(5): 1328-1333.
- Soule, H. D., J. Vazquez, et al. (1973). "A human cell line from a pleural effusion derived from a breast carcinoma." *J Natl Cancer Inst* **51**(5): 1409-1416.
- Sovak, M. A., R. E. Bellas, et al. (1997). "Aberrant nuclear factor-kappaB/Rel expression and the pathogenesis of breast cancer." *J Clin Invest* **100**(12): 2952-2960.
- Stal, O., S. Sullivan, et al. (1995). "c-erbB-2 expression and benefit from adjuvant chemotherapy and radiotherapy of breast cancer." *Eur J Cancer* **31A**(13-14): 2185-2190.
- Staller, P., J. Sulitkova, et al. (2003). "Chemokine receptor CXCR4 downregulated by von Hippel-Lindau tumour suppressor pVHL." *Nature* **425**(6955): 307-311.
- Steinhardt, A. A., M. F. Gayyed, et al. (2008). "Expression of Yes-associated protein in common solid tumors." *Hum Pathol* **39**(11): 1582-1589.
- Sternlicht, M. D. (2006). "Key stages in mammary gland development: the cues that regulate ductal branching morphogenesis." *Breast Cancer Res* **8**(1): 201.
- Strieter, R. M., P. J. Polverini, et al. (1995). "The functional role of the ELR motif in CXC chemokine-mediated angiogenesis." *J Biol Chem* **270**(45): 27348-27357.
- Taichman, R. S., C. Cooper, et al. (2002). "Use of the stromal cell-derived factor-1/CXCR4 pathway in prostate cancer metastasis to bone." *Cancer Res* **62**(6): 1832-1837.
- Takahashi, Y., Y. Miyoshi, et al. (2005). "Down-regulation of LATS1 and LATS2 mRNA expression by promoter hypermethylation and its association with biologically aggressive phenotype in human breast cancers." *Clin Cancer Res* **11**(4): 1380-1385.
- Tanaka, Y. (2002). "[Chemokines in health and diseases]." *J UOEH* **24**(1): 27-35.
- Tarasova, N. I., R. H. Stauber, et al. (1998). "Spontaneous and ligand-induced trafficking of CXC-chemokine receptor 4." *J Biol Chem* **273**(26): 15883-15886.
- Tarrant, T. K. and D. D. Patel (2006). "Chemokines and leukocyte trafficking in rheumatoid arthritis." *Pathophysiology* **13**(1): 1-14.
- Thakur, A., Y. Sun, et al. (2008). "Anti-invasive and antimetastatic activities of ribosomal protein S6 kinase 4 in breast cancer cells." *Clin Cancer Res* **14**(14): 4427-4436.

- Tolia, N. H. and L. Joshua-Tor (2007). "Slicer and the argonautes." Nat Chem Biol **3**(1): 36-43.
- Tone, Y., K. Furuuchi, et al. (2008). "Smad3 and NFAT cooperate to induce Foxp3 expression through its enhancer." Nat Immunol **9**(2): 194-202.
- Tran, D. Q., H. Ramsey, et al. (2007). "Induction of FOXP3 expression in naive human CD4+FOXP3 T cells by T-cell receptor stimulation is transforming growth factor-beta dependent but does not confer a regulatory phenotype." Blood **110**(8): 2983-2990.
- Tsuji-Takayama, K., M. Suzuki, et al. (2008). "IL-2 activation of STAT5 enhances production of IL-10 from human cytotoxic regulatory T cells, HOZOT." Exp Hematol **36**(2): 181-192.
- Tsuji-Takayama, K., M. Suzuki, et al. (2008). "The production of IL-10 by human regulatory T cells is enhanced by IL-2 through a STAT5-responsive intronic enhancer in the IL-10 locus." J Immunol **181**(6): 3897-3905.
- Tuefferd, M., J. Couturier, et al. (2007). "HER2 status in ovarian carcinomas: a multicenter GINECO study of 320 patients." PLoS One **2**(11): e1138.
- Tyner, S. D., S. Venkatachalam, et al. (2002). "p53 mutant mice that display early ageing-associated phenotypes." Nature **415**(6867): 45-53.
- Unitt, E., A. Marshall, et al. (2006). "Tumour lymphocytic infiltrate and recurrence of hepatocellular carcinoma following liver transplantation." J Hepatol **45**(2): 246-253.
- van Loosdregt, J., Y. Vercoulen, et al. (2010). "Regulation of Treg functionality by acetylation-mediated Foxp3 protein stabilization." Blood **115**(5): 965-974.
- Varney, M. L., S. L. Johansson, et al. (2006). "Distinct expression of CXCL8 and its receptors CXCR1 and CXCR2 and their association with vessel density and aggressiveness in malignant melanoma." Am J Clin Pathol **125**(2): 209-216.
- Varney, M. L., A. Li, et al. (2003). "Expression of CXCR1 and CXCR2 receptors in malignant melanoma with different metastatic potential and their role in interleukin-8 (CXCL-8)-mediated modulation of metastatic phenotype." Clin Exp Metastasis **20**(8): 723-731.
- Veikkola, T. and K. Alitalo (1999). "VEGFs, receptors and angiogenesis." Semin Cancer Biol **9**(3): 211-220.
- Ventura, A., D. G. Kirsch, et al. (2007). "Restoration of p53 function leads to tumour regression in vivo." Nature **445**(7128): 661-665.
- Vigouroux, S., E. Yvon, et al. (2003). "Induction of antigen-specific regulatory T cells following overexpression of a Notch ligand by human B lymphocytes." J Virol **77**(20): 10872-10880.
- Walsh, T., S. Casadei, et al. (2006). "Spectrum of mutations in BRCA1, BRCA2, CHEK2, and TP53 in families at high risk of breast cancer." JAMA **295**(12): 1379-1388.
- Wander, S. A., D. Zhao, et al. (2013). "PI3K/mTOR inhibition can impair tumor invasion and metastasis in vivo despite a lack of antiproliferative action in vitro: implications for targeted therapy." Breast Cancer Res Treat **138**(2): 369-381.
- Wang, B., D. Lin, et al. (2003). "Multiple domains define the expression and regulatory properties of Foxp1 forkhead transcriptional repressors." J Biol Chem **278**(27): 24259-24268.
- Wang, J., J. Cai, et al. (2011). "Silencing of CXCR4 blocks progression of ovarian cancer and depresses canonical Wnt signaling pathway." Int J Gynecol Cancer **21**(6): 981-987.

- Wang, J., A. Ioan-Facsinay, et al. (2007). "Transient expression of FOXP3 in human activated nonregulatory CD4+ T cells." *Eur J Immunol* **37**(1): 129-138.
- Wang, J., T. Murakami, et al. (2001). "Gene gun-mediated oral mucosal transfer of interleukin 12 cDNA coupled with an irradiated melanoma vaccine in a hamster model: successful treatment of oral melanoma and distant skin lesion." *Cancer Gene Ther* **8**(10): 705-712.
- Wang, J., Y. Shiozawa, et al. (2008). "The role of CXCR7/RDC1 as a chemokine receptor for CXCL12/SDF-1 in prostate cancer." *J Biol Chem* **283**(7): 4283-4294.
- Wang, L., R. Liu, et al. (2009). "Somatic single hits inactivate the X-linked tumor suppressor FOXP3 in the prostate." *Cancer Cell* **16**(4): 336-346.
- Wang, X. C., Y. P. Wu, et al. (2009). "Suppression of anoikis by SKP2 amplification and overexpression promotes metastasis of esophageal squamous cell carcinoma." *Mol Cancer Res* **7**(1): 12-22.
- Wang, Y., Q. Dong, et al. (2010). "Overexpression of yes-associated protein contributes to progression and poor prognosis of non-small-cell lung cancer." *Cancer Sci* **101**(5): 1279-1285.
- Weigel, D., G. Jurgens, et al. (1989). "The homeotic gene fork head encodes a nuclear protein and is expressed in the terminal regions of the Drosophila embryo." *Cell* **57**(4): 645-658.
- Weng, A. P., A. Shahsafaie, et al. (2003). "CXCR4/CD184 immunoreactivity in T-cell non-Hodgkin lymphomas with an overall Th1- Th2+ immunophenotype." *Am J Clin Pathol* **119**(3): 424-430.
- WHO.int. (2013). "Breast cancer: Prevention and control." Retrieved 1-7-2013, 2013, from <http://www.who.int/cancer/detection/breastcancer/en/index1.html>.
- Wiley, H. E., E. B. Gonzalez, et al. (2001). "Expression of CC chemokine receptor-7 and regional lymph node metastasis of B16 murine melanoma." *J Natl Cancer Inst* **93**(21): 1638-1643.
- Wilson, C. B., E. Rowell, et al. (2009). "Epigenetic control of T-helper-cell differentiation." *Nat Rev Immunol* **9**(2): 91-105.
- Winkelstein, W., Jr. (2006). "Janet Elizabeth Lane-Clayton: a forgotten epidemiologic pioneer." *Epidemiology* **17**(6): 705.
- Wolf-Yadlin, A., N. Kumar, et al. (2006). "Effects of HER2 overexpression on cell signaling networks governing proliferation and migration." *Mol Syst Biol* **2**: 54.
- Woo, E. Y., C. S. Chu, et al. (2001). "Regulatory CD4(+)CD25(+) T cells in tumors from patients with early-stage non-small cell lung cancer and late-stage ovarian cancer." *Cancer Res* **61**(12): 4766-4772.
- Wu, B., E. Y. Chien, et al. (2010). "Structures of the CXCR4 chemokine GPCR with small-molecule and cyclic peptide antagonists." *Science* **330**(6007): 1066-1071.
- Wu, C. C., M. L. Chan, et al. (2005). "Pristimerin induces caspase-dependent apoptosis in MDA-MB-231 cells via direct effects on mitochondria." *Mol Cancer Ther* **4**(8): 1277-1285.
- Wu, Y., M. Borde, et al. (2006). "FOXP3 controls regulatory T cell function through cooperation with NFAT." *Cell* **126**(2): 375-387.
- Xiao, S., H. Jin, et al. (2008). "Retinoic acid increases Foxp3+ regulatory T cells and inhibits development of Th17 cells by enhancing TGF-beta-driven Smad3

- signaling and inhibiting IL-6 and IL-23 receptor expression." *J Immunol* **181**(4): 2277-2284.
- Xiong, G., C. Wang, et al. (2012). "RORalpha suppresses breast tumor invasion by inducing SEMA3F expression." *Cancer Res* **72**(7): 1728-1739.
- Xiong, Y., G. J. Hannon, et al. (1993). "p21 is a universal inhibitor of cyclin kinases." *Nature* **366**(6456): 701-704.
- Xu, M. Z., T. J. Yao, et al. (2009). "Yes-associated protein is an independent prognostic marker in hepatocellular carcinoma." *Cancer* **115**(19): 4576-4585.
- Xu, T. P., H. Shen, et al. (2013). "The impact of chemokine receptor CXCR4 on breast cancer prognosis: A meta-analysis." *Cancer Epidemiol* **37**(5): 725-731.
- Xu, T. P., H. Shen, et al. (2013). "The impact of chemokine receptor CXCR4 on breast cancer prognosis: A meta-analysis." *Cancer Epidemiol*.
- Yamagiwa, S., J. D. Gray, et al. (2001). "A role for TGF-beta in the generation and expansion of CD4+CD25+ regulatory T cells from human peripheral blood." *J Immunol* **166**(12): 7282-7289.
- Yang, L., D. E. Anderson, et al. (2008). "IL-21 and TGF-beta are required for differentiation of human T(H)17 cells." *Nature* **454**(7202): 350-352.
- Yang, T. Y., S. C. Chen, et al. (2000). "Transgenic expression of the chemokine receptor encoded by human herpesvirus 8 induces an angioproliferative disease resembling Kaposi's sarcoma." *J Exp Med* **191**(3): 445-454.
- Yao, Z., Y. Kanno, et al. (2007). "Nonredundant roles for Stat5a/b in directly regulating Foxp3." *Blood* **109**(10): 4368-4375.
- Ye, J., C. Ma, et al. (2013). "Specific Recruitment of gammadelta Regulatory T Cells in Human Breast Cancer." *Cancer Res* **73**(20): 6137-6148.
- Yiu, G. K. and A. Toker (2006). "NFAT induces breast cancer cell invasion by promoting the induction of cyclooxygenase-2." *J Biol Chem* **281**(18): 12210-12217.
- Yu, D. and M. C. Hung (2000). "Role of erbB2 in breast cancer chemosensitivity." *Bioessays* **22**(7): 673-680.
- Yuan, X. L., L. Chen, et al. (2010). "Elevated expression of Foxp3 in tumor-infiltrating Treg cells suppresses T-cell proliferation and contributes to gastric cancer progression in a COX-2-dependent manner." *Clin Immunol* **134**(3): 277-288.
- Zabel, B. A., Y. Wang, et al. (2009). "Elucidation of CXCR7-mediated signaling events and inhibition of CXCR4-mediated tumor cell transendothelial migration by CXCR7 ligands." *J Immunol* **183**(5): 3204-3211.
- Zagzag, D., Y. Lukyanov, et al. (2006). "Hypoxia-inducible factor 1 and VEGF upregulate CXCR4 in glioblastoma: implications for angiogenesis and glioma cell invasion." *Lab Invest* **86**(12): 1221-1232.
- Zeelenberg, I. S., L. Ruuls-Van Stalle, et al. (2003). "The chemokine receptor CXCR4 is required for outgrowth of colon carcinoma micrometastases." *Cancer Res* **63**(13): 3833-3839.
- Zhang, B., L. H. Ji, et al. (2013). "Skp2-RNAi suppresses proliferation and migration of gallbladder carcinoma cells by enhancing p27 expression." *World J Gastroenterol* **19**(30): 4917-4924.
- Zhang, F., G. Meng, et al. (2008). "Interactions among the transcription factors Runx1, RORgamma and Foxp3 regulate the differentiation of interleukin 17-producing T cells." *Nat Immunol* **9**(11): 1297-1306.

- Zhang, H. Y. and H. Sun (2010). "Up-regulation of Foxp3 inhibits cell proliferation, migration and invasion in epithelial ovarian cancer." *Cancer Lett* **287**(1): 91-97.
- Zhang, K., E. Rodriguez-Aznar, et al. (2012). "Lats2 kinase potentiates Snail1 activity by promoting nuclear retention upon phosphorylation." *EMBO J* **31**(1): 29-43.
- Zhao, B., L. Li, et al. (2010). "A coordinated phosphorylation by Lats and CK1 regulates YAP stability through SCF(beta-TRCP)." *Genes Dev* **24**(1): 72-85.
- Zhao, B., X. Wei, et al. (2007). "Inactivation of YAP oncoprotein by the Hippo pathway is involved in cell contact inhibition and tissue growth control." *Genes Dev* **21**(21): 2747-2761.
- Zhao, Y., W. Jian, et al. (2013). "RNAi silencing of c-Myc inhibits cell migration, invasion, and proliferation in HepG2 human hepatocellular carcinoma cell line: c-Myc silencing in hepatocellular carcinoma cell." *Cancer Cell Int* **13**(1): 23.
- Zheng, K., H. Y. Li, et al. (2010). "Chemokine receptor CXCR7 regulates the invasion, angiogenesis and tumor growth of human hepatocellular carcinoma cells." *J Exp Clin Cancer Res* **29**: 31.
- Zheng, S., J. Huang, et al. (2011). "17beta-Estradiol enhances breast cancer cell motility and invasion via extra-nuclear activation of actin-binding protein ezrin." *PLoS One* **6**(7): e22439.
- Zheng, S. G., J. H. Wang, et al. (2006). "TGF-beta requires CTLA-4 early after T cell activation to induce FoxP3 and generate adaptive CD4+CD25+ regulatory cells." *J Immunol* **176**(6): 3321-3329.
- Zheng, Y., S. Z. Josefowicz, et al. (2007). "Genome-wide analysis of Foxp3 target genes in developing and mature regulatory T cells." *Nature* **445**(7130): 936-940.
- Zhou, B. P., M. C. Hu, et al. (2000). "HER-2/neu blocks tumor necrosis factor-induced apoptosis via the Akt/NF-kappaB pathway." *J Biol Chem* **275**(11): 8027-8031.
- Zhou, H. and H. H. Tai (2000). "Expression and functional characterization of mutant human CXCR4 in insect cells: role of cysteinyl and negatively charged residues in ligand binding." *Arch Biochem Biophys* **373**(1): 211-217.
- Zhou, L., J. E. Lopes, et al. (2008). "TGF-beta-induced Foxp3 inhibits T(H)17 cell differentiation by antagonizing RORgamma function." *Nature* **453**(7192): 236-240.
- Zhou, N., Z. Luo, et al. (2002). "Exploring the stereochemistry of CXCR4-peptide recognition and inhibiting HIV-1 entry with D-peptides derived from chemokines." *J Biol Chem* **277**(20): 17476-17485.
- Ziegler, S. F. (2006). "FOXP3: of mice and men." *Annu Rev Immunol* **24**: 209-226.
- Zlotnik, A., A. M. Burkhardt, et al. (2011). "Homeostatic chemokine receptors and organ-specific metastasis." *Nat Rev Immunol* **11**(9): 597-606.
- Zlotnik, A. and O. Yoshie (2000). "Chemokines: a new classification system and their role in immunity." *Immunity* **12**(2): 121-127.
- Zorn, E., E. A. Nelson, et al. (2006). "IL-2 regulates FOXP3 expression in human CD4+CD25+ regulatory T cells through a STAT-dependent mechanism and induces the expansion of these cells in vivo." *Blood* **108**(5): 1571-1579.
- Zou, W. (2006). "Regulatory T cells, tumour immunity and immunotherapy." *Nat Rev Immunol* **6**(4): 295-307.

- Zuo, T., R. Liu, et al. (2007). "FOXP3 is a novel transcriptional repressor for the breast cancer oncogene SKP2." J Clin Invest **117**(12): 3765-3773.
- Zuo, T., L. Wang, et al. (2007). "FOXP3 is an X-linked breast cancer suppressor gene and an important repressor of the HER-2/ErbB2 oncogene." Cell **129**(7): 1275-1286.

	Chapter
General introduction	1
General materials and methods	2
Study of FOXP3 expression in normal and malignant breast cell lines	3
<i>In vitro</i> modelling of FOXP3 expression in normal and malignant breast cell lines	4
<i>In vivo</i> levels of FOXP3 and CXCR4 expression in breast cancer samples	5
Discussion	6
List of references	7
Appendices	8

8 Appendices

A

```

1 TTGAGCAAGGACCCGATGCCCAACCCAGGCTGSCAAGCCCTGSCCCTTCCTTGGCCCTTGGCCATCCCAAGGAGCTGSCCAGCTGAGGAGCTGACCCAAAGCTCAGACCTGCTGGGGGCCCGGGGCCAGG 140
1 ttggacaaggacccgatgcccaacccaggctggcaagccctggcccttctcttggcccttggccatccccaggagcctgcccagctggagggctgcacccaagcctcagacctgctgggggcccggggccaggy 140

141 GGGAACTTCCAGGGCCGAGATCTTCAGAGCGGGGCCATGCTCTCTCTTCTTGAACCCCATGSCACCATGSCAGCTGCCAGCTGCCCCACTGCCCCAGTATGCTGGTGGCACCCTCCGGGGCACGGCTGGGGCCCT 280
141 gggaaacttcagggccgagatcttcagagcggggcccattgctctcttcttgaaccccatgscaccatgscagctgccagctgcccactgcccactgctcagtggtggcaccctccggggcacggctggggccct 280

281 TGCCCCACTTACAGGCACTCTCCAGGACAGGCCACATTCATGCACAGCTCTCAACGGTGGATGCCAGGCCGAGCCCTGTGCTGAGGTGCACCCCTGGAGAGCCAGCCATGATCAGCTCAGCCACCCACC 420
281 tgccccacttacaggcaactctccaggacaggccacatttcacacagctctcaacggtggatgccagccggagccctgtgctgaggtgcacccctggagagccagccatgatcagctcacaccaccacc 420

421 ACCGCCACTGAGGGTCTTCTCCCTCAAGGCCCGGCTGGCTCCACCTGGGATCAACGTGGCCAGCTGGAATGGGTGTCCAGGAGCCGGGCACTGCTCTGCACCTTCCCAAAATCCAGTGCACCCAGGAAGGACAGC 560
421 accgccactgagggcttctccctcaaggcccgccctggcctccacctgggatcaacgtggccagctggaatgggtgtccaggagccgggcaactgctctgcacctcccaaatccagtgccaccaggaaggaagacac 560

561 CTTTCGGCTGTGCCCCAGAGCTCTTACCCACTGCTGCAAAATGGTGTCTGCAAGTGG 618
561 ctttcggctgtgccccagagctcttaccactgctgcaaaatggtgtctgcaagtgg 618

```

B

```

1 ACAAGGACCCGATGCCCAACCCAGGCTGSCAAGCCCTGSCCCTTCCTTGGCCCTTGGCCATCCCAAGGAGCTGSCCAGCTGAGGAGCTGACCCAAAGCTCAGACCTGCTGGGGGCCCGGGGCCAGG 140
1 acaaggacccgatgcccaacccaggctggcaagccctggcccttctcttggcccttggccatccccaggagcctgcccagctggagggctgcacccaagcctcagacctgctgggggcccggggccaggggga 140

141 ACCTTCCAGGGCCGAGATCTTCAGAGCGGGGCCATGCTCTCTCTTCTTGAACCCCATGSCACCATGSCAGCTGCACTG----- 223
141 accttcagggccgagatcttcagagcggggcccattgctctcttcttgaaccccatgscaccatgscagctgcccactgcccactgctcagtggtggcaccctccggggcacggctggggcccttggc 280

224 -----CTCAACGGTGGATGCCAGGCCCGGACCCCTGTGCTGAGGTGCACCCCTGGAGAGCCAGCCATGATCAGCTCAGCCATCAGCCACCCACCAGC 315
281 ccacttacaggcaactctccaggacaggccacatttcacacagctctcaacggtggatgccacgcccggagccctgtgctgaggtgcacccctggagagccagccatgatcagcctcacaccaccaccag 420

316 CCAGTGGGGTCTTCTCCCTCAAGGCCCGGCTGGCTCCACCTGGGATCAACGTGGCCAGCTGGAATGGGTGTCCAGGAGCCGGGCACTGCTCTGCACCTTCCCAAAATCCAGTGCACCCAGGAAGGACAGCACCCTT 455
421 ccactggggcttctccctcaaggcccgccctggcctccacctgggatcaacgtggccagcctggaatgggtgtccaggagccgggcaactgctctgcacctcccaaatccagtgccaccaggaaggaagacacctt 560

456 TCGGCTGTGCCCCAGAGCTCTTACCCACTGCTGCAAAATGGTG 498
561 tgggtgtgccccagagctcttaccactgctgcaaatggtg 603

```

Appendix 1 – Sequencing of *FOXP3* in HMEpC using *FOXP3* primer region 1
Sequencing data from *FOXP3FL* (upper band on gel) with primer set 1 (A), *FOXP3A3* (lower band on gel) from primer set 1 (B).

A

```

      *      *      *      *      *      *      *      *      *      *      *      *      *      *
1 TTCCAAATCCAGTGCACCCAGGAAGGACAGCACCCCTTTCGGCTGTGCCCCAGAGCTCTACCCACTGCTGGCAAAATGGTGTCTGCAAGTGGCCCGGATGTGAGAAGGTCTTCGAAGAGCCAGAGGACTTCCTCAAGCA 140
|||||
1 ttcccaaatcccaagtgccaccaggaaggacagccaccttccggctgtgccccagagagctctaccacctgtgtggcaaatggtgtctgcaagtggcccgagatgtgagaaggtcttcgaagagccagagagacttccccaagca 140
      *      *      *      *      *      *      *      *      *      *      *      *      *      *

141 CTGCCAGGCGGACCATCTTCTGGATGAGAAGGSCAGGSCACAATGTCTCTCCAGAGAGAGATGATACAGTCTCTGGAGCAGCAGCTGGTGTCTGGAGAAGGAGAAGCTGAGTGCCATGCAGGCCACCTGGCTGGGAAAA 280
|||||
141 ctgccagggcgaccactctcttgatgagaaggcgaggccacaatgtctctccagagagagatggttacagttctctggagcagcagctggtgtctggagaaggagaagctgagtgccatgcagggccacacctgggtgggaaaa 280
      *      *      *      *      *      *      *      *      *      *      *      *      *      *

281 TGGCACTGACCAAGGCTTTCATGTGGCATCATCCGACAAGGGCTCCTGCTGCATGCTAGTCTGTGCGAGCCCAAGGCCCTGTGCTCCAGCCTGGTCTGGCCCCCGGAGGCCCTGACAGCCTGTTTGTGTCGGGAGG 420
|||||
281 tggcactgaccaaggcttctctgtgcatcatccgacaagggtcctctgctgcatctgtgctgtgagcagcagggccctgtgtctccagcctggtgtgtgccccgggagggccctgacagcctgtttgtgtccggagg 420
      *      *      *      *      *      *      *      *      *      *      *      *      *      *

421 CACCTGTGGGGTAGCCATGGAACAGCACATTCACAGATTCTCCACAACATGAGTACTTCAAGTTCACAACATGCGACCCCTTTCACCTACGCCACGCTCAITCGCTGGGCCATCTTGGAGGCTCCAGAGAAGCA 560
|||||
421 cacctgtgggtagccatggaaacagcacattccagagttcctccacaacatggactacttcaagttccacaacatgcgacccctttcacctagccacgctcatccgctgggacctctggaggtccagagaagca 560
      *      *      *      *      *      *      *      *      *      *      *      *      *      *

```

B

```

      *      *      *      *      *      *      *      *      *      *      *      *      *      *
1 CAGAGTTCCTCCACAACATGGACTACTTCAAGTTCACACATGCGACCCCTTTCACCTACGCCACGCTCATCGCTGGGCCATCTCTGGAGGCTCCAGAGAAGCAGCGGACACTCAATGAGATCTACCACTGGTTCACA 140
|||||
1 cagagttcctccacaacatggactacttcaagttccacaacatgogaccccttccacctacgccaagctcatccgtgggacctctggaggctccagagaagcagcgagcactcaatgagatctaccactggttcaca 140
      *      *      *      *      *      *      *      *      *      *      *      *      *      *

141 CCGATGTTGCTTCTTCAGAAACCATCTGCCACTGGAAGACGCCATCCGCCACAACCTGAGTCTGCACAAGTGTCTTGTGCGGGTGGAGAGCGAGAAGGGGGCTGTGTGGACCTGGATGAGCTGGAGTTCGCGAA 280
|||||
141 cgcattgttgccttcttcagaaacctcctgccacctggaagaagccatccggccacaacctgagctctgcacaaagtcttctgtcggggtggagagcgagaagggggctgtgtggacctggatgagctggagttccgcaa 280
      *      *      *      *      *      *      *      *      *      *      *      *      *      *

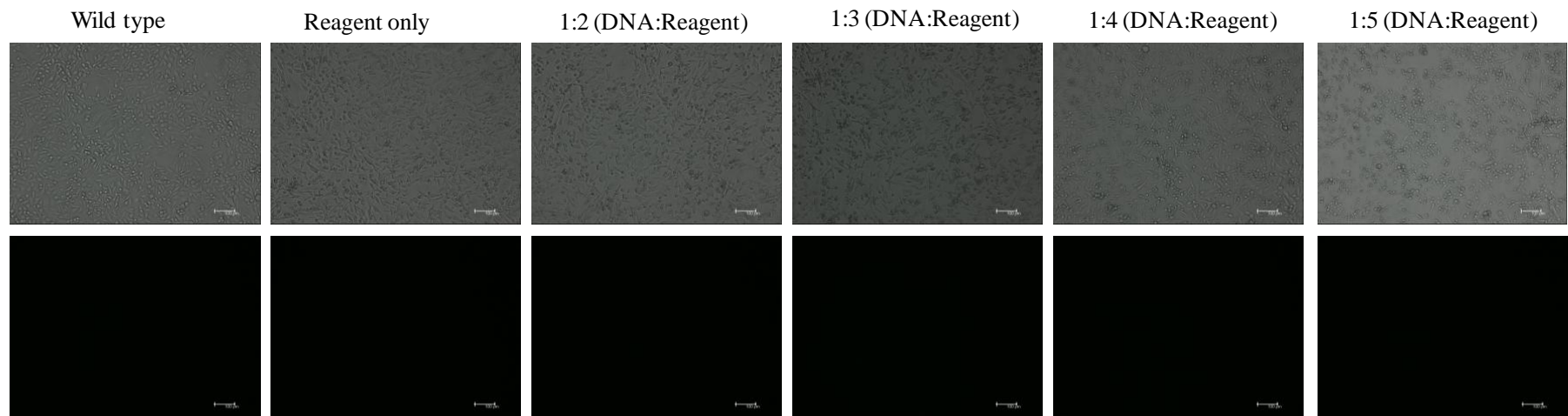
281 GAAACGGAGCCAGAGGCCAGAGTGTTCACACCTACACCTGGCCCCCTGACCTCAAGATCAAGGAAAGGAGGATGGAGAACAGGGGCCAAACTGGTGGAGGCGCAGAGGTGGTGGGGGCGAGGATGATAGGCCCTGGA 420
|||||
281 gaaacggagccagagggccagcaggtgttccaacctacacctggccccctgacctcaagatcaaggaaaggaggatggagcgaacagggggccaaactggtgggagggcagaggtggtggggggcaggggatgtagggcctgga 420
      *      *      *      *      *      *      *      *      *      *      *      *      *      *

421 TGTGCCACAGGGACCAAGAGTGAAGTTTCCACTG 456
|||||
421 tgtgccacagggaccagaagtgaagtttccactg 456
      *      *      *      *      *      *      *      *      *      *      *      *      *      *

```

Appendix 2 – Sequencing of *FOXP3* in HMEpC using FOXP3 primer set 2 and 3

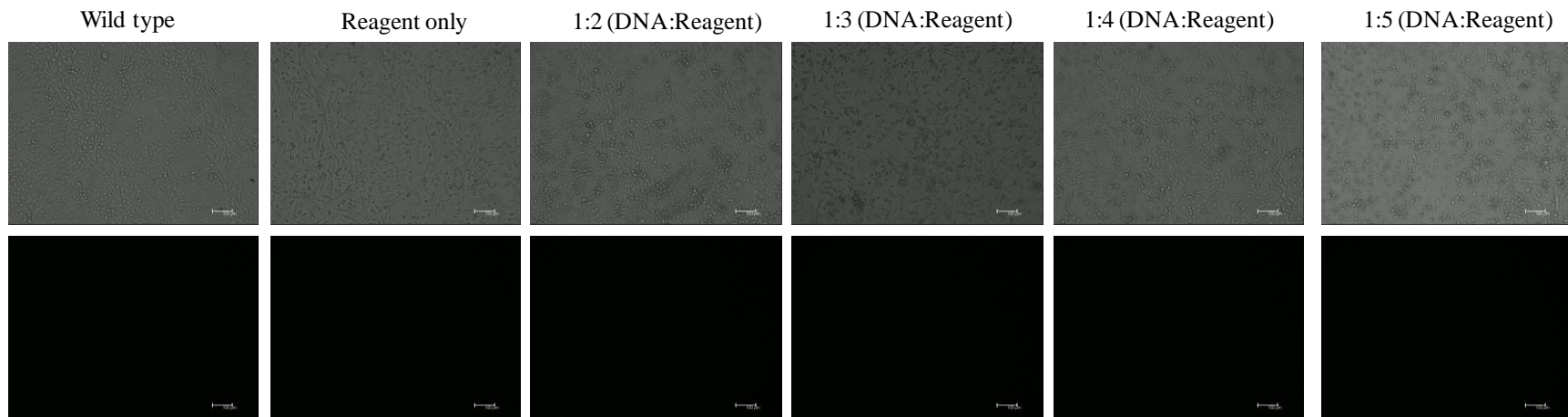
Sequencing data from *FOXP3* with primer set 2 (A), *FOXP3* from primer set 3 (B).



Appendix 3 – Optimisation of pmaxGFP transfection into MDA-MB-231 using JetPRIME® after 24 hours

MDA-MB-231 were transfected with 2µg of PmaxGFP plasmid using varying ratios of JetPRIME® reagent from 1:2 to 1:5 (µg of DNA: µl of reagent) .

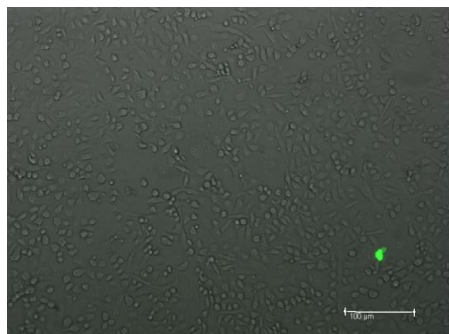
To avoid cytotoxicity, after 48 hours transfection complexes were removed and replaced with growth media without antibiotics. Transfection efficiency was determined by IF microscopy after 24 hours



Appendix 4 – Optimisation of pmaxGFP transfection into MDA-MB-231 using JetPRIME® after 48 hours

MDA-MB-231 were transfected with 2µg of PmaxGFP plasmid using varying ratios of JetPRIME® reagent from 1:2 to 1:5 (µg of DNA: µl of reagent). Transfection efficiency was determined by IF microscopy after 48 hours

Brightfield/FITC merge

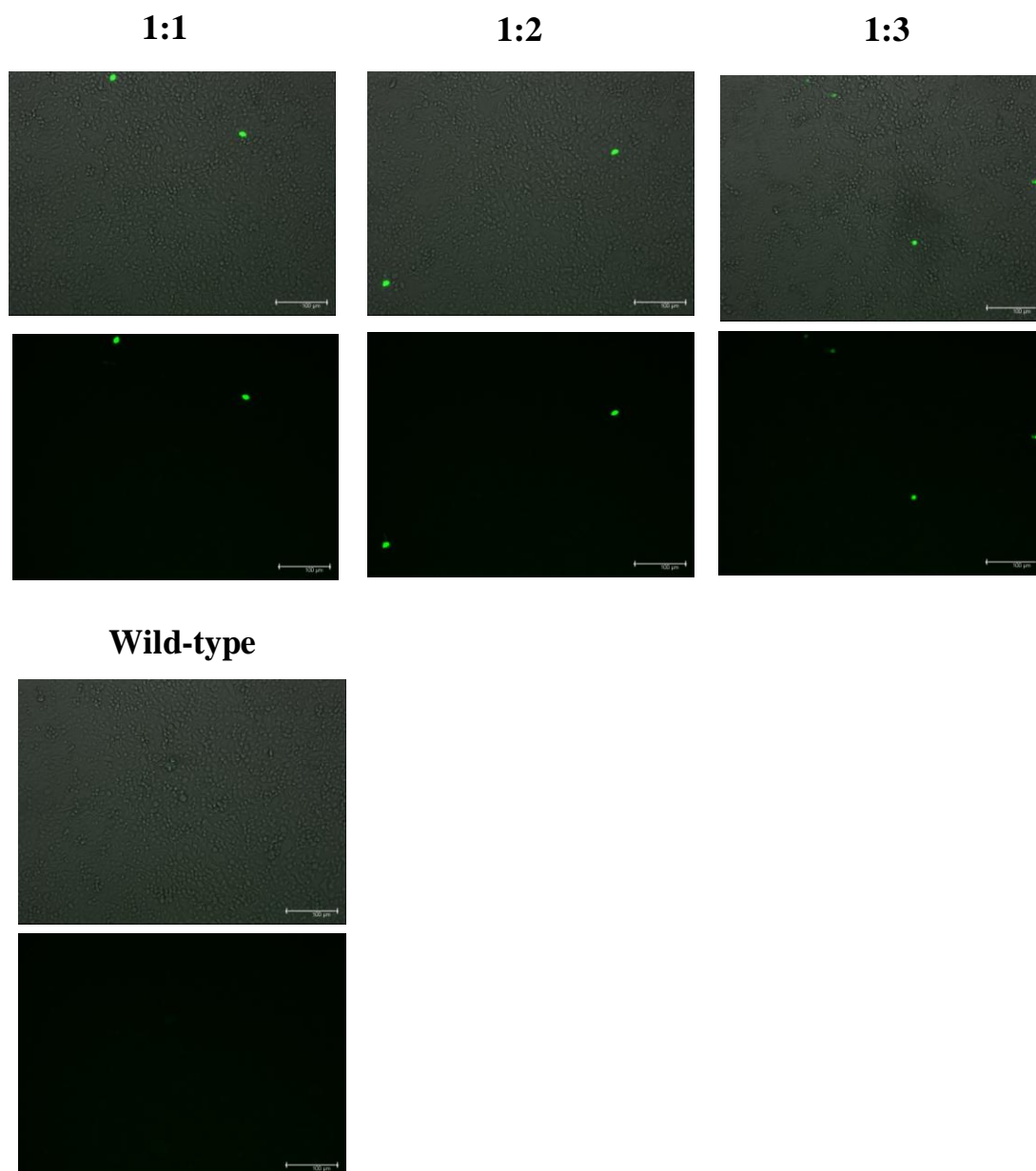


FITC



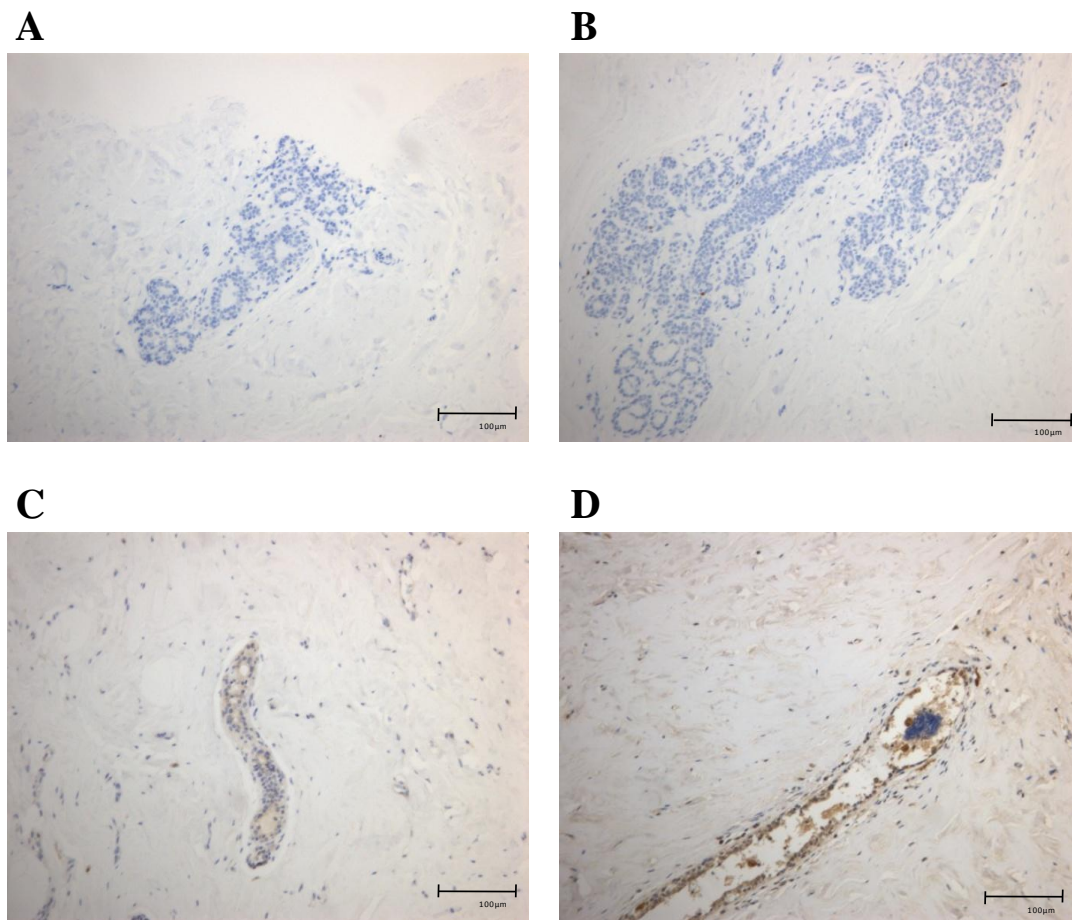
Appendix 5 – Transfection of pmaxGFP into MDA-MB-231 using GeneJuice® after 24 hours

MDA-MB-231 were transfected with 2ug of pmaxGFP plasmid using GeneJuice® according to the manufacturers recommended protocol (2μg of DNA: 6μl of reagent). Transfection efficiency was determined by IF microscopy after 24 hours.



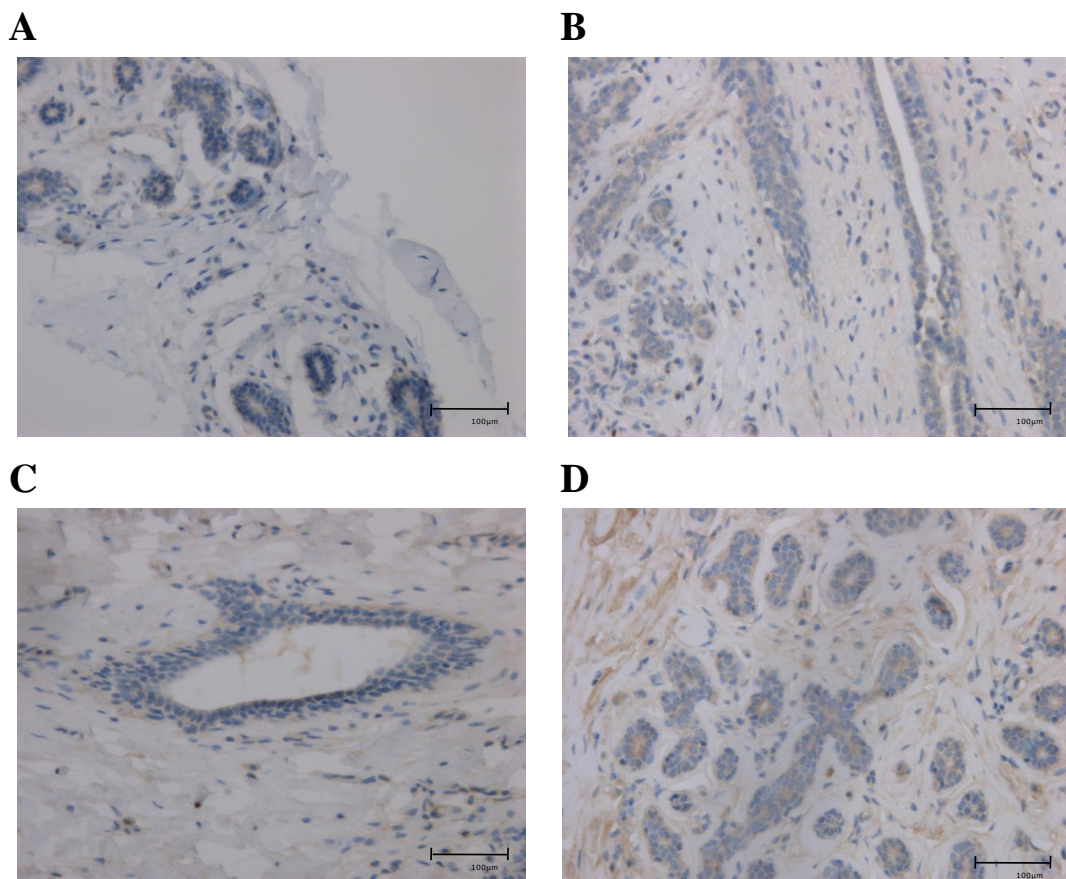
Appendix 6 – Optimisation of pmaxGFP transfection into MDA-MB-231 using TurboFect™ after 24 hours

MDA-MB-231 were transfected with 2 μ g of PmaxGFP plasmid using varying ratios of TurboFect™ reagent from 1:1 to 1:3 (μ g of DNA: μ l of reagent). Transfection efficiency was determined by IF microscopy after 24 hours



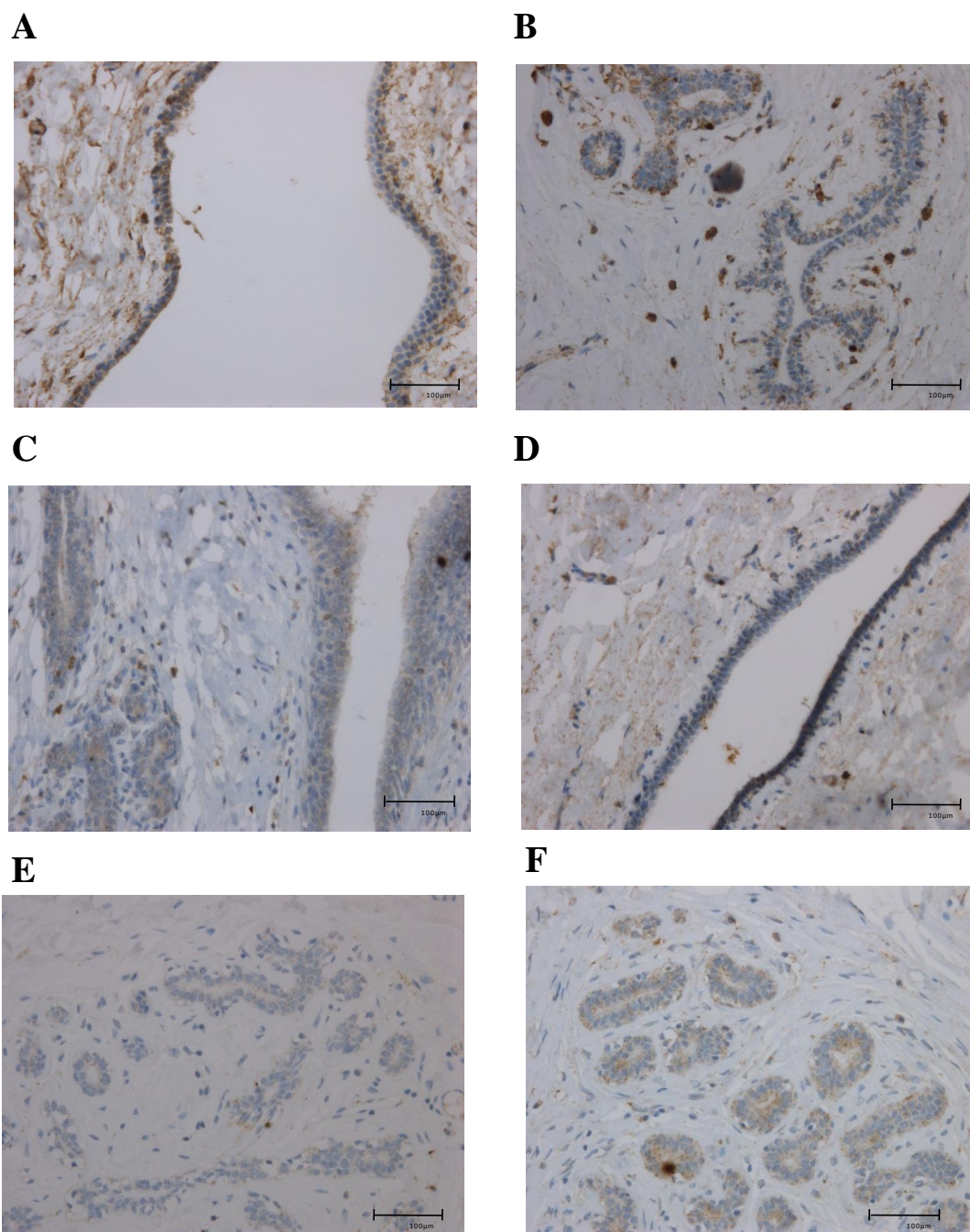
Appendix 7 – Attempted FOXP3 staining using the autostainer link 48 with FOXP3 antibody clone 236A/E7

Normal breast tissue from breast reduction surgery was stained for FOXP3 by Ms Denise Woolley using autostainer link 48 within the QE Hospital. Antigens were retrieved using a high pH buffer for 60 minutes and slides were stained for 40 minutes with the primary human anti-FOXP3 antibody at dilutions 1:150 (A), 1:100 (B), 1:50 (C), and 1:25 (D).



Appendix 8 – Optimisation FOXP3 staining using the BenchMark ULTRA with anti-FOXP3 antibody (clone 159D) using the ultraview detection kit

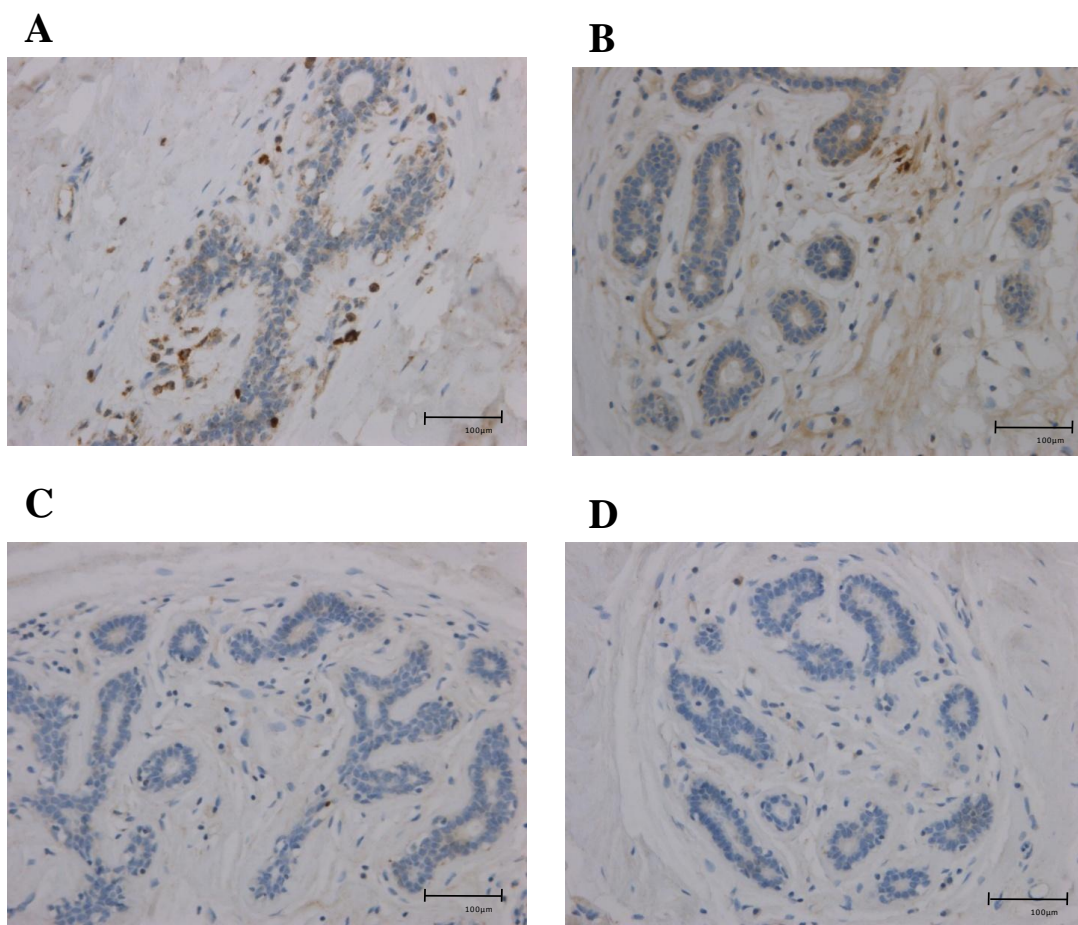
Normal breast tissue from breast reduction surgery was stained for FOXP3 by Ms Anna Long using the BenchMark ULTRA within the RVI Hospital. Antigens were retrieved using Cell Conditioning solution-1 (high pH buffer) for 60 minutes. Slides were stained with the primary human anti-FOXP3 antibody for 40 minutes at the dilutions 1:100 (**A**), 1:50 (**B**), 1:25 (**C**), 1:10 (**D**). All slides received 4 minutes amplification



Appendix 9 – Optimisation FOXP3 staining using the BenchMark ULTRA with anti-FOXP3 antibody (clone 159D) using the optiview detection kit

Normal breast tissue from breast reduction surgery was stained for FOXP3 by Ms Anna Long using the BenchMark ULTRA within the RVI Hospital. Antigens were retrieved using Cell Conditioning solution-1 (high pH buffer) for 60 minutes. Slides were stained for 40 minutes with a human anti-FOXP3 antibody at the dilutions; 1:100 (**A**), 1:50 (**B**), 1:50 + 12 minutes of amplification (**C**) and 1:25 +8 minutes amplification (**D**).

Alternatively antigens were retrieved using a pressure cooker with citrate buffer (**E**) or Tris/EDTA (**F**) with primary antibody dilutions at 1:50 for 40 minutes.



Appendix 10 – Optimisation FOXP3 staining using BenchMark ULTRA with anti-FOXP3 antibody (clone 159D) using the optiview detection kit (2)

Normal breast tissue from breast reduction surgery was stained for FOXP3 by Ms Anna Long using the BenchMark ULTRA within the RVI Hospital. Antigens were retrieved using Cell Conditioning solution-1 (high pH buffer) for 30 minutes. Slides were stained for 40 minutes with anti-FOXP3 antibody at the dilutions 1:50 (**A**) and 1:25 (**B**). Alternatively antigens were retrieved using Cell Conditioning solution-2 (low pH buffer) and stained with anti-FOXP3 primary antibody at the dilutions 1:50 (**C**) or (**D**) 1:25 for 40 minutes.

Appendix 11:

A list of the posters, presentations, publications, prizes throughout duration of this PhD as listed below:

Posters:

- Mammary gland biology – Gordon Conference, Stowe, VT, US (June 2013)

Presentations:

- Institute of Cellular Medicine (ICM) research seminar series (2011)
- Women's cancer detection society (WCDS) annual committee meeting (2011 & 2012)
- Applied immunobiology and Transplantation seminar series (2012 & 2013)
- North-East postgraduate research conference (NEPG) (2011)
- Boston Brandeis University – Invited guest speaker (June, 2013)

Publications:

- **Douglass S**, Ali S, Meeson AP, Browell D, Kirby JA (2012) The role of FOXP3 in the development and metastatic spread of breast cancer. *Cancer Metastasis Rev*;31(3-4):843-54
- Asghar K, Brain J, Palmer JM, **Douglass S**, Naemi F, Kirby JA, Ali S (2013) Immunoregulatory activity of Indoleamine 2, 3-dioxygenase in the pathogenesis of Primary Biliary Cirrhosis (*Manuscript pending result*).
- **Douglass S** *et al* (2013), Dysregulated FOXP3 in breast epithelia promotes an aggressive phenotype and increases site-specific metastasis in breast cancer (*manuscript in preparation*)

Prizes:

- Travel grant awarded by British society of immunology (competitive basis) - £1000, 2013
- Travel grant awarded by Newcastle University graduate school (competitive basis) - £800, 2013

Memberships:

- British association for cancer research (BACR) (2010-Present)
- British society for immunology (BSI) (2010-Present)